Function of SUMO-like proteases SENP1, SENP2 and NEDP1 *in vivo*

Heidi M. Mendoza
School of Biomedical Sciences
University of St. Andrews

A thesis submitted for the degree of Doctor of Philosophy
September 2004

I, Neil M. Mackay, hereby certify that this thesis, which is approximately 31000 words in length, has been written by me, that it is the record of work carried out by me and that it has not been submitted in any previous application for a higher degree.

date 14/12/04 signature of candidate

I was admitted as a research student in Sept 2000 and as a candidate for the degree of Doctor of Philosophy in Sept 2000; the higher study for which this is a record was carried out in the University of St Andrews between 2000 and 2004.

date 14/12/04. signature of candidate .

I hereby certify that the candidate has fulfilled the conditions of the Resolution and Regulations appropriate for the degree of Doctor of Philodophy in the University of St Andrews and that the candidate is qualified to submit this thesis in application for that degree.

date 14/12/04 signature of supervisor

In submitting this thesis to the University of St Andrews I understand that I am giving permission for it to be made available for use in accordance with the regulations of the University Library for the time being in force, subject to any copyright vested in the work not being affected thereby. I also understand that the title and abstract will be published, and that a copy of the work may be made and supplied to any *bona fide* library or research worker.

date 14/12/04 signature of candidate

CONTENTS

List of Figures

List of Tables

List of Abbreviations

ADP	Adenosine diphosphate
AMP	Adenosine monophosphate
APC	Anaphase promoting complex
APL	Acute promyelocytic leukemia
APP-BP1	Amyloid precursor protein-binding protein 1
A. thaliana	*Arabidopsis thaliana*
ATP	Adenosine triphosphate
bp	Base pairs
BSA	Bovine serum albumin
CDK	Cyclin-dependent kinase
cDNA	Complementary DNA
CKI	Cyclin-dependent kinase inhibitor
C. elegans	*Caenorhabditis elegans*
D-MEM	Dulbecco's modified Eagle's medium
DNA	Deoxyribonucleic acid
D. melanogaster	*Drosophila melanogaster*
DTT	Dithiothreitol
DUB	Deubiquitination enzyme
E. coli	*Escherichia coli*
E1	Activating enzyme
E2	Conjugating enzyme
E3	Ligation enzyme
ECL	Enhanced chemiluminescence
EDTA	Ethylenediaminetetracetic acid

FCS	Foetal calf serum
GST	Glutathione S-transferase
h	Hour(s)
HA	Haemagglutinin
HECT	Homology to E6-AP C-terminus
Ig	Immunoglobulin
IκB	Inhibitor kappa B
IPTG	Isopropyl-b-D-thiogalactopyranoside
IVTT	*In vitro* transcription translated
kDa	Kilo Dalton
LB	Luria-Bertani broth
LPS	Lipopolysaccharide
Mdm2	Mouse double minute 2
min	minute(s)
MW	Molecular weight
NBs	Nuclear bodies
NEDD8	Neuronal precursor cell expressed developmentally downregulated protein 8
NF-κB	Nuclear factor-kappa B
NLS	Nuclear localisation signal
NP-40	Nonidet P-40
NPC	Nuclear pore complex

PAGE	Polyacrylamide gel electrophoresis
PBS	Phosphate buffered saline
PCR	Polymerase chain reaction
PML	Promyelocytic leukaemia protein
PVDF	Polyvinylidene difluoride
RanGAP	Ran GTPase activating protein
RanBP	Ran binding protein
RNA	Ribonucleic acid
RSC	Random sequence control
RT-PCR	Reverse transcriptase PCR
SAE1	SUMO activating enzyme subunit1
SAE2	SUMO activating enzyme subunit2
S. cerevisiae	*Saccharomyces cerevisiae*
S. pombe	*Schizosaccharomyces pombe*
SCF	Skip1, cullin, F-box complex
SDS	Sodium dodecyl sulphate
SENP	Sentrin-specific protease
SUMO	Small ubiquitin-like modifier
SUSP1	SUMO-specific protease 1
TNFα	Tumour necrosis factor alpha
Tris	2-amino-2-(hydroxymethyl) propane-1, 2-diol
Ub	Ubiquitin
UBA1	Ubiquitin activating enzyme
Ubc	Ubiquitin conjugating enzyme
UBL	Ubiquitin-like modifiers

UBP	Ubiquitin-specific processing proteases
UCH	Ubiquitin C-terminal hydrolase
UDP	Ubiquitin domain protein
Ulp	Ubiquitin-like protease
VHL	von Hippel-Lindau
WT	Wild type
X. laevis	*Xenopus laevis*

Abbreviations for amino acids

Alanine	ala	A
Arginine	arg	R
Asparagine	asn	N
Aspartic acid	asp	D
Cysteine	cys	C
Glutamine	gln	Q
Glycine	gly	G
Histidine	his	H
Isoluecine	ile	I
Leucine	leu	L
Lysine	lys	K
Methionine	met	M
Phenylalanine	phe	F
Proline	pro	P
Serine	ser	S
Threonine	thr	T
Tryptophan	try	W
Tyrosine	tyr	Y
Valine	val	V

ACKNOWLEDGEMENTS

I would like to acknowledge my two supervisors, Professor Ron Hay and Dr. Barbara Ink, for their guidance and encouragement throughout my PhD. Barbara deserves a special mention for setting up the project so well and for sharing her enthusiasm with me.

I would also like to thank all of the St. Andrews lab for their scientific advice and for creating such a great atmosphere to work in. In particular Dr. Lin-nan Shen for his stimulating discussions about the proteases. Thanks also to the Glaxo lab for making my time at Glaxo so enjoyable.

Finally, thanks to Mum, Dad, Simon, Frost, and Roy for their love and support which made this all possible.

ABSTRACT

The ubiquitin-like protein SUMO is attached to a subset of proteins and participates in a wide range of cellular processes. Here I report the characterisation of SENP1 and SENP2, human SUMO specific proteases. Expressed and purified SENP1 and SENP2 cleave the inactive precursor forms of SUMO-1, SUMO-2 and SUMO-3 after the diglycine motif to generate the mature forms that are capable of being conjugated to substrate proteins. In addition SENP1 and SENP2 display isopeptidase activity to deconjugate SUMO-1 and SUMO-2 from modified proteins. Exogenous expression of SENP1 and SENP2 resulted in the deconjugation of SUMO-1, SUMO-2 and SUMO-3 from modified substrates *in vivo*. Deconjugation was not observed after exogenous expression of C548A SENP2 or C603A SENP1, where the cysteine residue predicted to supply the active site nucleophile is changed to alanine. Expressed SENP2 was almost exclusively nuclear and accumulated in discrete nuclear "speckles" and at the nuclear rim. Expressed SENP1 was present at the nuclear rim, in a few nuclear dots, and free in the nucleoplasm at interphase. SENP1 depletion with siRNA has shown that SENP1 is required for progression through cytokinesis in mammalian cells. In addition, SENP1 depleted cells accumulate SUMO-2, but not SUMO-1 at the midbody during cytokinesis. Expression of GFP tagged SENP1 has shown very low levels of the wt

SENP1 protease are present at the midbody. However, the catalytically inactive mutant of SENP1 accumulates at the midbody and causes the accumulation of SUMO-2, but not SUMO-1. A 3D reconstruction of z-sections taken through the SENP1 structure at the midbody has revealed that SENP1 forms a ring. SENP1 and SENP2 belong to a family of enzymes that are likely to be involved in controlling the dynamic equilibrium that establishes the SUMO modified state of proteins *in vivo*.

The ubiquitin-like protein NEDD8 is essential for activity of SCF-like ubiquitin ligase complexes and inhibits the transcriptional activity of p53. Here I identify and characterize NEDP1, a human NEDD8 specific protease. NEDP1 is highly conserved throughout evolution and equivalent proteins are present in yeast, plants, insects and mammals. Bacterially expressed NEDP1 is capable of processing NEDD8 *in vitro* to expose the diglycine motif required for conjugation and can deconjugate NEDD8 from modified substrates. NEDP1 appears to be specific for NEDD8 as neither ubiquitin nor SUMO bearing C-terminal extensions are utilized as substrates. Inhibition studies and mutagenesis indicate that NEDP1 is a cysteine protease with sequence similarities to SUMO specific proteases and the class of viral proteases typified by the adenovirus protease. *In vivo* NEDP1 deconjugates NEDD8 from a wide variety of substrates including the cullin component of

SCF-like complexes. Thus NEDP1 is likely to play an important role in ubiquitin mediated proteolysis by controlling the activity of SCF complexes.

1 INTRODUCTION

Reversible post-translational modification provides a means for cells to swiftly alter protein function in response to changes in the environment. Small molecule modifications such as acetylation and phosphorylation are well-known mechanisms of changing protein function. An additional sophisticated method of altering the function of proteins is reversible covalent modification with another protein. Covalent modification with a small protein provides a large and varied surface area with which to regulate interaction with other cellular components. The first discovered and most extensively characterised small protein modifier is ubiquitin.

Proteins that have regions of homology to ubiquitin can be divided into two groups: ubiquitin domain proteins (UDP) and small ubiquitin-like modifiers (Ubl) [1]. UDPs contain a ubiquitin-like domain, but are often much larger than ubiquitin and do not covalently modify other proteins. UDPs include parkin, DSK2, ubiquilin, Rad23, and Fau and the ubiquitin-like domain is involved in mediating protein-protein interactions and interaction with the proteasome.

Since the discovery of ubiquitin as a covalent modifier other proteins have been identified that are also small covalent modifiers [2]. Some Ubls

such as NEDD8, FAT-10, and ISG15/UCRP are highly homologous to ubiquitin while others like SUMO, URM1, APG8, and APG12 are only distantly related to ubiquitin. A hallmark of Ubls is the existence of a highly conserved di-glycine motif at or near the C-terminus of the protein. Exceptions to this rule include both APG8 and APG12 which have a single glycine and Hub1 which has a di-tyrosine motif. The only certain method of determining that a protein is a Ubl rather than a UDP is experimental evidence of covalent modification. Small ubiquitin-like proteins will be discussed in detail below.

1.2 UBIQUITIN

Ubiquitin is a small 76 amino acid protein modifier that was discovered to regulate the degradation of many cellular proteins through the formation of ubiquitin chains attached to a lysine in the target protein [3, 4]. Modification of a protein with four or more ubiquitins linked through their lysine 48 residues classically targets proteins to the 26S proteasome complex for ATP dependent degradation of the target protein and recycling of ubiquitin. Processing of ubiquitin conjugated protein by the proteasome releases short peptides, short peptides conjugated to ubiquitin, and polyubiquitin chains. De-ubiquitinating isopeptidases and C-terminal hydrolases are able to

release ubiquitin from ubiquitin conjugates and polyubiquitin chains and are important for the generation of free ubiquitin [3]. Isopeptidases may also deconjugate specific ubiquitin conjugates to prevent their degradation. Many proteins are phosphorylated prior to ubiquitination which is one mechanism by which proteins are marked for degradation [4]. Examples of proteins regulated in this manner include β-catenin and IκBα [5]. Other types of ubiquitination such as mono-ubiquitination and ubiquitin chains formed through lysine 63 of ubiquitin do not target proteins for degradation, but may be involved in control of signal transduction pathways, subcellular targeting, or alteration of protein function. Ubiquitination of some plasma membrane proteins targets them for endocytosis and lysosome mediated degradation [6, 7]. The first identified ubiquitinated protein was histone2A which is a relatively stable protein [8]. p53 is a well-known tumour suppressor that is dysfunctional in many tumours and is known to be regulated by ubiquitination [9]. Classically, in normal physiological conditions p53 is constantly turned over due to ubiquitination and subsequent degradation mediated by the ubiquitin ligase, mdm2. Pro-apoptotic signals block the ubiquitination of p53 thus promoting its stability and activation. Activation of p53 results in a halt in cell cycle progression and/or induction of apoptosis. Ubiquitination of p53 can be regulated both by alteration in ligation and by de-ubiquitination. Abnormalities in ubiquitin conjugation and deconjugation have been implicated in disease processes [10, 11].

1.1.1 Mechanism of ubiquitin conjugation

Ubiquitin conjugation requires the sequential activity of three enzymes, an activating enzyme (E1), a conjugating enzyme (E2), and a ubiquitin ligase (E3), which conjugate the C-terminal glycine of ubiquitin to a lysine in the target protein [4]. The E1 enzyme utilises ATP to catalyse the adenylation of the C-terminal glycine residue (Gly 76) of ubiquitin and releases PPi. Activated ubiquitin is then attached to a cysteine residue of the E1 in a thiolester linkage. Then activated ubiquitin is transferred to a cysteine residue of an E2 via a trans-esterification reaction. Finally ubiquitin is covalently attached to a cysteine in the target protein. Ubiquitin E3 ligases facilitate the addition of ubiquitin to the ε-amino group of a lysine in the target protein. While only one E1, UBA1, has been discovered in humans, there are at least 25 E2-like proteins and an even greater number of E3s. Although there is very little evidence for direct interaction between E2 and substrate, it is apparent that many E2s have specific substrates whilst others are more general. Only 11 of the 25 E2s have been demonstrated to function as ubiquitin conjugation enzymes. E3s encompass a wide range of proteins and there is little sequence homology between subgroups of E3s. The mechanisms by which E3s promote ligation are quite different, some bind directly to substrate whilst others have an indirect interaction through an

adapter molecule [4]. The main three families of E3 ligases are; N-end rule E3 ligases, HECT domain E3s, and RING E3s. The first discovered family of ubiquitin ligases was the N-end rule E3 ligases which bind substrates that have basic or hydrophobic N-terminal amino acids. The HECT domain containing family of E3 ligases forms a thiolester intermediate with ubiquitin, whilst the RING finger E3 ligases mediate ubiquitin transfer directly from E2 to substrate. The RING finger ligase family includes a number of modular E3 ligase complexes; including SCF (Skp1 cullin F box) and APC (anaphase promoting complex) complexes. Substrate specificity is likely to arise from the specific conjugation of ubiquitin due to the various combinations of E2s and E3s and from the activities of de-ubiquitinating enzymes [4].

1.1.2 Ubiquitin ligases

1.1.2.1 SCF and APC: Cell cycle regulators

Progression through the cell cycle is controlled by cyclin dependent kinases (CDK). CDKs are regulated by cyclins, positive regulatory subunits, and cyclin dependent kinase inhibitors (CKI), negative regulatory subunits. Phosphorylation dependent ubiquitin mediated degradation results in sequential progress through the stages of the cell cycle. The APC and SCF

Ub E3s are responsible for the degradation of specific cyclins or CKIs at key points in the cell cycle [12, 13].

SCF complexes are modular E3s composed of at least a Ub E2, a cullin, skp1, Rbx a RING domain protein, and an F-box containing protein (Fig. 1) . The F-box protein and skp1 mediate substrate specificity through protein-protein interaction domains and skp1 also links F-box proteins to the core subunits of the SCF complex. A large number of F-box containing proteins have been identified and provide an elegant means of generating substrate specificity. In addition the activity of SCF complexes is regulated through the neddylation of the cullin subunit and through the association of hrt1/rbx1/roc1, a ring finger containing protein [12-14]. An essential function of SCF^{cdc4} is to promote the G1⇒S transition of the cell cycle through degradation of sic1, a CKI which inhibits S phase promoting CDK complexes. Accumulation of G1-CDKs at the end of G1 results in the phosphorylation of sic1, thus marking it for ubiquitination by SCFs and removing a block of S phase entry [4]. In addition SCFs also destroy positive regulatory G1 cyclins, cln1 and cln2, by utilising a different F-box protein, Grr1 [14].

The anaphase promoting complex (APC) is an E3 composed of at least 10 subunits in mammals and is responsible for chromosome

segregation and exit from mitosis (Fig. 1) [4, 13]. Substrates of APC contain a destruction box and include mitotic cyclins and anaphase inhibitors. One key target for destruction by the APC is an inhibitor of sister chromatid segregation, Pds1 [15]. Pds1 binds and inhibits the cysteine protease Esp1. Degradation of Pds1 by the APC releases Esp1 which is then able to cleave proteins responsible for maintaining sister chromatid cohesion, thus allowing sister chromatid separation. In eukaryotic cells at the spindle assembly checkpoint all chromatids must be aligned appropriately at the metaphase plate for anaphase to occur. Misaligned or lagging chromosomes induce a checkpoint arrest. One part of this checkpoint is inhibition of APC by Mad2 which inhibits degradation of Pds1 and B cyclins [15].

1.1.2.2 Hypoxia sensing ubiquitin E3s

von Hippel-Lindau syndrome is usually a hereditary disease in which individuals are predisposed to a wide range of highly vascularised tumours as a consequence of a mutation in the tumour suppresser VHL [16]. Current research has revealed that the VHL protein is part of a hypoxia sensing ubiquitin ligase complex analogous to the SCF. The VHL complex comprises VHL, elongin C, elongin B, cullin2, Rbx, and an E2 (Fig.1). In normal oxygen conditions (normoxia) the VHL complex rapidly degrades factors required for induction of angiogenesis, the hypoxia inducible factors

HIF-1α, HIF-2α, and HIF-3α. HIF prolyl-hydroxylases (PHD) 1, 2, and 3 utilise oxygen to hydroxylate a proline residue in HIF-1 subunits. PHD2 is responsible for the hydroxylation of HIF1-α in normoxia [17]. Hydroxylated HIF is ubiquitinated by VHL-E3 and degraded in a proteasome dependent manner. In this manner PHD2 functions as an oxygen sensor which transmits changes in oxygen levels through HIF-1α. Under low oxygen conditions HIFs are stabilised and regulate the expression of genes required for angiogenesis. Mutation of VHL in VHL syndrome or in sporadic tumours, may inactivate the VHL E3 ligase complex, thus stabilising HIF. Highly vascularised tumours could occur due to constitutive activation of hypoxia inducible genes.

1.1.3 De-ubiquitinating enzymes

Sequencing of the human genome has identified more than 90 putative de-ubiquitinating enzymes, thus allowing significant determination of substrate specificity through de-ubiquitination [3, 18]. There are two types of de-ubiquitinating enzymes, ubiquitin C-terminal hydrolases (UCH) and Ub specific proteases (UBP). Ubiquitin is synthesised as poly-ubiquitin chains or Ub-ribosomal fusions and must be processed prior to conjugation. The C-terminus of cellular Ub can form various types of linkages: to the alpha-amino group of the ubiquitin precursor, to the epsilon lysine in protein or

small peptide conjugates, or ester and thiol linkages, all of which must be removed to generate free ubiquitin.

UCHs contain a conserved catalytic region and prefer small leaving groups so typically hydrolyse C-terminal esters or amides of ubiquitin. UCHs exhibit tissue specific expression; UCH-L1 is expressed in neuronal cells, UCH-L3 is expressed in heamatopoeitic, lung and brain cells [18].

UBPs are much larger than UCHs and are able to deconjugate ubiquitin chains as well as remove ubiquitin from substrates. Efforts to characterise UBP function through deletion studies have been complicated as loss of free ubiquitin chains may inhibit the proteasome and result in generic phenotypes which mask phenotypes associated with the mis-regulated degradation of essential cellular proteins. In fact this may reflect the essential role UBPs have in the breakdown of free ubiquitin chains. IsoT (Ubp14p in yeast) is known to remove remnant peptides generated by the action of the proteasome, from the C-terminus of ubiquitin. IsoT then releases one ubiquitin at a time from the free ubiquitin chain [19]. In spite of difficulties in determining the substrate specificities of individual UBPs, roles for UBPs have been discovered in memory and neurodegeneration, development, chromatin condensation, and oncogenesis.

In some cases of familial Parkinson's disease (PD), mutations which cause a partial loss of catalytic activity are found in UCH-L1 [11]. It is likely that accumulation of a specific substrate or set of substrates may be a causal factor in the neurodegeneration observed in these families. A neuronal UCH has also been discovered to be important for long term facilitation in *Aplysia*. The expression of *Aplysia* UCH (Ap-UCH) is induced by the neurotransmitter 5-hydroxytryptamine (5-HT). The role of Ap-UCH is to degrade an inhibitor of protein kinase A. Prolonged activation of PKA is necessary for long-term facilitation to occur [18].

The fat facets (FAF) gene encodes for a UBP which is an essential regulator of cell fate determination in *Drosophila melanogaster* [20]. A FAF null mutant has abnormal ovarian and eye development. Examination of eye morphology in FAF null mutants revealed more than the normal eight photoreceptors in each eye unit, indicating a loss of regulated apoptosis during development.

The de-ubiquitination of histones has been shown to be important in chromatin condensation and control of gene expression. A newly characterised UBP, UBP-M, has been implicated in the control of chromosome condensation at mitosis. Ubp-M can de-ubiquitinate histone2A *in vitro* and is phosphorylated at the onset of mitosis, suggesting that Ubp-M

may regulate proteins involved in chromatin condensation and gene expression in a cell cycle dependent manner [3].

Uncontrolled activation of proteins involved in signal transduction is associated with oncogenesis. Signal transduction is regulated at many levels by ubiquitin mediated degradation and it is likely that loss or mutation of UBPs would result in the mis-regulated turnover of signalling proteins. Different types of ubiquitin chains linked through lysine 6, 11, 29, or 63 have been shown to be involved not in proteosomal degradation, but in activation of signal transduction. The expression of UBPs, DUB1 and DUB2 are induced by cytokines and may de-ubiquitinate the receptors induced by them to inhibit signalling [21]. Loss of UBPs may cause oncogenesis through prolonged signal activation. CYLD is a tumour suppresser which encodes a UBP. Loss or mutation of both copies of CYLD results in cylindromatosis or turban tumour syndrome. CYLD was found to be a negative regulator of NF-$\varkappa$B induction, and inhibition of CYLD through small interfering RNA or overexpression of mutant CYLD results in enhanced tumour necrosis factor (TNF) induced NF-$\varkappa$B signalling [10, 22, 23]. TNF interaction with its receptor results in formation of lysine 63 linked poly-ubiquitin chain formation of TNF receptor associated factors (TRAFs). It is likely that the function of CYLD is to remove lysine 63 linked chains from TRAFs to terminate signalling. Loss of CYLD and enhanced NF-$\varkappa$B induction cause the

inappropriate expression of NF-κB responsive genes. NF-κB responsive genes are involved in inhibition of apoptosis, therefore, excessive NF-κB activation could allow the accumulation of mutations and inhibition of apoptosis resulting in the oncogenic transformation of cells. However, anti-inflammatory drugs which prevent the activation of NF-κB responsive genes block the inhibition of apoptosis seen in cells depleted of CYLD and may provide a treatment for cylindromatosis [10].

1.2 SUMO (SMALL UBIQUITIN-LIKE MODIFIER)

SUMO is the best characterised ubiquitin-like modifier, and may modify a broad range of cellular proteins [24, 25]. The effects of SUMO modification are diverse and are specific to the protein which is modified. SUMO was first discovered in *Saccharomyces cerevisiae*, but has since been found in most higher eukaryotes. The number of SUMO genes varies quite remarkably from only one SUMO in *S. cerevisiae* and *C. elegans* , 8 in *A. thaliana*, and at least three SUMO genes and many pseudogenes in humans.

In addition to SUMO-1, there are two other SUMO isoforms in humans, SUMO-2 and SUMO-3. SUMO-2 and SUMO-3 are 95% identical to

each other and approximately 47% identical to SUMO-1 [26]. Interestingly SUMO-2 and SUMO-3 contain SUMO consensus sites at their N-termini and as a consequence can form SUMO chains *in vitro* and *in vivo* [27, 28]. Conjugation of SUMO-2 and SUMO-3 to high molecular weight proteins is dramatically increased after heat shock, oxidative stress or ethanol treatment [27]. The functional significance of SUMO chains is currently unknown it is likely that SUMO chains are involved in the stress response.

Overexpression studies have shown that most SUMO substrates may accept any SUMO member, but it is likely that substrates may be preferentially conjugated to either SUMO-1, -2, or -3 under physiological conditions. Preferential modification of a substrate by SUMO-1 or SUMO-2/-3 may have distinct consequences *in vivo*. Monitoring of SUMO conjugation at endogenous levels has revealed that ranGAP1 is preferentially conjugated to SUMO-1 [27], while LEF1 [29] and topoisomerase II [30] are conjugated to SUMO-2, -3.

Unlike the majority of ubiquitinated proteins, acceptors of SUMO modifications are not targeted for degradation. In the case of the transcriptional inhibitor IκBα the target lysine for SUMO-1 modification is the same as that of ubiquitin conjugation, thus blocking ubiquitination at that residue and stabilising the protein [31]. A growing number of transcription

factors have been shown to be SUMO modified. In most cases modification leads to transcriptional repression. SUMO modification may also alter a proteins subcellular localisation. The interaction of Ran GTPase activating protein 1 (RanGAP1) with the Ran-GTP-binding protein 2 (RanBP2) at the cytoplasmic face of the nuclear pore complex is dependent on SUMO-1 conjugation of RanGAP1 at Lys526 [32, 33]. Modification of the promyelocytic leukaemia protein (PML) targets it to distinct nuclear bodies [34-36] and is required for Daxx recruitment to these structures [37, 38].

1.2.1 Mechanism of SUMO conjugation

The SUMO conjugation cascade is analogous to, but distinct from, ubiquitin conjugation (Fig. 2). Although SUMO is only 18% identical to ubiquitin, the structure of SUMO determined by NMR spectroscopy closely resembles that of ubiquitin [39]. SUMO surface residues are very different from ubiquitin, enabling different protein interactions. SUMO is synthesised as a precursor which must be processed by SUMO specific proteases prior to conjugation (Fig. 3). In addition SUMO proteases are responsible for the deconjugation or removal of SUMO from its target substrates. While ubiquitin will often modify any of a number of lysines on a target protein, SUMO modification usually requires a consensus motif (ψKxE) where ψ is a large hydrophobic amino acid and x is any amino acid [40]. Unlike ubiquitin

the SUMO E1 and E2 enzymes are sufficient for conjugation *in vitro* [31]. The SUMO E1 is a heterodimer composed of SAE1/SAE2 in humans or Aos1p /Uba2p in yeast that are homologous to the N-terminal and C-terminal portions of ubiquitin E1 respectively [41-44]. Unlike ubiquitin only one SUMO E2 has been characterised, Ubc9 [45, 46]. In fact Ubc9 was initially believed to be a Ub conjugating enzyme due to primary sequence similarity to known ubiquitin E2s [47].

SUMO E1 catalyses the adenylation of the C-terminal glycine of SUMO (Fig. 2). Activated SUMO is then conjugated via a thiolester linkage to a cysteine of the E1. A transesterification reaction then takes place between SUMO attached to cysteine of the E1 to a cysteine of the E2 Ubc9. The final step is covalent attachment of SUMO via its C-terminal glycine to a lysine through an amide linkage in the target substrate.

1.2.2 SUMO E3 ligases

Aos1, uba2, ubc9, and a conserved SUMO motif are sufficient for SUMO conjugation *in vitro* [40]. This has lead to the idea that unlike Ub conjugation, SUMO conjugation did not require E3 ligases. In 2001 the first SUMO ligases siz1 and siz2 were discovered in *S. cerevisiae* [48]. Siz1 was required for the conjugation of SUMO to septins *in vivo* and enhances septin

conjugation *in vitro*. Deletion of both siz1 and siz2 prevents the conjugation of most, but not all cellular SUMO substrates. Intriguingly siz1 and siz2 double deletion mutants are viable indicating that the basal level of SUMO conjugation is sufficient for viability. This suggests either that other SUMO ligases exist in *S. cerevisiae* or that some substrates do not require an E3. The most closely related human proteins to siz1 and siz2 are the Protein Inhibitors of Activated STAT (PIAS) family. There are five members of the PIAS family of proteins and each has a conserved DNA binding domain and a Ub-E3-like ring domain. Investigation of PIAS 1, 3, x, ß, γ revealed that all are capable of SUMO E3 ligase activity *in vitro* and *in vivo* and that this activity is mediated by the ring domain *in vivo* [49]. The SUMO modification of p53, LEF1, and Sp3 have been demonstrated to be enhanced by PIAS proteins [49-51]. Recently a SUMO E3 ligase, Pli1p has been discovered in fission yeast. Pli1p is homologous to PIAS proteins and contains a RING domain which is required for SUMO ligase activity. Pli1p enhances the SUMOylation of Rad22p, a known *S. pombe* SUMO substrate, *in vitro*. Deletion of Pli1p causes a reduction in global SUMOylation and an increase in free SUMO. Pli1p null cells are sensitive to thiabendazole, a microtubule de-stabilising agent, show increased minichromosome loss, and have increased telomere length. It is speculated that the phenotype of Pli1p null yeast reflects a role for Pli1p in centromere and telomere maintenance [52]. PIAS proteins have been implicated in a wide range of cellular processes

and it will be important to re-examine the role of PIAS proteins with respect to their functions as E3 ligases.

Two other proteins have been discovered to act as E3 ligases in higher eukaryotes, RanBP2/Nup358 and polycomb group 2 (Pc2). RanBP2/Nup358 is a component of the ranGTPase cycle at the nuclear pore complex (NPC). It is a large protein with distinct domains, none of which bear any resemblance to known E3s. A 33 kDa region between IR1 and IR2 has been shown to interact with ubc9 and enhance SUMO transfer from ubc9 to sp100 [53]. The presence of Ubc9 also at the NPC suggests that SUMO modification of some substrates may be linked to nuclear import [54].

Pc2 is a chromatin associated protein which forms complexes involved in transcriptional repression [55]. It has been shown that Pc2 enhances sumoylation of the transcriptional co-repressors CtBP1 and CtBP2 and recruits them to repression domains [56]. Pc2 is not homologous to any known E3s.

Overexpression studies have shown that most SUMO E3s will enhance the modification of most SUMO substrates *in vivo*, perhaps reflecting their participation in larger E3 complexes. SUMO modification may mediate transcriptional repression through the recruitment of repressive factors or

alternatively may sequester transcription factors in nuclear domains [49]. SUMO ligases are the most recently discovered components of SUMO conjugation machinery and much remains to be elucidated about their modes of action and substrate specificity.

1.2.3 SUMO proteases

1.2.3.1 Yeast SUMO proteases

S. cerevisiae Ubiquitin-like specific protease (ScUlp1)

The first SUMO specific protease, ScUlp1, was isolated in a screen for *S. cerevisiae* proteins able to cleave an artificial SUMO substrate *in vitro.* A second *S. cerevisiae* SUMO specific protease, ScUlp2, was identified through sequence similarity to ScUlp1. ScUlp1 and ScUlp2 share a conserved C-terminal catalytic domain, but are not conserved in the N-terminal region. ScUlp1 is required for cell viability and deletion of Ulp1 results in cells arrested at the G2/M stage of cell cycle [57]. Similarly deletion of Ubc9 also causes the arrest of cells at the G2M stage of the cell cycle [47]. ScUlp1 is mainly responsible for precursor processing [57]. To determine whether SUMO processing or deconjugation activity of ScUlp1

was required for viability, ScUlp1 deletion mutants were complemented with mature SUMO. Exogenous expression of mature SUMO partially restored growth, suggesting that the SUMO processing activity of ScUlp1 is a proportion of the requirement for viability [57]. Overexpression of ScUlp2 was unable to compensate for the lethality of ScUlp1 deletion demonstrating non-redundant functions of the SUMO proteases in yeast [57]. ScUlp2 is only required for viability at high temperatures. Deletion of ScUlp2 results in pleiotropic phenotypes including enhanced chromosome loss rates, sensitivity to DNA damaging drugs, and impaired recovery from induced cell cycle arrest [58]. Prior to characterisation as a SUMO protease the ScUlp2 gene was discovered to be a high copy suppressor of defects in chromatid cohesion [59]. Deletion of ScUlp2 results in defects in centromeric cohesion which are linked to mis-regulated SUMO modification of topoisomerase II [60]. Deletion of both ScUlp1 and ScUlp2 compensates for loss of viability and defects seen in single deletions, which can only partially be attributed to a defect in precursor processing [58].

ScUlp1 is targeted to the NPC via karyopherins whilst ScUlp2 is present within the nucleoplasm [61]. Deletion experiments have shown that the protease domain is necessary, and sufficient, for the essential function of ScUlp1 in cell cycle progression. In addition the N-terminal domain is required for a proportion of substrate targeting with regions positively

regulating ScUlp1 substrate specificity and regions which negatively regulate specificity for ScUlp2 substrates [62]. Removal of the N-terminal domain of ScUlp1 allows for compensation of Ulp2 deletion defects at low levels of expression of ScUlp1.

In 2000 Mossessova and Lima solved the crystal structure of ScUlp1-SUMO by using sodium borohydride to trap an analogue for the tetrahedral catalytic intermediate resulting in a covalent thiohemiacetyl bond between the ScUlp1 active site cysteine and the C-terminal glycine of SUMO. The interaction between ScUlp1 and SUMO is an extensive hydrophilic interface composed of polar and charged residues and nearly half a dozen mixed salt bridges. In contrast the interaction between UCH Yuh1 and ubiquitin is mostly hydrophobic with some polar interactions and only one salt bridge [63]. Selectivity for the di-glycine motif of SUMO is the consequence of a constricted hydrophobic tunnel near the active site composed of Cys-580, Ser-513, His-514, Try-448, and Try-515 [64]. However the catalytic site lies within a shallow narrow cleft that would allow large SUMO modified proteins to come into close proximity of the catalytic site for deconjugation. The general base His-514 co-ordinates the active site cysteine Cys-580 which is stabilised by Asp-531. Cys-580 and Gln-574 create the oxyanion hole [64].

S. pombe Ulp1 (SpUlp1)

In *Schizosaccharomyces pombe* a Ulp1-like protease SpUlp1 has been characterised. Unlike *S. cerevisiae*, neither SpUlp1 nor SpSUMO is essential for cell viability [65, 66]. Although SpUlp1 is not essential, deletion causes slow growth, sensitivity to UV radiation and reduced levels of SpSUMO conjugates. In addition SpUlp1 deletion causes irregular cell shape, nuclear displacement, and multiple septation. Overexpression of mature SUMO-GG does not rescue the slow growth or sensitivity to UV radiation phenotypes but does restore levels of SpSUMO conjugates to levels seen in wt cells [66]. These data suggest that while SpUlp1 is responsible for a proportion of precursor processing, the slow growth and UV sensitivity phenotypes are the result of loss of SpUlp1 deconjugation activity. Like ScUlp1, SpUlp1 is localised to the nuclear periphery, however SpUlp1 shows a diffuse nuclear localisation during mitosis [66].

1.2.3.2 Mammalian SUMO proteases

Classification of SUMO proteases using Barrett's system [67], groups SUMO proteases within the C48 family of cysteine proteases which is most closely grouped to the adenovirus protease family C5. Shortly after the discovery of Ulp1 as a cysteine protease two mammalian SUMO proteases

were cloned and characterised. Murine SMT3IP1 was shown to be a nucleolar SUMO protease [68] whilst human SENP1 was a nuclear SUMO protease [69]. Subsequently the human SUMO proteases were further characterised and these later discoveries will be discussed in the relevant chapters.

Increased SUMO modification has been detected after exposure of cells to different stresses. Levels of SUMO-1 modified p53 increase after exposure of cells to UV light [70], while treatment of cells with camptothecin results in increased modification of topoisomerase I by SUMO-1 [71]. Increased SUMO modification observed under these conditions could result from accelerated conjugation of SUMO to substrates or from selective inhibition of SUMO deconjugation.

In August 2004 the crystal structure of the SENP2 catalytic domain (residues 364-589) was resolved alone (2.2 Å) and in complex with SUMO-1 (2.8 Å). Similarly to the Ulp1-ScSUMO complex, sodium borohydride was used to trap a reduced deacylation intermediate of the proteolytic reaction. The distance between the sulphur atom of the active site cysteine and the carbonyl of glycine-97 in SUMO-1 is consistent with a covalent bond between the two [72]. The crystal structure of SENP2 alone and in complex with SUMO revealed no major conformational changes in SENP2 structure

although there was a slight opening of the catalytic site to accommodate SUMO. The interactions between SENP2 and SUMO were mainly comprised of a conserved salt bridge (SENP2 Asp-413-SUMO Arg-63) and a hydrophobic interaction between SENP2 (Phe-441) and a hydrophobic pocket of residues Leu-65, Arg-63, Tyr-91 from SUMO-1. Similarly to ScUlp1-ScSUMO, two tryptophans form a constricted hydrophobic tunnel near the active site thus creating an absolute requirement for two glycine residues N-terminal to the cleavage site of SUMO-1. Analysis of the enzymatic activity of SENP2 processing of the SUMO-1, -2, -3 precursors revealed a greater efficiency in SUMO-2 precursor cleavage as compared to SUMO-1 or SUMO-3 [72]. These differences in processing efficiency could largely be abrogated by inter-changing the C-terminal tails between SUMO precursors or adding a second di-glycine C-terminal to the natural di-glycine of SUMO. These data suggest that the C-terminal extensions of SUMO precursors may provide a method of regulating processing *in vivo*. However both the structure resolution and enzymatic analysis were determined only for the catalytic domain of SENP2. The N-terminal region is likely to possess important elements for determining substrate specificity. Although this may occur primarily through sub-cellular localisation, it is also possible that there are regions important in substrate interactions which have not been included in this research.

1.2.3.3 Other SUMO specific proteases

SUMO specific proteases have also been identified and characterised in *Xenopus laevis* and *D. melanogaster*. In *X. laevis* two isoforms of SUMO proteases exist; XSENP1a and XSENP1b. The catalytic domains of these proteases are most similar to hSENP1 although the N-terminal regions are not highly homologous to hSENP1. Overexpression of XSENP1 inhibited normal head formation in *X. laevis* [73]. In *D. melanogaster* two SUMO proteases have been identified; DmUlp1 and DmUlp2, which are orthologues of ScUlp1 and ScUlp2 respectively. DmUlp1-GFP is localised to the nucleoplasmic face to the NPC. Depletion of DmUlp1 changes the spectrum of SUMO conjugates in cells and may regulate the nuclear/cytoplamic partitioning of SUMO [74].

1.2.4 Biological roles of SUMO modification

1.2.4.1 RanGAP1-SUMO modification alters protein localisation

RanGAP1, a protein involved in nuclear transport, was one of the first proteins shown to be modified by SUMO at Lys526 [32, 33]. RanGAP1 is present in the cytoplasm and at the cytoplasmic side of nuclear pore complexes (NPC) in cells. SUMO modification is required for targeting of

RanGAP1 to the NPC and mutation of the SUMO modified lysine blocks NPC localisation [75, 76]. In addition SUMO has been shown to be required for targeting ranGAP1 to kinetochores during mitosis [77].

1.2.4.2 SUMO modification opposes ubiquitination

The transcription factor NF-$\varkappa$B is held inactive in the cytoplasm through interaction with the inhibitory $\varkappa$B (I$\varkappa$B) protein. Activation of NF-$\varkappa$B requires the phosphorylation dependent ubiquitination and degradation of I$\varkappa$B [78]. Free NF-$\varkappa$B then translocates to the nucleus and activates expression of responsive genes involved in the inflammation response. Newly synthesised I$\varkappa$B translocates to the nucleus and associates with NF-$\varkappa$B. The NF-$\varkappa$B-I$\varkappa$B complexes are then exported to the cytoplasm [79]. In 1998 Desterro and colleagues showed that I$\varkappa$Bα is SUMO modified on the same lysine which is utilised for ubiquitination. Furthermore SUMO modified I$\varkappa$Bα is resistant to ubiquitination and degradation, creating a protected pool of NF-$\varkappa$B which cannot be activated. The proportion of SUMO modified I$\varkappa$B varies in different cell lines and may provide a general mechanism for regulating the total amount of inducible NF-$\varkappa$B [31].

SUMO modification of Huntingtin (Htt), the protein which accumulates in and is responsible for neurodegeneration seen in Huntington's disease (HD),

also occurs on the same lysine residues utilised for ubiquitination [80]. As for IκBα, SUMO modification blocks ubiquitination and stabilises Htt. Stabilisation of Htt exacerbates neurodegeneration in *a D. melanogaster* model of HD.

Proliferating cell nuclear antigen (PCNA), a protein involved in DNA replication and repair, is also ubiquitinated and SUMO modified on the same lysine (Lys-164). However modification of Lys-164 is not linked to protein turnover, but to regulation of PCNA function. SUMO modification inhibits PCNA repair function while ubiquitin is important in Rad6 dependent DNA repair. Lysine 63 linked ubiquitin chains are required for error free DNA repair. Mono-ubiquitination may be involved in error prone DNA repair [81]. SUMO and ubiquitin modification of PCNA is antagonistic and mutually exclusive, and provides an example of a protein which is exquisitely regulated through post-translational modification.

NEMO (NF-κB essential modifier), the regulatory subunit of the IKK complex is also SUMOylated and ubiquitinated on the same residues [82]. DNA damage induces SUMOylation of NEMO on lysines 277 and 309. Mutation of lysines 277 and 309 abrogates SUMO modification and blocks NF-κB activation. SUMO modified NEMO translocates to the nucleus and is subsequently ubiquitinated. Ubiquitination of NEMO is involved in IKK

activation which activates NF-κB. In this case, co-ordinated sequential modification by SUMO then ubiquitin is required to signal DNA damage and activate NF-κB.

1.2.4.3 SUMO modification mediates transcriptional repression

Of the known SUMO modified substrates a high proportion have roles in transcriptional regulation [50, 83, 84]. SUMO modification causes transcriptional activation of p53 [70, 85] but is mostly involved in mediating transcriptional repression as observed for Sp3 [51, 86], ELK-1 [87], and p300 [88]. p300 and ELK-1 have domains which mediate repression that were subsequently discovered to possess consensus SUMO modification motifs. p300 is a transcriptional regulator that can activate and repress transcription in a context specific manner. Mutation of the lysines in the p300 repression domain relieves repression. Fusion of SUMO to the DNA binding domain of a GAL4 reporter construct causes repression in reporter assays, demonstrating the intrinsic repressive capacity of SUMO [86]. SUMO dependent recruitment of histone deacetylases (HDACs) to transcription factors and change in the histone code may provide a general mechanism by which SUMO mediates repression. Co-expression of SENP2 has been used to relieve repression of ELK-1, p300, and sp3 [86-88]. Phosphorylation of the ELK-1 transcription factor by a MAPkinase results in loss of SUMO

modification and loss of transcriptional repression [87]. Deconjugation of SUMO from transcription factors by SUMO proteases may provide a method of rapidly reversing SUMO mediated transcriptional repression.

1.3 NEDD8

NEDD8 (neuronal development down-regulated protein 8) was initially isolated in mice [89] and the human NEDD8 was subsequently shown to be a small ubiquitin-like modifier [90]. NEDD8 conjugation is further discussed in Chapter 4.

1.4 ISG15 (INTERFERON STIMULATED GENE)/UCRP (UBIQUITIN CROSS REACTIVE PROTEIN)

ISG15 (interferon stimulated gene)/UCRP (ubiquitin cross reactive protein) was identified over 20 years ago and was the first ubiquitin-like protein to be discovered. ISG15 contains two ubiquitin-like domains in tandem and is synthesised as a precursor that is processed prior to conjugation. Expression and conjugation of ISG15 are up-regulated in response to interferon, lipopolysaccharides, and viral infection. The E1 for

ISG15, UBE1L, was identified as a protein inhibited during influenza virus infection [91]. UbcH8, a ubiquitin E2 enzyme, has recently been shown to be an ISG15 conjugation enzyme [92]. UBP43/USP18 was originally proposed to be a ubiquitin specific protease, but was later shown to be specific for ISG15. At least one other ISG15 protease is likely to exist, as mice UBP43/USP18 knock-out cells are still able to process the ISG15 precursor [93]. An assay developed to trap Ubls and their specific conjugating/deconjugating enzymes has demonstrated an interaction between ISG15 and T/USP5 (isoT), a protease previously reported to be ubiquitin specific [94]. Therefore, isoT is a possible candidate for ISG15 precursor processing. Substrates for ISG15 conjugation include serpin2a, stat1, and ERK1. ISG15 is localised to intermediate filaments and is involved in regulation of signal transduction and the immune response [95].

1.5 URM1 (UBIQUITIN RELATED MODIFIER)

Similarities to the ubiquitin conjugation pathway exist in prokaryotes. In particular the molybdopterin and thiamine biosynthetic pathways utilise E1-like enzymes that bear mechanistic and sequence homology to Ub activating enzymes [96]. These E1-like enzymes, MoeB and ThiF, transfer a sulphur atom to the C-terminus of the short peptides MoaD and ThiS respectively.

Remarkably these polypeptides, MoaD and ThiS, terminate in a di-glycine motif. Furukawa and colleagues used the sequences of MoaD and ThiS to search the *S. cerevisiae* genome ORFs for homologous proteins. They identified URM1 (ubiquitin related modifier), which is approximately 20% identical to MoaD and ThiS, but is not homologous to ubiquitin. In humans a protein that is 42% identical to *S. cerevisiae* URM1 has also been identified. Interestingly URM1 has no amino acids following the C-terminal di-glycine, therefore negating the need for precursor processing proteases. URM1 forms a thiolester with Uba4, an E1 that is homologous ubiquitin E1 [97], but the existence of an E2, E3, or specific isopeptidase has yet to be demonstrated. The substrates, and therefore functions of URM1, are currently unknown.

1.6 APG12 AND APG8

Two ubiquitin-like conjugation systems Apg12 and Apg8 were discovered through investigation of autophagy defective mutants in *S. cerevisiae*. Autophagy is the process through which bulk components of the cytoplasm are degraded. Although unrelated in sequence to ubiquitin, Apg12 was demonstrated to be conjugated to Apg5 in a manner similar to ubiquitin conjugation [98]. The activating enzyme Apg7 is homologous to

ubiquitin E1s. Interestingly, the E2 for Apg12 was demonstrated to be Apg10, a protein that is not similar in sequence to any known E2s and may represent a new class of ubiquitin-like conjugating enzymes [98]. Apg12 is synthesised as a mature protein which has a single glycine at its C-terminus rather than the di-glycine found in most other small modifiers. It is likely that the main or only substrate for Apg12 modification is Apg5 and that this conjugation may be irreversible. The absence of an Apg12 precursor or evidence for deconjugation implies that a specific isopeptidase is not required for Apg12. All of the components of the Apg12 conjugation pathway are required for autophagy in yeast. Apg12, Apg5, Apg7, and Apg10 are conserved in humans and constitute a homologous Apg12 conjugation system [99]. In both mammalian and yeast cells Apg12 conjugation is required for autophagosome formation.

Apg8/AUT7 was discovered in the same investigation of autophagy defective mutants as Apg12, as well as in another autophage defect screen [100, 101]. Apg8/AUT7 like Apg12 has a single glycine at the C-terminus although Apg8 is synthesised as a precursor. The E1 enzyme Apg7 is dual specific for Apg8/AUT7 and Apg12 activation. The E2 enzyme for Apg8/Aut7 is Apg3/AUT1 which bears weak homology to Apg10 [101]. Apg8/AUT7 is the first small protein modifier that is known to be conjugated through its amino group to a phospholipid, phosphatidylethanolamine (PE),

which mediates its membrane association. Apg4/AUT2 was also identified in the autophagy defective mutants screen, and is distantly related to de-ubiquitinating proteases. Apg4/AUT2 is the Apg8/AUT7 specific protease and is able to process Apg8/AUT7 precursor as well as deconjugate Apg8/AUT7 from PE. The human homologue of Apg4/AUT2 has recently been shown to interact with four mammalian members of the Apg8-like family [102, 103]. Apg8 has three known homologues in humans, GATE-16 (golgi-associated ATPase enhancer 16 kDa), MAP1-LC3 (microtubule associated protein light chain 3), and GABARAP (gamma-aminobutyric acid receptor associated protein) all of which are associated with membrane processes. In addition a fourth member of the family Apg8L (Apg8-like) has recently been reported [102]. Interestingly, the crystal structure of GATE-16 revealed the conserved ubiquitin super-fold even though GATE-16 does not share sequence homology with ubiquitin [104]. Although GATE-16, MAP1-LC3, and GABARAP are conjugated by mammalian homologues of Apg7 [105] and Apg3/AUT1 [106], the substrates they are conjugated to and their roles are still unknown.

1.7 HUB1/UBL5/BEACON

Hub1 is a small ubiquitin-like protein that was identified in *S. cerevisiae* and is highly conserved in humans [107] [108]. Unique to Hub1 is a C-

terminal di-Tyrosine motif that is followed by a single amino acid. Dittmar and colleagues reported that expression of Hub1 minus the C-terminal amino acid resulted in a greater level of Hub1 conjugates than when the full-length protein was expressed [108]. This lead Dittmar et. al. to conclude that Hub1 was processed by an unidentified protease and then conjugated. Luders and colleagues have recently reported evidence to the contrary. Luders et. al. demonstrated that Hub1 still interacts with proteins when expressed with a large C-terminal tag, when grown in the presence of NEM which should inhibit conjugation enzymes, and when cells have been ATP depleted therefore suggesting that Hub1 is not conjugated, but instead forms tight non-covalent interactions in cells [109]. In addition, the Hub1 crystal structure shows that the di-Tyrosine lies on the last beta-sheet of the ubiquitin-like structure, in contrast to SUMO, NEDD8, and ubiquitin which all have their di-glycine at the end of a C-terminal extension [110]. The position of the di-tyrosine in the Hub1 crystal structure makes it a poor candidate for conjugation.

1.8 FAT-10/DIUBIQUITIN

FAT-10 was originally discovered in 1996 through sequencing of the MHC class I locus and was found to be conserved in mice and humans.

FAT-10 consists of two ubiquitin domains connected by a linker region and may have a role in cytokine induced apoptosis. Interestingly the C-terminal domain terminates in a di-glycine suggesting that FAT-10 may function as a ubiquitin-like modifier. Inducible expression of FAT-10 in a stable cell line revealed a FAT-10 monomer and a number of slower migrating FAT-10 reactive species [111]. The possibility that these slower migrating species are FAT-10 covalent conjugates is supported by the finding that the bands are resistant to boiling and ß-mercaptoethanol treatment although they could also be polymers. In addition mutation of the C-terminal di-glycine motif abolishes the formation of these complexes. Although it is likely that FAT-10 is a ubiquitin-like modifier it is unknown whether the modification is reversible and which enzymes are involved in its conjugation.

1.8 AIMS OF THE PROJECT

The aim of this research was to identify and characterise novel SUMO-like specific proteases. To demonstrate substrate specificity the catalytic domains of putative SUMO proteases are to be expressed and tested in *in vitro* processing and deconjugation assays. To confirm substrate specificity *in vivo*, cellular deconjugation assays are to be developed. Localisation and siRNA studies will be used to understand the function of SUMO-like proteases *in vivo*.

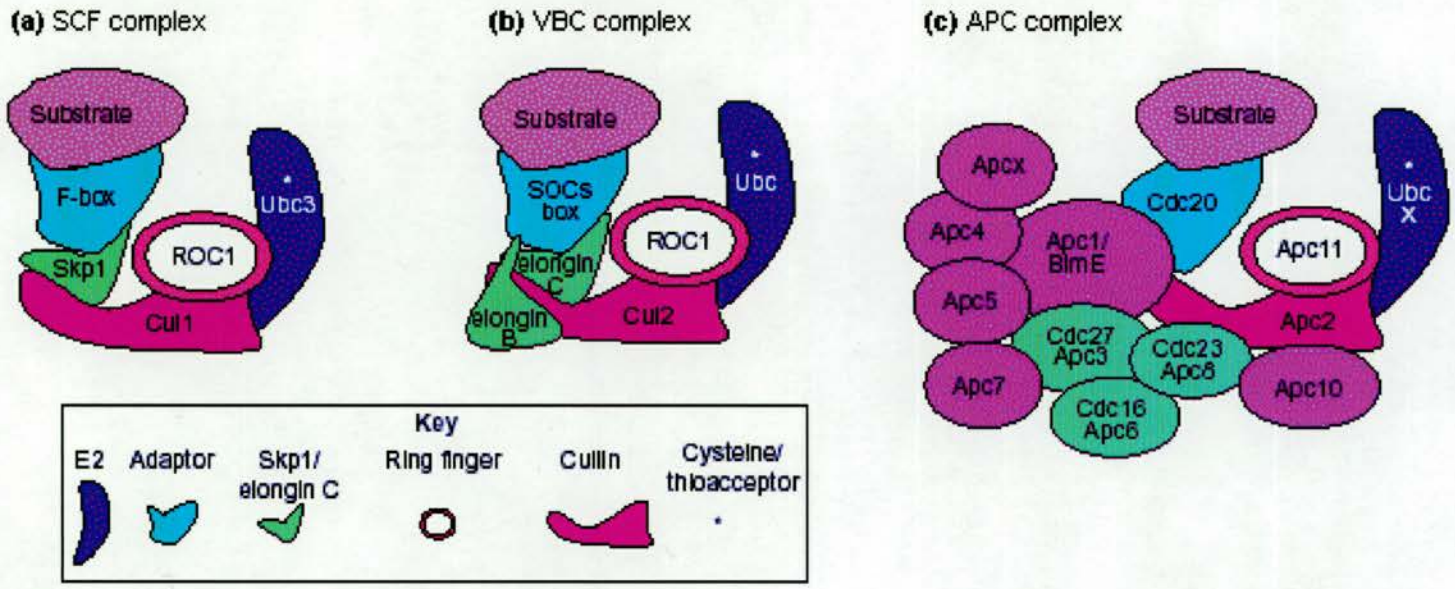

Figure 1: Comparison of SCF, VBC, and APC ubiquitin ligase complexes.

a. SCF (Skp1-Cullin-F-box) ligases. The F-box protein recruits the substrate and interacts with skp1. Skp1 bridges the F-box protein and substrate to the cullin, which binds a RING protein and the ubiquitin E2. b. VCB complex (VHL-Elongin B-Elongin C). The substrate (e.g. Hif-1alpha) interacts with the SOCS box containing protein (e.g. VHL). The SOCS box containing protein binds elongin B/C which interacts with the cullin. c. APC (anaphase promoting complex). Apc2 is a homologue of a Cullin protein. Apc11 is a RING finger protein.

Adapted from (9)

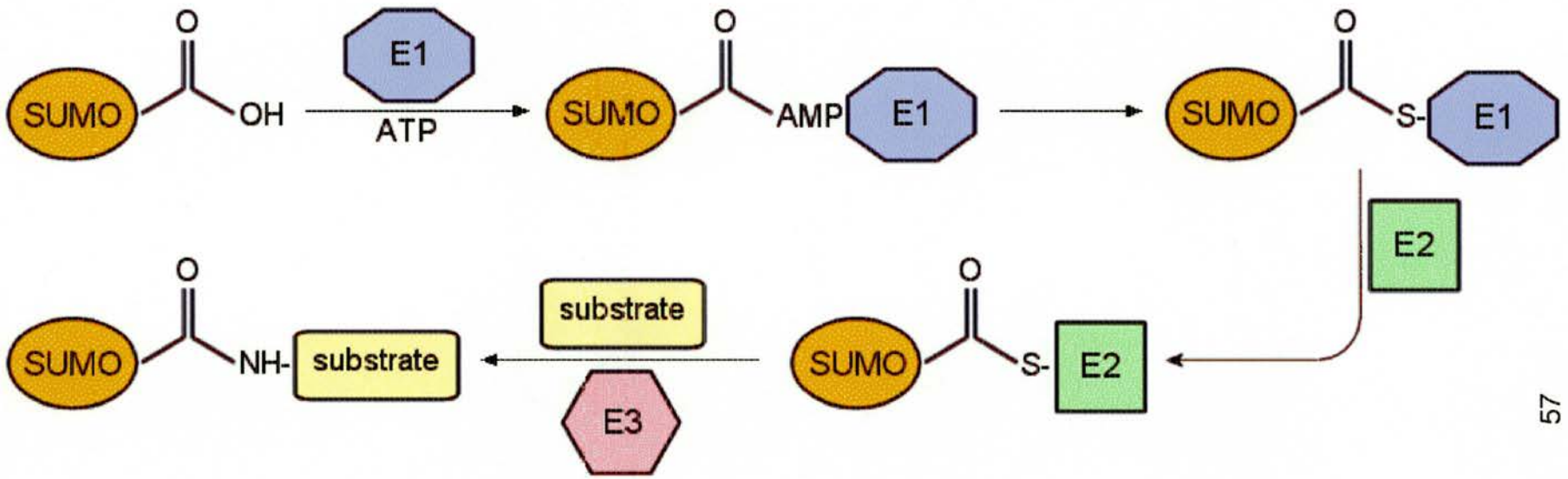

Figure 2: Mechanism of SUMO conjugation.

The SUMO activating enzyme (E1) is a heterodimer composed of SAE1/SAE2. Ubc9 is the only known SUMO conjugating enzyme (E2). Known SUMO E3s include PIAS proteins, RanBP2, and Pc2.

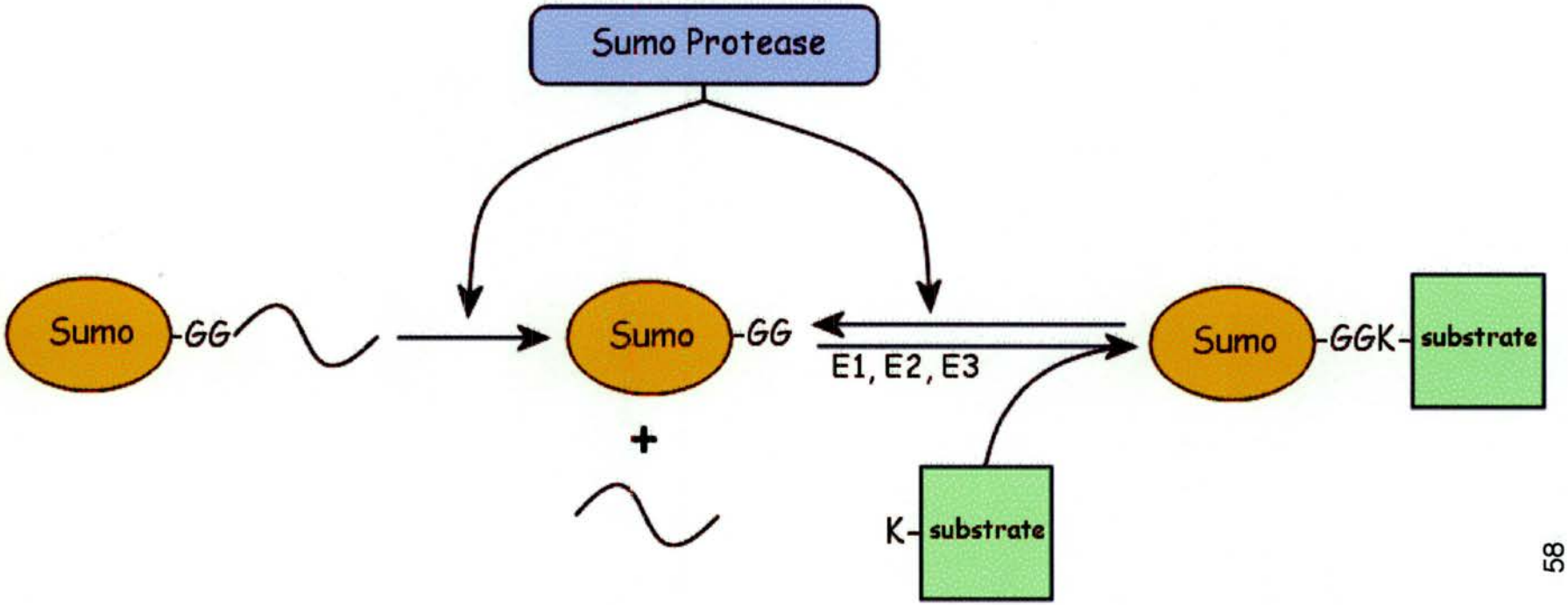

Figure 3: Role of SUMO proteases in SUMO processing and deconjugation.

2 MASTER MATERIALS AND METHODS

Reagents were acquired from Sigma unless otherwise specified.

2.1 ANTIBODIES

HA-SUMO-1, HA-SUMO-2, and HA-SUMO-3 were detected in Western blot experiments using mouse monoclonal antibody 12CA5, obtained from BabCO (at a 1:5000 dilution), which recognises YPTDVPDYA from influenza HA.

SENP2 was detected in experiments using rabbit Ab A1 directed against peptide CSGGKERDRRTD from the N-terminal domain of SENP2 and antigen affinity purified prior to use. For Western blotting the antibody was used at a 1:300 dilution. For fluorescence Ab A1 was used at 1:200. For analysis of specificity a trace amount of peptide was taken up in 100 μl of water. 15 μl of this solution was pre-incubated with antibody for 1 hour prior to use for Western blots. Pre-immune serum taken from the rabbit prior to immunization was used in control blots at 1:2000.

Sheep anti-mouse and anti-rabbit horseradish-peroxidase-conjugated IgG (Amersham Pharmacia Biotech) were used at 1:5000 dilution to detect primary antibody.

FITC conjugated donkey anti-mouse and Texas-Red conjugated donkey anti-rabbit antibodies were used at the 1:300 dilution (Jackson Immunoresearch).

NEDP1 was detected in Western blot experiments using sheep affinity purified NEDP1 directed against purified NEDP1 at 1:10000 dilution.

Phalloidin conjugated to Texas-Red, a gift from E. Flitney, was used in fluorescence at 1:20 dilution.

PML was detected in immunofluorescence experiments using mouse mAb 5E10 (1:10 dilution) obtained from R. van Driel [112].

GST-Ub-His-PK was detected in Western blot experiments using mouse monoclonal anti-sv5 PK 336 antibody (at a 1:1000 dilution), kindly provided by Prof. Randall [113].

GST-Nedd8-Myc-6His and His-NEDD8 were detected in Western blot experiments, at a 1:2000 dilution, using mouse monoclonal anti-His antibody obtained from Amersham Pharmacia Biotech.

Anti-Myc 9E10 monoclonal mouse antibody, provided by D. Girdwood was used at a 1:500 dilution in Western blot experiments to detect Cul-4A-Myc.

Tubulin was detected in immunofluorescence using mouse monoclonal anti-alpha tubulin N356 (Amersham Life Sciences) at 1:250 dilution.

Endogenous SUMO-1 was detected in immunofluorescence experiments using SUMO-1(FL1-101) sc-9060 rabbit polyclonal IgG (Santa Cruz Biotechnology) at a 1:50 dilution.

Endogenous SUMO-2/-3 were detected in immunofluorescence experiments using Sentrin-2(SUMO-3) rabbit polyclonal IgG (51-9100 Zymed) at 1:100 dilution.

Endogenous CSN7 was detected in Western blots using rabbit anti-CSN7 (Affiniti) at a 1:2000 dilution.

2.2 AFFINITY PURIFICATION OF NEDP1 ANTIBODY

Coupling of GST-NEDP1 to beads

15.4 mg of GST-NEDP1 was dialysed against 1.5 l coupling buffer (0.2 M $NaHCO_3$, 0.5 M NaCl pH 8.3) for 5 h with 3 changes of coupling buffer. 3 g of beads (N-hydroxysuccinimidyl activated agarose 4 % beaded agarose (Sigma H-8280)) slurry was resuspended in 50 ml of 1 mM HCl, then washed in 200 ml of coupling buffer. The bead slurry was resuspended in GST-NEDP1 solution. The solution was then mixed by rotation for 2 h at room temperature. The beads were then poured into a column and the protein solution was recycled three times through the column. Protein binding to beads was monitored by Bradfords assay. Buffer A (0.5 M NaCl, 0.5 M ethanolamine pH 8.3) and Buffer B (0.1 M NaAcetate, 0.5 M NaCl pH 4) were used for washing the beads. 30 ml volumes of Buffer A, Buffer B, and Buffer A were used to serially wash the beads. The beads were then left for 20 min prior to 30 ml washes with Buffer B, Buffer A, Buffer B. The beads were then stored in 0.5 M NaCl, PBS, 0.1 % azide at 4°. The column was washed in 100 ml of coupling buffer prior to use.

Affinity purification of NEDP1 antibody

15 ml of the third bleed from sheep was diluted with 150 ml PBS and passed through a 0.2 µm filter. The antibody was passed over the GST-NEDP1 column twice using Bradfords assay to monitor antibody binding. The column was then washed with 40 ml of 0.5 M NaCl, 1 mM Tris-HCl (pH 7.5). The antibody was eluted using 10 ml of 0.1 M glycine pH 2.25. 500 µl fractions were collected into eppendorfs containing 50 µl 1 M Tris-HCl pH 8. Fractions containing antibody were pooled and BSA was added to 1mg ml^{-1}, glycerol to 10 % (w/v), and azide to 0.1 %. The antibody was stored at – 70 °C. The column was washed and stored in PBS, 0.5 M NaCl, 0.1 % azide at 4 °C.

2.3 BACTERIA

E. coli DH5α (genotype: ϕ80d*lac*ZΔM15, *rec* A1, *end* A1, *gyr* A96, *thi*-1, *hsd* R17 (r_k-,m_k+), *sup* E44, *rel* A1, *deo*R, Δ(*lac*ZYA-*arg*F)U169) was used for routine DNA preparation.

E. coli B834 (F^-, *ompT*, *hsdS*$_B$, (R_B-, m_B-), *dcm*, *gal*) was used for protein expression unless otherwise stated.

E. coli BL21DE3 (F^-, *ompT*, *hsdS*$_B$, (R_B-, m_B-), *dcm*, *gal(DE3))*

Bacteria were grown in Luria-Bertani (LB) broth with antibiotics added when required.

2.3.1 Preparation of chemically competent DH5α cells

A single colony was picked from a freshly streaked agar plate and grown overnight at 37 °C. LB was then inoculated with 1/100 of overnight culture and grown at 37 °C at 120 rpm until an optical density of approximately 0.6 was reached. The culture was incubated on ice for 30 minutes. The culture was then centrifuged at 3000 rpm for 5 minutes at 4 °C. Each 50ml pellet was then resuspended in 12.5 ml of 100mM $CaCl_2$ and 12.5 ml of 40mM $MgSO_4$ (freshly mixed and pre-chilled), then incubated on ice for a further 30 minutes. The cells were centrifuged at 3000 rpm for 5 minutes at 4 °C. Then pellets were resuspended in 2.5 ml of 100 mM $CaCl_2$ and 2.5 ml of 40 mM $MgSO_4$. Glycerol was added to competent cells prior to snap-freezing in liquid nitrogen and storage at –70 °C.

2.3.2 Transformation of chemically competent cells

50 μl of chemically competent cells were transformed with approximately 0.2 μg of DNA. Cells were incubated with DNA on ice for 30 min, followed by a heat-shock of 3 min at 42 °C and a further 30 min incubation on ice. 1 ml of warm LB was added to cells and incubated for 1 hour prior to plating on agar in the presence of a selective antibiotic.

2.4 CELL CULTURE AND TRANSFECTIONS

2.4.1 SUMO and NEDD8 deconjugation assays

SUMO protease deconjugation assays were performed in COS7 cells grown in Dulbecco's modified Eagle's medium supplemented with 10 % foetal bovine serum. For analysis of SUMO protease deconjugation activity, 9.6 cm^2 wells of subconfluent cells were transfected using Lipofectamine according to the instructions provided by the manufacturer. The expression constructs for various proteases and either HA-SUMO-1, HA-SUMO-2, or HA-SUMO-3 (1 μg of total plasmid DNA) were cotransfected as indicated in

the figures. Cell extracts were prepared for Western blot using RIPA lysis buffer as detailed in '2.20 Preparation of cell extracts'. NEDD8 deconjugation assays were performed similarly using His-NEDD8 and NEDP1 wild type or mutant or empty vector as indicated.

2.4.2 NEDD8 deconjugation assays and purification of His6-tagged NEDD8 Cul-4A conjugates

COS7 cells were grown in Dulbecco's modified Eagle's medium supplemented with 10% foetal bovine serum. For analysis of NEDP1 deconjugation activity *in vivo*, 25 cm^2 flasks of sub-confluent cells were co-transfected with the expression constructs for NEDP1 and His-NEDD8 (10.6 μg of total plasmid DNA) as indicated in the figures.

Forty-eight hours after transfection COS7 cells were lysed in 5 ml of 6 M guanidinium-HCl, 0.1 M Na_2HPO_4/NaH_2PO_4, 0.01 M Tris-Hcl pH 8.0, 5 mM imidazole and 10 mM β-mercaptoethanol per 25 cm^2 flask. After sonication the lysates were mixed with 50 μl of Ni^{2+}-NTA-agarose beads prewashed with lysis buffer and incubated for 2 hours at room temperature. The beads were successively washed with the following: 6 M guanidinium-HCl, 0.1 M Na_2HPO_4/NaH_2PO_4, 0.01 M Tris-HCl pH 8.0, 10 mM β-mercaptoethanol; then 8 M urea, 0.1 M Na_2HPO_4/NaH_2PO_4, 0.01 M Tris-HCl pH 8.0, 10 mM β-

mercaptoethanol; then 8 M urea, 0.1 M Na_2HPO_4/NaH_2PO_4, 0.01 M Tris-HCl pH 6.3, 10 mM β-mercaptoethanol (buffer A) plus 0.2 % Triton-X-100; then buffer A and finally buffer A plus 0.1 % Triton-X-100. After the last wash with buffer A, His-NEDD8 was eluted with 200 mM imidazole in 5 % SDS, 0.15 M Tris-HCl pH 6.7, 30 % glycerol, 0.72 M β-mercaptoethanol. The eluates were subjected to SDS-PAGE (10%) and the proteins transferred to a PVDF membrane. Western blotting was performed with a mAb against the Myc tag.

2.4.3 Immunofluorescence analysis

HeLa cells were grown in Dulbecco's modified Eagle's medium supplemented with 10 % foetal bovine serum. For analysis of the cellular localisation of proteins, 13 mm coverslips of subconfluent cells were transfected with plasmids expressing the protein of interest, with 0.2 μg total DNA and 0.6 μl of Fugene as indicated.

2.4.4 Six-well plate luciferase transfections

HeLa cells were grown to 50 % confluency in 6 well plates and then transfected with a ratio of 3:1 (Fugene μl:DNA μg) as specified by the manufacturers (Roche). Cells were transfected with 100 ng of reporter

plasmid (p3EnhConALuc), NEDP1 wt or NEDP1 mut (amounts as indicated), and pcDNA3 to bring the final amount of DNA to 1 µg. 24 h after transfection the cells were stimulated with 10 ng ml^{-1} TNF for 6 hours then lysed and analysed for luciferase activity as detailed in '2.17 Luciferase assays'.

2.4.5 siRNA transfection

For immunofluorescence, 13 mm coverslips of 30-50% confluency were serially transfected with 80 nM, 50 nM, and 50 nM, in a total volume of 200 µl, of SENP1 siRNA or random sequence control (RSC) siRNA using oligofectamine (Invitrogen) as directed by the manufacturer. Cells were fixed 24 h after the last transfection.

For cell cycle analysis, 6 well plates of 30-50 % confluent HeLa cells were transfected serially with 100 nm then 50 nM (100µl total volume) of RSC, SENP1, or SENP2 siRNA respectively. 24 h after the last transfection cells were harvested for flow cytometry.

For analysis of cell viability, 96 well plates of 30-50 % confluent HeLa cells were transfected twice at 0 h and 72 h with 50 nM of siRNA duplexes, in a total volume of 100 µl, using oligofectamine. Cells were split at 48 hours to maintain logarithmic growth and analysed for cell viability at 96 h.

For real-time quantitative RT-PCR analysis HeLa cells were transfected once with 100 nM RSC or SENP1 siRNA, in a total volume of 100 μl, then harvested 24 h post transfection.

For luciferase assays HeLa57A cells were grown to 30 % confluency in 96 well plates, then serially transfected with 80 nM then 50 nM siRNAs, in a total volume of 100 μl, using oligofectamine (Invitrogen) as directed by the manufacturer's instructions. 24 hours after the last transfection, cells were stimulated for 6 h with 10 ng ml^{-1} TNF then lysed and analysed for luciferase activity.

6 well plates for siRNA transfection and analysis of NEDP1 protein knock-down were transfected similarly, but scaled up for 6 well plates and transfected in 1 ml final volume. The cells were lysed using RIPA buffer as detailed in '2.2 Preparation of cell extracts'.

Small interfering RNAs (siRNAs) were obtained from Eurogentec in a desalted deprotected form. siRNA duplexes were prepared and stored according to the manufacturer's instructions.

SENP1 sense 5'- GACUCCAACUCCCAGUUCUdTdG-3'

SENP1 anti-sense 5'- AGAACUGGGAGUUGGAGUCdTdT-3'

RSC sense 5'-GCUAUGUGACGUAGAGCGAdTdT-3'

RSC anti-sense 5'-UCGCUCUACGUCACUAGCdTdT-3'

SENP2 sense 5'-GAGUGACAGUUACCCGAGAUU-3'

SENP2 anti-sense 5'-UCUCGGGUAACUGUCACUCUU-3'

NEDP1 sense 5'-CUGGCCUUUGUGGAAGAGAdTdT-3'

NEDP1 antisense 5'-UCUCUUCCACAAAGGCCAGdTdT-3'

2.5 CELL VIABILITY ASSAY

The CellTitre 96 non-radioactive cell proliferation kit (Promega) was used to measure cell viability as directed by the manufacturers instructions. Mitochondrial mediated reduction of tetrazolium salt into a fomazan is the basis of this assay.

2.6 cDNA CLONING

Isolation of SUMO-like proteases and sub-cloning into expression vectors was part of a collaboration with Dr. B. Ink (GlaxoSmithKline).

2.6.1 Cloning of SENP2

A BLAST search of the public databases was performed using the 181 amino acids of the protease domain of the yeast Ulp1 where a human gene, KIAA1331, was identified. The partial sequence of KIAA1331 was BLAST searched against the EST database and an EST, AA700122, was found that extended the N-terminus by 100 amino acids. EST aa700122 was then blast searched against the genomic DNA database and the genomic clones AC068379 and AC069420 were identified. The intron/exon boundaries of SENP2 could then be identified by comparing the genomic and EST sequences. To confirm and identify a cDNA containing the full-length gene, oligonucleotides (5'-GTAGGAGGGGATACCAACTGGAGCCTG-3' and 5'-CGCAATTTGAAAGCACTACTTAGGATT TC-3') were designed that flanked the region of the protease domain of SENP2 and a lung cDNA library from Origene was screened to identify bacterial clones containing the cDNA. Positive clones from the library were then rescreened using a primer in the vector, pCMV6-XL4, to detect the 5' end of the gene and a gene specific primer in the protease domain to detect the 3' end. The clone containing the longest insert was determined by DNA sequence analysis. The 5' end of SENP2 was confirmed by performing RACE on cerebellum cDNA. Marathon Ready cDNA (ClonTech) was used for analysis of the 5' end of SENP2. An

adaptor primer for the 5' end and two gene specific primers (5'-GCGAATTTGAAAGCACTACTTAGGATTTC-3' or 5-GTGCCGAGAATCCTAACCAGCCATC-3') for the 3' end were used in PCR to determine the 5' end of SENP2. Fragments generated in the reaction using the two different primers were analysed by DNA sequence analysis and found to contain a similar 5' end as the cDNA clone from the lung cDNA library.

Site-directed mutagenesis of SENP2 –pCMV-XL4 SENP2 (C548A) mut

The active cysteine residue was altered using the QuikChange system (Stratagene). Template DNA used in the mutagenesis contained the full-length gene of SENP2 under control of the CMV promoter. Mutagenic oligonucleotides (5'-CAGCTGAATGGGAGTGATGCTGGAATGTTTACTTG-3' and 5'-CAAGTAAACATTCCAGCATCACTCCCATTCAGCTG -3') were used to alter the active cysteine (TGT) to an alanine (GCT). The complete coding region of SENP2 was sequenced to verify that the cysteine had been altered to alanine and no other nucleotides had been altered.

Sub-cloning of SENP2 wt and mut into pEGFP-C1

pGFP-C1-SENP2 plasmid for the expression of GFP-SENP2(wt) was constructed by PCR amplification of SENP2 cDNA with the primers 5'-GCGAGATCTATGTACAGATGGCTGGTTAGGATT-3' and 5'CGCGAATTCTCACAGCAACTGCTGATG-3'. The PCR product was restricted with Bgl II and EcoRI before insertion into a similarly restricted pEGFP-C1 (ClonTech). pGFP-C1-SENP2(C548A) for the expression of GFP-SENP2(C548A) was constructed by PCR amplification of SENP2(C548A) cDNA using the same primers.

Cloning of SENP2(-NLS) into pcDNA3.1/V5-His TOPO for expression in mammalian cells

pcDNA3.1/V5-His TOPO SENP2(-NLS) for the expression of SENP2(-NLS) was constructed by PCR amplification of SENP2 cDNA with the primers 5'-ACCATGGATTGCTTTATTCACCAAGTGAAAAACAGTC-3' and 5'-TCACAGCAACTGCTGATGAAGGATTTCC-3'. The PCR product was inserted into pcDNA3.1/V5-His TOPO vector (Invitrogen).

Cloning of SENP2 protease domain as a GST fusion for bacterial expression

pGEX-2T-SENP2$_{368-589}$ plasmid for expression of the protease domain of SENP2 was constructed by PCR amplification of SENP2 cDNA with the

primers 5'-TTGAGATCTCTTACAGAGGACATGGAAAAG-3' and 5'-ATTGAATTCTCACAGCAACTGCTGATGAAG-3'. The PCR product was restricted with Bgl II and EcoRI before insertion into a BamHI and EcoRI restricted pGEX-2T. pGEX-2T-SENP2(C548A)$_{368-589}$ was constructed as above by amplifying SENP2 (C548A) cDNA.

2.6.2 Cloning of SENP1

pEGFP-C1-SENP1 plasmid for the expression of GFP-SENP1(wt) was constructed by PCR amplification of SENP1 cDNA with the primers 5'-GCGAGATCTATCGATGATATTGCTGATAGGATG-3' and 5'-CGCGCGGAATTCTCACAAGAGTTTTCGGTGGAGGAT-3'. The PCR product was restricted with Bgl II and EcoRI before insertion into a similarly restricted pEGFP-C1. Construction of pEGFP-C1-SENP1(mut) for the expression of GFP-SENP2(mut) was constructed by PCR amplification of pcDNA-SENP1(mut) using the same primers.

2.6.3 Cloning of NEDP1

A blast search of a number of protein databases was performed using the 181 amino acids of the protease domain of the yeast Ulp1 where a number of Ulp-like genes were identified. Hidden Markov Model (HMM)

searches (using the HIMMER suite) of a translated EST assembly database with HMMs generated from protein multiple sequence alignments of the Ulp-like proteins identified NEDP1.

To confirm and identify a cDNA containing the full-length gene of NEDP1, PCR analyses of tissues of human cDNA (Clontech) were used to determine expression of NEDP1. Oligonucleotides (5'-GATCCGCCAAGCTGGCTCAATGACC-3' and 5'-GCGTGAACTGAGTTGCTCCTGCTATGG-3') were designed that flanked the region of the protease domain and cDNAs were screened for expression. A kidney cDNA library from Origene was screened to identify bacterial clones containing the cDNA. Positive clones from the library were then rescreened using a primer in the vector, pCMV6-XL4, to detect the 5' end of the gene. The clone containing the longest insert was determined by DNA sequence analysis. A stop codon in the 5'UTR was used as confirmation that the cDNA was a full-length gene. Oligonucleotides (5'-GCCACCATGGACCCCGTAGTCTTG-3' and 5'-CTACTACTTTTTAGCAAGTGTGGCAATGAG-3') of the coding region including the stop codon of NEDP1 were designed for cloning NEDP1 into the pcDNA3.1/V5-His vector (Invitrogen). This construct was used for further analysis.

Site-directed mutagenesis of NEDP1

Site-directed mutagenesis using the QuikChange system (Stratagene) was used to alter the active cysteine residue. The template DNA used in the mutagenesis contained the full-length gene of NEDP1 under control of the CMV promoter. Mutagenic oligonucleotides (5'-CCAACAAAACAGCTATGACGCTGGGATGTACGTGATATG -3' and 5'-CATATCCGTACATCCCAGCGTCATAGCTGTTTTGTTGG -3') were used to alter the active cysteine (TGT) to an alanine (GCT). The complete coding region of NEDP1 was sequenced to verify that the cysteine had been altered to alanine and no other nucleotides had been altered.

Cloning of GST-NEDP1 for the expression of NEDP1 in bacteria

pGEX-4T3-NEDP1 plasmid for the expression of NEDP1 was constructed by PCR amplification of NEDP1 cDNA with the primers 5'-GCAGAATTCCGACCCCCTAGTCTTGAGTTAC-3' and 5'-CCAGCTCGAGCTACTTTTTAGCAAGTGTGGC-3'. The PCR product was restricted with EcoRI and XhoI before insertion into a similarly restricted pGEX-4T3. pGEX-4T3-NEDP1mut(C163A) was constructed as above by amplifying NEDP1(C163A) cDNA.

2.6.4 Other plasmids

pGEX-2T-Ub-His-PK for the expression of GST-Ub-His-PK was constructed by PCR amplification of pGST-UbGG [114] with the primers 5'-GCGGGATCCCAGATCTTCGTGAAGACCCTG-3' and 5'-GCGGAATTCCACCACCTCTCAGACGCAGGAC.-3'. The PCR product was restricted with BamHI and EcoRI prior to insertion into a similarly restricted pGEX-2T-His-PK vector.

Plasmids HA-SUMO-1, -2 and –3, and pcDNA3-PML were a gift from Dr. M. Tatham.

Plasmids pcDNA3-HDAC [115], pcDNA3-p53 [70], pcDNA3-IkBa [116] and pEnhConALuc were available in the lab.

The construct pGST-H-PK was the gift of Prof. Randall.

Plasmids pGST-NEDD8-Myc-His and pGST-NEDD8-GG were the gift of Prof. Yasuda.

The pGEX2T-His-PK plasmid was the gift of Dr. Liu.

pGEX-His-NEDD8 was the gift of Dr. L. Shen.

2.7 DNA PREPARATION

The preparation of plasmid DNA was carried out using Qiagen maxi, mini, and gel extraction kits as per the manufacturer's instructions. Purification of PCR products was carried out using PCR Clean-Up kits (Promega) as per the manufacturer's instructions. Restriction enzymes were obtained from Promega. VENT DNA polymerase (New England Biolabs) was used for PCR. Concentration and purity of all DNA preparations was determined using optical density readings at wavelengths 260 nm and 280 nm.

2.8 DNA SEQUENCING

All DNA constructs were verified by automated DNA sequencing on an ABI PRISMTM 377 DNA Sequencer (St. Andrews University DNA sequencing unit).

2.9 FLOW CYTOMETRY

For FACS analysis, 6-well plates of log phase HeLa cells were detached in 0.05 % w/v di-potassium EDTA in PBS, then fixed in 70 % ethanol, digested with RNase A (40μg/ ml), and stained with propidium iodide (100μg/ ml). (Becton-Dickson).

2.10 IMMUNOFLUORESCENCE ANALYSIS

Transfected cells were fixed with 4 % paraformaldehyde/PBS for 10 min, then washed with PBS. The paraformaldehyde was then blocked with 100 mM glycine/PBS for 10 min twice. After washing with PBS the cells were then permeabilised with 0.2 % Triton X-100 for 10 min then washed with PBS. The coverslips were blocked with 0.5 % goat serum/PBS for 5 min.

Primary antibody was applied for 45 min in 0.5 % GSA/PBS then washed off with GSA/PBS. Secondary antibodies were applied for 30 min in 0.5 % GSA/PBS. Coverslips were washed first with GSA/PBS, then with PBS.

Coverslips were mounted in mowial containing DAPI. Localisation of proteins was examined with a 100× oil immersion lens using a Zeiss axiovert S100 2TV Deltavision restoration microscope (Applied Precision Inc.) running Softworx Collection and Imaging Software.

2.11 IMMUNOPRECIPITATION USING NEDP1 ANTIBODY

Binding of NEDP1 antibody to protein G beads

Solid NaCl was added to a 3 M concentration to 1 ml (approximately 1 mg) of affinity purified NEDP1 antibody or pre-immune antibody. Each sample was then diluted to 10 ml with Buffer A (50 mM boric acid, 3 M NaCl pH 9). 500 µl packed volume of protein G beads (Sigma) was used per sample. The beads were washed three times with 10 ml Buffer A prior to use. Antibody and beads were mixed by rotation for 1 h at room temperature. The beads were then washed twice with 10 volumes of buffer A, before resuspending in 10 volumes of buffer B (200 mM boric Acid, 3 M

NaCl pH 9). A sample of beads (10) µl was removed for analysis (pre-coupling sample). Dimethylpimelimidate (Sigma) solid was added to a final concentration of 12 mg ml^{-1} and mixed by rotation at room temperature for 1 h. A sample of beads 10 µl was removed for analysis (post-coupling sample). The reaction was stopped by washing the beads in 0.2 M ethanolamine pH 8. The beads were resuspended in 0.2 M ethanolamine pH 8 and mixed at room temperature for 2 h. The beads were then washed three times in 10 volumes of PBS prior to storage in PBS/ 0.1 % azide at 4 °C. Analysis of coupling success was performed by running pre-coupling and post-coupling samples on a 10 % SDS-PAGE gel.

Immunoprecipitation of endogenous NEDP1 from HeLa cytoplasmic extracts

30 µl packed volume of beads was used per 1 ml sample of cytoplasmic extract see '2.19 Fractionation of cytoplasmic, nuclear, and high-salt nuclear extracts'. The beads were washed twice with buffer D (0.1 M EDTA, 10 % glycerol, 0.1 % NP-40, 1 mM DTT, 0.15 M KCl 20 mM HEPES (pH 7.5)). Cytoplasmic extract was added and mixed for 3 h at room temperature. The beads were then washed three times with buffer D. A fourth wash was carried out using buffer D without glycerol or NP-40. Samples of the beads were then boiled in lysis buffer without ß-mercaptoethanol at 60 °C for 10

min and then analysed by SDS-PAGE and Western blotting as indicated in the figure.

2.12 *IN VITRO* EXPRESSION OF PROTEINS

In vitro transcription/translation of proteins was performed using 1 μg of plasmid DNA and a wheat germ coupled transcription/translation system according to the manufacturer's instructions (Promega). ^{35}S Methionine (Amersham Pharmacia Biotech) was used in the reactions to generate radiolabelled protein.

2.13 *IN VITRO* SUMO CONJUGATION ASSAYS

^{125}I-SUMO-1 conjugation of GST-$PML_{485-495}$ was performed in 350 μl containing 80 μg ^{125}I-labeled SUMO-1, an ATP regenerating system, and buffer (50 mM Tris (pH 7.5), 5mM $MgCl_2$, 2 mM ATP, 10 mM creatine phosphate, 3.5 units·ml^{-1} creatine kinase, 28 μg Ubc9, 4.8 μg SAE1/SAE2, and 240 μg GST-PML). The reaction was incubated at 37° C for 8 h. ^{125}I-SUMO-1 conjugated to substrate was bound to glutathione agarose beads, washed and stored at 4° C prior to use in deconjugation assays. SUMO-1

conjugation to GST-ranGAP$_{418-587}$ was performed similarly. Radiolabelled GST-ranGAP$_{418-587}$ was conjugated to unlabelled SUMO-1 or SUMO-2 similarly.

SUMO-1 conjugation to ^{35}S labelled substrates PML, HDAC, p53 and IκB was performed in 100 μl volumes containing an ATP regenerating system and buffer 2 mM ATP, 5mM $MgCl_2$, 50 mM Tris (pH 7.5), 10 mM creatine phosphate, 3.5 units·ml^{-1} creatine kinase. The assay contained 1.2 μg of purified recombinant SAE1/SAE2, 6.5 μg Ubc9, 100 μg SUMO-1 and 10 μl of ^{35}S methionine labelled substrate . Reactions were incubated at 37° C for IκBα (4 h), HDAC (45 min), p53 and PML (1 h). Conjugation was terminated by the addition of iodoacetamide to 10 mM and incubated at 20° C for 30 min. The iodoacetamide was quenched by the addition of β-mercaptoethanol to 15 mM and incubated at 20° C for 15 min. The reactions were stored at –20° C prior to use.

2.14 *IN VITRO* NEDD8 CONJUGATION

In vitro transcription and conjugation of Cul-2 was performed using 1 μg of plasmid DNA and a rabbit reticulocyte lysates coupled transcription/ translation system (Promega) in the presence of 3 μg of GST-NEDD8-GG for

2 h at 30° C. ^{35}S Methionine (Amersham Pharmacia Biotech) was used in the reactions to generate radiolabelled protein. Conjugation was terminated by the addition of iodoacetamide to 10 mM and incubated at 20° C for 30 min. Iodoacetamide was quenched by the addition of β-mercaptoethanol to 15 mM and incubated at 20° C for 15 min. If not used immediately the reaction was stored at –20 °C.

2.15 *IN VITRO* DECONJUGATION ASSAYS

2.15.1 SUMO deconjugation assays

All deconjugation assays were performed in buffer containing 2 mM $MgCl_2$, 5 mM β-mercaptoethanol, and 50 mM Tris (pH 7.5). GST-PML-^{125}I-SUMO-1 deconjugation was performed in 20 μl containing GST-PML-^{125}I-SUMO-1 and between 0.5 μg and 0.003 μg of GST-SENP2$_{368-589}$. Reactions were incubated at 37° C for 3 h with agitation every 15 min. After termination with SDS sample buffer containing β-mercaptoethanol, reactions were fractionated by electrophoresis in polyacrylamide gels (10 %) containing SDS, stained, and destained prior to analysis by phosphorimaging.

^{125}GST-ranGAP$_{418-587}$-SUMO-1/2 deconjugation was performed in 20 μl containing ^{125}GST-ranGAP$_{418-587}$-SUMO-1/2 and between 1 μg and 0.015 μg of GST-SENP2$_{368-589}$. Reactions were terminated and analysed as above.

Deconjugation of ^{35}S methionine labelled PML-SUMO-1, HDAC-SUMO-2, p53-SUMO-1 and IκB-SUMO-1 was performed in 20 μl containing 15 μl of ^{35}S labelled conjugated substrate and between 0.5 μg and 0.008 μg of GST-SENP2$_{368-589}$. Reactions were incubated at 37° C for 3 h. After termination with SDS sample buffer containing β-mercaptoehtanol, reaction products were fractionated by electrophoresis in polyacrylamide gels (8 – 10 %) containing SDS, stained, destained and dried prior to analysis by phosphorimaging.

2.15.2 NEDD8 deconjugation assays

Deconjugation of ^{35}S methionine labelled Cul-2-NEDD8 was performed in 10 μl containing 3 μl of ^{35}S labelled conjugated substrate, 2 μg of GST-NEP1 in 50 mM Tris pH 7.5, 2mM $MgCl_2$ and 5 mM β-mercaptoethanol. Reactions were incubated at 37 °C for 3 h terminated with SDS sample buffer containing β-mercaptoethanol and the reaction products were fractionated by electrophoresis in polyacrylamide gels (8%) containing SDS, stained, destained and dried prior to analysis by phosphorimaging.

2.16 *IN VITRO* PROCESSING ASSAYS

2.16.1 SUMO processing assays

SUMO processing assays were performed in 10 μl containing 2 μg of full length SUMO-1, SUMO-2, or SUMO-3 proteins, 50 mM Tris (pH 7.5), 2 mM $MgCl_2$, 5 mM β-mercaptoethanol, and between 0.008 μg and 0.5 μg of GST recombinant protease. For analysis of active site mutant protease, 2 μg of SUMO-1 precursor was incubated with 0.5 μg of recombinant protease. Reactions were incubated at 37° C for 3 h. After termination with SDS sample buffer containing β-mercaptoethanol, the reaction products were fractionated by gel electrophoresis in SDS-PAGE gels (12 %), stained and destained. For MALDI-TOF mass spectrometry analysis 2 μg of SUMO precursor was incubated with 1μg of GST-$SENP2_{368-589}$ for 3 h at 37° C. All recombinant and cleaved SUMO protein masses were verified by MALDI-TOF mass spectrometry on a Micromass TofSpec 2E mass spectrometer (Micromass, Manchester, UK; University of St. Andrews Mass Spectrometry Service).

2.16.2 In vitro *NEDD8 processing assays*

NEDD8 processing assays were performed in 20 μl containing 6 μg of GST-NEDD8-Myc-His6, 50 mM Tris pH 7.5, 2 mM $MgCl_2$, 5 mM β-mercaptoethanol and between 166 ng and 0.07 ng of GST-NEDP1. Reactions were incubated at 37 °C for 3h. After termination with SDS sample buffer containing β-mercaptoethanol, reaction products were fractionated by gel electrophoresis in 12.5 % polyacrylamide gels containing SDS, stained and destained. Reactions were also subjected to Western blot using anti-His antibody.

NEDD8, SUMO, and Ub processing assays were performed in 20 μl containing 2 μg of substrate (GST-NEDD8-Myc-His6, GST-UB-H-P, or SUMO-1) and 0.5 μg of GST-NEDP1 or GST-NEDP1mut. All processing assays were performed in buffer containing 50 mM Tris pH7.5, 2 mM $MgCl_2$, and 5 mM β-mercaptoethanol for 3 h at 37 ° C. After termination with SDS sample buffer containing β-mercaptoethanol, the reaction products were fractionated by gel electrophoresis in 12.5 % polyacrylamide gels containing SDS. NEDD8 and Ubiquitin processing assays were further subjected to Western blot using either anti-His antibody or anti-PK SV5 antibody.

Protease inhibition assays were performed in 10 μl containing 1 μg of substrate (GST-NEDD8-Myc-His6) and 50 ng of GST-NEDP1. Assays were performed in 50 mM Tris pH 7.5 containing either NEM (5, 2.5 mM) or EDTA (50 mM, 30 mM, 10 mM) as indicated. Protease was pre-incubated with either inhibitor or buffer for 5 min prior to the addition of substrate and then further incubated at 37 ° C for 3h. After termination with SDS sample buffer containing β-mercaptoethanol, the reaction products were fractionated by gel electrophoresis in 12.5 % polyacrylamide gels containing SDS, stained and destained.

2.17 LUCIFERASE ASSAYS

2.17.1 Six-well plate luciferase assays

All buffers and plates were kept on ice where possible. 6 well plates of cells were washed twice with PBS, then 200 μl of luciferase lysis buffer was added (9.2 mM KH_2PO_4, 90.8 mM K_2HPO_4, 0.5 mM DTT and 0.2 % Trition X-100). The cells were scraped then mixed by pipetting and spun at 13000 rpm in a benchtop centrifuge for 30 seconds. 50 μl of lysate was injected with luciferase assay buffer (25 mM Tris-phosphate pH 7.8, 2 mM $MgCl_2$, 1 mM DTT, 1 % Triton X-100, 15 % glycerol, 1 mM ATP, 0.15 mM luciferin

(Sigma L6882), 1 % BSA) using a Lumat LB 901 Berthold luminometer that also measured luciferase activity. Activity is expressed as fold activation.

2.17.2 96-well plate luciferase assays

All buffers and plates were kept on ice where possible. 100 µl of lysis buffer was added per well of 96 well plates and mixed by pipetting. 50 µl of each sample was transferred to a 96 well plate (Perkin Elmer) for luciferase assay analysis. Activity was measured using a 96 well luminometer (MicroLumat LB 96P BerthoLD) that also measures luciferase acticity. Activity is expressed as fold activation.

2.18 MASS SPECTROMETRY

The processing reactions (20 μl, 10 pmoles/μL) were desalted on-line through a XTerra MS C8 5 mm 2.1x10mm column, eluting with an increasing acetonitrile concentration (2% acetonitrile, 98% aqueous 1% formic acid to 98% acetonitrile, 2% aqueous 1% formic acid) and delivered to an electrospray ionisation mass spectrometer (LCT, Micromass, Manchester, UK) which had previously been calibrated using myoglobin. An envelope of multiply charged signals was obtained and deconvoluted using MaxEnt1 software to give the molecular weight of the protein.

2.19 PREPARATION OF CYTOPLASMIC, NUCLEAR, AND HIGH SALT NUCLEAR EXTRACTS

5 l of HeLa suspension cells were prepared for extraction by centrifugation at 4000 rpm at 4° C for 30 min. The cell pellet was washed in ice-cold PBS and re-centrifuged. The cell pellet was washed in 2 pellet volumes of hypotonic buffer (10mM Hepes pH 7.5, 1.5 mM $MgCl_2$, 10 mM KCl, 0.5mM DTT + protease inhibitor (Roche complete EDTA-free protease inhibitor tablet)) and mixed by inversion. The cells were pelleted by centrifugation at 1000g for 5 min at 4°C in a benchtop centrifuge. 2 pellet

volumes of hypotonic buffer was added to the pellet, mixed by inversion, and poured into a Dounce homogeniser and incubated on ice for 10 min. The cell membranes were disrupted using 15 strokes of the Dounce homogeniser. The lysate was then spun at 1000g for 20 min at 4°C. The supernatant was the cytoplasmic lysate (SN1). The pellet was then respun at 18000 rpm for 20 min at 4°C. The supernatant (SN2) was aspirated and discarded, the pellet was retained for the nuclear extract. 0.11 volumes of buffer B (0.3 M Hepes pH 7.5, 1.4 M KCl, 30 mM $MgCl_2$, + Roche complete EDTA-free protease inhibitor tablet) was added to SN1 and then spun at 100000 g for 35 min at 4°C. The supernatant was removed and dialysed against Buffer D (20mM Hepes pH 7.5, 0.1 mM EDTA, 10% glycerol, 0.1 % NP-40, 1mM DTT, 0.15 M KCl) overnight, giving the cytoplasmic fraction. The nuclear pellet was resuspended in two volumes of Buffer C (20mM Hepes pH 7.5, 1.5 mM $MgCl_2$, 10mM KCl, 0.5 mM DTT, and protease inhibitor tablet). The nuclear pellet was mixed using three strokes of the Dounce homogeniser, incubated on ice for 30 min, and then centrifuged at 18 000 rpm for 30 min at 4°C. The supernatant was removed and dialysed against Buffer D overnight, giving the nuclear extract. The pellet was then resuspended in two volumes of high salt extraction buffer (20 mM Hepes pH 7.5, 1 M NaCl, 1.5 mM $MgCl_2$, 0.2 mM EDTA, 0.5 mM DTT, 25 % glycerol, 1 % NP-40, and protease inhibitor tablet) using 10 strokes of the Dounce homogeniser and incubated on ice for 10 min. The lysate was then spun at

35000 rpm for 35 min at 4°C. The supernatant was removed and dialysed overnight against buffer D, giving the high salt nuclear extract.

2.20 PREPARATION OF CELL EXTRACTS

Unless otherwise stated cell extracts were prepared for lysis in SDS sample buffer (5% SDS, 0.15 M Tris HCl pH 6.7, 30 % glycerol) diluted 1:3 in RIPA buffer (25 mM Tris pH 7.2, 50 mM NaCl, 0.5 % NP-40, 0.5 % deoxycholate, 0.1 % SDS, 0.1 % azide) containing 10 mM iodoacetamide and complete EDTA-free protease inhibitor tablets (Roche) freshly added. After addition of lysis buffer the cells were agitated for 5 min. β-mercaptoethanol was then added to a concentration of 1:20. Lysates were boiled for 10 min then sonicated briefly prior to loading onto a gel.

2.21 PROTEIN EXPRESSION AND PURIFICATION

GST-SENP2$_{368-589}$ fusion protein was expressed in *Escherichia coli* B834 grown to OD 0.6 at wavelength 600nm, then induced with 0.5 mM IPTG for 3 h at room temperature, and purified by affinity chromatography using glutathione agarose as described previously [117]. GST-SENP2$_{368-589}$ was

eluted with buffer containing 10 mM glutathione and stored at -70° C.

GST-NEDP1 [118] and GST-SENP1 $_{418-645}$ fusion proteins were expressed and purified similarly.

A *Drosophila* ubiquitin carboxyl terminal hydrolase was expressed in E. coli and purified as described [78].

GST-SUSP1 was a kind gift of Dr. J. Desterro.

GST-NEDD8-Myc-His and GST-Ub-His-PK were expressed in *E. coli* BL21 DE3 as described previously [68].

6-His NEDD8 was expressed and purified from E. coli Bl21(DE3) as described previously [118].

Expression and Purification of Recombinant Proteins – C52A SUMO-1, SUMO-1, SUMO-2, SUMO-3, Ubc9, SAE2/SAE1, and GST-PML (GST-TEV-$PML_{485-495}$) were expressed in, and purified from, *E. coli* B834 as described previously [28].

2.21.1 Quantitation of protein

Protein concentrations were determined using Bradfords reagent [119] (Biorad) and the absorbance at 595 nm was measured using a spectrophotometer.

2.21.2 SDS-PAGE and Western blotting

Protein samples were resuspended in Lysis buffer (20mM Tris-HCl pH 6.8, 2% SDS, 5% β-mercaptoethanol, 2.5% glycine and 2.5% bromophenol blue and denatured at 100°C for 5 min before loading on SDS-polyacrylamide gels. Biorad mingel equipment was used following the manufacturer's instructions. Gels were stained with Coomassie Blue (0.2% Coomassie brilliant blue R250, 5% methanol, 10% acetic acid). Gels for Western blotting were transferred onto polyvinylidene difluoride membrane using a wet blotting system (Biorad). Membranes were then blocked in PBS containing 10% skimmed milk powder and 0.1% Tween 20. Membranes were then incubated with primary antibody in PBS containing 5% skimmed milk powder and 0.1% Tween. Horseradish peroxidase conjugated antibodies were used as secondary antibodies. Antibody detection was performed using an ECL system.

2.22 RADIOIODINATION

SUMO-1 or GST-ranGAP$_{418-587}$ were radiolabelled with ^{125}I using the chloramine-T method as described previously for wt-SUMO-1 [45], except that the labelled protein was dialysed against 50 mM Tris pH 7.5, 1 mM DTT instead of passage over a P2-acrylamide gel column.

2.23 TAQMAN

RNA was isolated by a BIOMEK 2000 using a modified SV96 total RNA isolation system (PROMEGA) method. For each set of experiments three 96 well plates were set up. Plate 1 was designed to investigate expression of the test oligos (SENP1), plates 2 and 3 study expression of GAPDH with and without RT enzyme as positive and negative controls. For each well on the plate containing 5ul RNA template, a 20µl reaction volume was added, containing 12.5 µl '2x one-step RT-PCR mastermix (Applied Biosystems' (containing optimised volumes of $MgCl_2$, dNTP mix, and Taq polymerase), 1µl of 10µM forward primer, 1µl of 10µM reverse primer, 0.5µl of 5µM duel labelled FAM/TAMRA probe and 5µl water. PCR assays were performed on an ABI 7900 Sequence Detection system (Applied Biosystems) running the

cycling conditions: 45 °C for 10 minutes, 95 °C for 10 minutes, 40 cycles of 95 °C for 15 seconds, 60 °C for 1minute.

RT-PCR probes

SENP1 forward 5'-CAGACTCTGTGATTTTACTGAAAGTGAA-3'

SENP1 reverse 5'-TTGATCCACAGCTCTGCCTG-3'

SENP1 probe 5'-TTCCCAGACTCCAACTCCCAGTTCTACTTTCT-3'

GAPDH forward 5'-CAAGGTCATCCATGACAACTTTG-3'

GAPDH reverse 5'-GGGCCATCCACAGTCTTCTG-3'

GAPDH probe 5'ACCACAGTCCATCGGATCACTGCCA-3'

3. BIOINFORMATICS AND CHARACTERISATION OF NOVEL SUMO-LIKE PROTEASES

3.1 INTRODUCTION

In 1999 the first SUMO protease Ulp1 (Ubiquitin-like protease 1) was characterised in *Saccharomyces cerevisiae*. However unlike the SUMO conjugating enzymes Ubc9 and SAE1/2, which are homologous to ubiquitin conjugating enzymes, Ulp1 bears no sequence homology to known de-ubiquitinating enzymes (DUBs) or ubiquitin C-terminal hydrolases (UCH). Instead, Ulp1 is distantly related to adenovirus processing proteases [57]. Homology is confined to a C-terminal region in which all three of the catalytic residues from the adenovirus type 2 protease are conserved as well as an invariant glutamine (H, D, Q, C) (further termed catalytic domain). The adenovirus protease 2 and other related viral proteases process proteins with a Gly-Gly-X motif. The homology between Ulp1 and viral proteases probably represents a conserved mechanism for cysteine proteases to recognize and cleave after a di-glycine motif.

The sequence of the catalytic domain of Ulp1 was used to search the ENTREZ protein sequence database for related human proteases. Seven

human proteins were discovered which contained a conserved region homologous to the catalytic domain of Ulp1. An alignment of the conserved regions shows that the catalytic triad of Asp, Cys, and His is conserved (Fig. 4). Table 1 shows the homology between the catalytic domains of the human proteases and the catalytic domain of Ulp1. Of these seven proteases the most highly conserved is 35 % identical and the least conserved is 25 % identical to the catalytic domain of Ulp1. Two of the proteases, SENP7 and SENP6 (further termed SUSP1) have insertions within the catalytic domain, which is reflected in their gap scores of 23 % and 22 % respectively.

	% Identity	% Homology	%GAPS
SENP1	35	52	6
SENP2	33	50	11
SENP3	29	47	7
SENP5	30	49	8
SENP7	31	48	23
SUSP1/SENP6	28	45	22
NEDP1/SENP8	25	38	9

Table 1: Homology of SENPs and NEDP1 catalytic domains relative to the catalytic domain of ULP1

3.2 Results

As part of a collaboration, cDNAs for all seven of the putative SUMO proteases identified in the database search were isolated. cDNA libraries were screened by PCR to identify clones containing each of the proteases and positive clones were then sequenced to obtain the 5' and 3' ends of the longest inserts. RACE was performed on cerebellum cDNA to verify the 5' end of each protease. PCR analysis of cDNA from human tissues was used to verify that each of the proteases was expressed. Site-directed mutagenesis was used to mutate the putative active site cysteine to an alanine for each of the proteases. The full-length wild type (wt) proteases, as well as active site mutants (mut), were cloned into mammalian expression vectors for further study.

To determine the substrate specificity of these proteases *in vivo*, plasmids expressing each wt and active site mutant protease were co-transfected into COS7 cells along with plasmids expressing HA tagged SUMO-1, SUMO-2, or SUMO-3. As a joint experiment M. Tatham and I transfected cos7 cells with HA-SUMO and putative SUMO proteases. When HA-tagged SUMO is expressed in COS7 cells, it is conjugated to a range of cellular substrates that can be visualised as a SUMO ladder by Western blotting using an anti-HA specific antibody (Fig. 5). Deconjugation of SUMO

substrates can be demonstrated by loss or reduction of the SUMO conjugation ladder. When expressed in cells along with HA tagged SUMO, SENP1 and SENP2 were found to deconjugate SUMO-1, SUMO-2, and SUMO-3 from a broad range of substrates in this system as indicated by changes in the SUMO conjugation ladder (Fig. 5). However the mutant proteases, in which the active site cysteine was mutated to an alanine, were unable to deconjugate SUMO, thus demonstrating the requirement of this cysteine for catalytic activity. Previously SENP1 was characterised and published as a SUMO protease [69], which is confirmed by these data. SENP2 however was unpublished at the time and was chosen for further characterisation.

SENP3 is 83 % identical to a mouse protease, SMT3IP1, that was previously demonstrated to be a SUMO specific protease [68]. When expressed in cells along with tagged SUMO, human SENP3 was found to deconjugate SUMO-3 and to a lesser extent SUMO-2, but was ineffective or unable to deconjugate SUMO-1 (Fig. 6a). The cysteine to alanine mutant was catalytically inactive in this assay. In order to characterise SENP3 a peptide from the N-terminal domain was used to generate rabbit polyclonal antibodies specific for SENP3. To establish the subcellular localisation of SENP3 HeLa cells were transfected with SENP3 and stained with anti-SENP3 antibody. The majority of the expressed SENP3 was localised to the

nucleoli, but a small fraction was found free in the nucleoplasm (Fig. 6b). The possibility exists that the localisation of SENP3 restricts the access of SENP3 to a subset of SUMO modified substrates and is responsible for the lack of deconjugation seen in the SUMO-1 ladder. Alternatively elements of the N-terminal domain may inhibit or facilitate the deconjugation of a certain set of SUMO substrates.

The putative SUMO proteases SENP5 and SENP7 were also tested for the ability to deconjugate SUMO in COS7 cells. Two different splice variants of SENP7 were tested, a long variant (lv) and a short variant (sv). Transfection of SENP5 or SENP7 into cells did not result in a significant or reproducible change in the SUMO conjugation ladder (Fig. 7). Neither SENP5 nor SENP7 could be convincingly shown to be SUMO specific proteases in this assay. One possibility for this is that some SUMO proteases may be expressed in an inactive form and require activation. It is also possible that SUMO proteases exist which are highly specific even when over-expressed; in this case it would be difficult to observe the deconjugation of a single SUMO substrate in the presence of many other SUMO modified proteins. Alternatively the remaining proteases may not be SUMO specific proteases.

The least well-conserved protease, NEDP1, was predicted to be a SUMO protease based on sequence similarity to the Ulp1 catalytic domain. However NEDP1 was found to be inactive in SUMO processing and deconjugation assays *in vitro*. When co-transfected with HA-SUMO-1, -2, -3 into COS7 cells, no significant differences in the SUMO conjugation profiles were observed (Fig. 8).

NEDD8/Rub1 is another small ubiquitin-like modifier with a conjugation pathway analogous to ubiquitin conjugation. NEDD8 is 56 % identical and 76 % similar in sequence to ubiquitin and is conjugated to the cullin family of proteins. Although NEDD8 shows very low sequence homology to SUMO, the structures of both proteins are similar and contain the ubiquitin superfold [39, 120]. For this reason, we decided to test NEDP1 against NEDD8 (further discussed in Chapter 4). The unexpected discovery of NEDP1 as a NEDD8 specific protease supports the hypothesis that putative SUMO proteases that are inactive in SUMO assays may be specific for other small ubiquitin-like modifiers.

Previous research in our lab was unable to demonstrate that SUSP1 was a SUMO specific protease. Bacterially expressed GST-SUSP1 fusion protein was inactive in SUMO-1, -2, and -3 processing assays, and was also unable to deconjugate various ^{35}S or ^{125}I labelled SUMO modified substrates.

In addition, neither baculovirus expressed nor *in vitro* translated SUSP1 was active in similar processing or deconjugation assays. Expressed SUSP1 from mammalian cells was also inactive in all SUMO deconjugation assays. This previous research raised the possibility that SUSP1 is specific for ubiquitin or other small ubiquitin-like modifiers. In order to determine the specificity of SUSP1, GST-SUSP1 catalytic domain (CD) was purified from bacteria, incubated with NEDD8 precursor or ubiquitin precursor, and the reaction products were fractionated by SDS-PAGE and stained with Coomassie Blue (Fig. 9). NEDD8 and ubiquitin precursors were constructed with additional artificial C-terminal tags in order to more easily monitor the mass changes that would result from precursor processing. In the event of a mass change in the precursor, mass spectrometry would be used to confirm precise C-terminal processing. As positive controls NEDP1 and ubiquitin C-terminal hydrolase(CTH) were used to process the NEDD8 and ubiquitin precursors respectively. The SUSP1 catalytic domain was unable to process either the NEDD8 precursor or the ubiquitin precursor. As a result of purification a small fraction of the precursors were cleaved by endogenous exopeptidases, these breakdown products are indicated by '*'.

3.3 Discussion

The primary sequence alignment of the catalytic domains of the seven predicted SUMO proteases was used for phylogenetic analysis. The tree generated by the alignments splits the proteases into four subgroups (Fig. 10). One group contains SENP1 and SENP2, both of which deconjugate SUMO from a broad range of substrates *in vivo*. The closest related group to SENP1 and SENP2 contains SENP3 and SENP5. SENP3 could only deconjugate a fraction of SUMO-3 modified substrates even when over-expressed. Of the seven proteases studied SENP5 is most closely related to SENP3, but didn't conclusively deconjugate SUMO substrates when expressed in HeLa cells.

NEDP1 was not grouped with any of the other proteases, which reflects the fact that it was the least related to the other proteases. The surprising result that NEDP1 was a NEDD8 specific protease, even though it was initially predicted to be a SUMO specific protease based on sequence alignment, raises the possibility that SENP5, SENP7, and SUSP1 might not be SUMO proteases.

In 2000 Kim et. al reported that SUSP1 was a SUMO specific protease, based on characterisation of partially purified lysates from bacteria

expressing SUSP1 that were able to process a SUMO precursor [121]. However partially purified lysates could contain a number of exopeptidases that would act on a SUMO precursor. In order to conclude that the activity from the lysates was attributable to SUSP1, an appropriate control of lysates from bacteria expressing SUSP1 catalytically inactive mutant showing no processing would be required. Given the lack of appropriate controls in the SUSP1 characterisation, the specificity of SUSP1 has yet to be proven. SENP7 and SUSP1 are grouped together on the tree and lie between the known SUMO protease sub-groups and the NEDD8 protease NEDP1. Their position in the tree, in conjunction with lack of any clear SUMO deconjugating activity *in vivo*, would support the hypothesis that SENP7 and SUSP1 are proteases for other small ubiquitin-like modifiers.

Other small ubiquitin-like protein modifiers are also conjugated in a manner analogous to ubiquitin and SUMO. Some of these small modifiers bear high sequence homology to ubiquitin (NEDD8 58 % identical) and others do not (Apg12 (20%), URM1 (18 %), SUMO (18%)). Analysis of the tertiary structures of NEDD8, SUMO, and AUT7 reveals a common ubiquitin super-fold [39, 104, 120]. To date all the E1 and E2 conjugation enzymes for small ubiquitin-like modifiers share some sequence homology, suggesting a common structural mechanism for interacting with the ubiquitin super-fold structure. It is likely that the deconjugation proteases for these

small ubiquitin-like modifiers might also share some sequence homology. Some of the proteases may come from the proteases already designated as ubiquitin specific such as UBP43(USP18), which is now known to also be a protease for ISG15 [93], and others might emerge from proteases predicted to be SUMO specific proteases. One way of searching for possible substrates for SENP7 and SUSP1 would be to look within the families of ubiquitin-like proteins for modifiers that terminate in a di-glycine motif when mature and which have been shown to modify cell substrates in a dynamic manner. Although many ubiquitin-like proteins have yet to be thoroughly characterised, URM1, FAT10, FUB1, and ISG15 are possible candidate substrates for the uncharacterised SENPs.

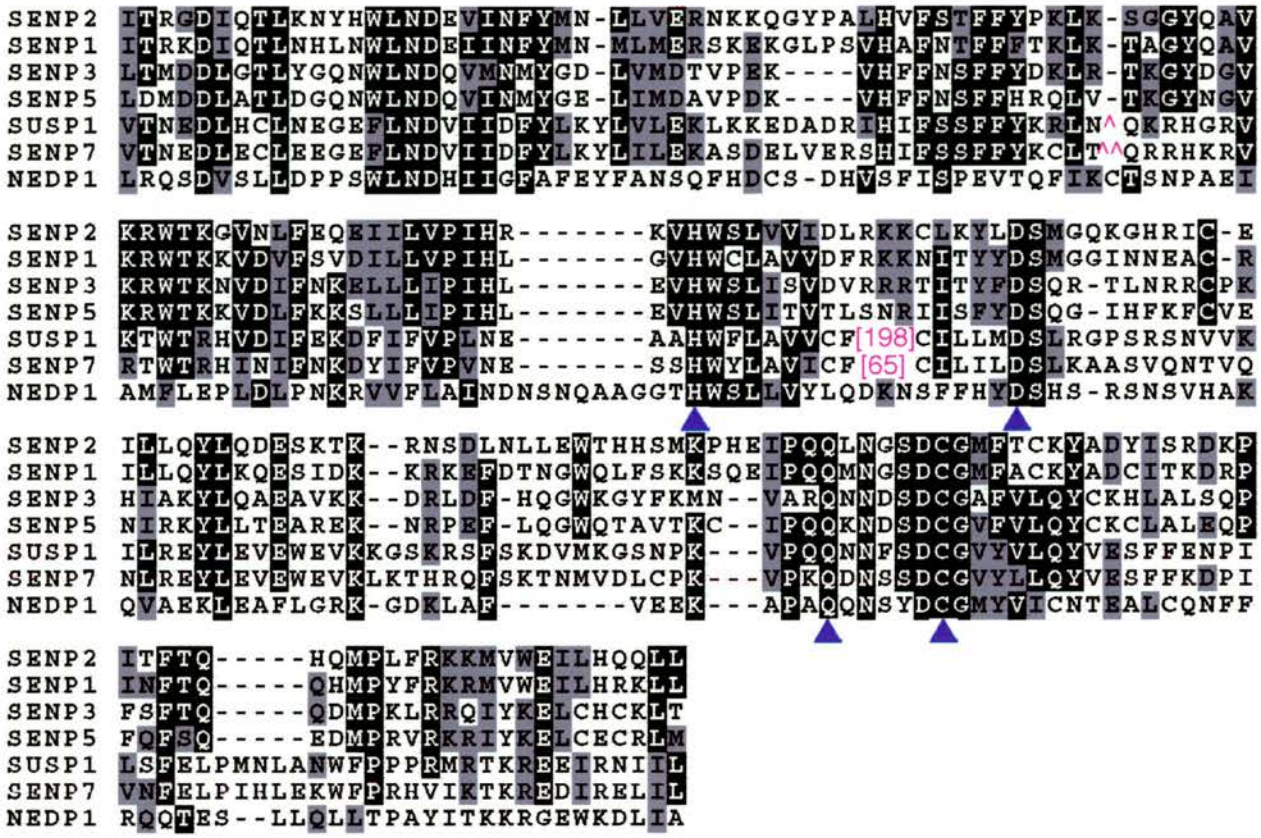

Figure 4: Primary sequence alignment of predicted human SUMO specific proteases. Primary sequence alignments of SENP1, SENP2, SENP3, SENP5, SENP7, SUSP1, and NEDP1. Residues which are identical or conserved in more than 50 % of the proteases are indicated by black shading and grey shading respectively. The catalytic triad of His (H), Asp (D), Cys (C), and an invariant Gln (Q) are indicated (▲). 15 (^) and 16 (^^) amino acid segments have been removed from SUSP1 and SENP7 respectively. All other segments deleted are indicated by the length of the deletion in [ ].

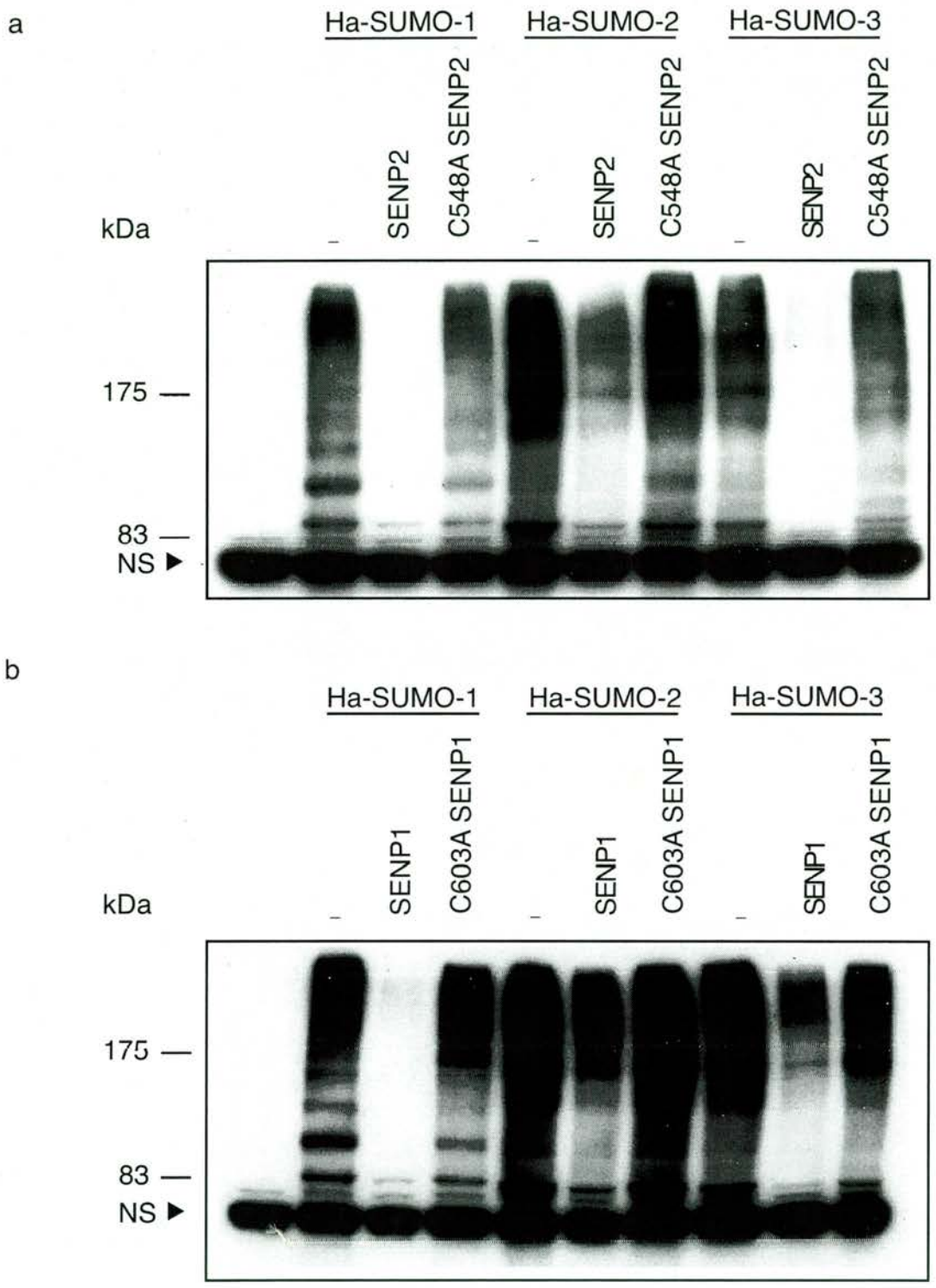

Figure 5: SENP2 and SENP1 are SUMO specific proteases *in vivo*.

COS7 cells were transfected with either empty pcDNA3 (-), or plasmids expressing HA-SUMO-1, HA-SUMO-2, HA-SUMO-3, SENP2, C548A SENP2, SENP1, or C603A SENP1 as indicated. Anti-HA Western blots were performed as detailed in methods and materials. A non-specific (NS) band is indicated along with molecular weight markers.

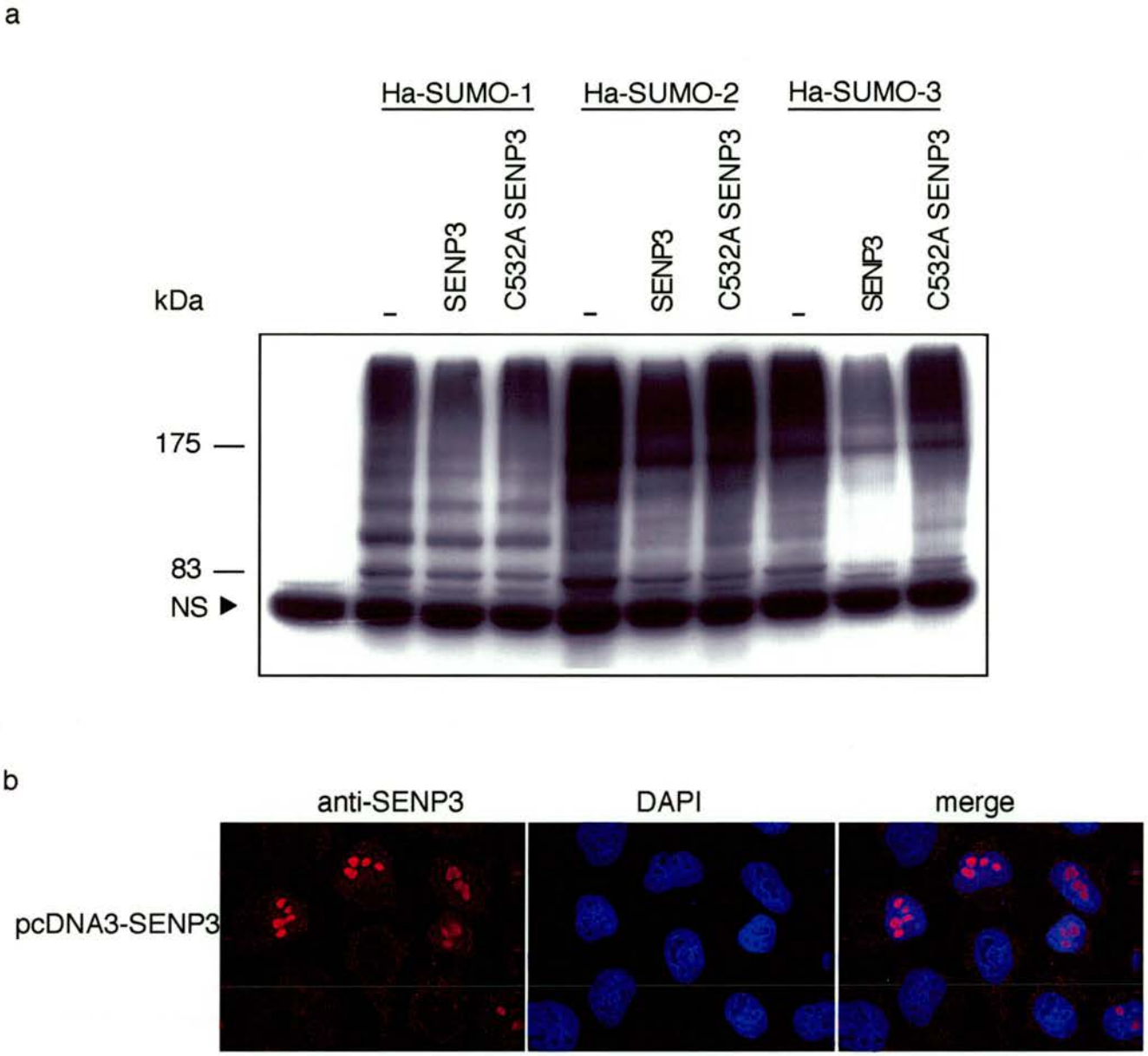

Figure 6: SENP3 is a nucleolar SUMO specific protease *in vivo*.

a. COS7 cells were transfected with either empty pcDNA3 (-), or plasmids expressing HA-SUMO-1, HA-SUMO-2, HA-SUMO-3, SENP3 or C532A SENP3 as indicated. Anti-HA Western blots were performed as detailed in methods and materials. A non-specific (NS) band is indicated along with molecular weight markers. b. Hela CD cells were transfected with pcDNA3-SENP3. Cells were stained with anti-SENP3 Ab and DAPI as indicated. SENP3 was localised to the nucleolus, but was also present in the nucleoplasm at lower levels.

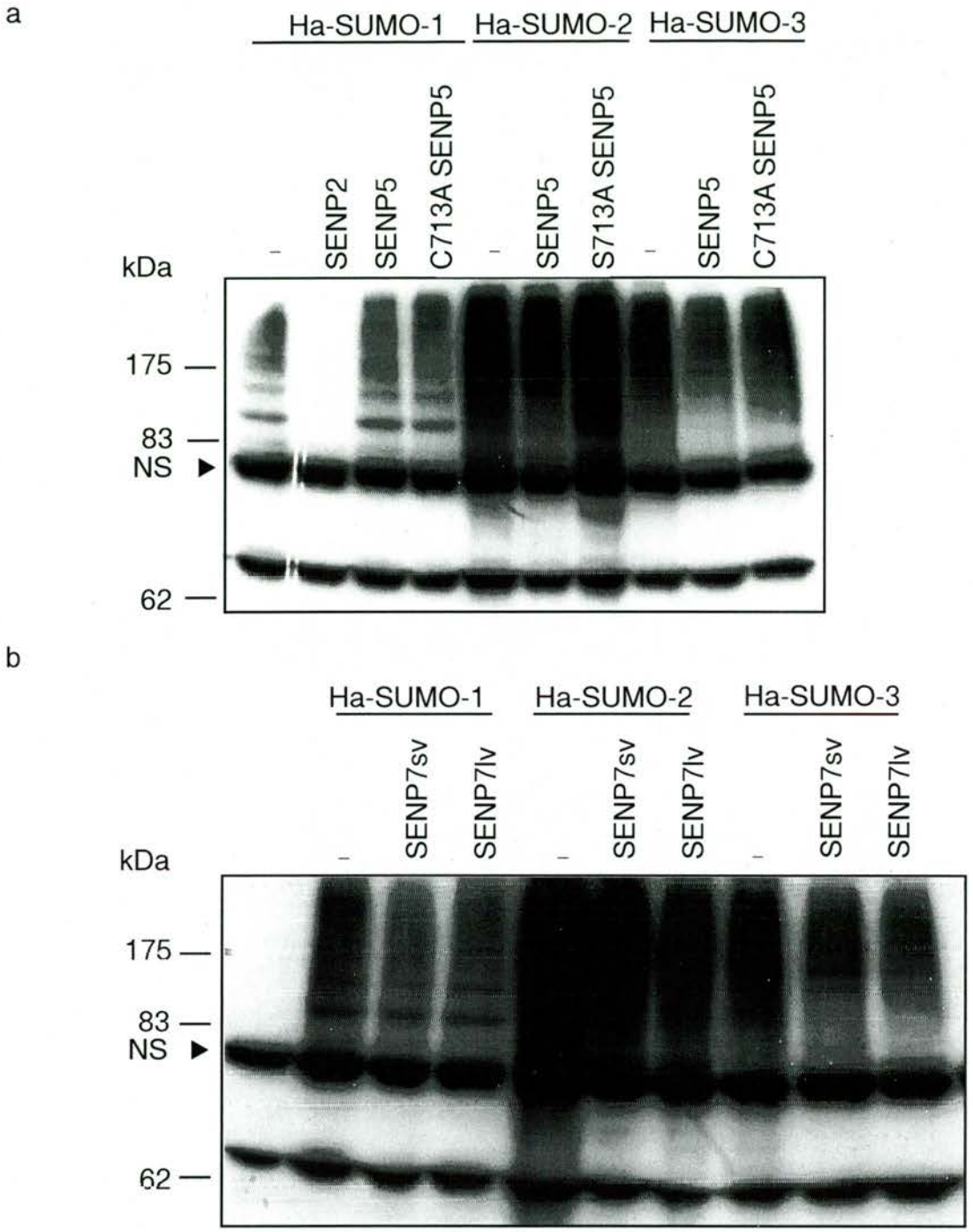

Figure 7: SENP5 and SENP7 do not significantly alter SUMO conjugation *in vivo*.

COS7 cells were transfected with either empty pcDNA3 (-), or plasmids expressing HA-SUMO-1, HA-SUMO-2, HA-SUMO-3,SENP7sv, SENP7lv, SENP5, or C713A SENP5 as indicated. Anti-HA Western blots were performed as detailed in methods and materials. A non-specific (NS) band is indicated along with molecular weight markers.

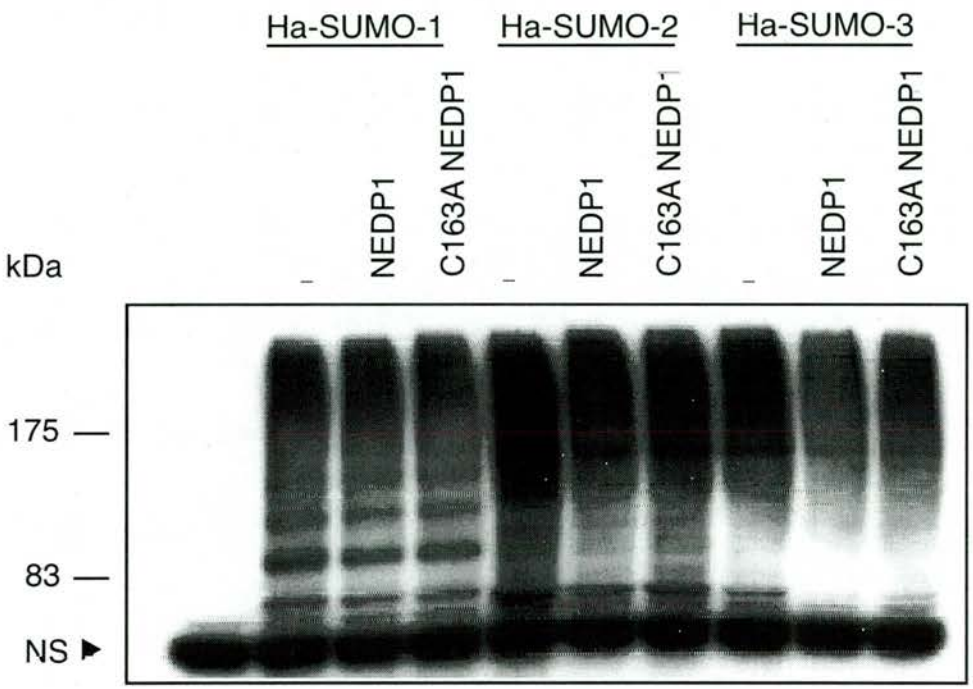

Figure 8: NEDP1 does not deconjugate SUMO *in vivo*.

COS7 cells were transfected with either empty pcDNA(-), or plasmids expressing HA-SUMO-1, HA-SUMO-2, HA-SUMO-3, NEDP1, or C163A NEDP1 as indicated. Anti-His Western blots were performed as detailed in methods and materials. A non-specific (NS) band is indicated along with molecular weight markers.

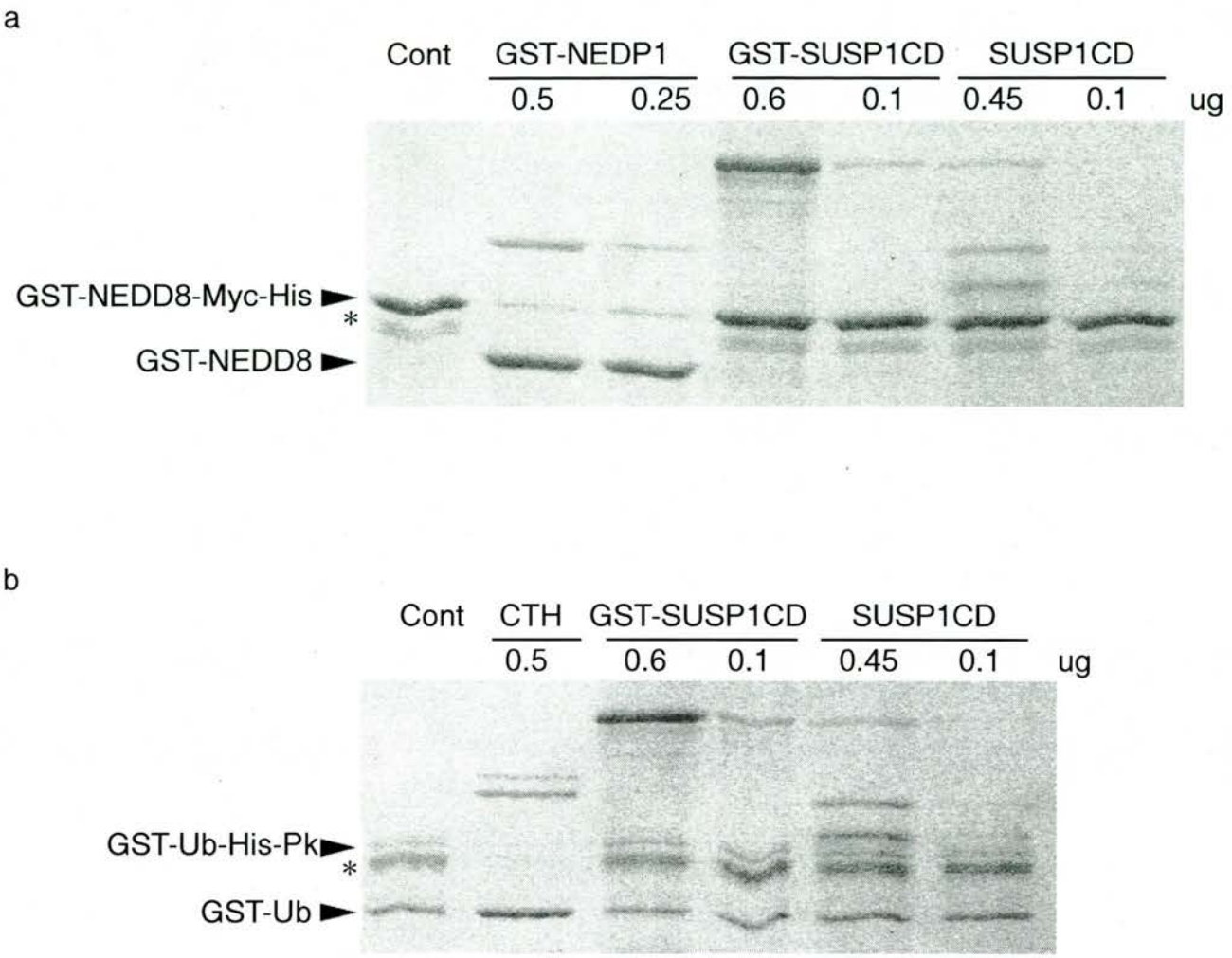

Figure 9: SUSP1does not process NEDD8 or Ub precursors *in vitro.*

a. 2 ug of GST-Ub-H-PK was incubated with Ubiquitin C-terminal hydrolase (Ub-CTH), GST-SUSP1CD, or SUSP1CD as indicated. b. 2 ug of GST-NEDD8-Myc-His was incubated with GST-NEDP1, GST-SUSP1CD, or SUSP1CD as indicated. All reaction products were fractionated by 12.5 % polyacrylamide gels containing SDS and Coomassie stained. Degradation products present in the purified precursors are marked by '*'.

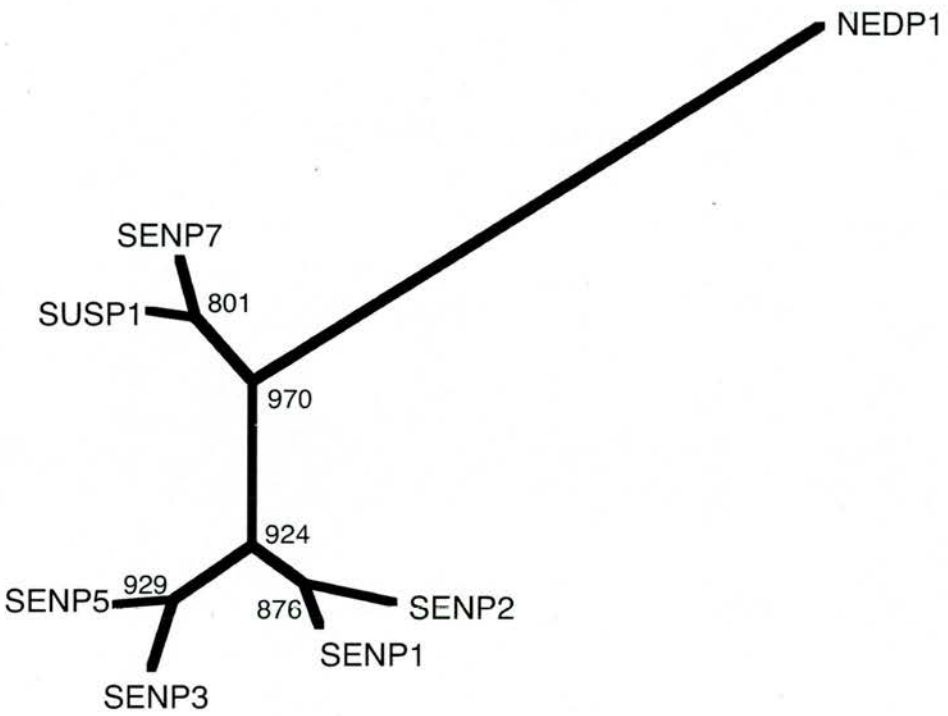

Figure 10: Phylogenetic analysis the seven human homologues to *S. cerevisiae* Ulp1. A primary sequence alignment of the catalytic domains of human proteases homologous to Ulp1 was used to generate this tree. The tree is an unrooted phylogram constructed using neighbor-joining method with bootstrap values displayed as a percentage of 1000 replications.

4. CHARACTERISATION OF NEDP1

4.1 INTRODUCTION

Ubiquitin and ubiquitin-like proteins are conjugated to acceptor lysine residues on target proteins and have diverse effects on the modified proteins. While conjugation of multiple copies of ubiquitin targets proteins for degradation via the proteasome, addition of SUMO or NEDD8 can alter the function of the conjugated protein [96]. Formation of the isopeptide bond between the C-terminal glycine of the ubiquitin-like protein and the ε-amino group of lysine in the modified protein is accomplished by an enzymatic cascade that typically involves three enzymes, E1 (activating enzyme), E2 (conjugating enzyme) and E3 (ligase). In the case of NEDD8, or its yeast equivalent Rub1, the ubiquitin-like protein is activated by a heterodimeric complex of APP-BP1 and Uba3, and is conjugated to substrates by the conjugating enzyme Ubc12 [122, 123]. Although an E3 ligase specific for NEDD8 has yet to be identified, the parallels with the ubiquitin and SUMO systems indicate that it is likely such an activity will exist. To date the main targets for NEDD8 modification that have been described are members of the Cullin family of proteins [122-128]. Cullins are important components of multiple ubiquitin ligase complexes that also contain Rbx1, Skp1 (or homologue) and a substrate receptor protein that contains an F-box motif.

These SCF-like complexes are responsible for the ubiquitination of proteins such as phosphorylated IκBα and hydroxylated HIF1α. Recently, p53 and mdm2 have been shown to be neddylated. Mdm2 was discovered to promote NEDD8 modification of p53 which resulted in an inhibition of p53 transcriptional activity [129]. Genetic experiments in yeast and plants indicate that Rub1 (NEDD8) modification is important for SCF ubiquitin ligase activity [122, 130-132], while biochemical experiments demonstrated that NEDD8 modification of Cul-1 was responsible for recruitment of the Ubc4-ubiquitin thioester to the SCF complex [133]. It has been demonstrated that the Rbx1 component of SCF complexes activates Ubc12 mediated NEDD8 modification of Cdc53 and Cul2 [126]. While a complete Rub1 (NEDD8) modification pathway is not required for the viability of *Saccharomyces cerevisiae* [122, 131] it is required for viability of *Schizosaccharomyces pombe* [132]. In ts41 hamster cells a temperature sensitive mutation in APP-BP1 results in cell cycle defects and indicates that NEDD8 modification is required for entry into mitosis and inhibition of entry into S-phase [134, 135]. Deletion of the Uba3 gene in mice leads to embryonic lethality and establishes an essential function of NEDD8 modification in higher eukaryotic cells [133]. *In vitro* ubiquitination of $p27^{Kip1}$ in cell extracts requires a continuously active NEDD8 conjugation system, thus suggesting the existence of isopeptidases that are capable of hydrolysing NEDD8 from Cul1 [136]. It is therefore likely that the extent of

NEDD8 modification is controlled by a dynamic equilibrium between NEDD8 modification, mediated by APP-BP1/Uba3 and Ubc12, and NEDD8 removal catalysed by NEDD8 specific proteases. A NEDD8 specific protease activity has been reported to be associated with the COP9 signalosome, and while a metalloprotease motif in Jab1/Csn5 is required for this activity, the isolated protein did not display NEDD8 protease activity [137, 138]. NEDD8, like all ubiquitin-like proteins, is synthesised as an inactive precursor and has to be processed by a NEDD8 specific protease to expose the diglycine motif at the C-terminus that is required for conjugation.

The aims of this research were: to express and purify NEDP1 from bacteria to verify NEDD8 specificity in a recombinant system; express NEDP1 and a catalytically inactive mutant in cells to test specificity; and to investigate the function of NEDP1 using siRNA.

4.2 Results

4.2.1 Cloning of cDNA encoding NEDP1

The NEDP1 coding region of 212 amino acids is composed of only 1 exon (data not shown) containing the complete coding region of the gene. Recognizable within the NEDP1 coding sequence is a 201 amino acid domain that is also present in the family of SUMO proteases. This domain contains the putative catalytic triad of histidine, aspartate and cysteine along with an invariant glutamine residue. NEDP1 has approximately 20% identity to the yeast and human Ulps (Fig. 4) but differs from other members of the yeast and human family of Ulp proteases in that the protein consists of just the protease domain with only short N and C terminal extensions. Interrogation of expressed sequence databases with the putative protease domain of NEDP1 revealed a highly conserved family of proteins that are present in all eukaryotes from *S. pombe* to *H. sapiens* (Fig. 11). Two NEDP1 like proteins are present in *S. pombe*, for clarity only one is shown.

4.2.2 Processing of GST-NEDD8 but not Ub or SUMO by NEDP1

To determine the biochemical activity of NEDP1, a 212 amino acid polypeptide corresponding to the complete coding region was expressed as

a fusion with glutathione S-transferase in bacteria. GST-NEDP1 was isolated by affinity chromatography and the purified proteins analysed by electrophoresis in a polyacrylamide gel containing SDS. Coomassie Blue staining revealed that the purified GST-NEDP1 was essentially homogenous (Fig. 12a). Although NEDP1 was expected to be a SUMO specific protease there was no evidence of activity against full length SUMO-1, SUMO-2 or SUMO-3 (Fig. 8).

Like SUMO, ubiquitin and NEDD8 are synthesized as inactive precursors that need to be precisely cleaved by proteases at a C-terminal diglycine motif prior to conjugation to their substrates. Recombinant GST-NEDD8-Myc-His, GST-Ub-H-P and full length SUMO-1 were expressed and purified from bacteria to provide model precursor substrates for NEDP1. To establish the specificity of NEDP1, 2 μg of SUMO-1, GST-Ub-H-P, or GST-NEDD8-Myc-His was incubated with 0.5 μg of GST-NEDP1 or a catalytically inactive form of the enzyme, GST-NEDP1mut. Processing of GST-NEDD8-myc-His6 and GST-Ub-H-P precursors were determined by Western blotting against the His and Pk tags respectively. NEDP1 was unable to process either SUMO-1 or Ub, but efficiently processed NEDD8 (Fig. 12b). To confirm that NEDP1 cleaved NEDD8 precisely after the second glycine in the GG motif a 6His version of NEDD8 was processed with NEDP1 and products of the cleavage reaction analysed by electrospray ionization mass

spectrometry (Fig. 13). The molecular mass of the processed NEDD8 corresponds precisely to cleavage after the second G in the diglycine motif. Thus NEDP1 is a NEDD8 processing enzyme. To determine the efficiency of NEDP1 processing GST-NEDD8-Myc-His was incubated with a range of concentrations of purified GST-NEDP1 and the reaction products were analysed by SDS-PAGE followed by Coomassie Blue staining (Fig. 14a). In the presence of 6 μg GST-NEDD8-Myc-His, 2 ng of NEDP1 is capable of processing greater than 50 % of the substrate in 3 h at 37 °C.

The sequence of NEDP1 suggests that it is a cysteine protease with the active site cysteine located at residue 163. To address this point a version of NEDP1 was created in which cysteine 163 was changed to alanine (NEDP1 mut). This protein was expressed in bacteria and purified to homogeneity (Fig. 12a). GST-NEDP1mut, in which putative active site cysteine 163 is mutated to an alanine, was unable to process NEDD8 (Fig. 12b). To verify that NEDP1 is a cysteine protease, processing assays were set up in the presence of NEM or EDTA. Although GST-NEDP1 processing activity was inhibited by 2.5 mM of NEM, addition of EDTA up to 50 mM had no effect on processing in this assay (Fig. 14b). Together with the lack of activity displayed by the C163A mutant these data indicate the NEDP1 is a NEDD8 specific cysteine protease.

Current research has shown a deneddylation activity associated with the COP9 signalosome [137, 138], although no deneddylation activity for purified recombinant subunits has been shown. To determine if NEDP1 interacted with the COP9 signalosome, NEDP1 was immunoprecipitated from HeLa cell lysates as detailed in 'Materials and Methods', followed by elution of NEDP1 from beads and analysis by SDS-PAGE and Western blotting. Pre-immune serum was used as a control. Previous research has shown that subunits of the COP9 signalosome co-purify [139]. For this reason Western blotting against one subunit was determined to be a reasonable indication of the presence of the COP9 signalosome. The eluate was probed with anti-csn7 to detect interaction with the CSN. csn7 was not detected in the NEDP1 immunoprecipitation under these conditions, although csn7 was present both in the raw lysates and in the unbound (UB) fraction (Fig. 15). To confirm that NEDP1 was being removed from the lysates, the unbound fraction of lysates incubated with pre-immune serum or NEDP1 antibody were probed for NEDP1. NEDP1 is present in the unbound fraction of the immunoprecipitation using pre-immune serum, but was absent from the unbound fraction that had been immunoprecipitated with NEDP1 antibody indicating that NEDP1 was efficiently immunoprecipitated.

4.2.3 NEDP1 deconjugates NEDD8 from Cul-2 in vitro

To determine whether NEDP1 is capable of acting as an isopeptidase in the presence of unrelated proteins an *in vitro* deconjugation assay was designed. Previously it has been demonstrated that cullin-4A could be conjugated to GST-NEDD8 during a transcription/translation reaction in rabbit reticulocyte lysates [123]. Cul-2 was therefore labelled with ^{35}S-methionine and conjugated to GST-NEDD8 during an *in vitro* transcription, translation reaction in rabbit reticulocyte lysates. Conjugation was terminated by incubation with iodoacetamide that also served to inhibit any endogenous NEDD8 proteases. After quenching of the iodoacetamide with β-mercaptoethanol the reaction products were used as substrates for NEDP1. Although Cul-2 has one major translated product there are two lower molecular weight species that may represent internal initiations. Full-length Cul-2 as well as incomplete translations were utilised by the conjugation machinery in the lysates for conjugation to GST-NEDD8. Incubation of the modified products with NEDP1 resulted in conversion of the modified to the unmodified form of Cul-2 (Fig. 16). Thus NEDP1 displays isopeptidase activity on a natural substrate in the presence of a large excess of unrelated proteins (from rabbit reticulocyte lysate extract).

4.2.4 NEDP1 deconjugates NEDD8 from modified Cul4 in vivo

To determine whether NEDP1 was active against a specific cullin family member *in vivo*, the cDNA encoding NEDP1 was transfected into COS7 cells along with expression plasmids for His-NEDD8 and Cul-4A-Myc. Cells were lysed under denaturing conditions and the His-NEDD8 conjugates were purified from cell lysates using Ni^{2}+-NTA-agarose beads. Bound proteins were separated by SDS-PAGE and subjected to Western blotting with an anti-Myc monoclonal antibody. Transfection of Cul-4A-myc, His-NEDD8, and empty expression vector allowed the purification of a His-NEDD8 modified Cul-4A-myc. Transfection of these constructs in the presence of NEDP1 resulted in the absence of NEDD8 modified Cul-4A. Transfection of the catalytically inactive NEDP1mut did not affect the modification state of Cul-4A. Western blotting of the unfractionated extract with anti-Myc antibody revealed that Cul-4A expression was not affected by NEDP1 or NEDP1 mut (Fig. 17). Thus NEDP1 is capable of acting as a NEDD8 specific cysteine protease that can deNEDDylate cullins *in vivo.*

4.2.5 Substrate specificity of NEDP1

To determine if NEDP1 displays a preference for particular NEDD8 conjugated substrates *in vivo* a NEDP1 expression vector was transfected

into COS7 cells along with the expression plasmid for His-NEDD8. As a control His-NEDD8 was transfected with empty expression vector or a vector encoding C163A NEDP1 where the cysteine residue predicted to supply the active site nucleophile was changed to alanine. 24 hrs post transfection NEDD8 modified conjugates were identified by Western blotting with an anti-His antibody.

Transfection of His-NEDD8 leads to the appearance of high molecular weight conjugates that disappear when NEDP1 is co-transfected. Co-transfection of catalytically inactive C163A NEDP1 does not alter the pattern of NEDD8 modified conjugates (Fig. 18). Therefore NEDP1 is active as a NEDD8 protease *in vivo* and is capable of deconjugating NEDD8 from all modified proteins detected *in vivo*.

4.2.6 Depletion of NEDP1 from HeLa cells results in changes in cell morphology and NF-kB activation

To further study the function of NEDP1 siRNA were generated against NEDP1 and the efficiency of NEDP1 depletion was determined in HeLa57A cells. For analysis of NEDP1 protein levels a NEDP1 specific antibody was raised against recombinant NEDP1 in sheep. The resultant NEDP1 serum was affinity purified as detailed in 'Materials and Methods'. The affinity of the

purified antibody for endogenous NEDP1 was analysed using lysates from HeLa57A. The predicted mass of NEDP1 is 24 kDa which corresponds to a band present in the untransfected control lysates (Fig. 19). Identification of this band as endogenous NEDP1 was further supported by expressed NEDP1 migrating at approximately the same size. To determine the efficiency of NEDP1 protein knock-down, HeLa cells were transfected twice in a total volume of 500 μl with 80 nM then 50 nM RSC or NEDP1 siRNA followed by lysis, SDS-PAGE, and Western blotting with anti-NEDP1 antibody. NEDP1 siRNA treatment reduced NEDP1 protein levels by approximately 75 % compared to RSC siRNA treated cells. A non-specific band was used to control for protein loading.

Current research is revealing a role for SUMO in transcriptional repression [140]. Although neddylation has been implicated in controlling the activity of ubiquitin ligase complexes the possibility also exists that NEDD8 may be involved in transcriptional repression. NF-κB activation was chosen for investigation of the effect of NEDP1 depletion as its activation involves both SCF-ubiquitin ligase machinery and transcriptional activation. The effect of NEDP1 depletion on the NF-κB pathway was analyzed using a HeLa57A cell line, which has a stably integrated NF-κB luciferase reporter. HeLa57A cells were depleted of NEDP1 by transfecting cells twice with 80 nM then 50 nM of either RSC or NEDP1 siRNA in a total volume of 100 μl.

The cells were then stimulated with TNF for 6 h and harvested for analysis of NF-κB activation as detailed in 'Materials and Methods'. Data are presented as fold NF-κB activation (Fig. 20). RSC siRNA treated cells or untreated control cells were activated 20-30 fold by 10 ng ml^{-1} of TNF. NEDP1 siRNA treated cells were activated 80-90 fold under the same stimulation conditions. If NEDP1 depletion results in elevated NF-κB activation, then it is reasonable to predict that NEDP1 over-expression would inhibit NF-κB activation. To examine the effects of NEDP1 over–expression on NF-κB activation, HeLa cells were transiently transfected with an NF-κB reporter plasmid (p3enhConALuc) and either empty vector (cont), NEDP1, or NEDP1 mut plasmids. Over-expression of NEDP1 or NEDP1 mut did not cause a significant inhibition of NF-κB activation in this assay (Fig. 21).

During NEDP1 depletion experiments it was apparent that after the second transfection cells treated with NEDP1 siRNA, but not RSC siRNA, became elongated with a fibroblast like morphology when viewed with phase contrast microscopy (Fig. 22). Examination of the actin and microtubule cytoskeleton by fluorescence microscopy revealed a decreased number of actin stress fibers in NEDP1 siRNA treated cells and further confirms the elongated morphology of the cells (Fig. 23).

4.3 Discussion

Here NEDP1, a NEDD8 specific protease present in human cells is described. NEDP1 is sensitive to the alkylating reagent N-ethylmaleimide and site directed mutagenesis indicates that the active site nucleophile is cysteine 163. The protein is highly conserved throughout evolution and is approximately 40% identical over the protease domain to two predicted gene products present in *S. pombe*. NEDP1 has highly related homologues in most organisms for which sequence information is available, suggesting that the homologues are also NEDD8 proteases. Sequence comparisons indicate that NEDP1 is unrelated to deubiquitinating enzymes although both are part of the cysteine protease superfamily. Although NEDD8 is much more similar to ubiquitin than SUMO, NEDP1 displays sequence similarity to the SUMO specific proteases including an arrangement of proposed catalytic residues (His-Asp-Cys) also present in yeast Ulp1 [64]. This suggests that NEDP1 is part of a distinct cysteine protease subfamily that contains SUMO specific proteases along with adenoviral [141] and other viral proteases. However the structural relatedness of NEDP1 to this class of cysteine proteases awaits the determination of its structure. Bacterially expressed and purified NEDP1 cleaves the NEDD8 precursor precisely after the diglycine motif, but is unable to utilise ubiquitin or SUMO with C-terminal extensions, indicating that NEDP1 is highly specific for NEDD8. This is in

contrast to two previously described proteases which utilized both NEDD8 and ubiquitin as substrates [142, 143] . In addition to processing NEDD8 precursor to the mature form NEDP1 is also capable of acting as a NEDD8 isopeptidase by deconjugating NEDD8 from Cul2 *in vitro. In vivo*, expressed NEDP1 removes NEDD8 from Cul4A. While Cullins are the main substrates for NEDD8 modification described to date it is clear that exogenous NEDD8 is conjugated to a large number of high molecular weight proteins that have apparent molecular weights that are considerably in excess of that predicted from NEDD8 modified Cullins. The identity of these NEDD8 modified proteins remains to be determined, but NEDP1 is capable of removing NEDD8 from all of the modified proteins. Thus NEDP1 appears to be highly specific for NEDD8 but is not specific with regard to the modified substrate when over-expressed.

An important role for a deNEDDylating activity is in the COP9 signalosome mediated removal of NEDD8 from Cullins [144, 145]. The COP9 signalosome is an 8 subunit multiprotein complex that is similar to the "lid" of the proteasome [145]. Within the COP9 signalosome, the Jab1/Csn5 subunit contains a JAMM motif that is predicted to form the active site of a metalloprotease [146]. Jab1/Csn5 is required for the deNEDDylation activity of the COP9 signalsome but it was reported that the deNEDDylation activity was sensitive to alkylating agents [137, 138] thus suggesting the

involvement of a cysteine protease. To address the possibility of NEDP1 recruitment to the COP9 signalosome, NEDP1 was immunoprecipitated and Western blotted for subunit 7 of the COP9 signalosome. Although no interaction could be demonstrated under these experimental conditions, this does not exclude the possibility of NEDP1 recruitment to the COP9 signalosome.

The NEDP1 siRNA studies revealed two observations; a change in cell morphology into elongated fibroblast-like cells, and an elevation in NF-κB activation when cells were stimulated with TNF. The change in cell morphology was not unsurprising as neddylation has been implicated in control of the cytoskeleton [147]. The observation that NEDP1 depletion results in elevation of NF-κB activation is intriguing, but it is difficult to predict where in the NF-κB signaling pathway the effect is occurring. If NEDP1 depletion decreases the rate of precursor processing of NEDD8 then the effects observed could be the result of having a limited pool of NEDD8 for conjugation. Alternatively, if NEDD8 processing is not limiting then the effect could be due to absence of deneddylation of a particular substrate. Surprisingly, overexpression of NEDP1 wt and mut had little effect on NF-κB activation. It is possible that NEDP1 is directed to a substrate by another protein which is in limited supply or that endogenous NEDP1 is already in abundance. Currently the cullin family of proteins are the most well

characterized targets for neddylation, and the de-/neddylation state of cullins has been implicated in controlling the activity of E3 ligases. Depletion of NEDP1 could result in the change of activity of E3 ligase complexes that could cause an enhancement in NF-κB activation. The ability of NEDD8 to inhibit the transcriptional activity of p53 leads to the possibility that other transcription factors may be neddylated [129]. It is conceivable that a change in the neddylation state of a transcription factor could be responsible for the enhancement of NF-κB activation. Alternatively, the neddylation state of as yet uncharacterized NEDD8 modified proteins upstream in the signal transduction pathway could be responsible for the enhanced NF-κB activity.

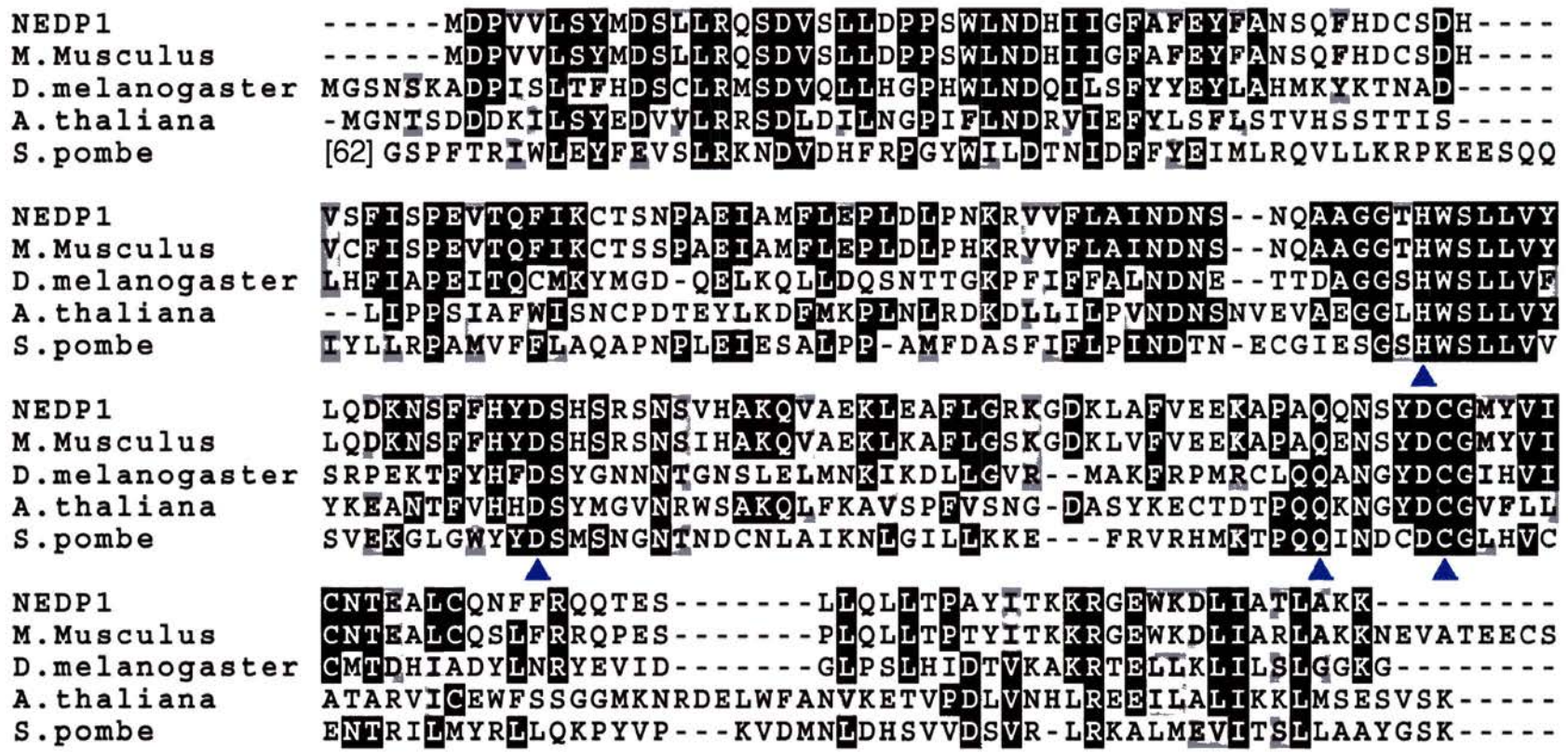

130

Figure 11: Conservation of NEDP1 between *M. musculus*, *D. melanogaster*, *A. thaliana*, and *S. pombe*

Primary sequence alignments of NEDP1 from *M. musculus*, *D. melanogaster*, *A. thaliana*, and *S. pombe*. The catalytic triad of His (H), Asp (D), Cys (C), and an invariant Gln (Q) are indicated (▲). Residues which are identical or conserved in more than 50 % of the proteases are indicated by black and grey shading respectively. An N-terminal deletion of 62 amino acids from the *S. pombe* protein is indicated in brackets. There is also another NEDP1 homologue in *S.pombe* which is not shown.

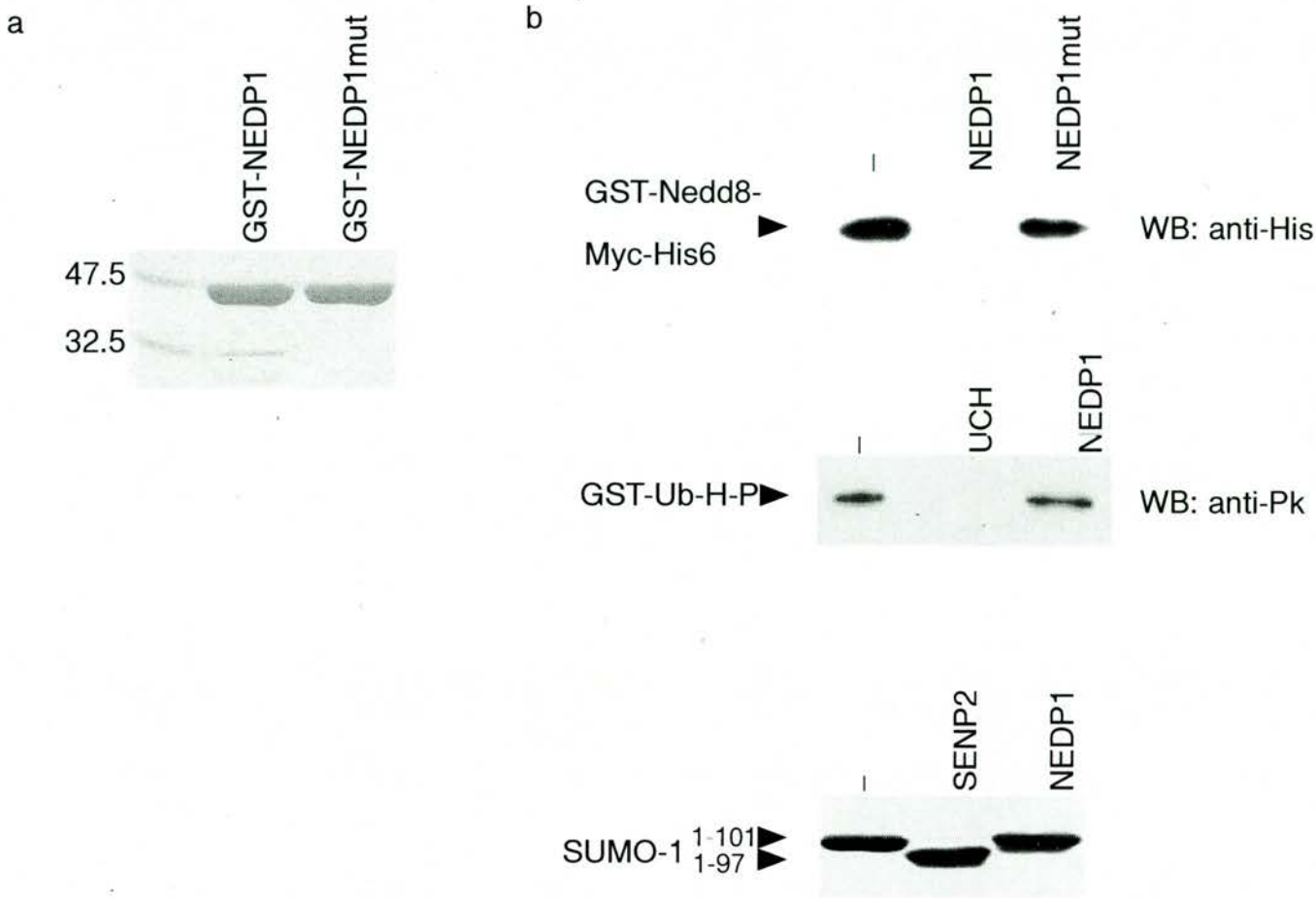

Figure 12: NEDP1 is a NEDD8 specific protease *in vitro*.

a. Coomassie-stained SDS-polyacrylamide gel containing 3 ug of recombinant purified NEDP1 and NEDP1mut as indicated. b. 2ug of GST-Ub-H-PK, GST-Nedd8-Myc-His6, or SUMO-1_{1-101} was incubated with 0.5 ug of GST-NEDP1, GST-NEDP1mut, SENP2 or Ubiquitin C-terminal hydrolase (UCH) as indicated. All reaction products were fractionated by 12.5 % polyacylamide gels containing SDS. NEDD8 and Ubiquitin processing assays were further subjected to Western blot using either anti-His antibody or anti-PK SV5 antibody as detailed under "Experimental Procedures". SUMO processing was analysed by Coomassie blue staining.

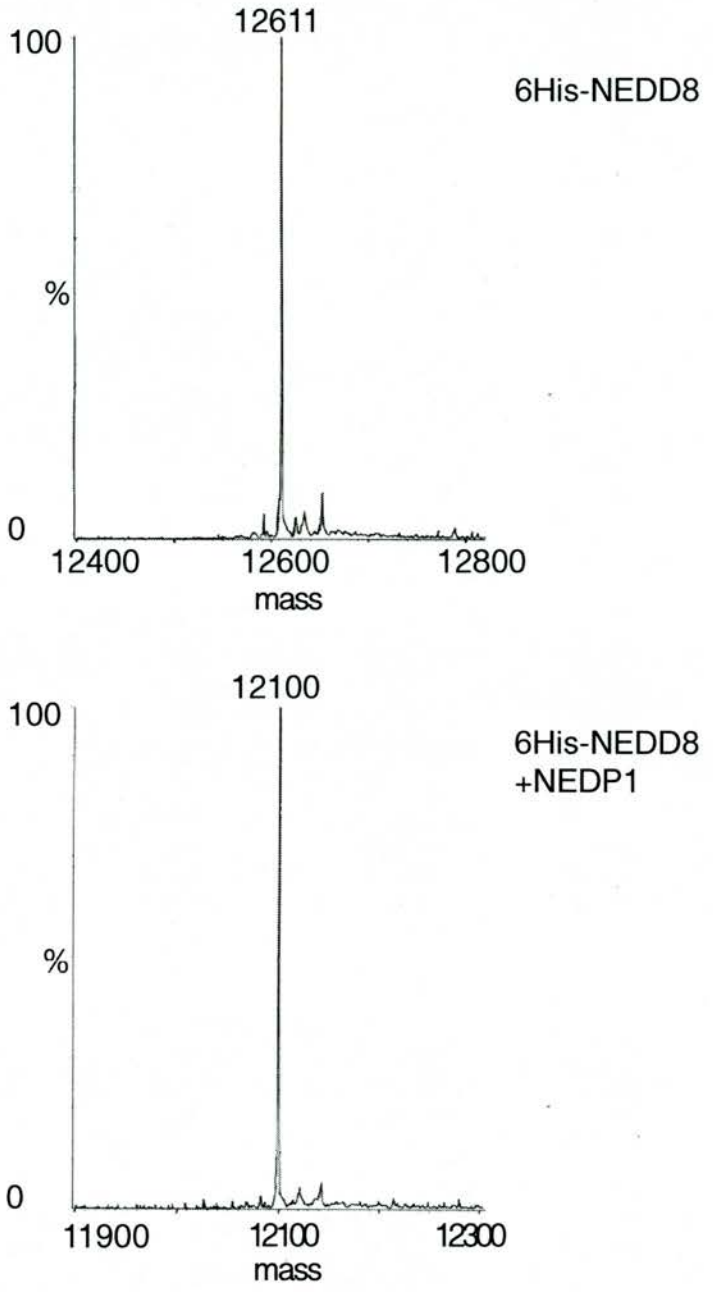

Figure 13: NEDP1 precisely processes the NEDD8 precursor to generate mature NEDD8. 6His-NEDD8 and 6His-NEDD8 processed with NEDP1 were analysed by electrospray ionisation mass spectrometry. Experimentally derived molecular masses are indicated. Calculated molecular mass for unprocessed 6His-NEDD8 is 12611.33 while that of 6His-NEDD8 terminating after the GG motif is 12099.75.

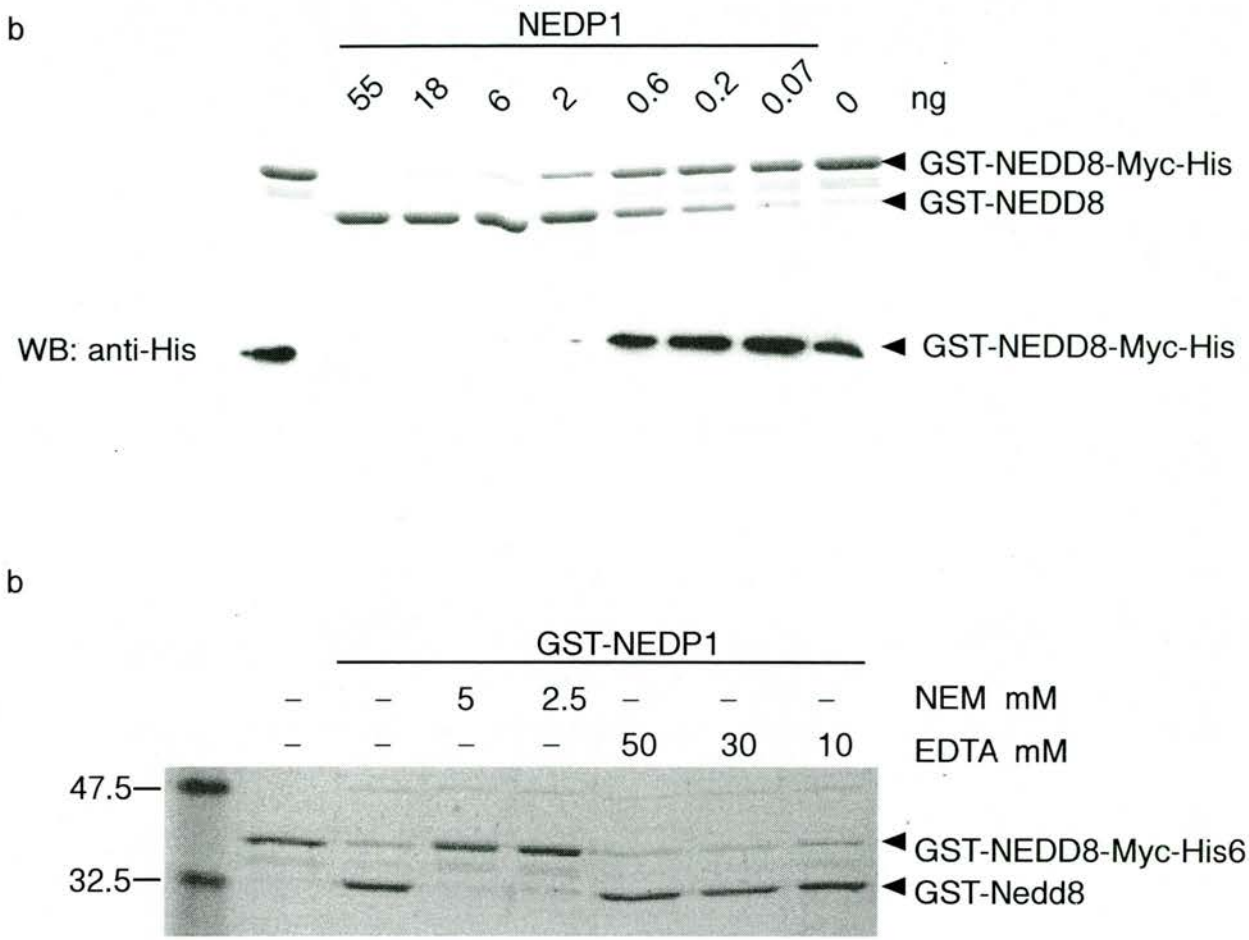

Figure 14: Processing of NEDD8 by NEDP1.

a. Coomassie-stained SDS-polyacrylamide gel showing 2 ug of full-length recombinant GST-NEDD8-Myc-His6 incubated with varying concentrations of GST-NEDP1 (166, 55, 18, 6, 2, 0.6, 0.2, 0.07 ng). The reaction products were further subjected to Western blot using anti-His antibody. GST-NEDD8-Myc-His6 and GST-NEDD8 are indicated.

b. Coomassie-stained SDS-polyacrylamide gel showing 1 ug of full-length recombinant GST-NEDD8-Myc-His6 incubated with 50 ng of GST-NEDP1 in the presence of either N ethylmaleimide (NEM), EDTA, or buffer. GST-NEDD8-Myc-His6 and GST-NEDD8 are indicated.

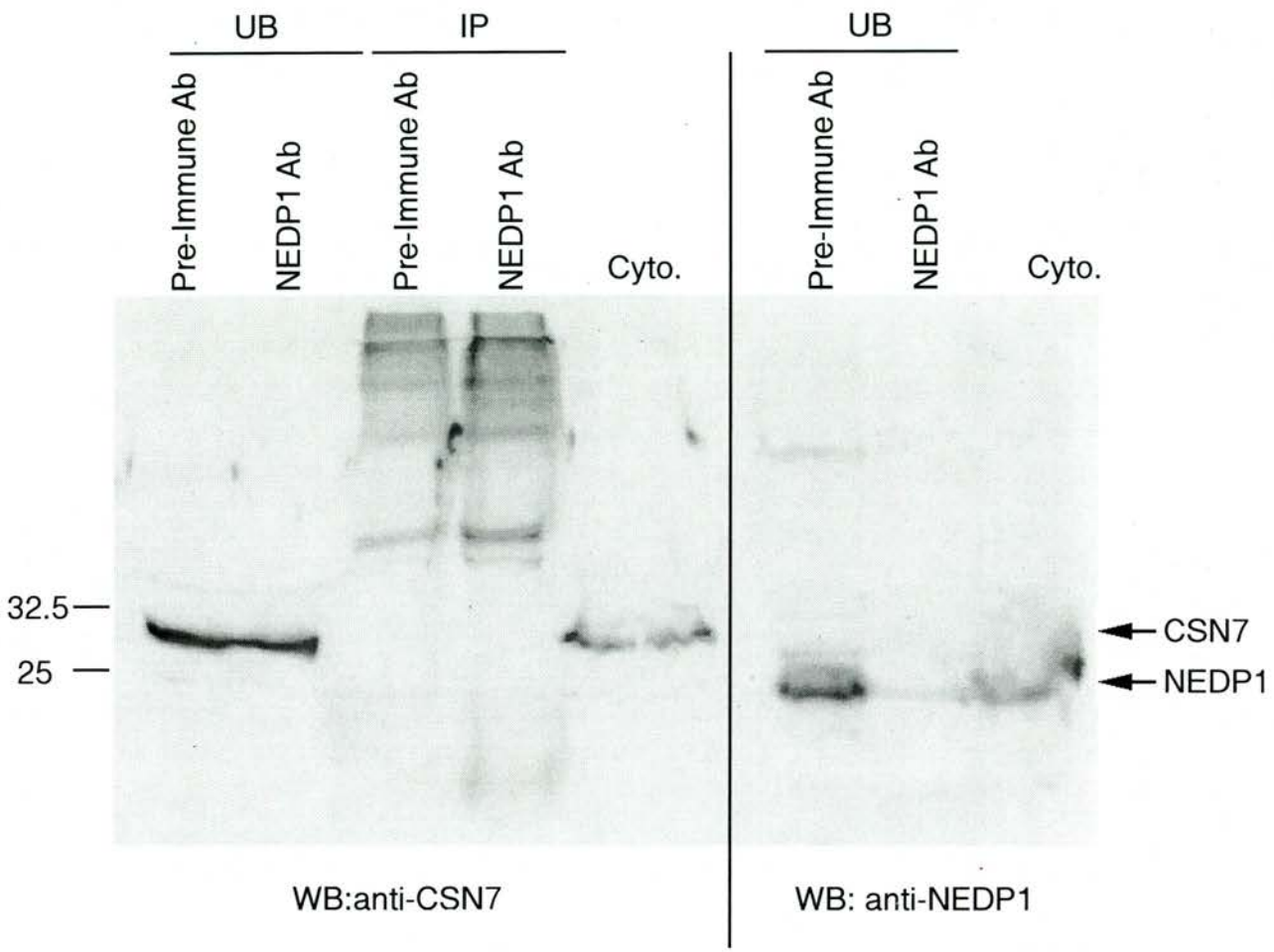

Figure 15: Immunoprecipitated NEDP1 does not interact with subunit 7 of the COP9 signalosome.

Endogenous NEDP1 was immunoprecipitated from HeLa cell cytoplasmic extracts using affinity purified NEDP1 antibody or pre-immune serum as detailed in 'Materials and Methods'. Unbound (UB), immune-precipitated (IP), and raw cytoplasmic extracts were analysed by SDS_PAGE and Western blotting with anti-CSN7 or anti-NEDP1 antibody as indicated.

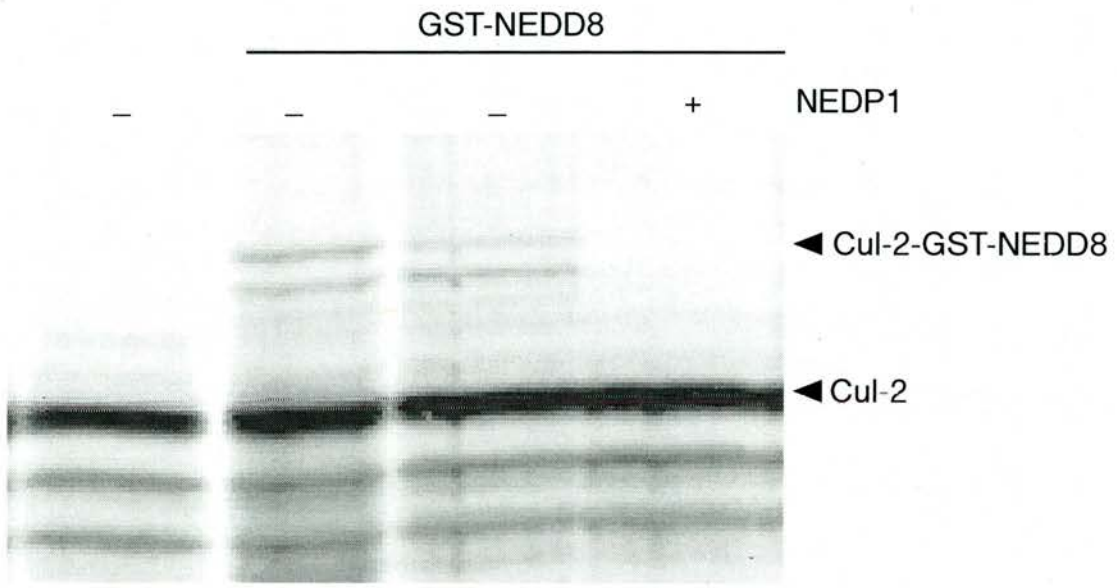

Figure 16: NEDP1 deconjugates NEDD8 from modified cullins *in vitro*.

GST-NEDP1 catalysed deconjugation of Cul-2-GST-NEDD8. GST-NEDD8 modified ^{35}S Cul-2 was incubated with 2 ug of GST-NEDP1 for 3 h at 37^0C. Reaction products were analysed by SDS-PAGE and radioactive species detected by phosphorimaging. The positions of Cul-2- GST-NEDD8 and unmodified Cul-2 are indicated.

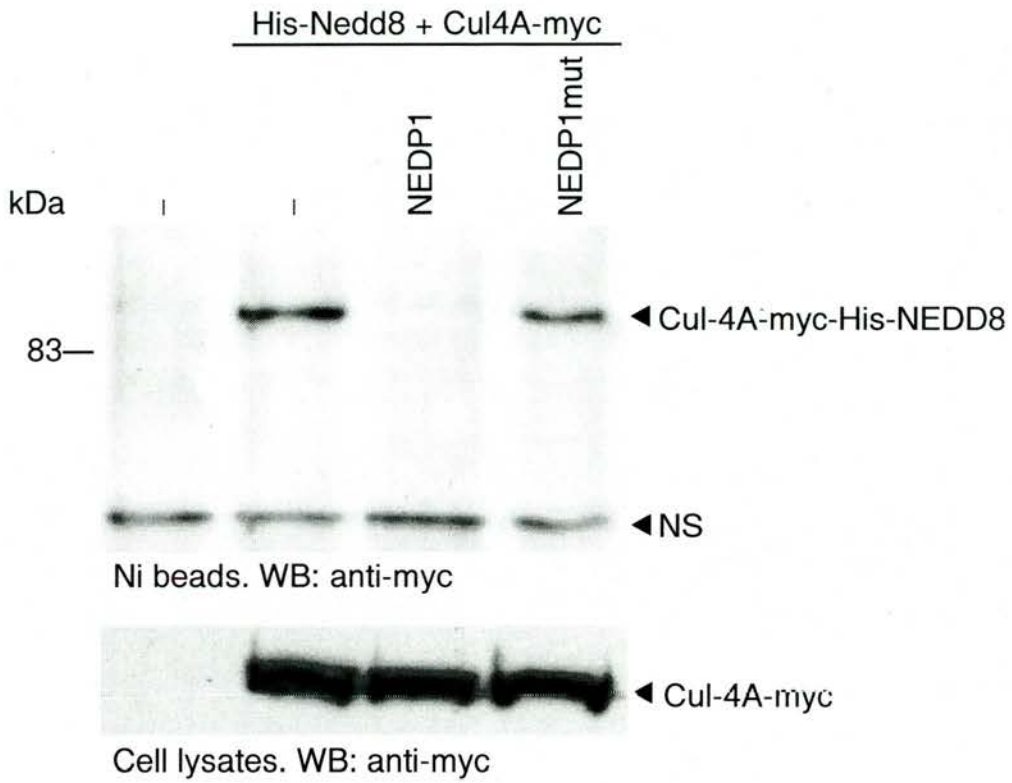

Figure 17: NEDP1 deconjugates NEDD8 from modified Cullin-4A *in vivo.*

COS7 cells were transfected with either empty pcDNA3 (-), or plasmids expressing Cul-4A-Myc, His-NEDD8, NEDP1, or NEDP1mut as indicated. His-NEDD8 conjugates were purified on Ni2+-agarose and conjugates were fractionated by gel electrophoresis in SDS-PAGE gels (8 % polyacrylamide). Anti-Myc Western blots were performed as detailed under "Experimental Procedures". A non-specific (NS) band is indicated along with the molecular weight markers.

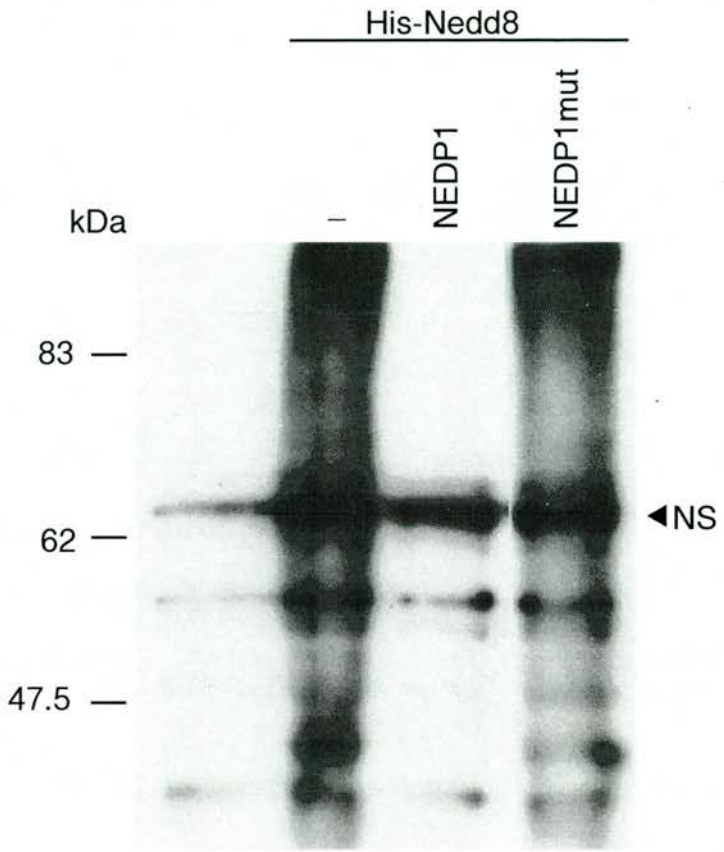

Figure 18: NEDP1 deconjgates NEDP1 *in vivo*.

COS7 cells were transfected with either empty pcDNA3 (-), or plasmids expressing His-NEDD8, NEDP1, or NEDP1mut as indicated. Anti-His Western blots were performed on cell lysates as detailed under "Experimental Procedures". A non-specific (NS) band is indicated along with molecular weight markers.

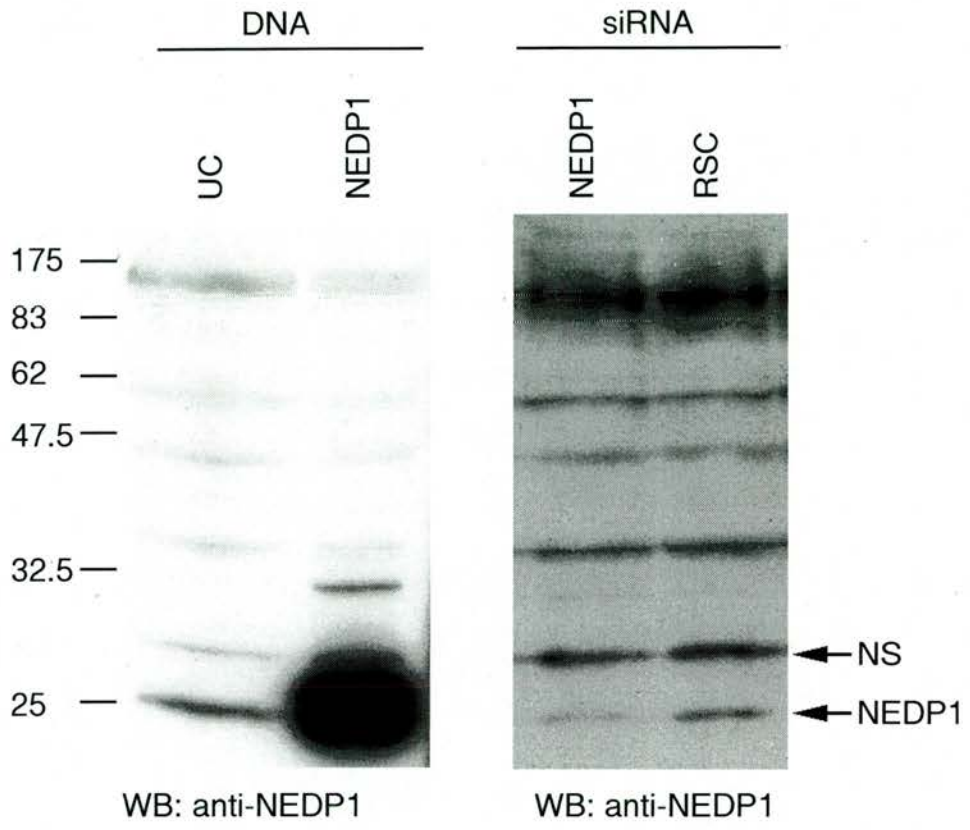

Figure 19: NEDP1 depletion in HeLa cells.

HeLa57A cells expressing NEDP1 and untransfected control cells (UC) were harvested as detailed in 'Materials and Methods' followed by SDS-PAGE and Western blotting with affinity purified NEDP1 antibody. Both endogenous and expressed NEDP1 migrated at approximately 25 kDa. HeLa57A cells were transfected twice with either RSC or NEDP1 siRNA and harvested 24 h after the last transfection. Lysates were then subjected to SDS-PAGE followed by Western blotting for analysis of NEDP1 protein knock-down. A non-specific band (NS) is indicated along with molecular weight markers.

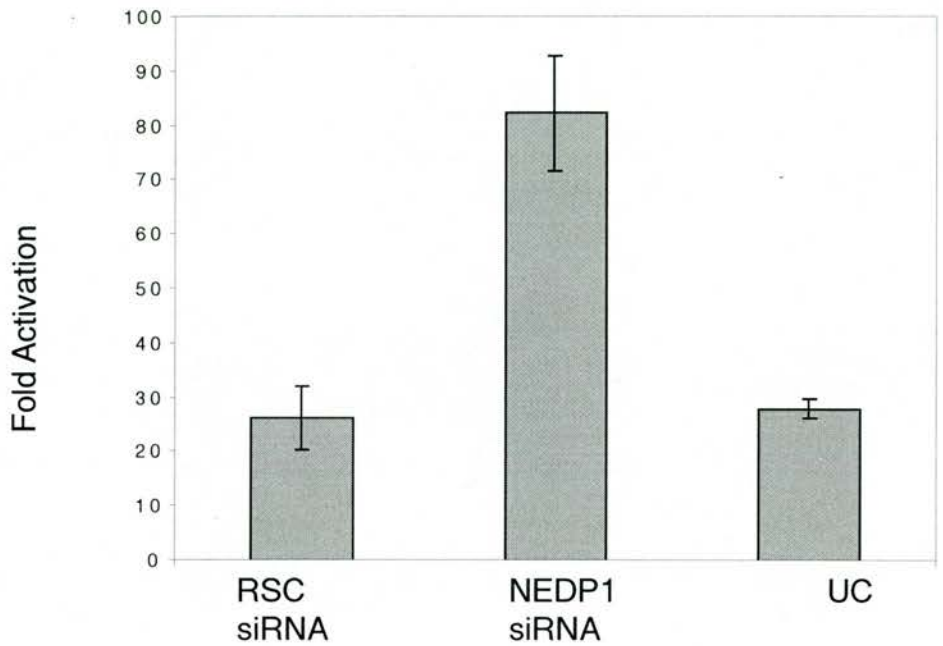

Figure 20: NEDP1 depletion enhances NF-kappaB activation.

HeLa57A cells with a stably integrated luciferase reporter, were transfected twice (80 nm and 50nm) with RSC or NEDP1 siRNA. Untransfected cells (UC) were included as an additional control. 24 h after the last transfection the cells were stimulated with 10 ng ml^{-1} TNF for 6 h prior to lysis and analysis of NF-kB activation. Data are presented as fold activation of stimulated cells compared to unstimulated treated cells. Each condition was performed in triplicate. These data are a representative of six separate experiments.

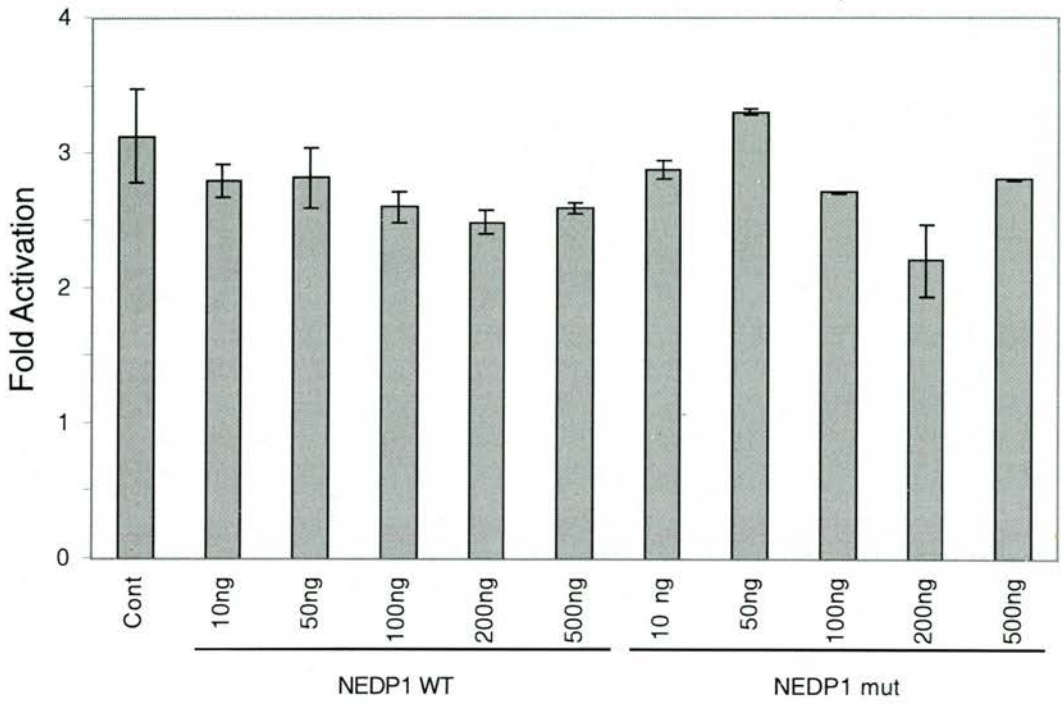

Figure 21: NEDP1 overexpression has no significant effect on NF kB activation.

HeLa cells were transfected with an NF-kB luciferase reporter (p3enhConALuc) and either empty vector, NEDP1, or NEDP1 mut as indicated. 36 h after transfection cells were stimulated with 10 ng ml^{-1} for 6 h prior to lysis and analysis of NF-kB activation. Each point represents triplicate stimulated and unstimulated wells represented as fold activation.

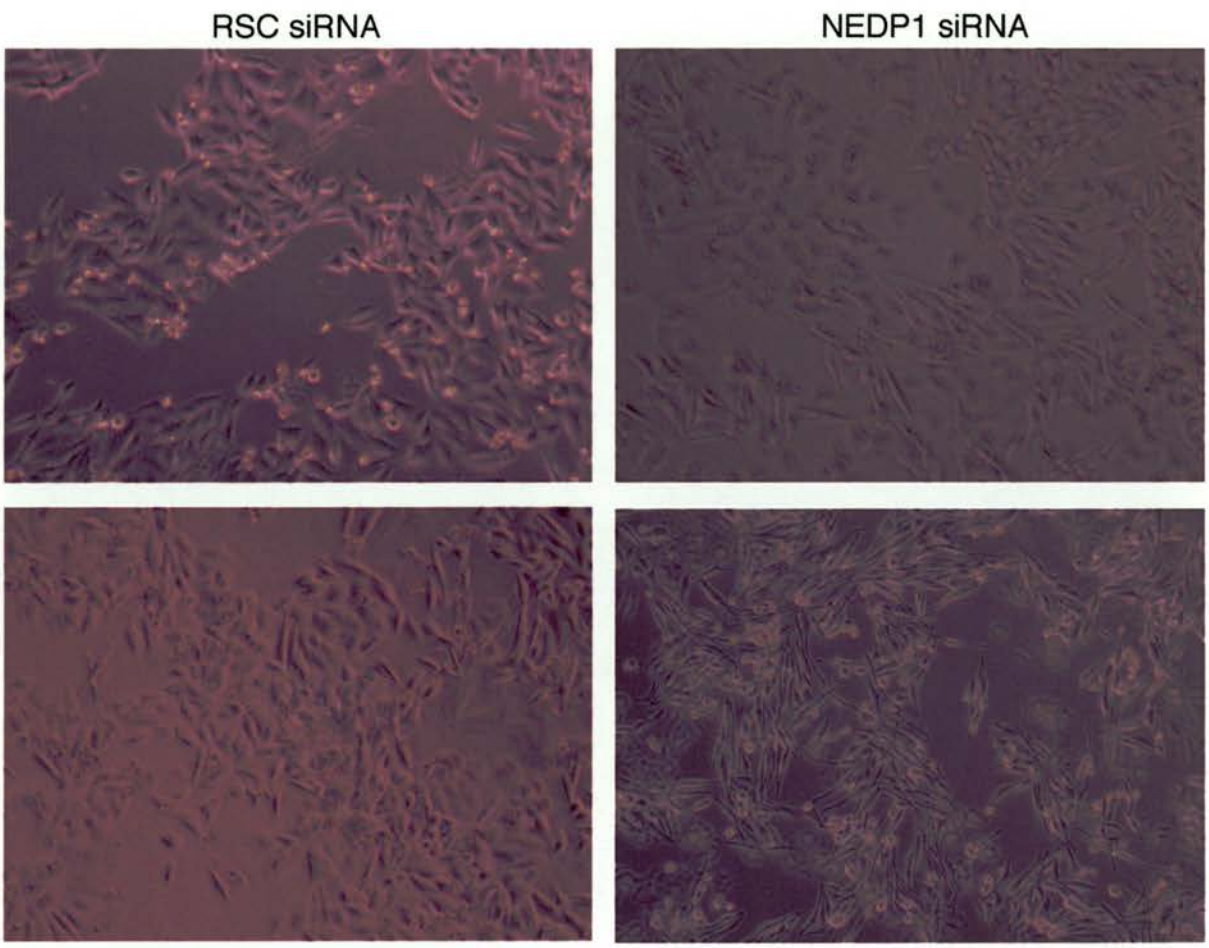

Figure 22: NEDP1 depletion causes cells to elongate.

Phase contrast micrographs of HeLa57A cells treated with RSC or NEDP1 siRNA as detailed in "Materials and Methods". Cells were visualised 24 h after last siRNA transfection.

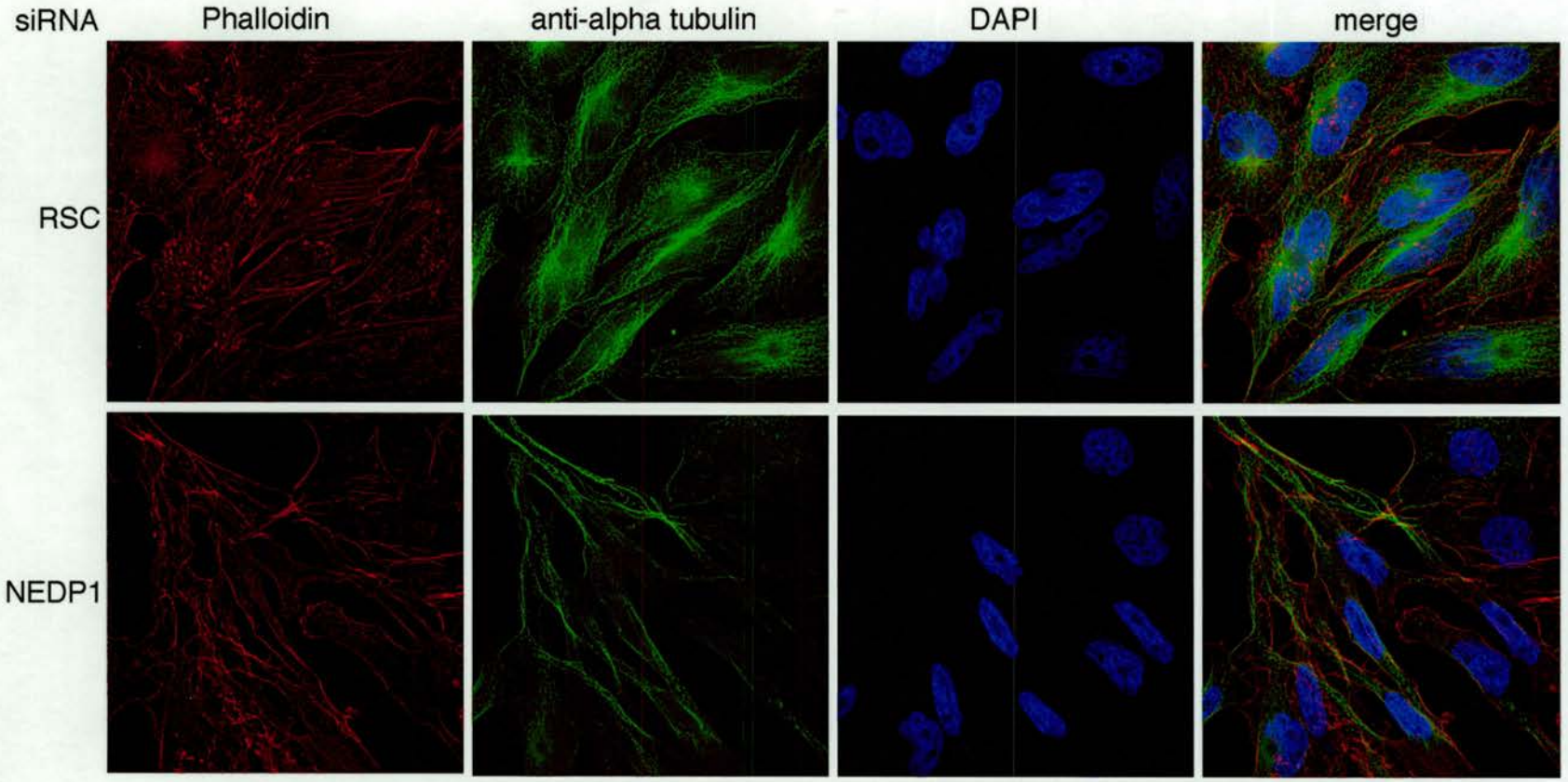

Figure 23: Effect of NEDP1 depletion on the cytoskeleton.

Hela57A cells were transfected with RSC or NEDP1 siRNA as detailed in 'Materials and Methods'. 24 h after the last transfection the cells were fixed and stained with phalloidin, anti-alpha tubulin antibody, and DAPI as indicated.

5. Characterisation of SENP2

5.1 Introduction

SUMO deconjugation is carried out by SUMO specific proteases which cleave the isopeptide bond between SUMO and the bound protein. These proteases are also responsible for cleavage of the SUMO precursors to expose the carboxyl terminal glycine residue that is conjugated to acceptor lysines in the target protein At the start of this project, *S. cerevisiae* Ulp1 and Ulp2 and two mammalian proteases SMT3IP1 and SENP1 had been identified as SUMO specific proteases [57, 58, 68, 69]. The catalytic domain of SENP2 was homologous to the SUMO specific proteases, but SENP2 was uncharacterised. For this reason SENP2 was chosen for characterisation as a putative SUMO specific protease. During the course of this research a number of other labs reported on mammalian SENP2. These results will be addressed in the discussion. The aims of the research were: to express and purify the SENP2 protease domain from bacteria in order to test the SENP2 SUMO specificity in a recombinant system; to express the full-length and catalytically inactive mutants of SENP2 in cells to determine substrate specificity; and to characterise the subcellular localisation *in vivo*.

5.2 Results

5.2.1 SENP2 acts as a SUMO specific protease in vivo

To establish that full length SENP2 is active *in vivo* the cDNA encoding SENP2 was inserted into a eukaryotic expression vector and transfected into COS7 cells along with expression plasmids for either HA-SUMO-1, HA-SUMO-2 or HA-SUMO-3. As controls the HA versions of SUMO were also cotransfected with empty expression vector or a vector encoding C548A SENP2 where the cysteine residue predicted to supply the active site nucleophile is changed to alanine. After 36h SUMO-modified species in cell extracts were revealed by Western blotting with an anti-HA monoclonal antibody. Transfection of HA-SUMO-1, HA-SUMO-2 or HA-SUMO-3 leads to the appearance of a number of high molecular weight SUMO modified species that are removed when SENP2 is cotransfected (Fig. 24a). Co-transfection of catalytically inactive C548A SENP2 does not alter the pattern of SUMO modified species. Thus SENP2 is active *in vivo* and is capable of deconjugating SUMO-1, SUMO-2 and SUMO-3 from a wide range of protein substrates.

For localisation experiments a GFP-SENP2 construct was created. In order to determine if GFP-SENP2 fusion was catalytically active, GFP-

SENP2 was transfected into COS7 cells along with the expression plasmids for either HA-SUMO-1, HA-SUMO-2 or HA-SUMO-3. After 36h SUMO-modified species in cell extracts were revealed by Western blotting with an anti-HA monoclonal antibody. Transfection of HA-SUMO-1 leads to the appearance of a number of high molecular weight SUMO modified species which are removed when GFP-SENP2 is co-transfected (Fig. 24b).

5.2.2 Expression and purification of the SENP2 protease domain as a GST fusion

To establish that the gene isolated encoded a SUMO-specific protease activity, the C-terminal region (aa368-589) containing the putative protease domain was expressed in bacteria as a fusion with glutathione S-transferase (Fig. 25a, b). GST-SENP2$_{368-589}$ was isolated by affinity chromatography and the purified protein analysed by electrophoresis in a polyacrylamide gel containing SDS (SDS-PAGE). Coomassie Blue staining demonstrated (Fig. 25c) that the purified GST-SENP2$_{368-589}$ was essentially homogenous.

5.2.3 SENP2 processes SUMO-1, SUMO-2 and SUMO-3

The ubiquitin-like proteins SUMO-1, SUMO-2 and SUMO-3 are all synthesised as inactive precursors which need to be precisely cleaved by

SUMO specific proteases to reveal the C-terminal diglycine motif, that is involved in conjugation to protein substrates (Fig. 26a). SUMO-2 and SUMO-3 are very similar (95% sequence identity), but are relatively different from SUMO-1 (50% sequence identity). Given this sequence diversity it was therefore important to determine if each of these ubiquitin-like proteins could be processed by SENP2. Full-length (unprocessed) forms of SUMO-$1_{(1-101)}$, SUMO-$2_{(1-103)}$ and SUMO-$3_{(1-95)}$ were incubated with a range of concentrations of purified GST-$SENP2_{368-589}$ and the products of the reaction analysed by SDS-PAGE followed by staining with Coomassie Blue. In the presence of roughly equal amounts of GST-$SENP2_{368-589}$, SUMO-1_{1-101}, SUMO-2_{1-103}, and SUMO-3_{1-95} are cleaved to their mature forms (Fig. 26b). In addition GST-SENP2(C548A)$_{368-589}$ in which the predicted active site cysteine had been mutated to an alanine was incubated with full-length SUMO-1. GST-SENP2(C548A)$_{368-589}$ was unable to process the SUMO-1 precursor (Fig. 26c).

While the reactions catalysed by SENP2 are consistent with cleavage after the di-glycine motifs this cannot be accurately determined by SDS PAGE. In each case samples were collected after incubation with SENP2 or after a control incubation lacking SENP2 and the products analysed by MALDI-TOF mass spectrometry. The experimentally determined masses of the products indicated that SUMO-1_{1-101} is cleaved by SENP2 to SUMO-1_{1-97}

(Fig. 27), SUMO-2_{1-103} is cleaved to SUMO-2_{1-92} (Fig. 28) and SUMO-3_{1-95} is cleaved to SUMO-3_{1-93} (Fig. 29). Thus SENP2 precisely processes SUMO-1, SUMO-2 and SUMO-3 to expose the C-terminal di-glycine motif that is conjugated to protein substrates.

5.2.4 SENP2 deconjugates SUMO-1 from modified substrates

To assess the ability of SENP2 to deconjugate SUMO from modified proteins two model substrates were used. GST fused to an 11 amino acid sequence containing the SUMO modification site located between amino acids 485-495 of PML (GST-PML) was conjugated to ^{125}I labelled SUMO-1 in the presence of SAE1/SAE2 and Ubc9 (Fig. 30a) [28]. GST fused to a peptide sequence containing the SUMO modification site located between amino acids 418-587 of ranGAP (GST-ranGAP) was conjugated to ^{125}I labelled SUMO-1 in the presence of SAE1/SAE2 and Ubc9 (Fig. 30a). The reaction products were purified by affinity chromatography on glutathione agarose and the eluted proteins used as a substrate for SENP2 (Fig. 30b,c) GST-PML-^{125}I-SUMO-1 or GST-ranGAP-^{125}I-SUMO-1 was incubated with a range of concentrations of SENP2, the reaction products fractionated by SDS-PAGE and ^{125}I-labelled species detected by phosphorimaging. SENP2 efficiently cleaves the isopeptide bond between the C-terminus of SUMO-1 and the lysine to which it is conjugated in GST-PML or GST-ranGAP (Fig.

31a, b). Radiolabelled GST-ranGAP was conjugated to SUMO-1 or SUMO-2 similarly to above, and also used as model substrates for GST-SENP2. GST-^{125}I-ranGAP-SUMO-1 or GST-^{125}I-ranGAP-SUMO-2 was incubated with a range of concentrations of SENP2, the reaction products fractionated by SDS-PAGE and ^{125}I-labelled species detected by phosphorimaging. SENP2 efficiently cleaves the isopeptide bond between the C- terminus of SUMO-1 or SUMO-2 and the lysine to which it is conjugated in ranGAP (Fig. 32).

While SENP2 is capable of acting as an isopeptidase on artificial substrates in a purified system it was important to establish that it could also act as an isopeptidase on natural substrates in the presence of unrelated proteins. Four well characterised substrates, PML [34], IκBα [31], HDAC4 [148], and p53 [70] were labelled with ^{35}S-Methionine during *in vitro* transcription, translation in a wheat germ extract. ^{35}S labelled p53, PML and IκBα were conjugated to SUMO-1 while HDAC4 was conjugated to SUMO-2 *in vitro* and the reactions were terminated by incubation with iodoacetamide. This also served to inhibit any endogenous SUMO-specific proteases. After quenching of the iodoacetamide with β-mercaptoethanol the reaction products were used as substrates for SENP2. PML incubation with SENP2 results in a dose dependent decrease in the SUMO modified form of PML (Fig. 33a). IκBα is modified predominantly at a single site and incubation of the modified material with SENP2 results in conversion of the modified to the

unmodified form of IκBα (Fig. 33b). The SUMO-1 and SUMO-2 modified forms of p53 and HDAC4 respectively were also deconjugated by SENP2 in a dose dependent manner (Fig. 33c, d). Thus SENP2 displays SUMO-1 and SUMO-2 isopeptidase activity on natural substrates in the presence of a large excess of unrelated proteins (from the wheat germ extract).

5.2.5 Subcellular localisation of SENP2

To establish the subcellular distribution of SENP2 HeLa cells were transfected with a construct expressing the full-length version of the protease. To detect the endogenous protease antibodies were raised against a peptide from the N-terminal domain of SENP2 and tested by Western blotting (Fig. 34). Affinity purified anti-SENP2 antibody recognised a protein of approximately 62 kDa from the high salt nuclear extract, which agrees with the predicted mass of SENP2 of 67 kDa. A number of bands were also present in the pre-immune Western blot. In order to verify that the anti-SENP2 antibody specifically recognised SENP2, both pre-immune serum and anti-SENP2 antibody were pre-incubated with the immunization peptide prior to Western blotting. The peptide blocked recognition of the 62 kDa band by the SENP2 antibody, but did not block any bands from the pre-immune blot. The anti-SENP2 antibody was used in immunofluorescence for recognition of endogenously and exogenously expressed SENP2.

Exogenously expressed SENP2 is located almost exclusively in the nucleus (as revealed by DAPI staining) and is predominantly located in discrete nuclear "speckles", (Fig. 35c). A proportion of SENP2 is also localised to the nuclear rim. While the catalytically inactive C548A SENP2 is also located in the nucleus, its distribution is different from that of the wild type protein and tends to be observed in very large numbers of "microspeckles" (Fig. 35d). An alternatively spliced variant of murine SENP2, SMT3IP2, is missing the N-terminal domain of SENP2 and is localised to the cytoplasm [114]. Inspection of the N-terminal region of SENP2 shows the presence of two potential nuclear localisation motifs that are absent from SMT3IP2 (Fig. 55). To determine if this N-terminal region was responsible for SENP2 nuclear localisation, an N-terminal deletion mutant was constructed that lacked the predicted NLS motifs (SENP2ΔNLS). Exogenously expressed SENP2ΔNLS is localised almost exclusively to the cytoplasm confirming that the N-terminal region is responsible for nuclear localisation (Fig. 35b).

Given the existence of alternatively localised spliced variants of SENP2, it was important to determine the localisation of endogenous SENP2 in human cells. In A549 cells most of the endogenous SENP2 was localised to the nucleus (Fig. 35a). While some punctate localisation was observed, it was impossible to show fine structure.

As SENP2 localises in nuclear dots it was of interest to investigate the localisation of SENP2 with a known SUMO modified substrate. PML is known to be SUMO modified and is targeted to nuclear bodies that contain other SUMO modified substrates therefore endogenous PML bodies were chosen for investigation. At low levels of expression GFP-SENP2 did not co-localise with PML bodies (Fig. 36a, b). Intriguingly, the catalytically inactive GFP-SENP2 C548A mut was found to co-localise with the majority of PML bodies (Fig. 36d).

5.3 Discussion

A human SUMO specific protease SENP2 was characterised. The expressed protein was shown to cleave the full-length unprocessed forms of SUMO-1, SUMO-2 and SUMO-3 to expose the C-terminal di-glycine that is conjugated to target proteins (Fig. 26). In addition the enzyme could act as an isopeptidase to deconjugate SUMO-1 and SUMO-2 from modified substrates (Figs. 31, 32, and 33). *In vivo* the overexpressed enzyme appeared to remove SUMO-1, SUMO-2 and SUMO-3 from the vast majority of proteins (Fig. 24). SENP2 wild type protease was almost exclusively nuclear and accumulated at the nuclear rim and in discrete nuclear "speckles" which at low levels of expression, did not co-localise with PML nuclear bodies (Fig. 36). Catalyticly inactive C548A SENP2 was also nuclear, but appeared to localise in a large number of "microspeckles". The reason for the difference in localisation of the wild type and mutant proteins is unclear but could be a consequence of a failure to remove SUMO from an important nuclear organiser. An alternative explanation is that SENP2 C548A is able to bind SUMO modified substrates, but is not released and consequently gets trapped with a substrate in nuclear bodies. Two other research groups have reported the localisation of SENP2 predominantly to the nucleoplasmic portion of nuclear pores, with only a small proportion of SENP2 present in nuclear dots [54, 149]. Differences in the proportions of

SENP2 targeted to nuclear dots or nuclear pores could be due to differences in fixation methods, constructs or cell types.

While the cellular localisation of human SENP2 is almost exclusively nuclear the cellular localisation of the corresponding mouse proteins SMT3IP2/Axam2 is reported to be predominantly cytoplasmic and in cytoplasmic vesicles surrounding the nucleus [114]. The likely explanation for this difference is that SENP2 contains additional sequences at the N-terminus that encode the putative nuclear localisation signal KRRR. It is not clear if the differences in length of the cDNAs isolated from mouse and human sources represent cell/species specific differences in alternative splicing. Irrespective of the reason for the shorter murine cDNA, the consequences on cellular localisation are dramatic and would be expected to have a substantial impact on substrate selection *in vivo*. Indeed SMT3IP2/Axam2 and Axam have been reported to effect the degradation of ß-catenin a cytoplasmic component of the Wnt signalling pathway [114, 150]. However, under the conditions of overexpression employed, exogenous SENP2 and SMT31P2/Axam2 both deconjugate tagged versions of SUMO-1, SUMO-2 and SUMO-3 from all the major substrates in the cell. Under normal circumstances it is likely that the cellular localisation of endogenous SENP2 will be tightly controlled as a means of restricting substrate specificity. Removal of the N-terminal domain of Yeast Ulp1 not only de-

localises it from the nuclear rim but also allows Ulp1 to deconjugate a wider range of SUMO modified substrate. As a consequence of this deregulation of substrate specificity, at low expression levels Ulp1 N-terminal deletion mutants can compensate for Ulp2Δ phenotypes when full-length Ulp1 cannot [62]. Database searching has revealed that in mammalian cells there are at least 7 genes which share a conserved SUMO specific protease domain, although it is clear that not all are SUMO specific proteases. While SMT31P1 is found in the nucleolus [68], SENP6 is cytoplasmic [121], and SENP1 is nuclear [69].

The function of SUMO specific proteases is two-fold: they generate mature SUMO by cleaving the precursor to expose the C-terminal diglycine motif that is conjugated to protein substrates and they deconjugate SUMO from modified substrates. It is clear that SUMO modification is a highly dynamic process with substrates experiencing rapid conjugation and deconjugation. In many cases the equilibrium established results in only a small proportion of the target protein being modified at a particular time. However it has been demonstrated that SUMO modification can be induced by a variety of agents [27, 35, 71] and this could either result from accelerated SUMO addition or inhibition of SUMO specific protease activity. The growing number of transcription factors known to be SUMO modified suggested that rapid sumoylation and desumoylation may be used to

regulate transcription. Over-expression of SENP2 and SuPr1 has been shown to relieve repression of p300 [88], and Elk-1 [87] through desumoylation of their repression domains. Best and colleagues have shown that over-expression of SuPr1 enhances transciptional activity of a c-jun reporter assay. However this enhancement is not dependent on the sumoylation status of c-jun, and also occurred with catalyticly inactive SuPr-1 [151]. It is possible that the catalyticly inactive SuPr-1 could be acting as a dominant negative, alternatively SuPr-1 interactions rather than catalytic activity could be responsible for regulation of transcription. The enhanced transcriptional activity of c-jun was dependent on the presence of PML suggesting that interaction with PML body components or PML itself is one mechanism through which SuPr-1 enhances transcription. The ability of SUMO proteases to remove SUMO from many substrates when over-expressed makes it imperative to ensure that the effects observed are due to a change in the sumoylation state of a specific protein, rather than an effect of global desumoylation. Establishing the role of SENP2 *in vivo* awaits genetic analysis in higher eukaryotes.

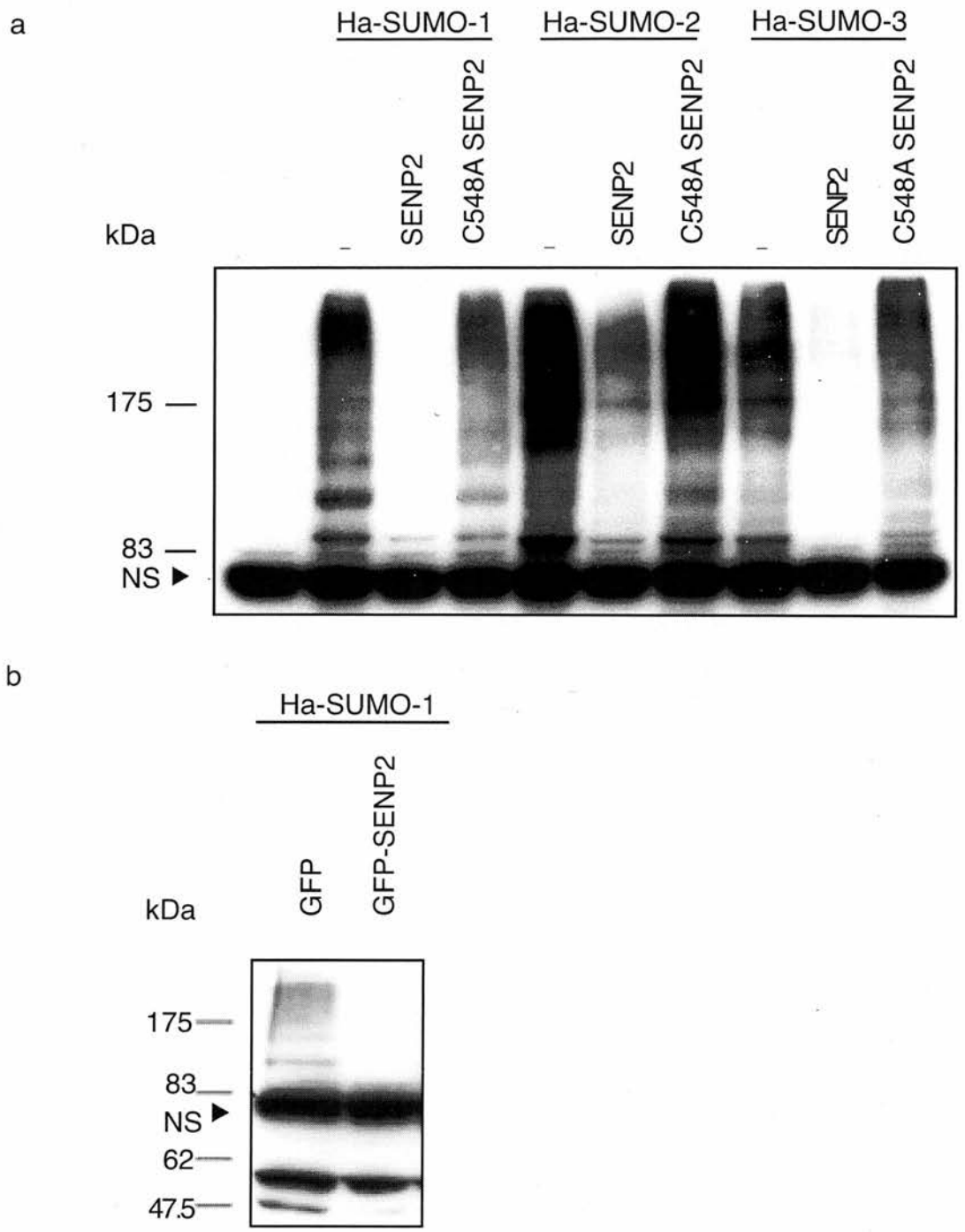

Figure 24: SENP2 acts as a SUMO specific protease *in vivo*.

a. COS7 cells were transfected with empty pcDNA3 (-), or plasmids expressing HA-SUMO-1, HA-SUMO-2, HA-SUMO-3, SENP2, C548A SENP2 as indicated. b. COS7 cells were similarly transfected with either HA-SUMO-1 and GFP or GFP-SENP2 as indicated. Anti-HA Western blots were performed on cell lysates as detailed under 'Materials and Methods'. A non-specific (NS) band is indicated along with molecular weight markers.

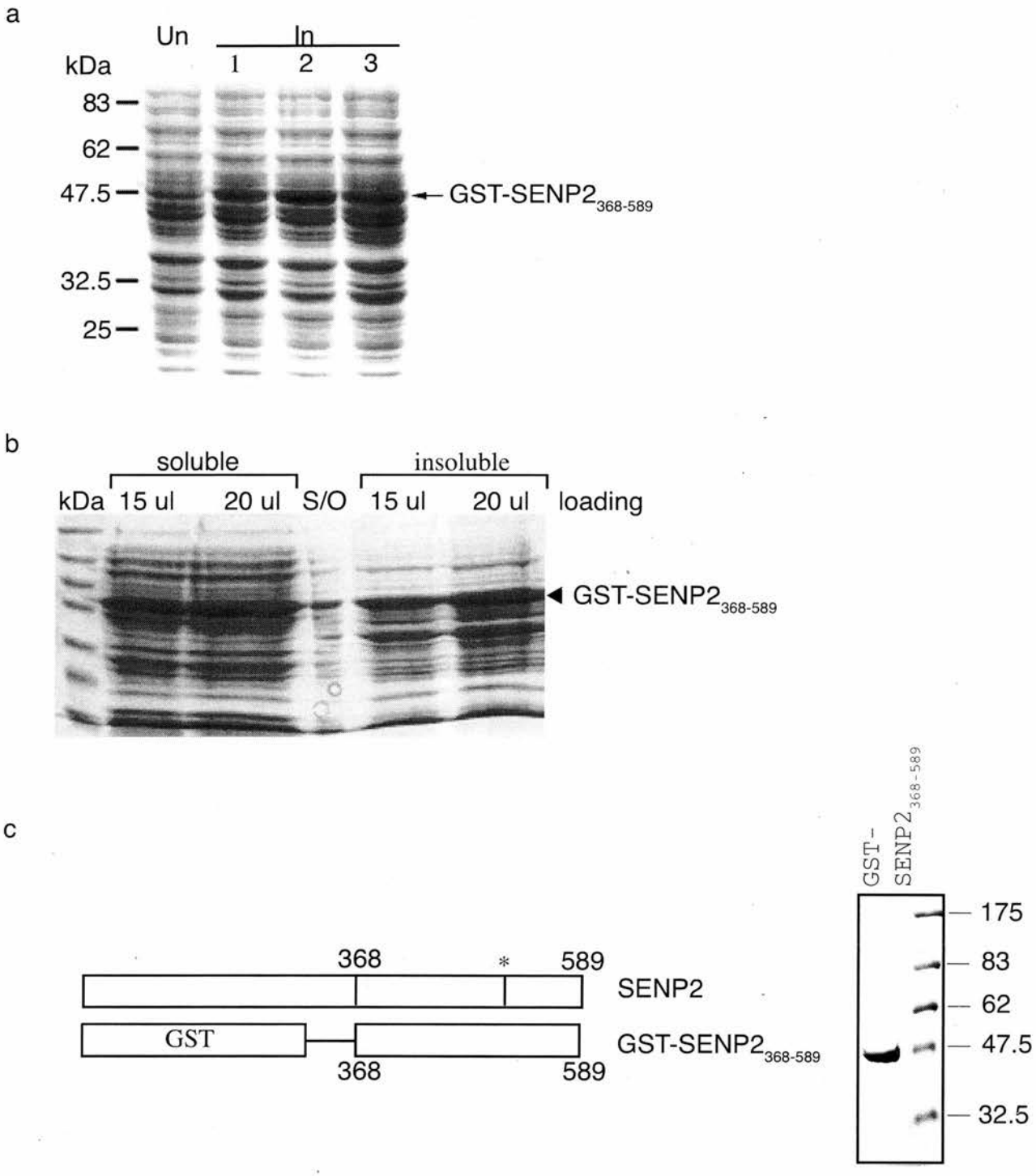

Figure 25: Expression and purification of GST-SENP2$_{368-589}$.

Coomassie-stained SDS- polyacrylamide gels showing a. Induction of GST-SENP2$_{368-589}$. b. Solubility of expressed GST-SENP2$_{368-589}$. c. 2 μg of the purified recombinant protein SENP2$_{368-589}$. Schematic of GST-SENP2$_{368-589}$ fusion and SENP2 proteins.

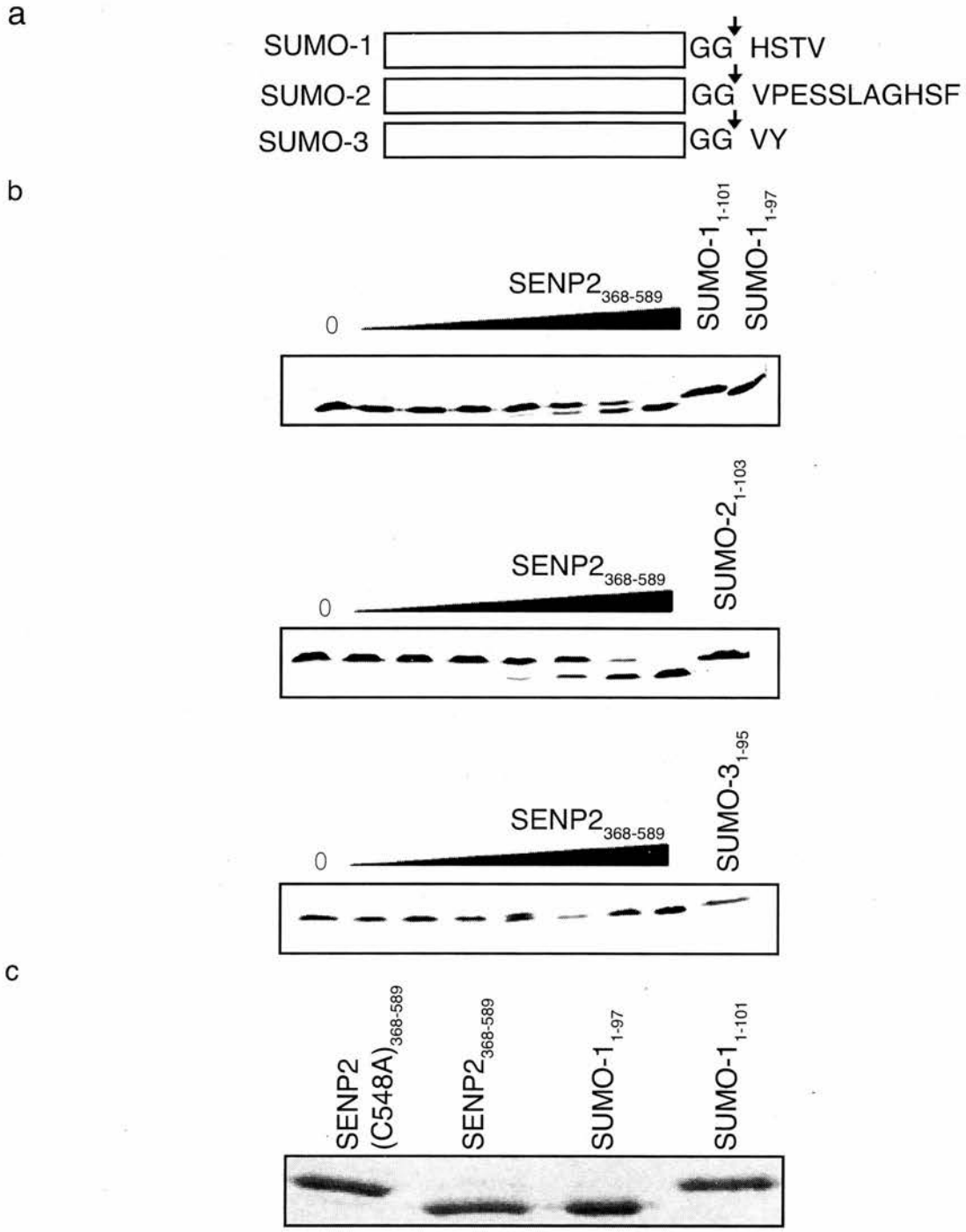

Figure 26: SENP2 processess SUMO-1, SUMO-2, and SUMO-3.

a. Coomassie-stained SDS-polyacrylamide gels showing 2 μg of full-length recombinant SUMO-1_{1-101}, SUMO-2_{1-103}, or SUMO-3_{1-95} incubated with varying concentrations of GST-SENP$2_{368-589}$ (0.008 μg to 0.5 μg). Recombinant SUMO-1_{1-101}, SUMO-1_{1-97}, SUMO-2_{1-103}, and SUMO-3_{1-95} in the presence or absence of protease are indicated. b. Coomassie-stained SDS-polyacrylamide gel showing 2 μg of full-length SUMO-1_{1-101} incubated with 0.5 μg of GST-SENP$2_{368-589}$ or GST-SENP2 $(C548A)_{368-589}$.

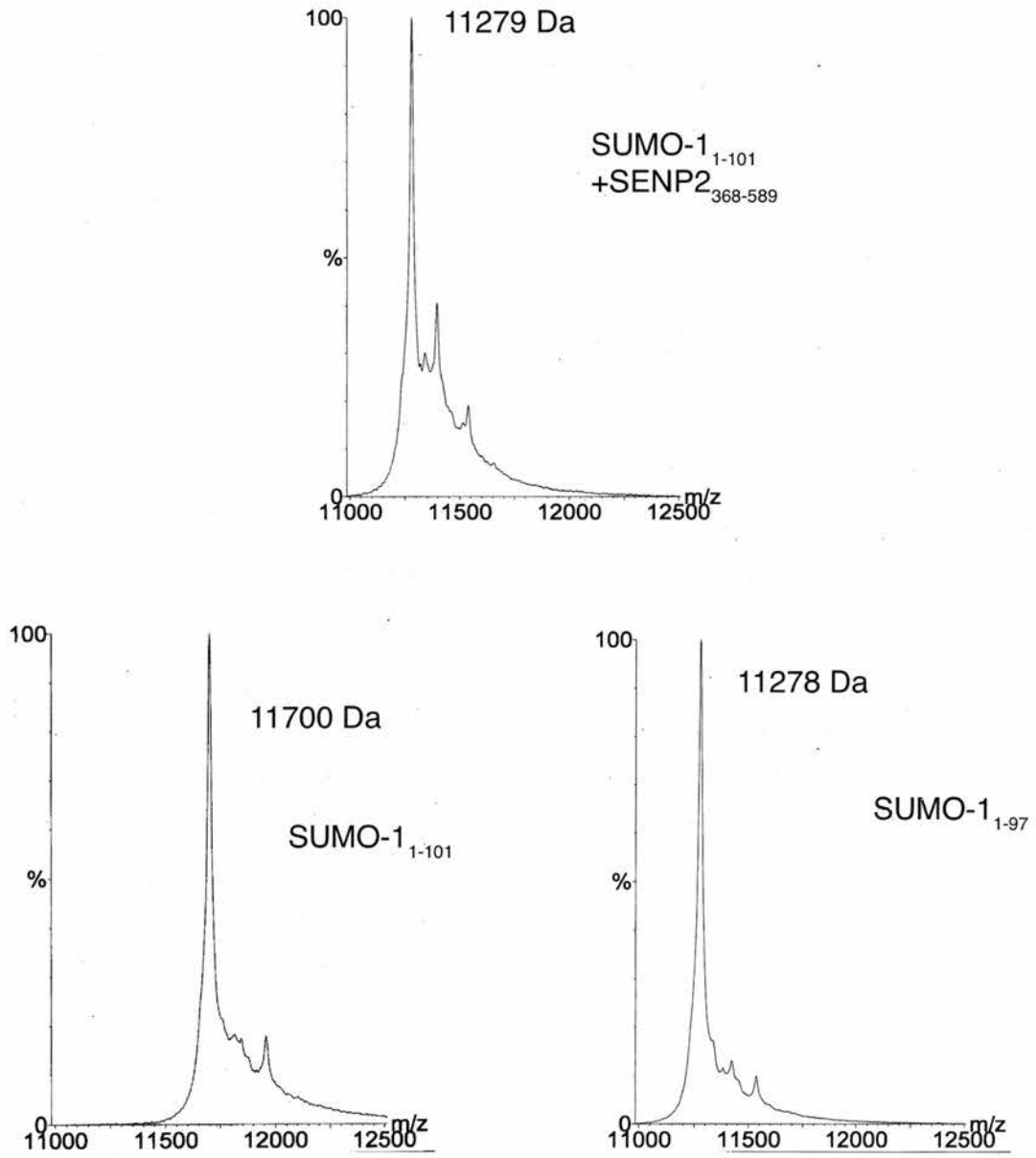

Figure 27: SENP2 processes the SUMO-1 precursor to mature SUMO-1.

GST-SENP2$_{368-589}$ processes SUMO-1$_{1-101}$ to SUMO-1$_{1-97}$. The SUMO-1$_{1-101}$ processing assay was set up and the products analysed by MALDI-TOF Mass Spectrometry as detailed under "Experimental Procedures". SUMO-1$_{1-101}$ incubated in the presence of GST-SENP2$_{368-589}$ has a mass of 11279 Da. Recombinant purified SUMO-1$_{1-97}$ mass 11278 Da. Recombinant purified SUMO-1$_{1-101}$ mass 11700 Da.

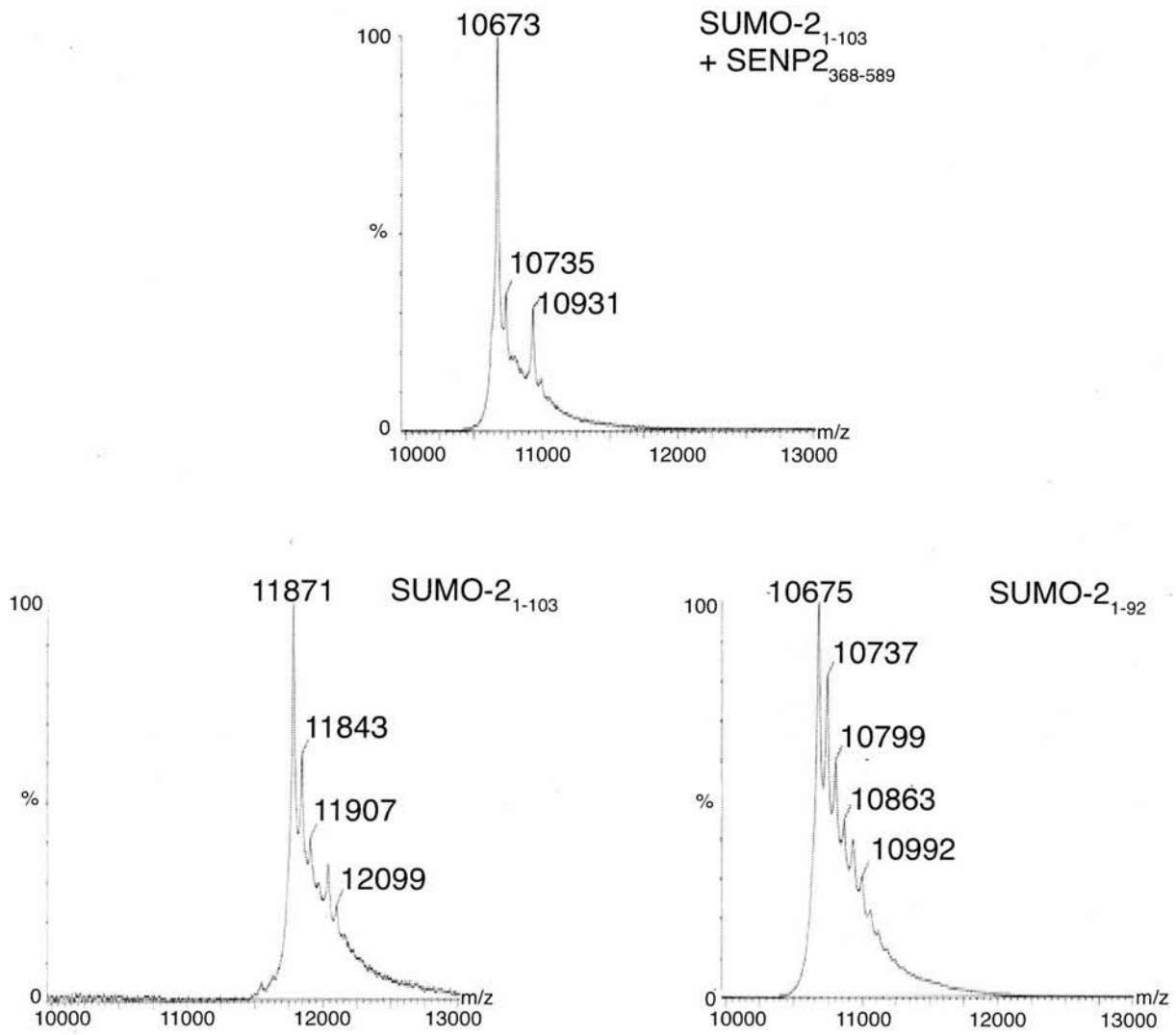

Figure 28: SENP2 processes the SUMO-2 precursor to mature SUMO-2.

GST-SENP2$_{368-589}$ processes SUMO-2$_{1-103}$ to SUMO-2$_{1-92}$. The SUMO-2$_{1-103}$ processing assay was set up and the products analysed by MALDI-TOF Mass Spectrometry as detailed under "Experimental Procedures". SUMO-2$_{1-103}$ incubated in the presence of GST-SENP2$_{368-589}$ has a mass of 10673 Da. Recombinant purified SUMO-2$_{1-92.}$ mass 10675 Da. Recombinant purified SUMO-2$_{1-103}$ mass 11871 Da.

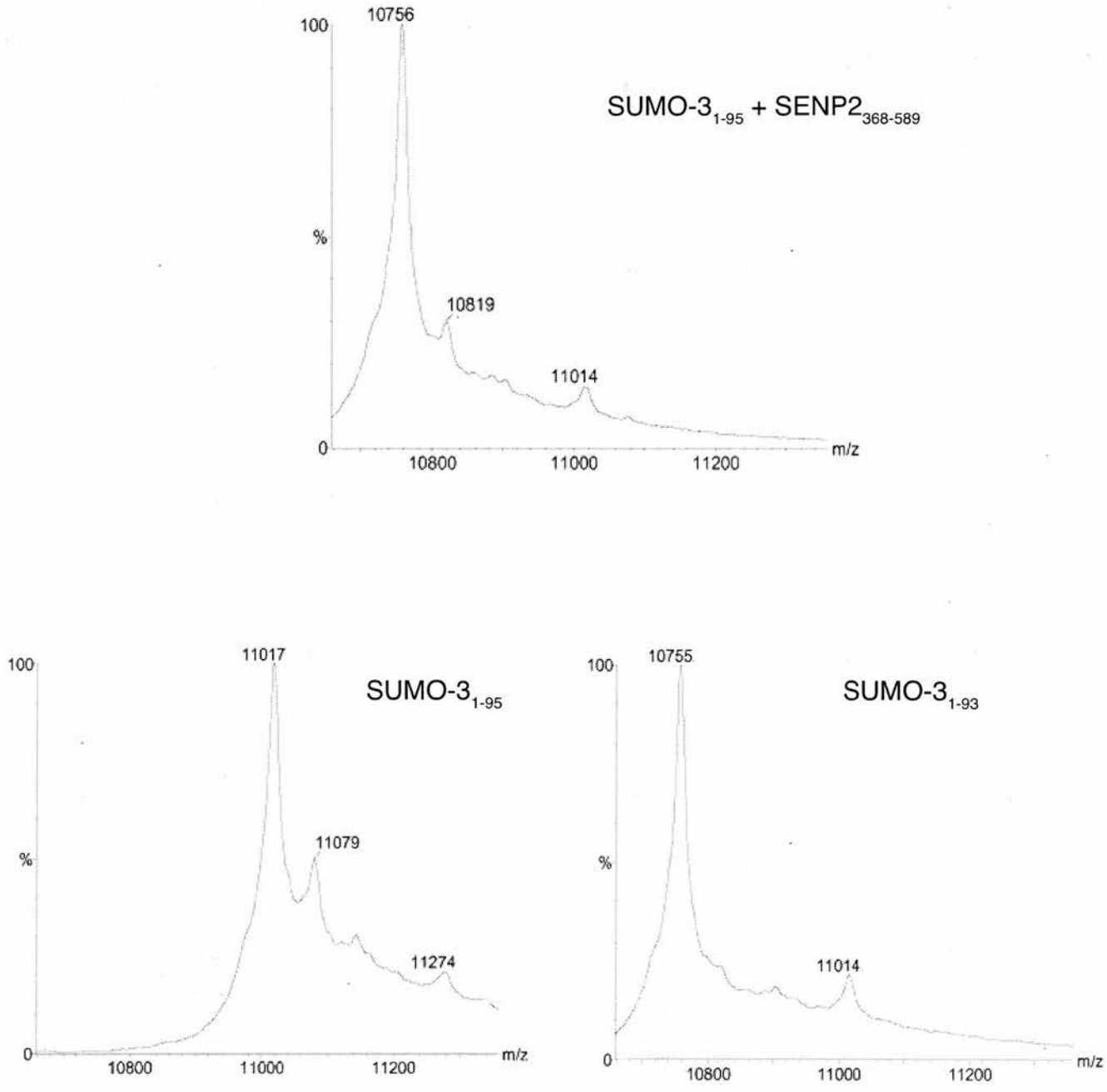

Figure 29: SENP2$_{368-589}$ processes the SUMO-3 precursor to mature SUMO-3.

GST-SENP2$_{368-589}$ processes SUMO-3$_{1-95}$ to SUMO-3$_{1-93}$. The SUMO-3$_{1-95}$ processing assay was set up and the products analysed by MALDI-TOF Mass Spectrometry as detailed under "Experimental Procedures". SUMO-3$_{1-95}$ incubated in the presence of GST-SENP2$_{368-589}$ has a mass of 10756 Da. Recombinant purified SUMO-3$_{1-93}$ mass 10755 Da. Recombinant purified SUMO-3$_{1-95}$ mass 11017 Da.

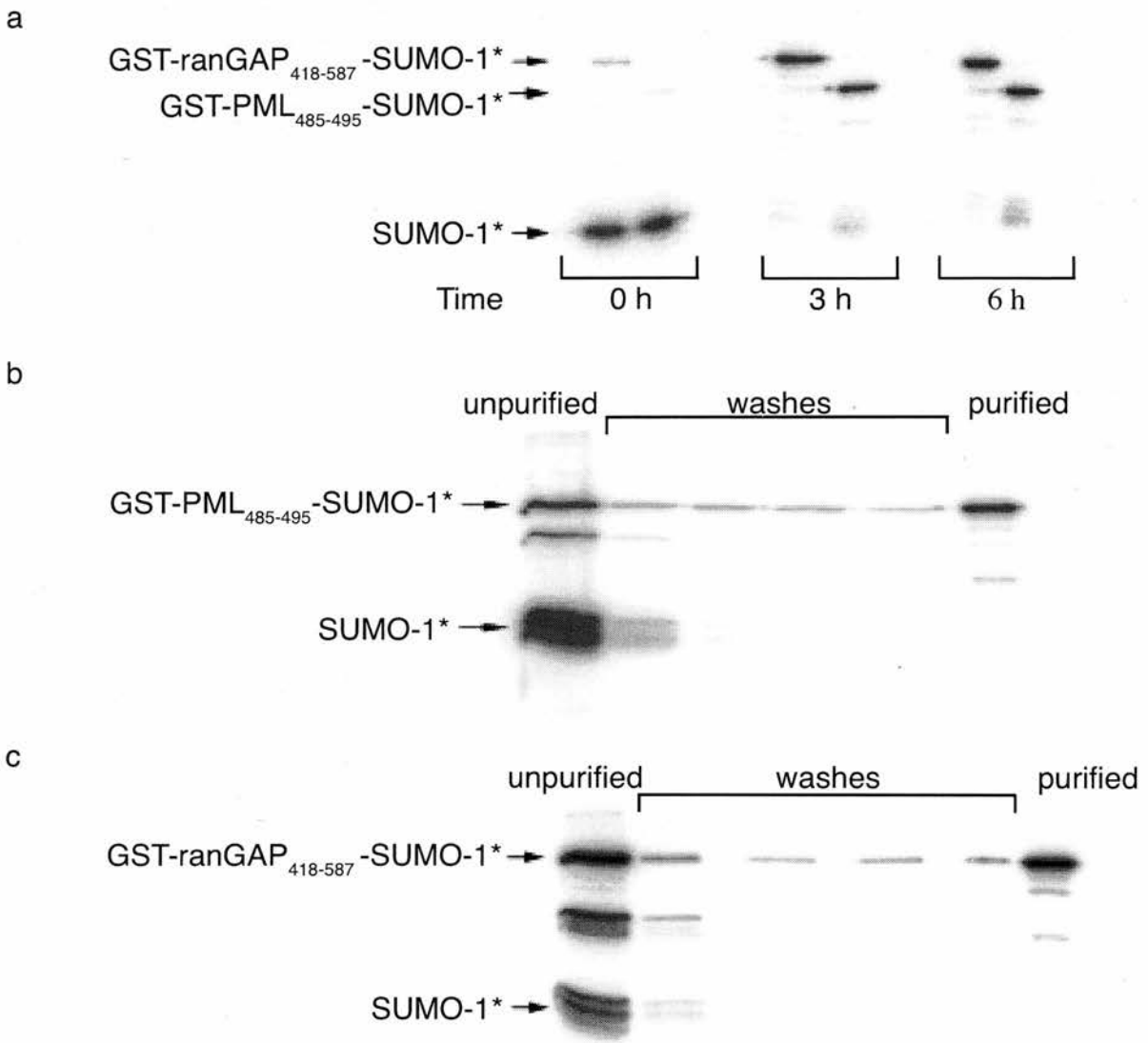

Figure 30: Conjugation and purification of radiolabelled ^{125}-SUMO-1 to GST-PML$_{485-495}$ and GST-ranGAP$_{418-587}$.

a. Purified GST-PML$_{485-495}$ and GST-ranGAP$_{418-587}$ were incubated with ^{125}-SUMO-1* as indicated in "Experimental Procedures". Timepoints were taken at 0, 3, 6 h to monitor SUMO conjugation. Samples were analysed by SDS-PAGE and dried gels were analysed by phosphorimaging. The positions of GST-ranGAP$_{418-587}$-SUMO-1*, GST-PML$_{485-495}$-SUMO-1*, and free SUMO-1* are indicated. b and c. SUMO conjugated to GST-substrate was purified by binding to glutathione agarose beads and washing the beads. Samples of unpurified, washes, and purified product were taken and analysed by SDS-PAGE and phosphorimaging. SUMO-1* conjugated product and free SUMO-1* are indicated. (*) indicates radioolabelling.

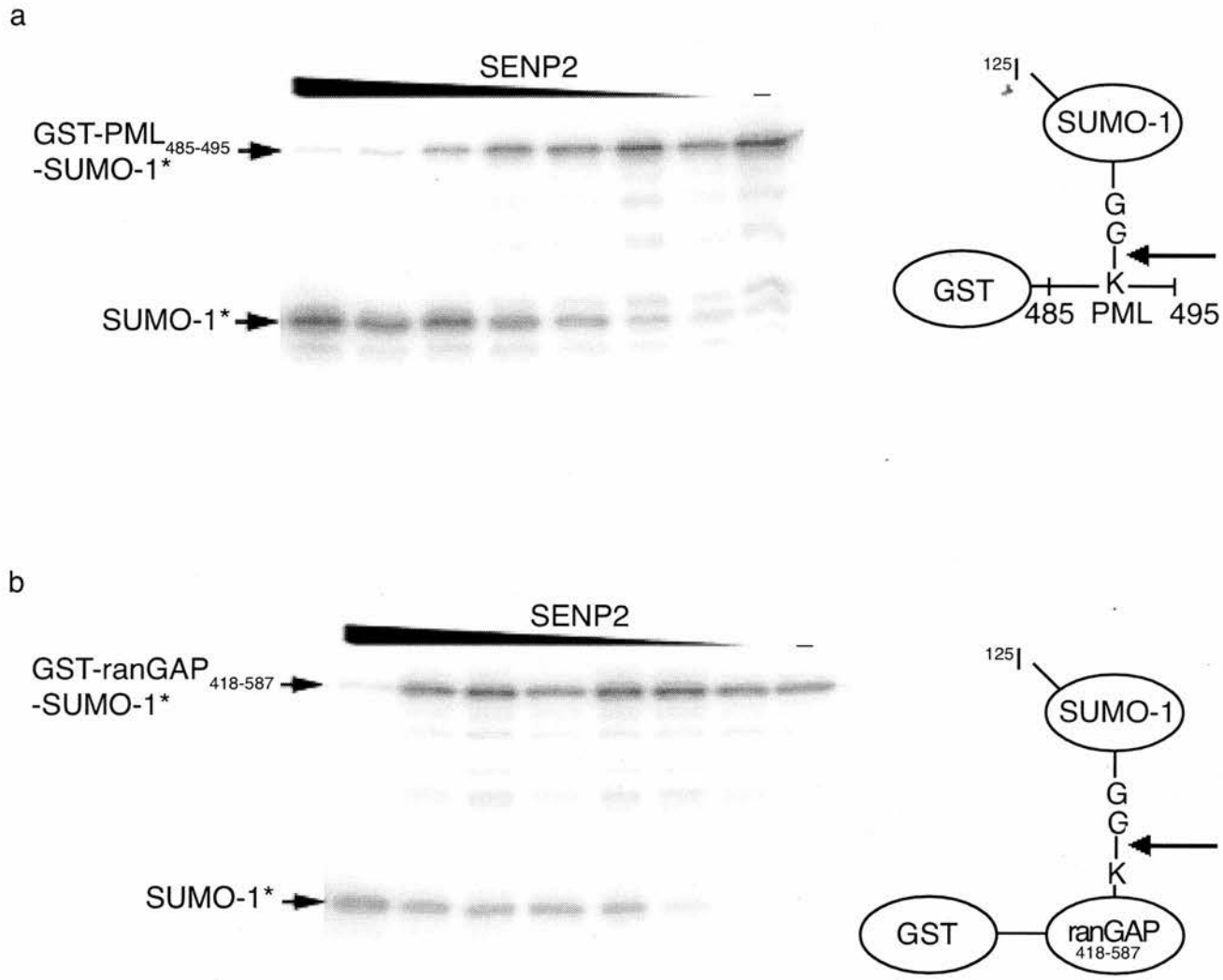

Figure 31: SENP2 deconjugates SUMO-1 from modified PML and RanGAP *in vitro*. GST-SENP2$_{368-589}$ catalysed deconjugation of GST-PML$_{485-495}$I-SUMO-1* (a) and GST-ranGAP$_{418-587}$-SUMO-1* (b). SUMO-1* modified GST-PML$_{485-495}$ or GST-ranGAP$_{418-587}$ was incubated with a range of concentrations of GST-SENP2$_{368-589}$ (0.008 μg to 0.5 μg) for 3 h at 37° C. Reaction products were analysed by SDS-PAGE and radioactive species detected by phosphorimaging. The positions of GST-PML$_{485-495}$-SUMO-1*, GST-ranGAP$_{418-587}$-SUMO-1* and free SUMO-1* are indicated. (*) indicates radiolabelling.

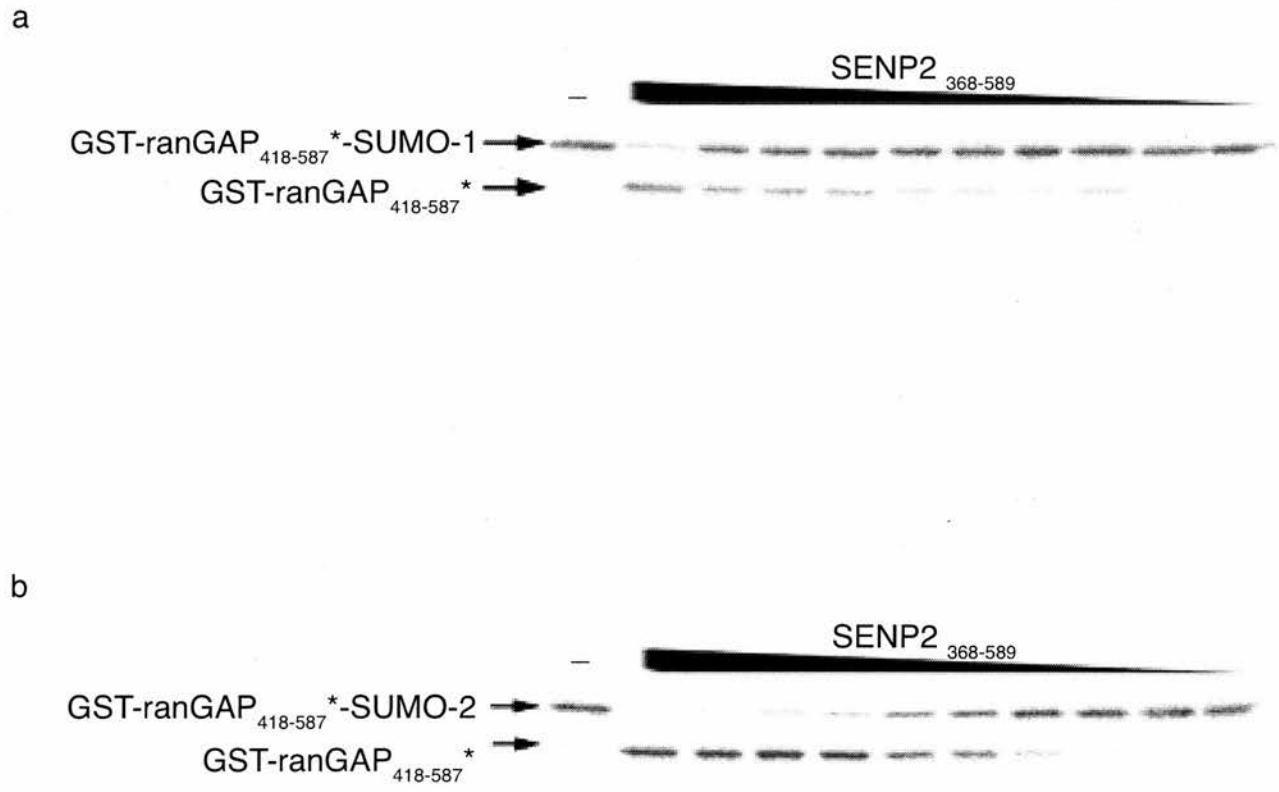

Figure 32: SENP2 deconjugates SUMO-1 and SUMO-2 from RanGAP *in vitro*.

GST-SENP2$_{368-589}$ catalysed deconjugation of GST-ranGAP$_{418-587}$*-SUMO-1/-2. SUMO-1 (a) or SUMO-2 (b) modified GST-ranGAP$_{418-587}$* was incubated with a range of concentrations of GST-SENP2$_{368-589}$ (0.008 μg to 0.5 μg) for 3 h at 37° C. Reaction products were analysed by SDS-PAGE and radioactive species detected by phosphorimaging. The positions of GST-ranGAP$_{418-587}$*-SUMO-1/-2 and unmodified GST-ranGAP$_{418-587}$* are indicated. (*) indicates radiolabelling.

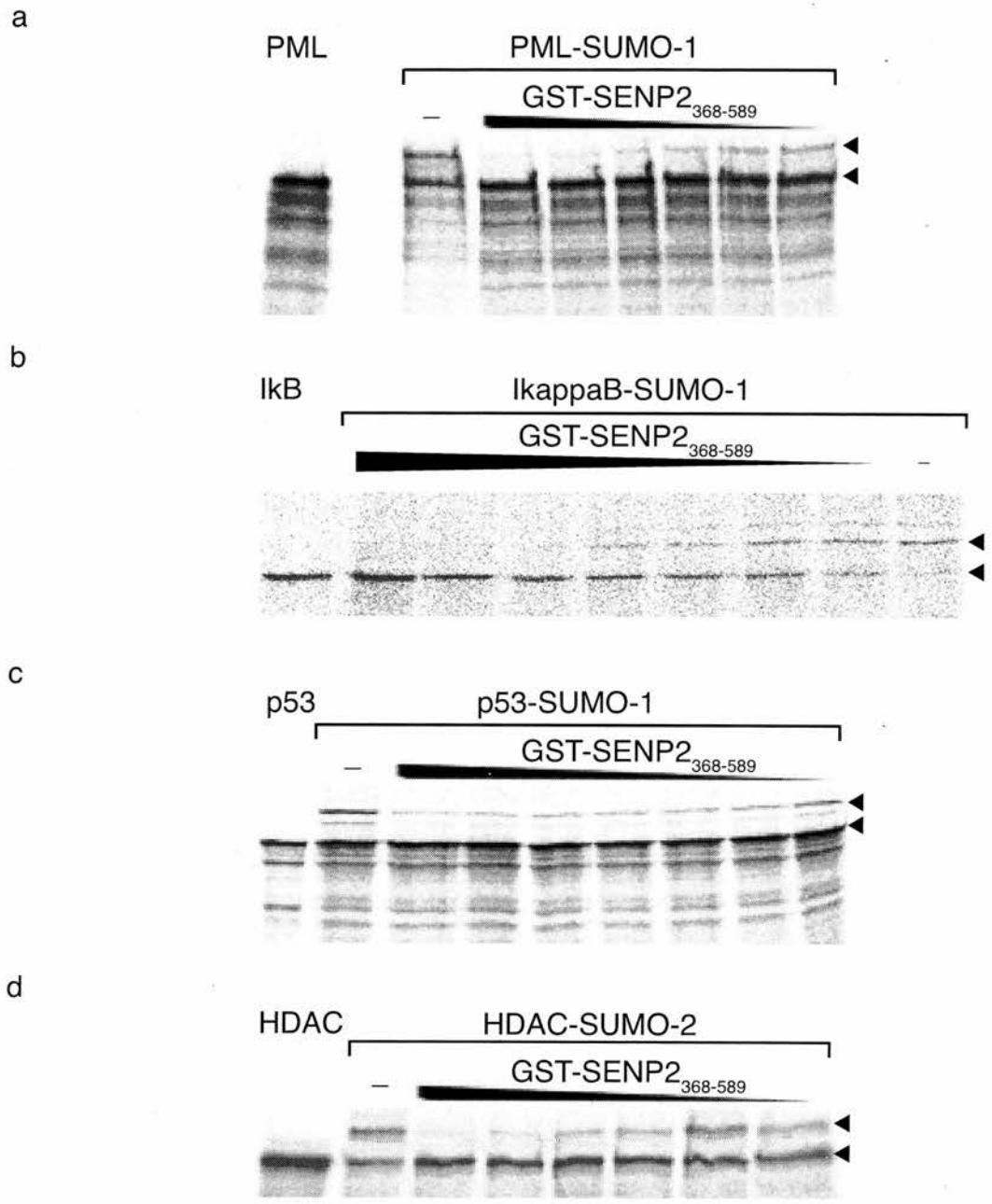

Figure 33: SENP2 deconjugates SUMO-1 and SUMO-2 from PML, IkappaBalpha, p53, and HDAC from rabbit reticulocyte lysates.

$GST\text{-}SENP2_{368\text{-}589}$ deconjugation of ^{35}S methionine labelled PML-SUMO-1, HDAC-SUMO-2, p53-SUMO-1 and IκB-SUMO-1. 15 μl of ^{35}S labelled substrate was incubated with $GST\text{-}SENP2_{368\text{-}589}$ (0.008 μg to 0.5 μg). Reaction products were analysed by SDS-PAGE and dried gels were analysed by phosphorimaging and show ^{35}S PML (3B), ^{35}S HDAC, ^{35}S p53 and ^{35}S IκB (3C) in both the free and SUMO conjugated forms as indicated.

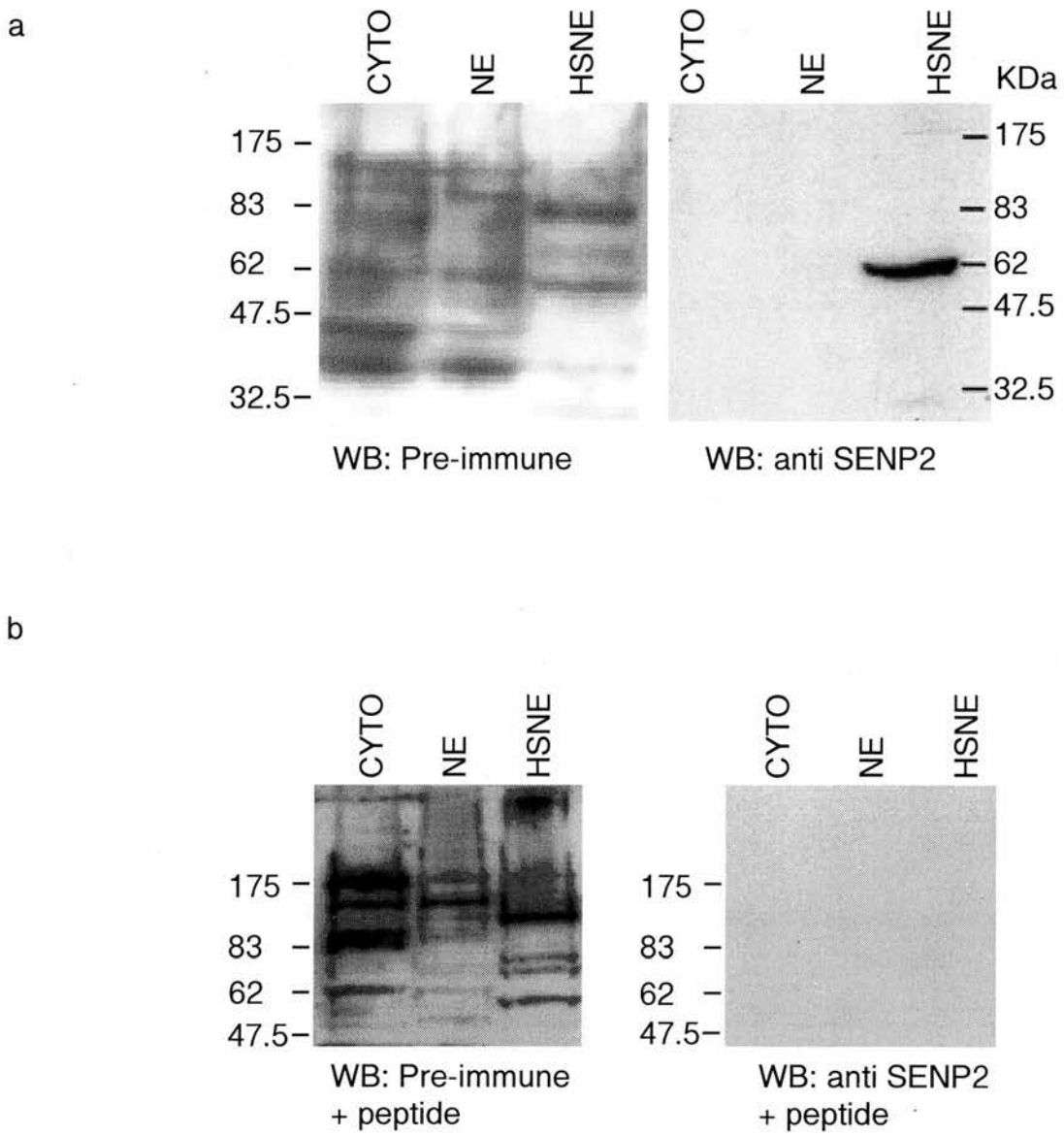

Figure 34: Western blotting demonstrates that SENP2 is localised to chromatin.

HeLa cells were fractionated as detailed in "Experimental procedures" to generate cytoplasmic (CYTO), nuclear (NE), and high salt nuclear fractions (HSNE). a. The fractions were analysed by SDS-PAGE and Western blotting using anti-SENP2 antibody. Under these conditions endogenous SENP2 is found in the high salt nuclear extract at approximately 62 kDa. b. A peptide competition assay performed on pre-immune and affinity purified anti-SENP2 specifically removed the 62 kDa band from the anti-SENP2 blot.

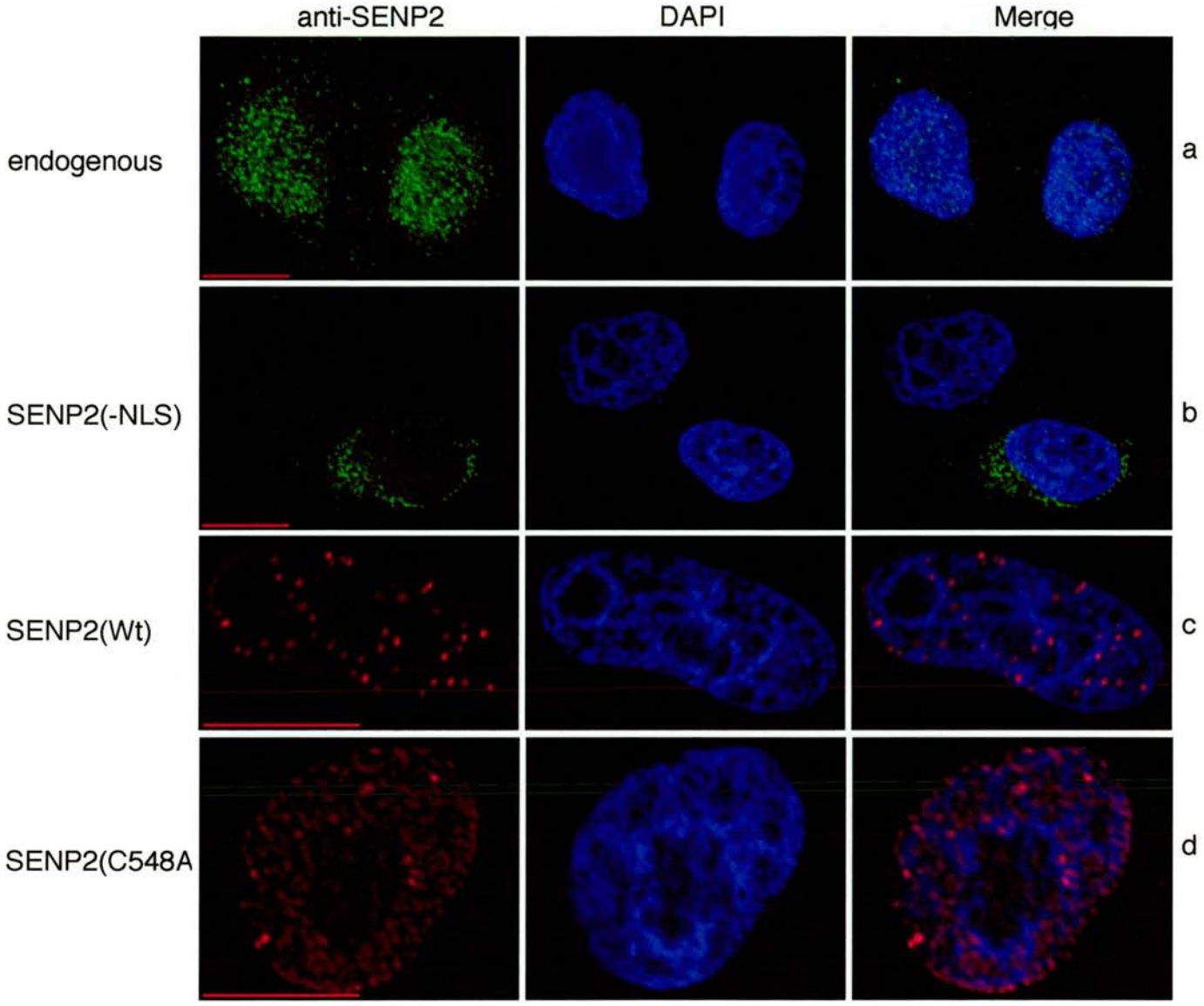

Figure 35: Subcellular localisation of SENP2.

a. The localisation of endogenous SENP2 was analysed in A549 cells using anti-SENP2 antibody. SENP2 was localised to the nucleus. b. Hela cells were transfected with SENP2 (Wt) of SENP2 (-NLS). Cells were fixed and then stained with anti-SENP2 antibody (green) and DAPI as indicated. SENP2(Wt) is localised to the nucleus while SENP2(-NLS) is localised to the cytoplasm. c. and d. HeLa CD cells were transfected with SENP2(Wt) or SENP2(C548A). Cells were then stained with anti-SENP2 (red), and DAPI as indicated. Both SENP2(Wt) and SENP2(C548A) were localised exclusively to the nucleus.

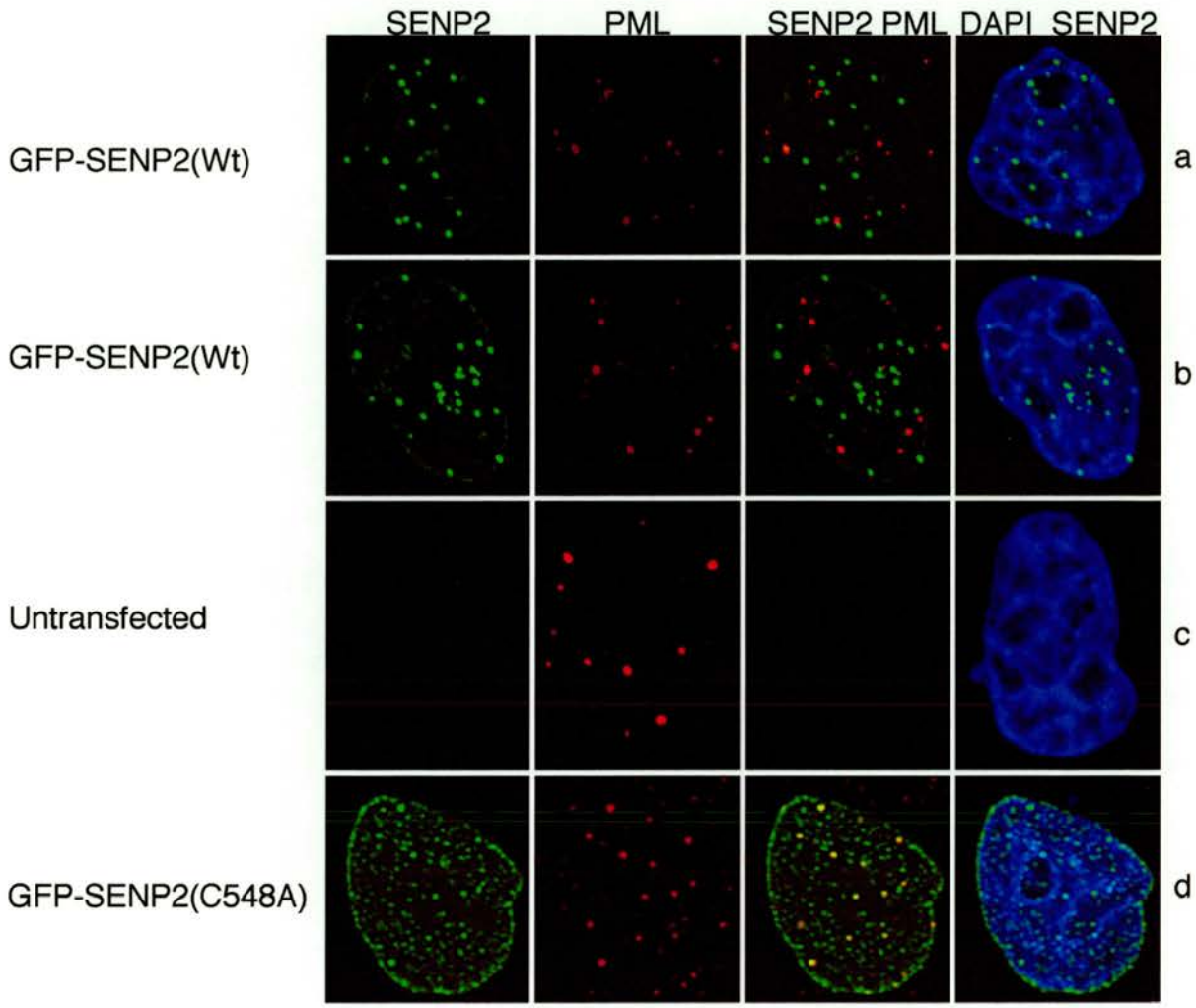

Figure 36: Localisation of SENP2 and PML

HeLa cells were transfected with GFP-SENP2(Wt) or GFP-SENP2(C548A). Cells were stained with anti-PML and DAPI as indicated.

Figure 55: Alignment of human SENP2 to mouse SMT3IP2.

Full-length amino acid alignment of human SENP2 and mouse SMT3IP2. Identical residues are indicated by ' * ', highly conserved residues (:), and loosely conserved residues ' . '. The predicted NLS motifs are boxed.

6. Characterisation of SENP1

6.1 Introduction

Mitosis and cytokinesis are very tightly regulated to ensure the accurate segregation of genetic and cytoplasmic material into two daughter cells (Fig. 37). Current research has focused on the regulation of chromatid separation and furrow ingression. Furrow ingression is the process by which the plasma membrane of a dividing cell ingresses and is pinched off to release two daughter cells. Investigation into the spatial regulation of cleavage ingression has shown that different organisms utilise different mechanisms for determining the plane of division. In animal cells the position of the plane of cleavage is determined by the position of the mitotic spindle. Yeast however orient the mitotic spindle relative to the predetermined cleavage plane. The structure responsible for furrow ingression in both animal cells and yeast is the actinomyosin contractile ring. After sister chromatid separation in anaphase the contractile ring compresses the central spindle, a bundle of anti-parallel microtubules formed between the separating chromatids. As the daughter cells drift apart, the central spindle microtubules become elongated and subsequently form the main structure of a slender cytoplasmic bridge separating the daughter cells, referred to as the

midzone (Fig. 37). At the centre of midzone microtubules, there is a gap that corresponds to the midbody, an electron dense structure that contains at least 35 proteins [152]. Abscission, the resolution of the cytoplasmic bridge between two daughter cells, is very poorly understood. Proteins implicated in abscission include kinases such as Aurora B [153] and polo-like kinase (Plk-1) [154]. Intriguingly, the maternal centriole has been shown to migrate to the vicinity of the midbody just prior to abscission and may provide temporal regulation of cytokinesis [155].

In the last few years mammalian SUMO specific proteases have been cloned and their specificity has been verified in *in vitro* and *in vivo* experiments [68, 69, 114, 149, 150, 156]. Yet the function of SUMO proteases in cells has remained elusive. It is likely that the equilibrium between conjugation and deconjugation is highly dynamic. Azuma and colleagues have demonstrated in *Xenopus* that topoisomerase II is maximally conjugated at metaphase with levels of conjugated species rapidly declining at the metaphase to anaphase transition [30]. In addition SUMO proteases can be activated rapidly and specifically due to certain cell stimuli such as: DNA damaging agents (our lab unpublished results) and heat shock [157]. However the individual proteases involved in each of these activities is unknown. All of the current research on SUMO proteases in cells is based on over-expression experiments and under these conditions SUMO

proteases may deconjugate the majority of SUMO substrates. In contrast elegant deletion experiments in yeast have enabled the characterisation of *S. cerevisiae* SUMO proteases ScUlp1 and ScUlp2 and *S. pombe* SUMO protease SpUlp1. Li and Hochstrasser have demonstrated that ScUlp1 is essential for cell cycle progression, with Ulp1Δ cells arresting at the G_2M phase of the cell cycle [57]. Although ScUlp2 is not essential for cell viability, loss of ScUlp2 causes pleiotropic defects, including temperature sensitivity, decreased chromosome stability, and increased sensitivity to DNA damaging agents. ScUlp2 was also isolated independently by a number of different groups as a high copy suppressor of chromatin cohesion defects [59, 60, 158]. SpUlp1Δ causes slow growth and sensitivity to ultraviolet radiation [66]. In addition some SpUlp1 null cells are multiply septated [66]. The requirement for temporally regulated SUMO conjugation and deconjugation in yeast raises the possibility that SUMO conjugation may also be required for cell cycle progression in higher eukaryotes. Indeed depletion of Ubc9 in chicken DT40 cells, using a tetracyclin repressible promoter, caused an increase in the number of cells containing multiple nuclei and a reduction in cell viablity [159]. This confirms that a role for SUMO conjugation during the cell cycle is conserved from yeast to higher eukaryotes. Yeast SUMO proteases are involved in the cell cycle and chromatid cohesion, thus it is likely that one or more mammalian SUMO proteases have similar functions.

The aims of this research were: to express and purify the SENP1 protease domain from bacteria in order to verify SUMO specificity in a recombinant system; to express full-length wt and catalyticly inactive mut in cells to confirm SUMO specificity; to characterise the subcellular localisation *in vivo*; and to investigate the function of SENP1 using siRNA.

6.2 Results

6.2.1 Expression and purification of the SENP1 protease domain as a GST fusion

To confirm that the gene isolated encoded a SUMO-specific protease, the C-terminal region (amino acids 418-645) of SENP1 containing the catalytic domain was expressed in bacteria as a fusion with glutathione S-transferase (Fig. 38). GST-SENP1$_{418-645}$ was isolated by affinity chromatography and the purified protein analysed by electrophoresis in a polyacrylamide gel containing SDS (SDS-PAGE). Coomassie Blue staining demonstrated that the purified GST-SENP1$_{418-645}$ was essentially homogeneous.

6.2.2 SENP1 processes SUMO-1, SUMO-2, and SUMO-3 precursors

SUMO-1, -2, -3 are synthesised as precursors which must be processed in cells to mature forms terminating in a di-glycine motif, prior to conjugation to substrates. To determine if SENP1 could process SUMO precursors, the SENP1 protease domain was expressed and purified from bacteria as a GST fusion. Purified GST-SENP1$_{418-645}$ was incubated with the SUMO-1, -2,

-3 precursors for 3 h at 37°C and the reaction products separated by SDS-PAGE and stained with Coomassie blue. Incubation of GST-SENP1 with the precursors for SUMO-1, SUMO-2, and SUMO-3 resulted in the appearance of a more rapidly migrating product that was consistent with cleavage of the precursors to the mature forms (Fig. 39). However the difference between precursor and mature SUMO-3 is only two amino acids, thus processing was difficult to determine by SDS-PAGE. To verify that the two C-terminal amino acids were being removed by SENP1, the SUMO-3 processing reaction was analysed by mass spectrometry (MALDI-TOF). SUMO-3 precursor mass of 11020 Da was decreased to 10755 Da when incubated with GST-SENP1$_{418-645}$ (Fig. 40). The experimentally determined mass of the products indicates that SENP1 processes SUMO-3$_{1-95}$ precisely to SUMO-3$_{1-93}$. Precise cleavage of SUMO-1 and SUMO-2 after the di-glycine motif was confirmed by MALDI-TOF mass spectrometry as described above (data not shown).

6.2.3 SENP1 deconjugates SUMO modified substrates in vitro

SUMO proteases have the potential to deconjugate SUMO from modified substrates as well as process SUMO precursors *in vivo*. Therefore, it was important to confirm the ability of SENP1 to deconjugate SUMO modified substrates *in vitro*. For this purpose a model SUMO modified substrate was generated. The SUMO modification site from PML (PML$_{485-495}$)

was expressed as a GST fusion and purified from bacteria. Purified GST-$PML_{485-495}$ was conjugated to ^{125}I radiolabelled SUMO-1 (SUMO-1*) using SAE1/2 and Ubc9 as detailed in 'Materials and Methods'. GST-$PML_{485-495}$ was purified from the conjugation reaction by glutathione affinity chromatography. The purified GST-$PML_{485-495}$-SUMO-1* was incubated with a range of concentrations of GST-$SENP1_{418-645}$ and the reaction products were fractionated by SDS-PAGE and analysed by phosphorimaging. SENP1 was able to efficiently cleave the isopeptide bond between the C-terminus of SUMO-1 and the lysine to which it was conjugated in PML (Fig. 41). While SENP1 was capable of acting as an isopeptidase in a purified system, it was important to establish the ability of SENP1 to deconjugate SUMO from natural substrates in the presence of unrelated proteins. For this purpose ^{35}S labelled SUMO modified substrates PML, HDAC4, and p53 were generated. PML, HDAC, and p53 were *in vitro* translated in the presence of ^{35}S-methionine using wheat germ extract. Labelled substrate was conjugated to SUMO using SAE1/2 and Ubc9 as detailed in 'Materials and Methods'. The conjugation reaction was terminated using iodoacetamide which also served to inhibit any endogenous proteases present in the extract. The iodoacetamide was quenched using ß-mercaptoethanol and the SUMO modified substrates were incubated with a range of concentrations of GST-$SENP1_{418-645}$ (Fig.42). The reaction products were fractionated by SDS-PAGE and analysed by phosphorimaging. In each

case incubation with GST-SENP1 converts the more slowly migrating SUMO modified species to the more rapidly migrating unmodified form. Thus SENP1 displays isopeptidase activity towards PML-SUMO-2, HDAC-SUMO-1, and p53-SUMO-1 in the presence of an excess of unrelated proteins from wheat germ extract.

6.2.4 SENP1 is localised to the nucleus during interphase

Previously characterised SUMO proteases have shown markedly different subcellular distributions. Therefore it was of interest to investigate the cellular localisation of SENP1. For this purpose SENP1 wt and SENP1 active site mutant (SENP1 mut) were expressed as GFP fusions in HeLa cells. At low levels of expression GFP-SENP1 was targeted to the nuclear rim and observed in the nucleoplasm (Fig. 43a). SENP1 also formed a small number of poorly defined nuclear dots. Staining of endogenous PML bodies showed that while GFP-SENP1 wt did not colocalise with PML bodies, occasional adjacent localisation occurred. When GFP-SENP1 mut is expressed at low levels its localisation is similar to that of the wt (Fig. 43b). However at higher levels of expression SENP1 mut protease forms a number of nuclear dots which colocalise with PML bodies (Fig. 43c).

6.2.5 Depletion of SENP1 causes SUMO-2, but not SUMO-1 to accumulate during cytokinesis

Genetic experiments from *S. cerevisiae* and *S. pombe* have implicated SUMO proteases in control of the cell cycle [57, 66]. To investigate the function of SENP1 in human cells small interfering RNAs (siRNAs) were used to deplete HeLa cells of SENP1 and then the ability of cells to proceed through the cell cycle was analysed. HeLa cells were transfected three times (80 nM, 50 nM, 50 nM final volume 100 μl) with either RSC, SENP1, or SENP2 siRNA then 72 h after transfection the cells were fixed and the distribution if SUMO-1 and SUMO-2 was monitored by immunofluorescence. Tubulin and DNA (DAPI) staining were used to determine the stage of cells in the cell cycle. A feature of SENP1 siRNA treated cells was that cells appeared to be undergoing aberrant cytokinesis with highly elongated midzones. While SUMO-2 did not normally accumulate in the midzone (Fig. 44a, b, h) it did accumulate along midzone microtubules in SENP1 depleted cells (Fig. 44c-f). A particularly striking feature of SENP1 depleted cells was the accumulation of SUMO-2 at the midbody in early cytokinesis. A higher magnification image of the midbody revealed that SUMO-2 accumulated in a double disc structure which overlaps with the ends of midzone microtubules (Fig. 44g).

Depletion of SENP1 did not affect SUMO-1 distribution during cytokinesis. SUMO-1 was present along midzone microtubules in both SENP1 (Fig. 45b, c) and RSC (Fig. 45a) treated cells. mRNA levels were monitored using quantitative RT-PCR of cells treated once with 100 nM siRNA then harvested 24 h later. SENP1 or RSC siRNA treated cells (Fig. 45d). SENP1 siRNA reduced SENP1 mRNA levels by approximately 80 % relative to RSC siRNA treated controls.

6.2.6 SENP1 is required for cell viability

Examination of SENP1 depleted cells by fluorescence revealed a high proportion of pyknotic and blebbing nuclei, consistent with an apoptotic phenotype (Fig. 45c-f) and (Fig. 45b). To further characterise this observation HeLa cells were transfected twice with SENP1, SENP2, or RSC siRNA (100 nM and 50 nM) and 48 h after treatment the proportion of cells at each stage in the cell cycle was determined by FACS analysis of propidium iodide stained cells. RSC and SENP2 treated conditions have 27 % and 18 % of cells in the subG1 gate, cells treated with SENP1 siRNA have 44 % of cells in the subG1 gate (Fig. 46a-c). This is consistent with SENP1 depletion being associated with an increase in apoptosis. To determine the ultimate consequences of SENP1 depletion cells were treated with RSC or SENP1 siRNA then analysed for cell viability after 96 h. Cells treated with RSC or

SENP2 siRNAs remained viable over the course of the experiment, whereas SENP1 depletion resulted in a dramatic loss in viability (Fig. 46c). Analysis of SENP1 depleted cells by immunofluorescence, stained for tubulin and DNA, revealed a characteristic phenotype of cells undergoing apoptosis during cytokinesis, as indicated by the presence of midzone microtubules and fragmented DNA (Fig. 46d). These data suggest that SENP1 depletion blocks cells in cytokinesis whereupon they undergo apoptosis.

6.2.7 SENP1 catalytically inactive mutant accumulates at the midbody during cytokinesis

As SUMO-2 accumulates at the midbody in SENP1 depleted cells, a reasonable hypothesis is that during a normal cell cycle SENP1 is required to deconjugate SUMO-2 modified substrates located at the midbody. To investigate the role of SENP1 in cytokinesis, SENP1 wt and SENP1 active site mutant (SENP1 mut) were expressed as GFP fusions in HeLa cells. Endogenous tubulin and DNA staining were used to determine the stage of cells in the cell cycle. GFP-SENP1 wt is expressed at very low levels in the midbody during cytokinesis and a faint signal can only be observed at high exposures (Fig. 47). In contrast the catalytically inactive SENP1 mut shows a striking accumulation at the midbody, an area characterised by a break in midzone microtubules. The accumullation of GFP-SENP1 mut at the

midbody was evident at early (Fig. 48a) and persisted through to late cytokinesis (Fig. 48b, c). A higher magnification of the midzone region demonstrated that GFP-SENP1 mut is present in the gap of midzone microtubules, but does not overlap with the ends of the microtubules (Fig. 48d). A 3D reconstruction of SENP1 mut midbody, using 30z sections through the midbody revealed that upon 90° rotation SENP1 mut was in the form of a ring (Fig. 48e). These data demonstrate that the catalytically inactive form of SENP1 accumulates at the midbody during mitosis and suggests that SENP1 is targeted to the midbody, but normally dissociates from the midbody after carrying out the desumoylation of proteins present at this structure. If this is the case then it would be expected that expression of a catalyticlaly inactive form of SENP1 would have similar consequences to siRNA mediated depletion of SENP1 by siRNA. HeLa cells were therefore transfected with GFP-SENP1 wt or GFP-SENP1 mut and the distribution of endogenous SUMO-1 and SUMO-2 determined by fluorescence microscopy. As expected GFP-SENP1 mut is prominently localised to the midbody and this is accompanied by the accumulation of SUMO-2, but not SUMO-1 at the midbody (Fig. 49a, b, and Fig. 50a, b). Under these conditions GFP-SENP1 wt was not detected at the midbody and did not alter the pattern of SUMO modified proteins in cells undergoing cytokinesis (Fig. 49c, d, Fig. 50c). In some cells expressing GFP-SENP1 mut DAPI staining revealed that DNA could be detected in the midzone. Higher magnification of one of these

midzone structures shows that the DNA is present across the midzone with at break at the SENP1 mut ring (Fig. 50d). This suggests that SENP1 mediated desumoylation may also be required for efficient chromosome segregation during mitosis.

6.2.8 SENP1 is involved in sister chromatid separation

Other defects in chromatid separation were also a feature of a proportion of cells expressing GFP-SENP1 mut. In some cells the chromatin failed to separate (Fig. 51) and in others the nuclear division was asymmetrical (Fig. 49b).

It is possible that SENP1 could be required at an earlier stage in mitosis, such as chromatid separation, and this could contribute to the observed chromatid separation defects and apoptosis. A preliminary examination of cells in early mitosis, either anaphase or metaphase, indicates that SENP1 depletion causes defects in chromatid alignment and or separation (Fig. 52). A proportion of cells have multiple spindle poles and many have DNA throughout the cell rather than aligned at the metaphase plate (Fig. 52). The control cells show correct alignment of the chromatids at metaphase and ordered movement to the poles as seen in anaphase (Fig. 52). In light of the chromatid separation defects observed when SENP1 was depleted, it was of

interest to determine the localisation of SENP1 during early mitosis. During metaphase, cells expressing GFP-SENP1 wt show diffuse SENP1 was well as a concentration of SENP1 to the spindle poles (Fig. 53a). Intriguingly SUMO-1 is also observed at the spindle poles (Fig. 53b).

6.3 DISCUSSION

To confirm the substrate specificity of SENP1, the SENP1 catalytic domain was expressed and purified from bacteria as a GST fusion protein. Purified SENP1 was able to process SUMO-1, SUMO-2, and SUMO-3 precursor proteins precisely to mature SUMO terminating in a di-glycine. In addition SENP1 could deconjugate model SUMO modified substrates, as well as natural substrates *in vitro*. Expression of SENP1 in HeLa cells confirmed the specificity of SENP1 as a SUMO protease *in vivo*. These data are in agreement with previously published data on SENP1 [69, 156, 160]. Localisation experiments concurred with previously published data showing that SENP1 was targeted to the nucleus during interphase. While SENP1 wt was not consistently localised to endogenous PML bodies, the catalytically inactive mutant co-localised with PML. It is possible that mutant SENP1 forms an unproductive complex with SUMO modified substrate(s) and consequently is trapped in nuclear bodies. These data are in agreement with results reported by Bailey and colleagues that show a catalyticly inactive SENP1 is also sequestered in exogenously expressed PML and HDAC4 nuclear bodies [156]. However HDAC4 normally localises to different nuclear domains than PML, so sequestration of catalyticly inactive mut by both HDAC4 and PML may be the result of over-expression, rather than specific targeting to these bodies.

siRNA to SENP1 were used to investigate the role of SENP1 *in vivo*. Depletion of SENP1 from HeLa cells results in aberrant cytokinesis and an accumulation of SUMO-2, but not SUMO-1 at the midbody. Consistent with this expression of a catalytically inactive version of SENP1 results in its accumulation at the midbody, whereas the wild type protease can be detected, but does not accumulate, at the midbody. These results suggest that SENP1 targeting to the midbody is a transient event, with SENP1 being released after the demodification of SUMO substrate(s). Intriguingly, SUMO-2 forms a double disc, the ends of which overlap with the tips of midbody microtubules while SENP1 forms a ring that lies at the centre of the midbody, between the SUMO-2 discs (Fig. 54).

This work is consistent with results on the *S. cerevisiae* orthologue of SUMO, which show that SUMO localises to the budneck, the yeast equivalent to midbody, and forms a transient ring structure that appears after anaphase and disappears before cytokinesis. In yeast the substrates for SUMO modification are the septin family of proteins which form a double ring structure at the yeast budneck. As the septin ring structure splits, the actinomysin contractile ring contracts [161]. If the SUMO modification sites of the septins are mutated, a septin ring is still able to assemble at the bud neck, but the ring is unable to disassemble at the onset of cytokinesis and

persists through subsequent cell divisions [162]. This investigation indicates that the role of SENP1 is to remove SUMO from midbody substrates during cytokinesis. The most likely candidates for SUMO modification at the midbody would be mammalian septins. A bioinformatic analysis of the mammalian septins reveals that septin 1, septin 3, and septin 10 each contain a consensus site for SUMO modification. Although mammalian septins are not as well characterised as their yeast orthologues, septins 9 and 5 are localised to the midzone and depletion of septin 9 caused binucleated cells which have arrested during cytokinesis [163]. It is important to determine whether the mammalian septins are also SUMO modified and if this modification is required for cytokinesis.

It is also possible that SUMO modified proteins other than septins may need to be desumoylated in order for cytokinesis to progress. In order to generate possible candidates an extensive literature search was undertaken to find proteins which are targeted to the midbody/midzone and also have a role in cytokinesis. Thirty-six proteins were found which satisfied both criteria. The sequences of these proteins were searched for consensus SUMO motifs. Of the thirty-six proteins, six proteins were found to possess consensus SUMO motifs (Table 2.)

	Midbody localisation	No. SUMO sites	SwissPro/TREMBLE ID
Citron kinase	Yes	7	Q87UQ9
ECT2	Yes	3	ECT2_HUMAN
CHO1/Mklp-1	Yes	2	KF23_HUMAN
Prc1	Yes	1	O43663
AIM-1	Yes	2	AURB_HUMAN
PTP-BL	Possibly	3	PTND_HUMAN

Table 2: Proteins which are localised to the midbody and possess SUMOylation motifs.

Intriguingly cells in which SENP1 had been depleted also exhibited defects in chromatid separation. Multiple spindle poles were often present and DNA was arrayed throughout the cell. Normally sister chromatids align along the metaphase plate and then very rapidly separate to opposite poles. A preliminary investigation of SENP1 and SUMO-1 early in mitosis demonstrates that both SUMO-1 and SENP1 are localised to the spindle poles in metaphase. It is possible that SENP1 or SUMO-1 may be involved in regulation of spindle pole body formation. This is one mechanism through which depletion SENP1 could cause anaphase defects. Alternatively, SENP1 depletion may interfere with sister chromatids separation at the kinetochore or along the chromatid arms. Consistent with these observations, *S. cerevisiae* SUMO proteases Ulp1 and Ulp2 and *S. pombe* Ulp1 are required for cell cycle progress [57, 66]. In particular ScUlp2 is linked to centromeric cohesion by deconjugation of SUMO modified

topoisomerase II [60] and in *X. laevis* topoisomerase II undergoes transient modification with SUMO-2 in mitosis [30]. In addition ScSUMO is required for chromosome segregation in *S. cerevisiae* [164] and scUlp2 is involved regulation of sister chromatid condensation [158]. The defects in chromosome segregation or separation that occur when SENP1 is depleted could also cause cells to undergo apoptosis through induction of the spindle assembly checkpoint

Much remains to be discovered about the role of SENP1 in mitosis. Future work should focus on the spatial and temporal regulation of SUMO and SENP1 during mitosis. In particular it will be essential to discover which proteins are SUMOylated and deSUMOylated in order to regulate chromosome separation and cytokinesis.

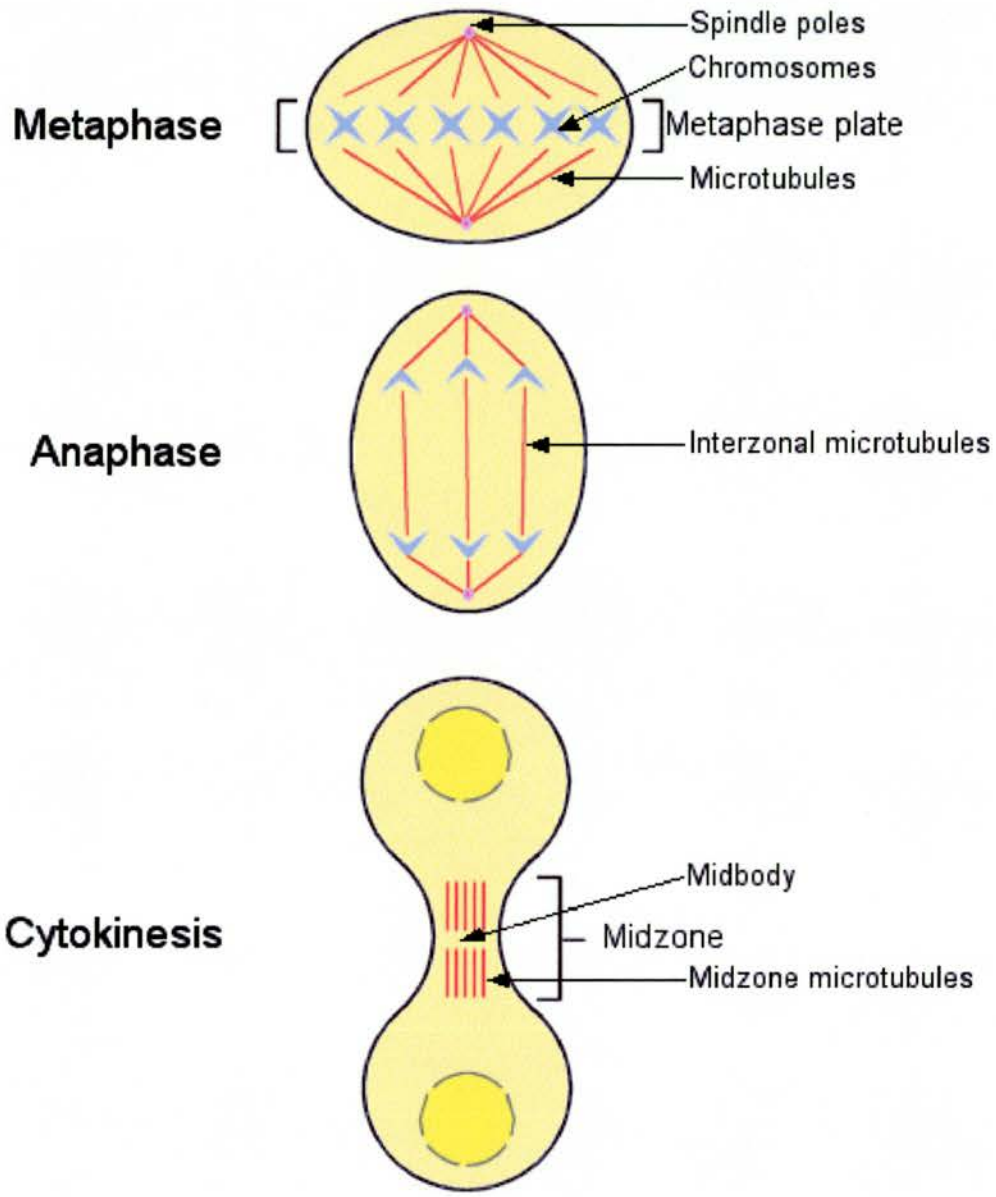

Figure 37: A representation of mammalian cells in metaphase, anaphase, and cytokinesis. Metaphase - condensed sister chromatids align at the equator of the cell (metaphase plate). Anaphase - Sister chromatids separate and moves to opposite spindle poles. The cell elongates and the cleavage furrow forms. Cytokinesis - The interzonal microtubles have been condensed into the midzone microtubules and form the main structure of a thin cytoplasmic bridge connecting two daughter cells. A break in midzone microtubules corresponds with an electron dense structure known as the midbody. Cytokinesis is completed when the midzone is pinched off.

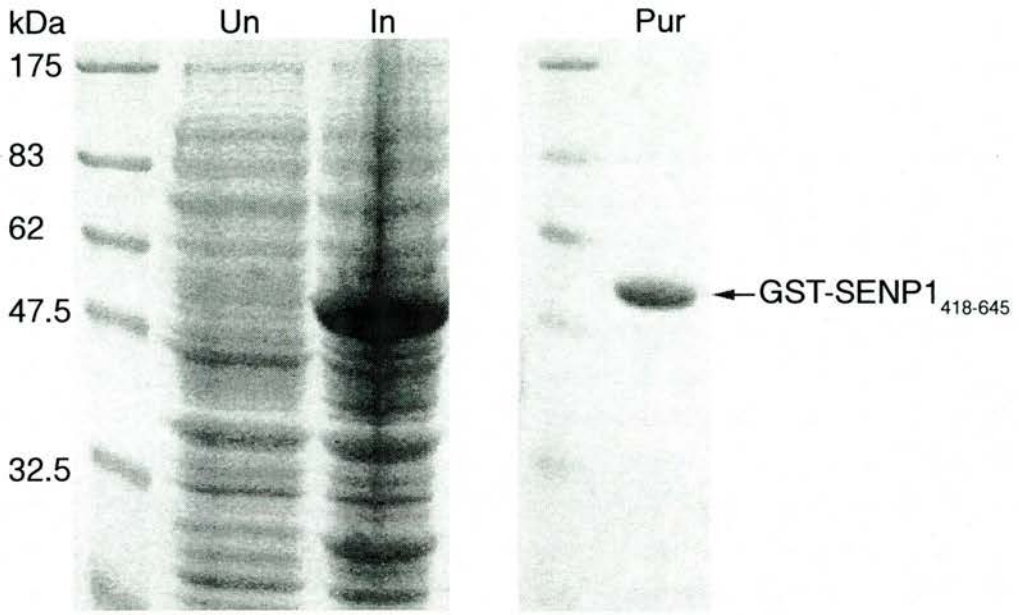

Figure 38: Expression and purification of GST-SENP1$_{418-645}$.

Coomassie-stained SDS-polyacrylamide gels showing uninduced (Un) bacteria , induction (In) of GST-SENP$_{418-645}$ and 2 ug the purified (Pur) protein SENP1$_{418-645}$.

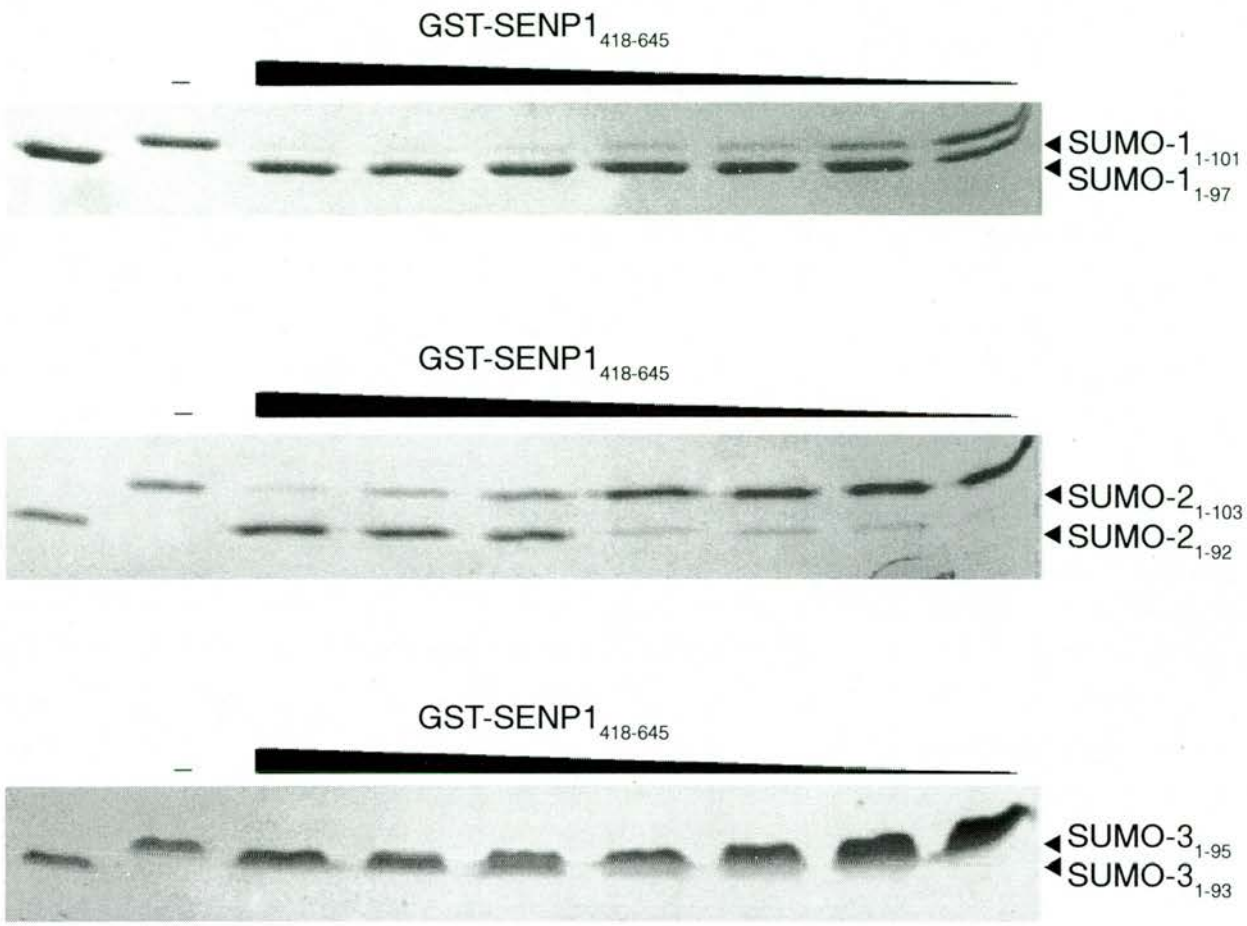

Figure 39: SENP1 processess SUMO-1, SUMO-2, and SUMO-3.

a. Coomassie-stained SDS-polyacrylamide gels showing 2 μg of full-length recombinant SUMO-1_{1-101}, SUMO-2_{1-103}, or SUMO-3_{1-95} incubated with varying concentrations of GST-SENP1$_{418-645}$ (0.008 μg to 0.125 μg). Recombinant SUMO-1_{1-101}, SUMO-1_{1-97}, SUMO-2_{1-103}, SUMO-2_{1-92}, SUMO-3_{1-93} and SUMO-3_{1-95} in the presence or absence of protease are indicated.

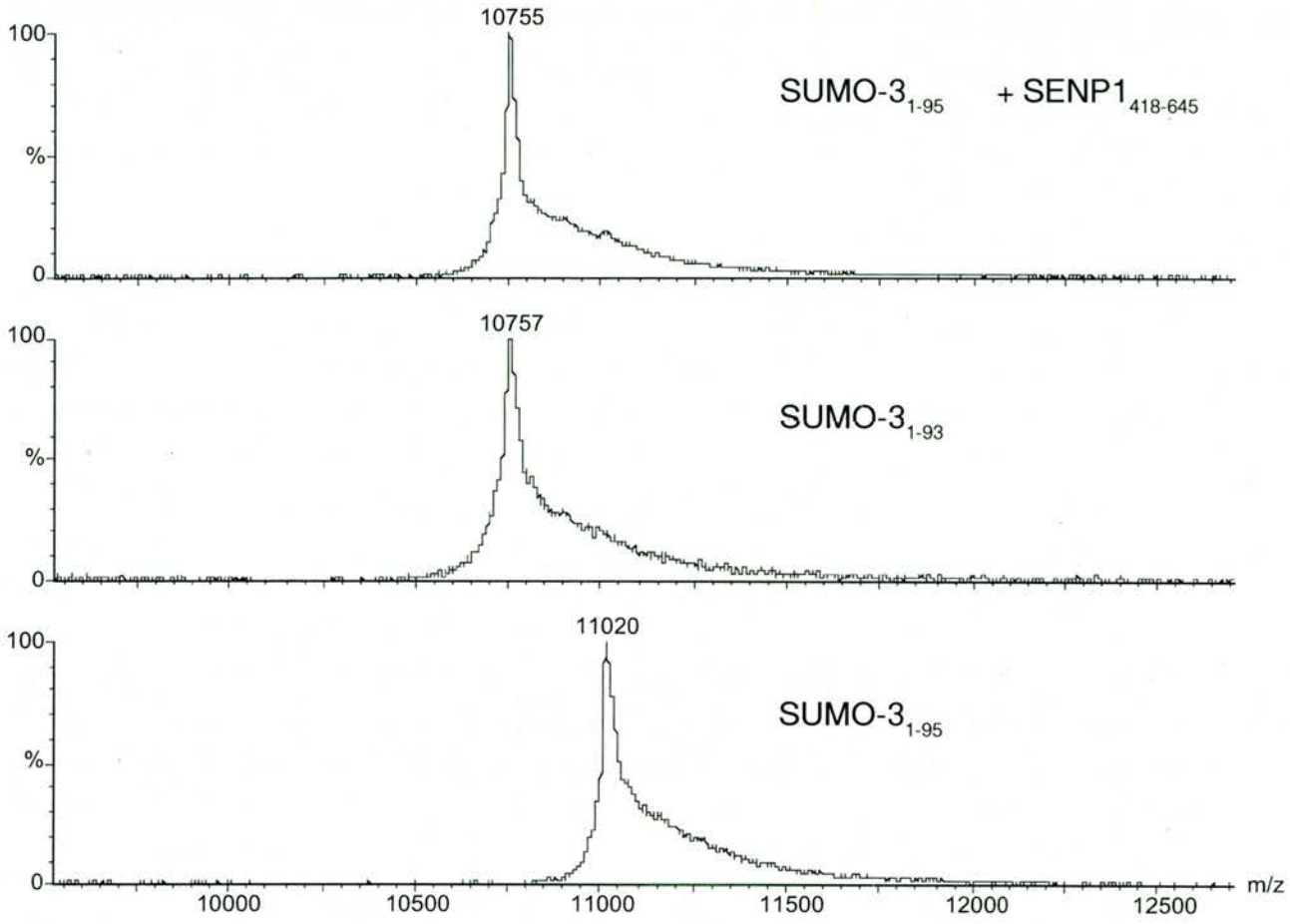

Figure 40: SENP1 processes the SUMO-3 precursor to mature SUMO-3.

GST-SENP1$_{418-645}$ processes SUMO-3$_{1-95}$ to SUMO-3$_{1-93}$. The SUMO-3$_{1-95}$ processing assay was set up and the products analysed by MALDI-TOF Mass Spectrometry as detailed under "Experimental Procedures". SUMO-3$_{1-95}$ incubated in the presence of GST-SENP1$_{418-645}$ has a mass of 10755 Da. Recombinant purified SUMO-3$_{1-93}$ mass 10757 Da. Recombinant purified SUMO-3$_{1-95}$ mass 11020 Da.

Figure 41: SENP1 deconjugates SUMO-1 modified PML *in vitro*.

GST-SENP1$_{418-645}$ catalysed deconjugation of GST-PML$_{485-495}$I^{125}SUMO-1 (SUMO-1*). SUMO-1* modified GST-PML$_{485-495}$ was incubated with a range of concentrations of GST-SENP1$_{418-645}$ (0.008 ug to 0.125 ug). Reaction products were analysed by SDS-PAGE and radioactive species detected by phosphorimaging. The positions of GST-PML$_{485-495}$-SUMO-1* and free SUMO-1* are indicated.

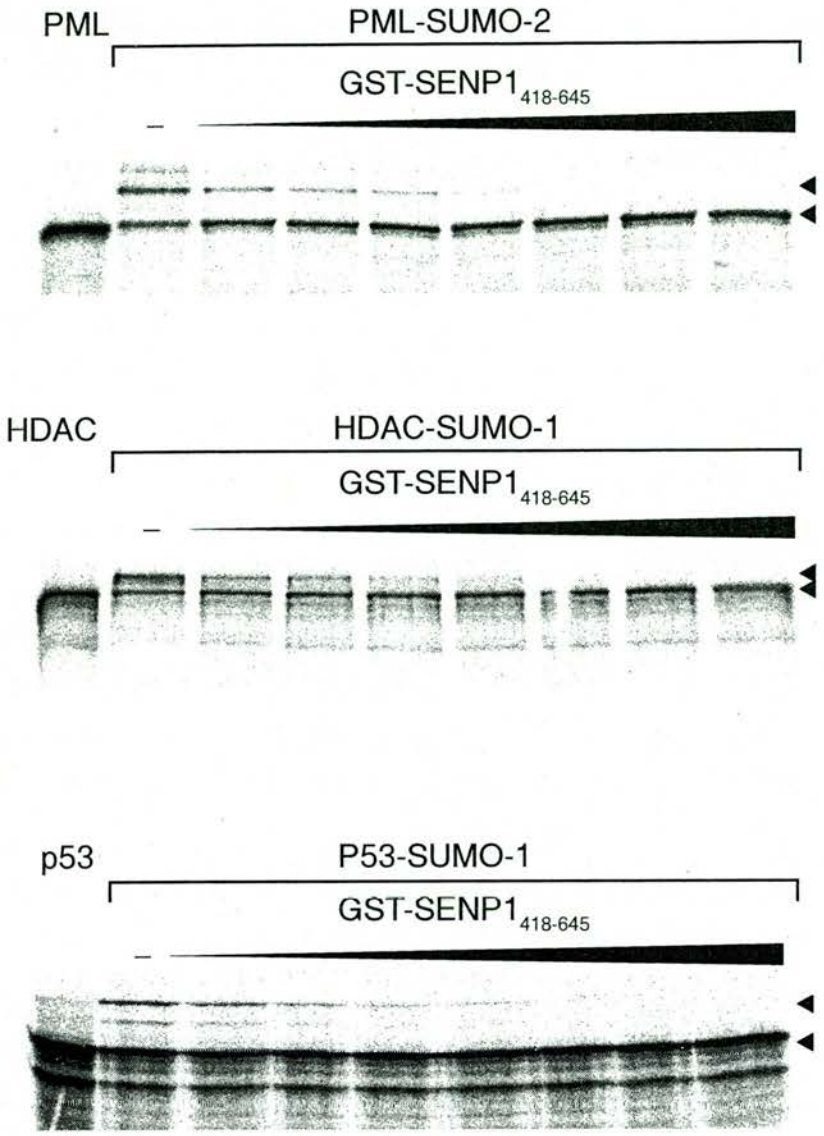

Figure 42: SENP1 deconjugates SUMO-1 and SUMO-2 from modified from PML, HDAC, p53 from rabbit reticulocyte lysates.

GST-SENP1$_{418-645}$ deconjugation of ^{35}S methionine labelled PML-SUMO-2, HDAC-SUMO-1, and p53-SUMO-1. 15 μl of ^{35}S labelled substrate was incubated with GST-SENP1$_{418-645}$ (0.008 μg to 0.5 μg). Reaction products were analysed by SDS-PAGE and dried gels were analysed by phosphorimaging and show ^{35}S PML, ^{35}S HDAC, and ^{35}S p53 in both the free and SUMO conjugated forms as indicated.

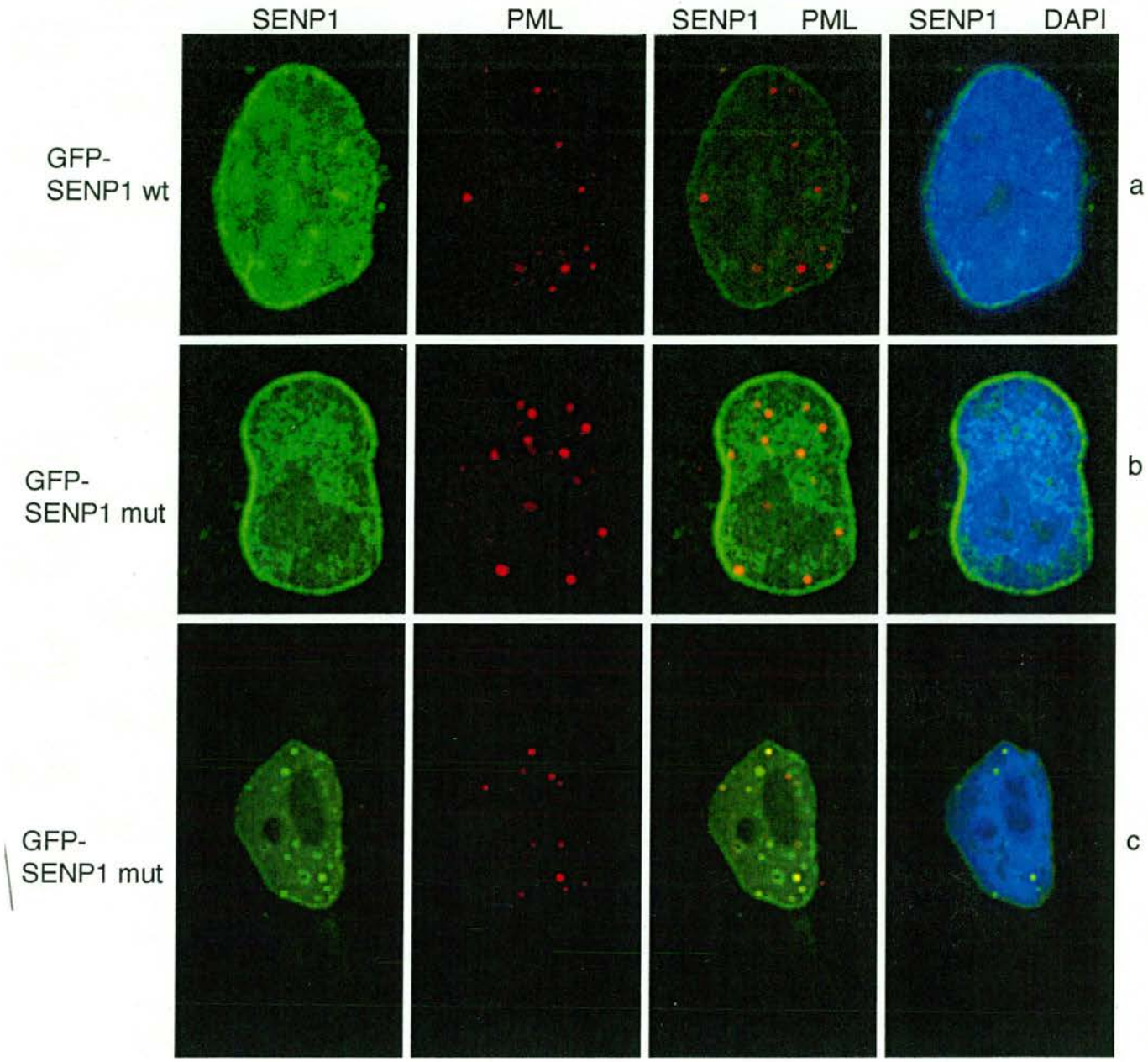

Figure 43: Localisation of SENP1 during interphase.

HeLa cells were transfected with GFP-SENP1 (a)wt or GFP-SENP1 mut (b and c). Cells were fixed with parafomaldehyde prior to staining with anti-PML and DAPI as indicated.

Figure 44: SENP1 depletion causes SUMO-2 to accumulate at the midbody.

HeLa cells were transfected with RSC (a, b, h) or SENP1 (c-g) siRNA and the distribution of endogenous SUMO-2 was monitored by immunofluorescence. Endogenous alpha-tubulin and DAPI staining were used to determine the cell cycle stage. Panels g and h show the midbody regions of c and a respectively at higher magnification.

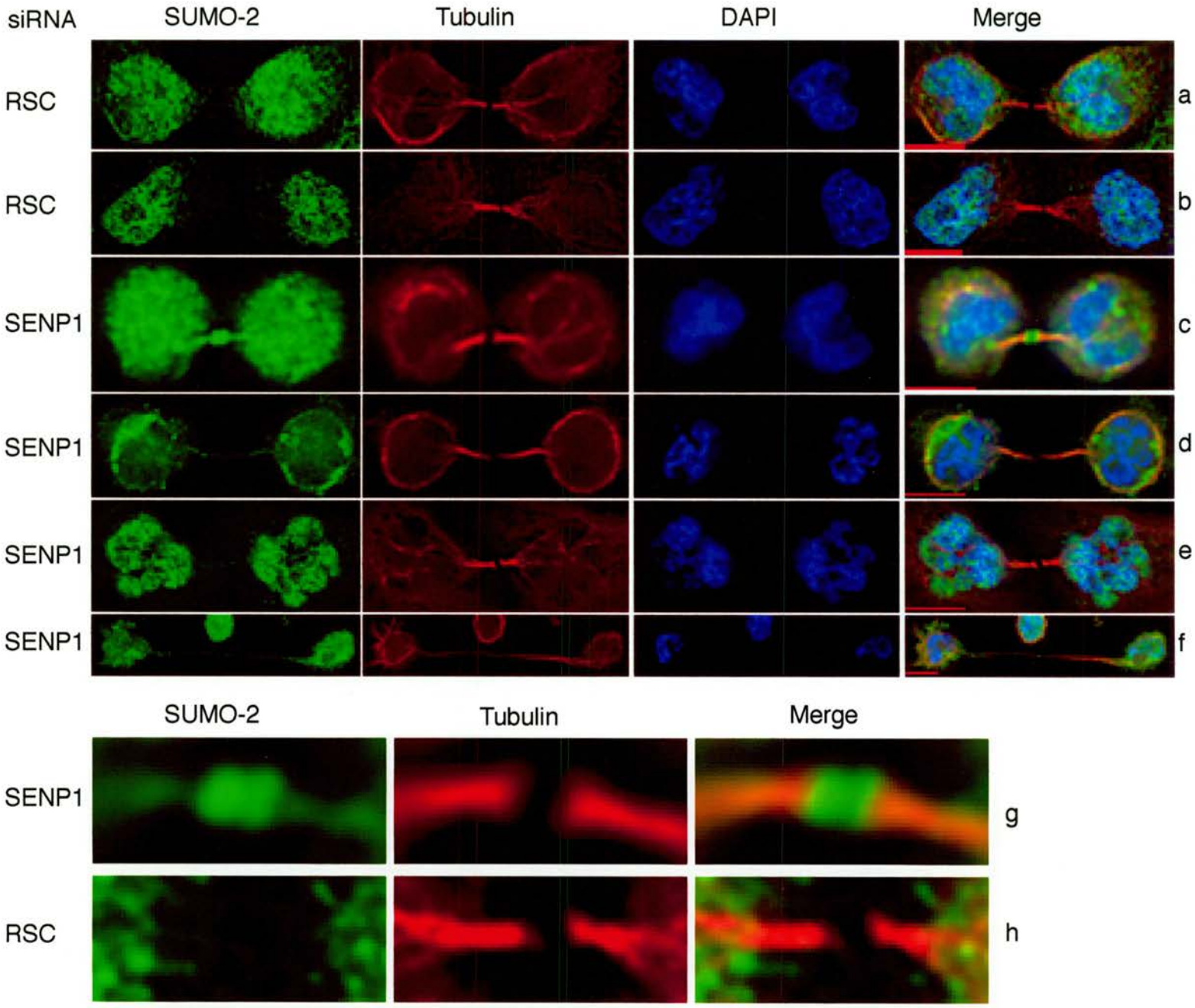
siRNA
SUMO-2
Tubulin
DAPI
Merge
RSC
a
RSC
b
SENP1
c
SENP1
d
SENP1
e
SENP1
f
SUMO-2
Tubulin
Merge
SENP1
g
RSC
h

Figure 45: SENP1 depletion does not cause SUMO-1 to accumulate at the midbody.

HeLa cells were transfected with RSC (a) or SENP1 (b and c) siRNA and the distribution of endogenous SUMO-1 was monitored by immunofluorescence. Endogenous alpha-tubulin and DAPI staining were used to determine the cell cycle stage. d. SENP1 mRNA levels were determined by quantitative RT-PCR after transfection of cells with RSC, SENP2 or SENP1 siRNA. Data were analysed from 6 replicates and variance is represented as % CV.

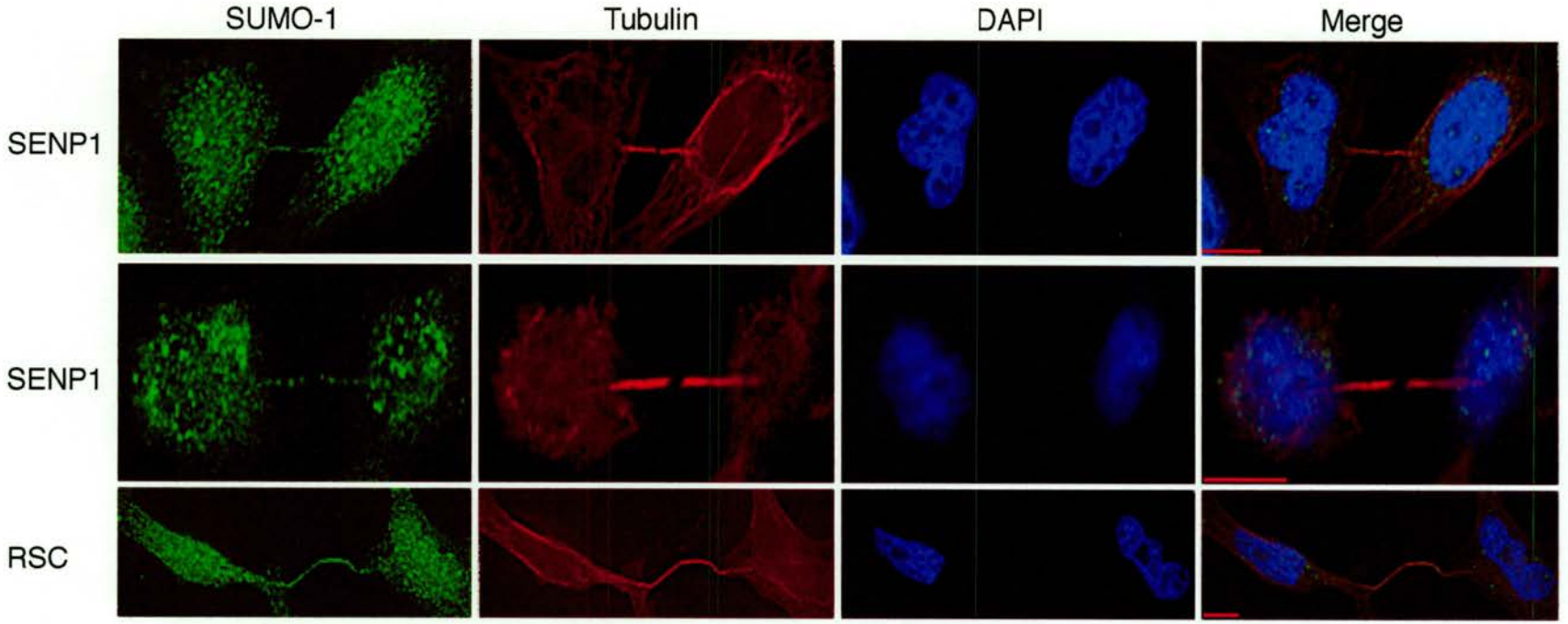
SUMO-1
Tubulin
DAPI
Merge
SENP1
SENP1
RSC
a
b
c

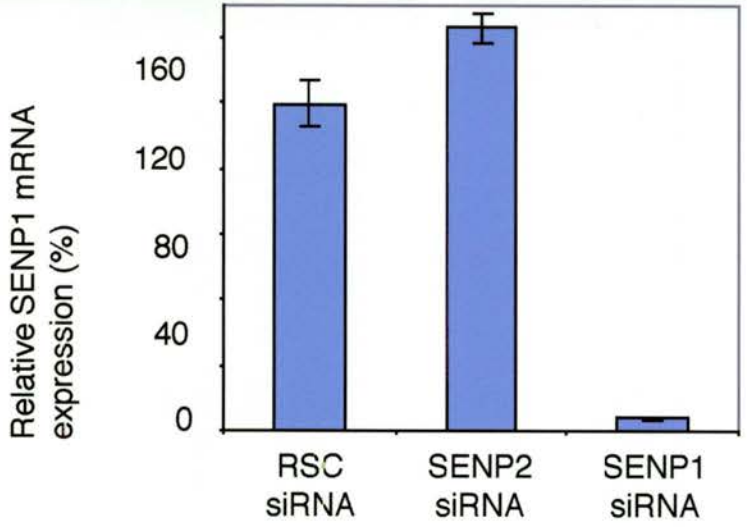
Relative SENP1 mRNA expression (%)
160
120
80
40
0
RSC siRNA
SENP2 siRNA
SENP1 siRNA
d

Figure 46: SENP1 is required for cell viability.

a. b. HeLa cells were transfected twice (100 nm and 50 nm) with RSC, SENP2, or SENP1 siRNA and harvested at 48 h. The effect on the cell cycle was determined by FACS analysis of propidium iodide stained cells. c. HeLa cells were transfected twice (50 nm) and analysed at 96 h post transfection for viability. Cell viability was measured using an MTT which is based on mitochondrial function. d. Phenotype of SENP1 siRNA treated cell stained with anti-alpha tubulin and DAPI. Scale bar 10 um.

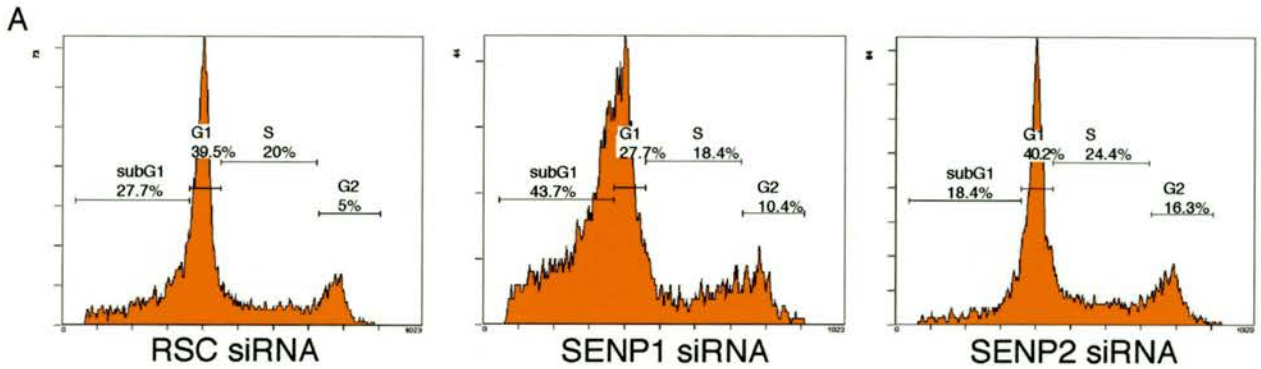
A
G1
39.5%
S
20%
subG1
27.7%
G2
5%
RSC siRNA
G1
27.7%
S
18.4%
subG1
43.7%
G2
10.4%
SENP1 siRNA
G1
40.2%
S
24.4%
subG1
18.4%
G2
16.3%
SENP2 siRNA

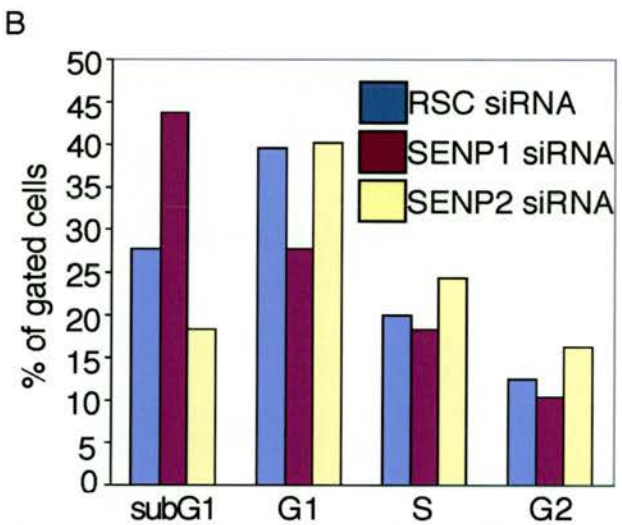
B
% of gated cells
50
45
40
35
30
25
20
15
10
5
0
RSC siRNA
SENP1 siRNA
SENP2 siRNA
subG1
G1
S
G2

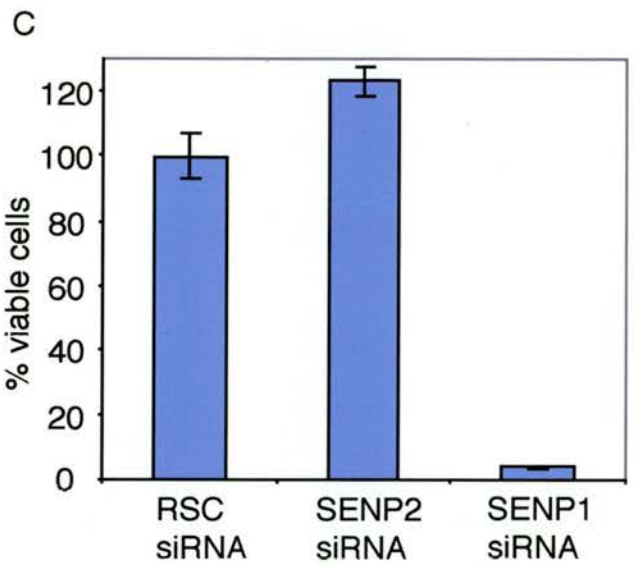
C
% viable cells
120
100
80
60
40
20
0
RSC siRNA
SENP2 siRNA
SENP1 siRNA

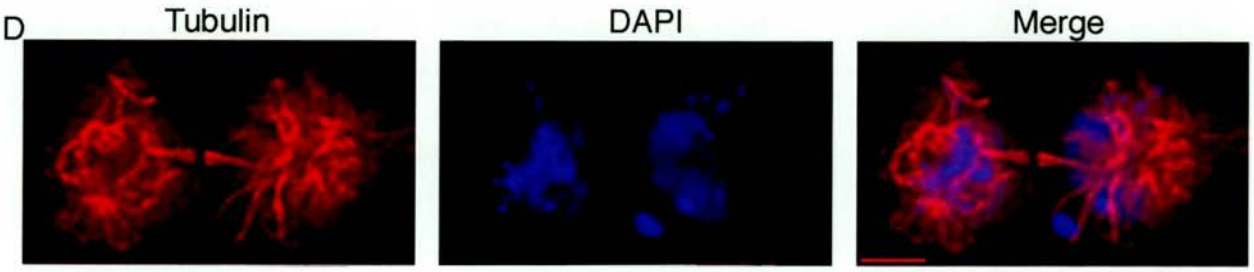
D
Tubulin
DAPI
Merge

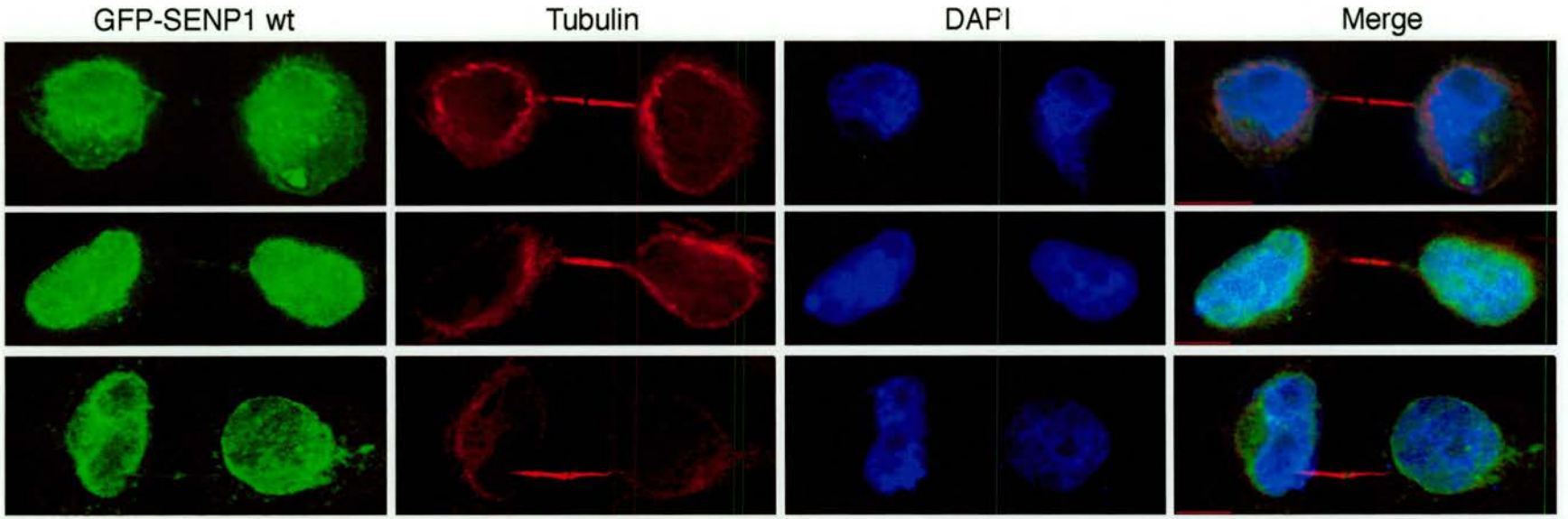

Figure 47: SENP1 wt is present at low levels in the midbody during cytokinesis.

a-c. HeLa cells were transfected with GFP-SENP1 wt then fixed and stained for tubulin and DAPI. In order to detect GFP-SENP1 wt at the midbody the gain was set 10 times higher than for GFP-SENP1 mut. Scale bars 10 um.

Figure 48: SENP1 mut accumulates at the midbody during cytokinesis.

a-d. HeLa cells were transfected with GFP-SENP1 mut then fixed and stained for tubulin and DAPI. The midbody region of b is shown at higher magnification in d. A 3D reconstruction of the GFP-SENP1 mut structure of the midbody was carried out using 30z sections. 0 degrees and 90 degrees rotation of the structure are shown in e. Scale bars 10 um.

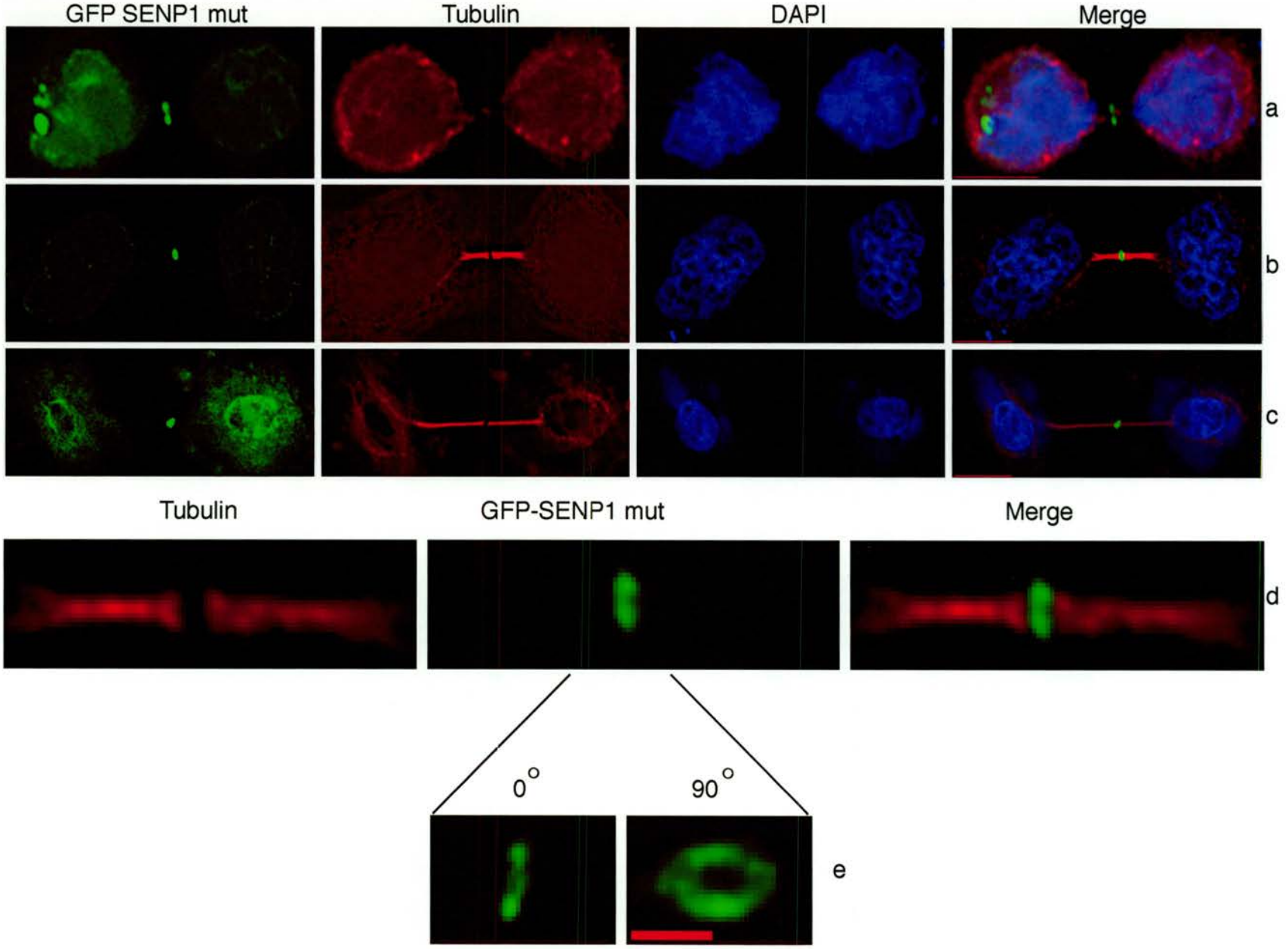
GFP SENP1 mut
Tubulin
DAPI
Merge
a
b
c
Tubulin
GFP-SENP1 mut
Merge
d
0°
90°
e

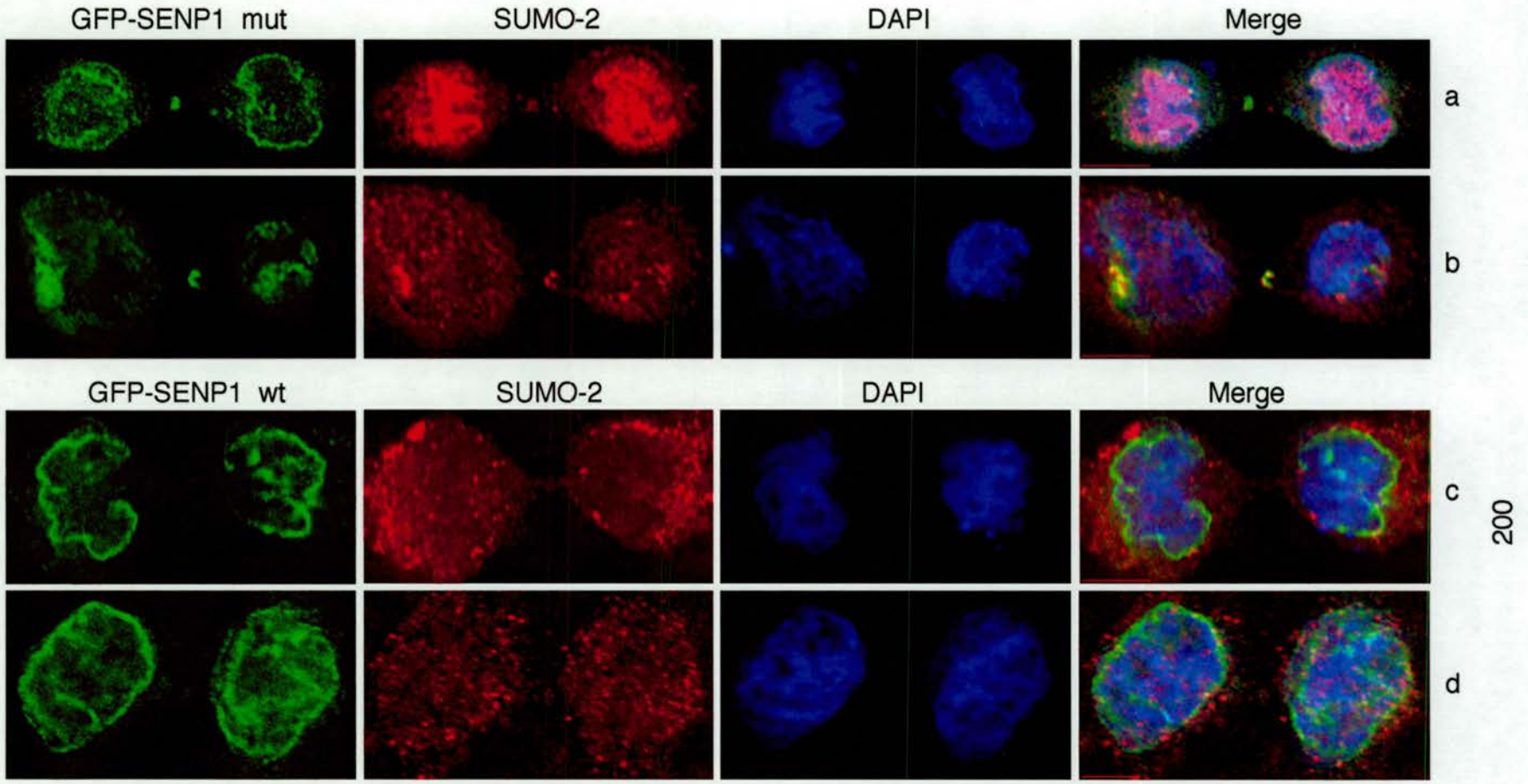

Figure 49: SUMO-2 is trapped at the midbody by expression of catalyticly inactive SENP1.

HeLa cells were transfected with either GFP-SENP1 wt (c and d) or GFP-SENP1 mut (a and b). The distribution of endogenous SUMO-2 was monitored by immunofluorescence. DNA was stained with DAPI.

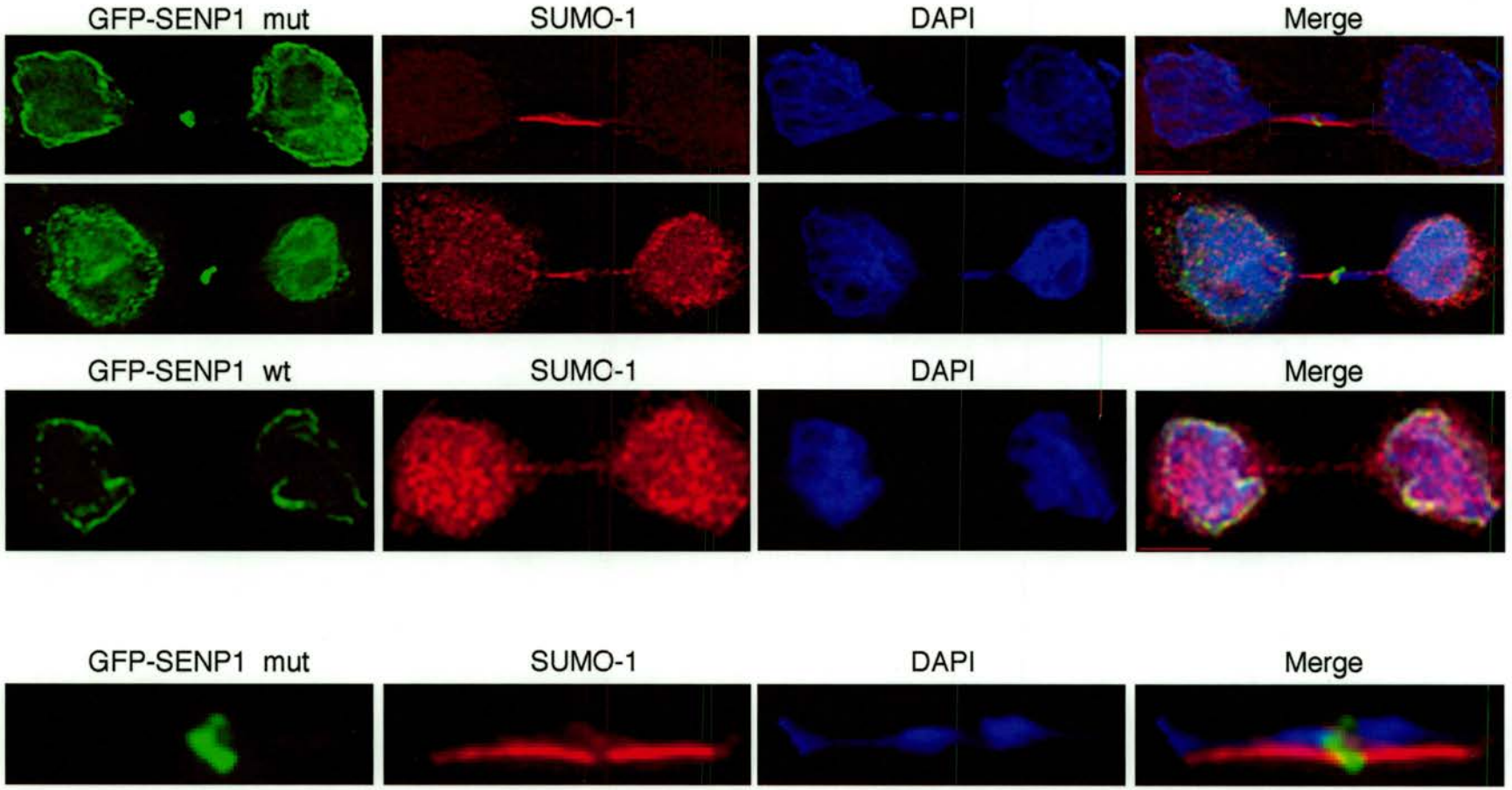

Figure 50: Expression of catalyticly inactive SENP1 causes aberrant chromatin segregation.

Hela cells were transfected with either GFP-SENP1 wt (c) or GFP-SENP1 mut (a, b, d). The distribution of endogenous SUMO-1 was monitored by immunofluorescence and DNA was stained with DAPI. A higher magnification of the midbody region from a is shown in d. Scale bars 10 um.

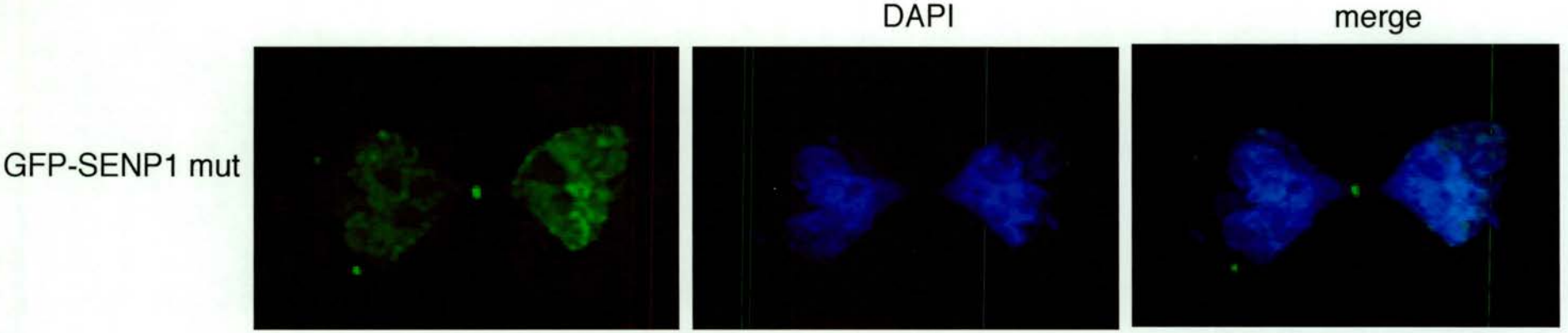

Figure 51: Expression of catalyticly inactive SENP1 causes defects in chromatin segregation.

HeLa cells were transfected with GFP-SENP1 mut. Cells were fixed with paraformaldehyde prior to staining for DAPI.

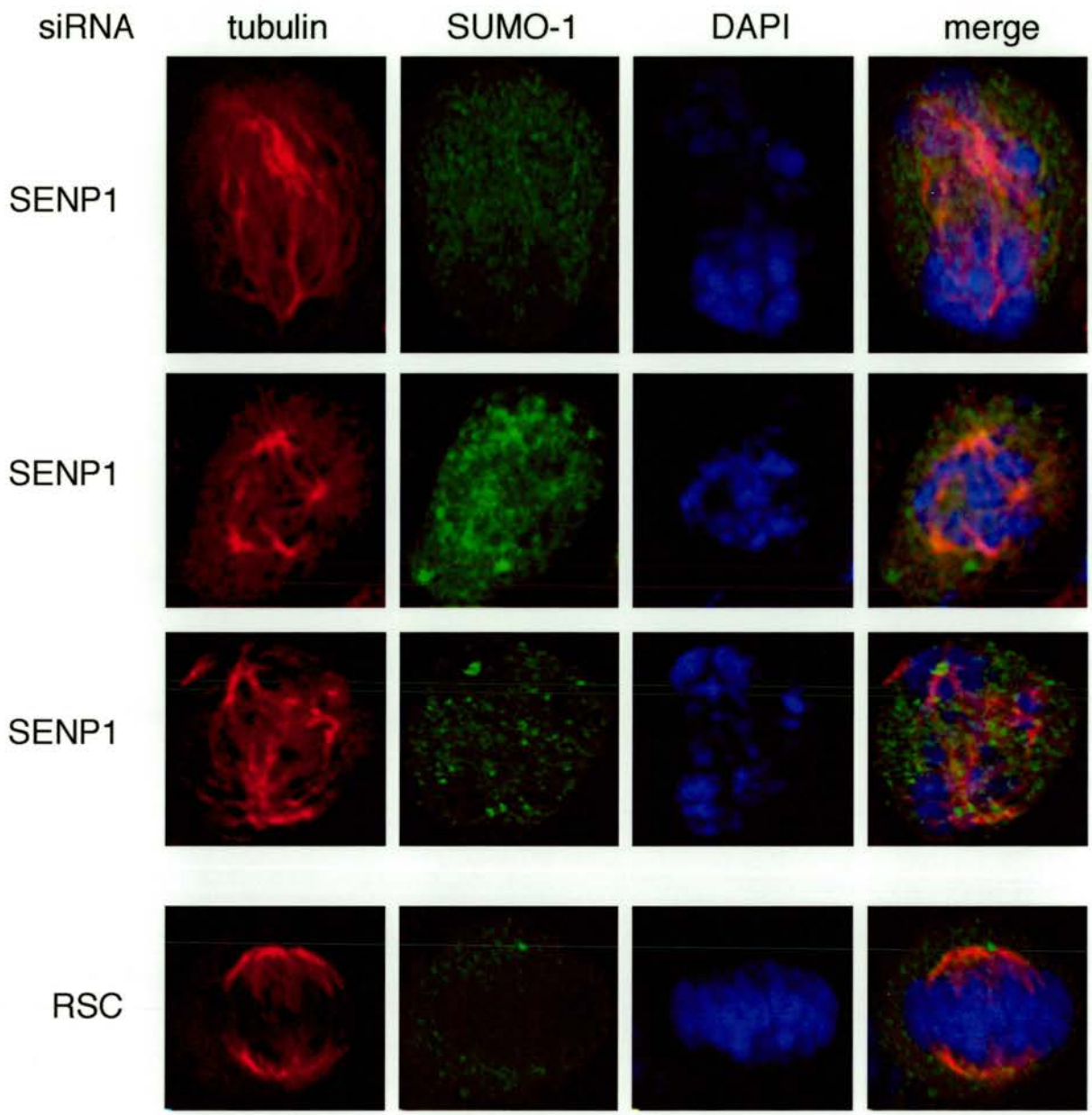

Figure 52: SENP1 depletion causes aberrant mitosis in HeLa cells.

HeLa cells were transfected with SENP1 (a-c) or RSC (d) siRNA and mitosis was monitored by immunofluorescence. Endogenous alpha-tubulin, SUMO-1, and DAPI were stained.

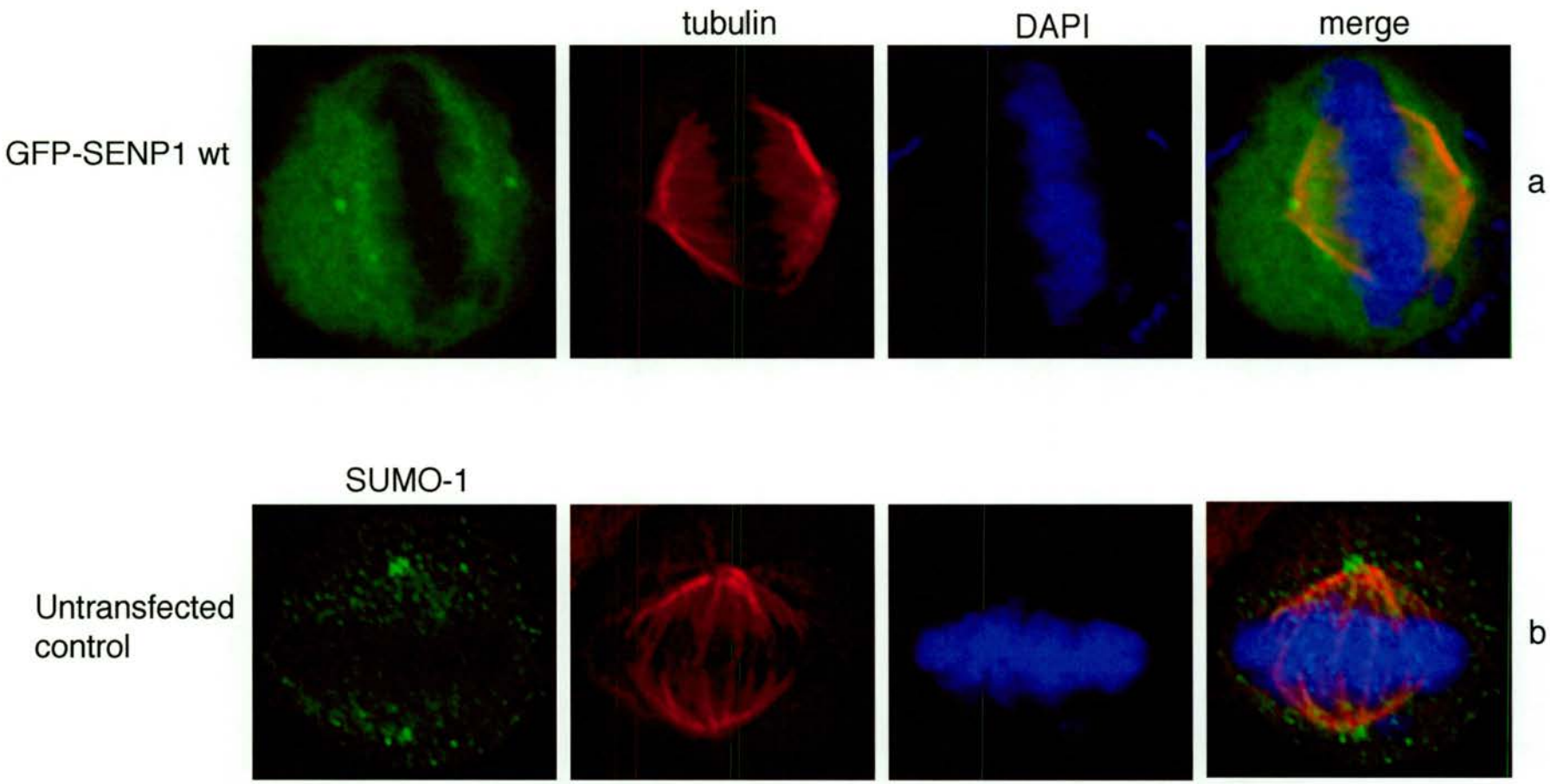

Figure 53: GFP-SENP1 wt and endogenous SUMO-1 are localised to the spindle poles at metaphase.

HeLa cells were transfected with GFP-SENP1 wt (a) or untransfected (b). Cells were fixed with paraformaldehyde prior to staining with anti-SUMO-1, anti-alpha tubulin, or DAPI as indicated.

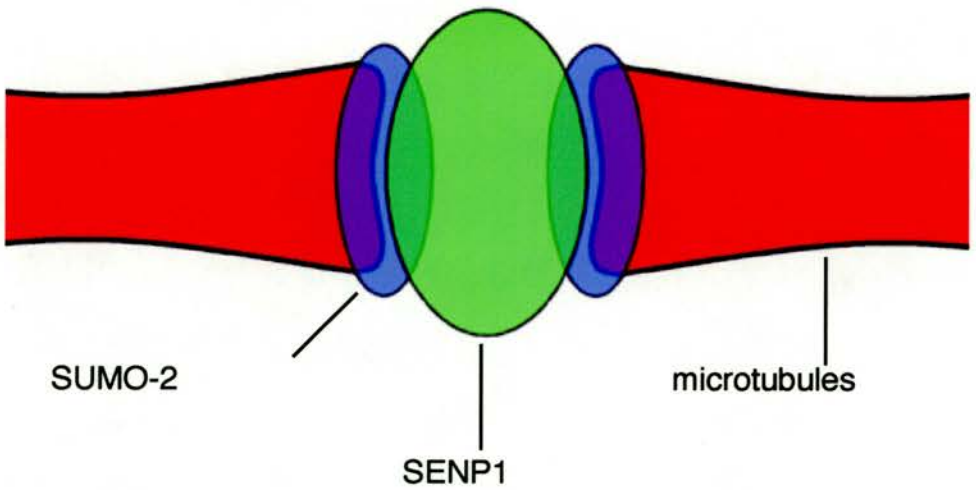

Figure 54: Diagramatic representation of the localisation of SENP1, SUMO-2, and microtubules at the midbody.

7. DISCUSSION

The aim of this research project was to identify and characterise novel SUMO-like specific proteases. Seven novel SUMO-like specific proteases were isolated and tested for SUMO specificity. SENP2 was demonstrated to be a new human SUMO specific protease. Surprisingly, NEDP1 was discovered to be a NEDD8 specific protease. NEDP1 can both process and deconjugate NEDD8, but it is currently unclear what the cellular function of NEDP1 is. The most well characterised NEDDylated substrates are the cullins, and NEDP1 is capable of removing NEDD8 from cullins both *in vitro* and *in vivo*. Depletion of NEDP1 from HeLa57A cells results in an enhanced activation of NF-$\varkappa$B. One possibility is that depletion of NEDP1 alters the activity of a cullin containing E3 ligase responsible for the degradation of a protein important for NF-$\varkappa$B activation. The recent discovery that the transcriptional activity of p53 is inhibited by Mdm2 mediated neddylation of p53 [129] leads to the possibility that other transcription factors are regulated by neddylation. It is perhaps more likely that depletion of NEDP1 alters the neddylation, and hence transcriptional activity, of a transcription factor involved in NF-$\varkappa$B activation. Another clue to the function of NEDP1, is the observation that NEDP1 depleted HeLa57A cells display an additional phenotypic change in morphology, with cells becoming elongated and spindly, suggesting that neddylation is involved in cytoskeletal regulation.

This is not without precedent as it has been previously shown in *C. elegans* that proteins of the NEDD8 conjugation pathway regulate the cytoskeleton [147]. Further investigation of the phenotypes of NEDP1 depletion should help clarify the role of NEDD8 proteases and function of NEDD8 conjugation in cells.

Here I also describe the identification and characterisation of SENP2, a previously unknown SUMO specific protease. SENP2 is able to process the SUMO precursors precisely to mature SUMO and to deconjugate SUMO both *in vitro* and *in vivo*. In addition I have demonstrated that SENP1 is a SUMO specific protease. Although both SENP1 and SENP2 are targeted to the nucleus during interphase their nuclear distribution is quite different. SENP1 wt is present primarily in the nuclear rim and nucleoplasm with only a small fraction being targeted to nuclear bodies. In contrast SENP2 is primarily targeted to nuclear bodies, with only a small proportion present in the nuclear rim. The localisation of the catalyticallly inactive mutants is also quite different. SENP2 mut forms a large number of microspeckles, whilst SENP1 forms a small number of nuclear dots. The localisation of SENP2, RanBP2, and Ubc9 to the nuclear pore strongly suggests that SUMOylation and deSUMOylation are linked to nuclear transport. A growing number of transcription factors are known to be regulated by SUMO modification, thus some of the SUMO proteases are likely to have role in transcription

regulation. The initial discovery that SENP2 is associated with chromatin suggests that SENP2 may be involved in the deSUMOylation of transcription factors. One approach to investigate the role of different SUMO proteases in the regulation of deSUMOylation would be to use siRNA to deplete individual proteases. When a transcription factor was discovered to be SUMO modified, the transcriptional activity could be measured under conditions in which individual SUMO proteases had been depleted.

From yeast to higher eukaryotes it is clear that regulated SUMO conjugation and deconjugation is required for cell cycle progression. Using SENP1 depletion and over-expression experiments, I have shown that SENP1 is required for cytokinesis in human cells. SENP1 is target to the midbody and forms a ring in cells in cytokinesis. Depletion of SENP1 or expression of catalytically inactive SENP1 causes the accumulation of SUMO-2, but not SUMO-1 at the midbody. In addition, depletion of SENP1 causes cells to undergo apoptosis, probably as a result of the induction of a cell cycle checkpoint. Although the targets for SENP1 deSUMOylation during cytokinesis are unknown, septins are likely candidates. Depletion of SENP1 also causes defects in chromatid separation with DNA becoming trapped across the midzone of cells in cytokinesis. Expression of SENP1 catalytically inactive mutant also causes asymmetric nuclear division. Thus it is likely that SENP1 has at least two roles in mitosis; it is required for sister

chromatid separation as well as for completion of cytokinesis. Again this parallels research in yeast, where it has been shown that overexpression of SUMO suppresses defects in chromatid cohesion. In addition ScUlp2 is involved in centromeric cohesion through deconjugation of SUMO modified topoisomerase II [60]. Topoisomerase II also undergoes transient modification with SUMO-2 during mitosis in *X. laevis* [30]. It is possible that depletion of SENP1 may cause defects in chomatid separation by altering topoisomerase II SUMO modification.

Much remains to be discovered about SUMO processes. How are they regulated? What are the substrate specificities of individual proteases? Will certain SUMO proteases be dedicated to precursor processing and others to deconjugation? From the wide variety of proteins known to be SUMO modified it is clear that SUMO proteases will be involved in a many cellular processes.

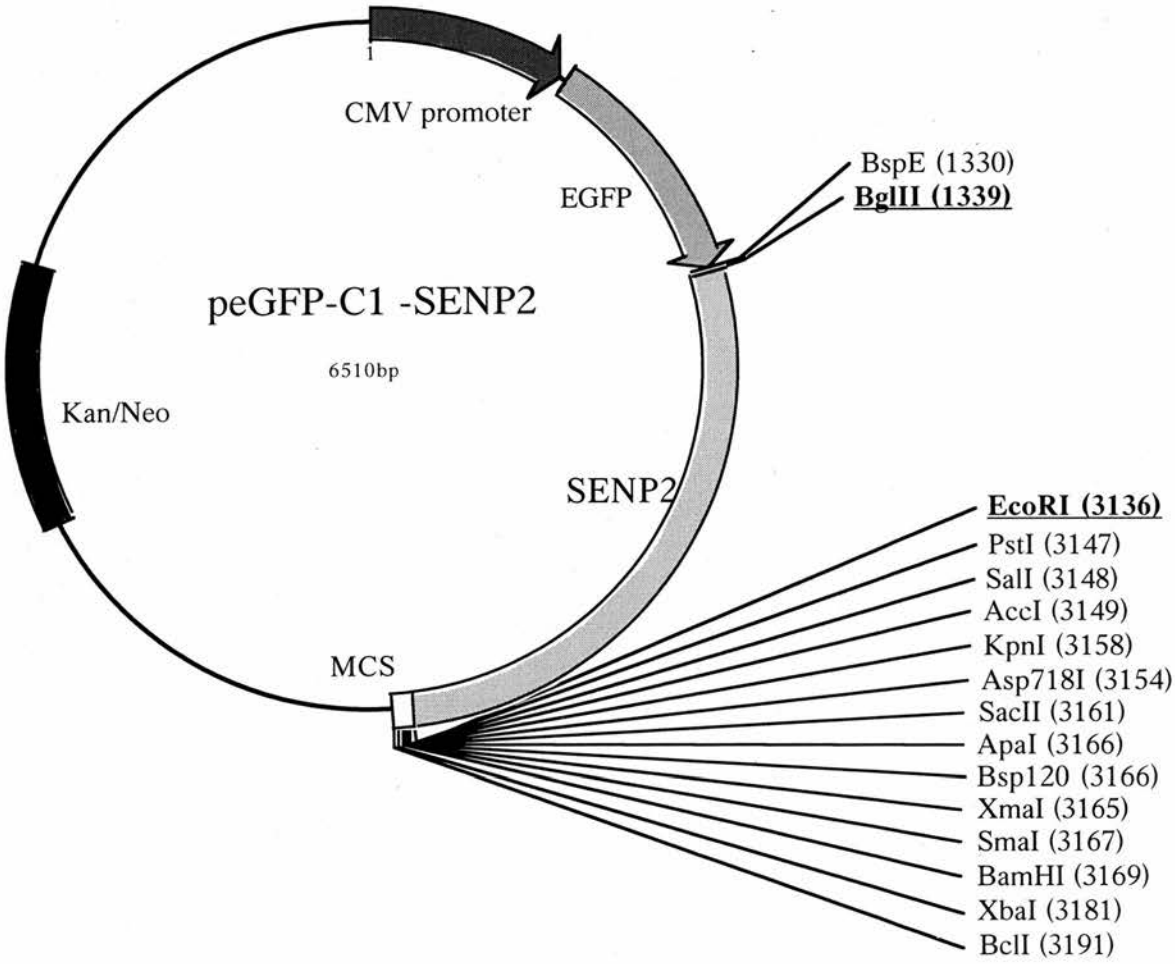

Cloning primers:

5'-GCGAGATCTATGTACAGATGGCTGGTTAGGATT-3'

5'-CGCGCGGAATTCTCACAGCAACTGCTGATG-3'

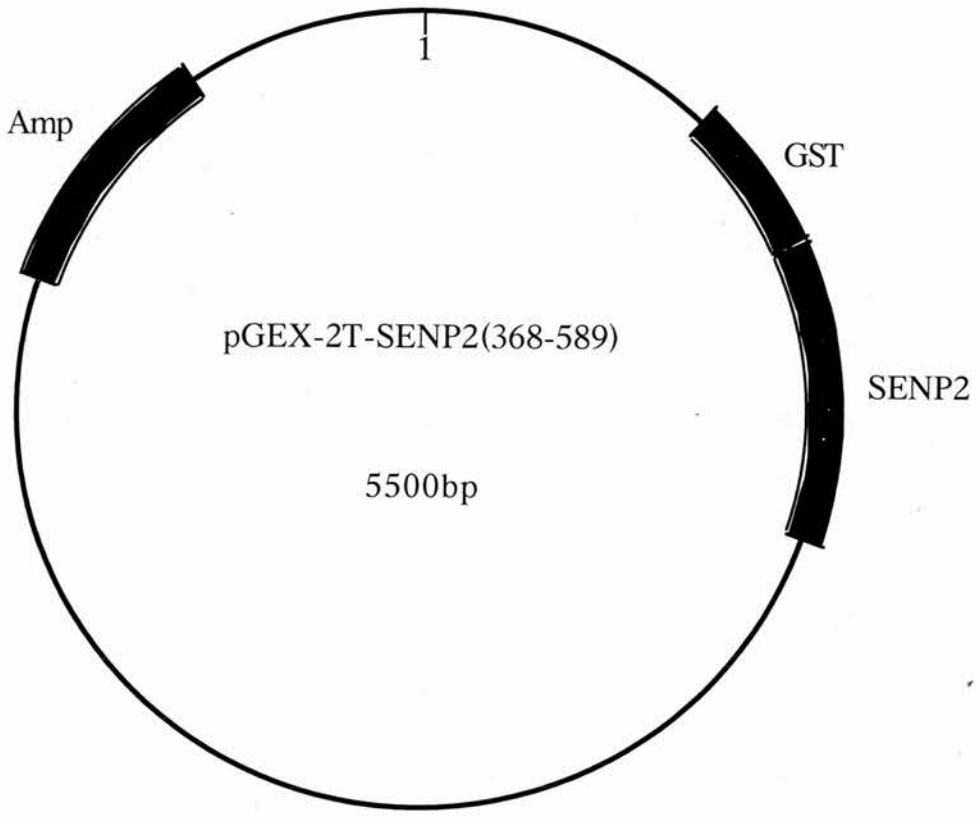

Cloning primers:

5'-TTGAGATCTCTTACAGAGGACATGGAAAAG-3'

5'-ATTGAATTCTCACAGCAACTGCTGATGAAG-3'

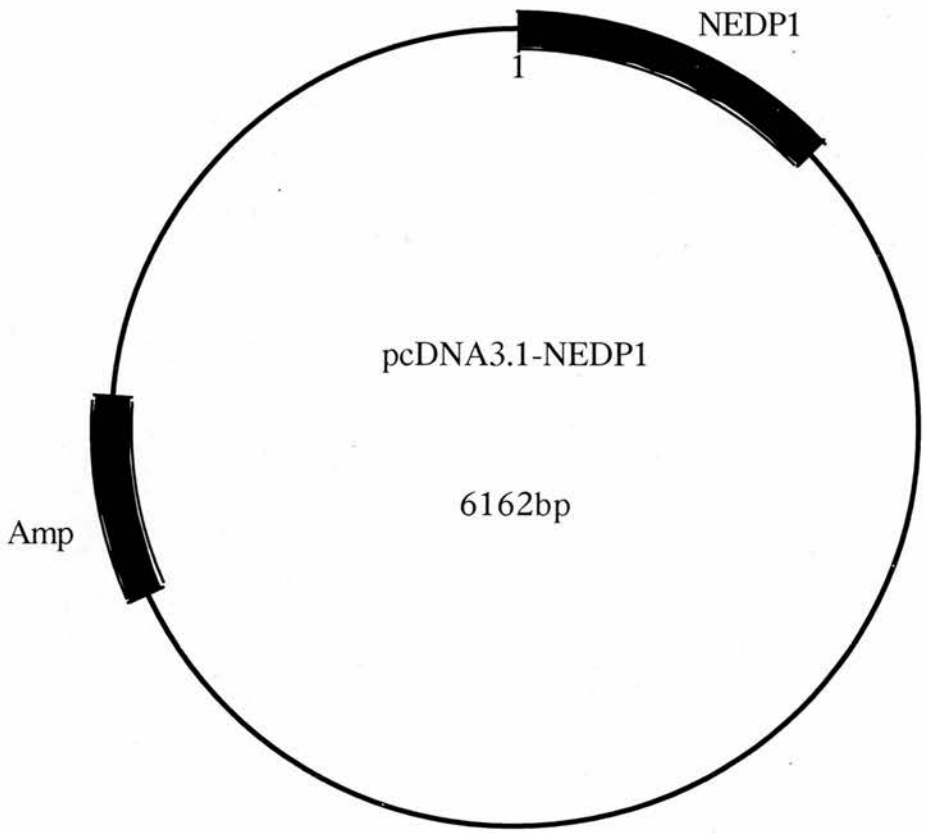

Cloning primers:

5'-GCCACCATGGACCCCGTAGTCTTG-3'

5'-CTACTACTTTTTAGCAAGTGTGGCAATGAG-3'

Antibody:

Bacterially produced full-length NEDP1 used to generate sheep anti-NEDP1

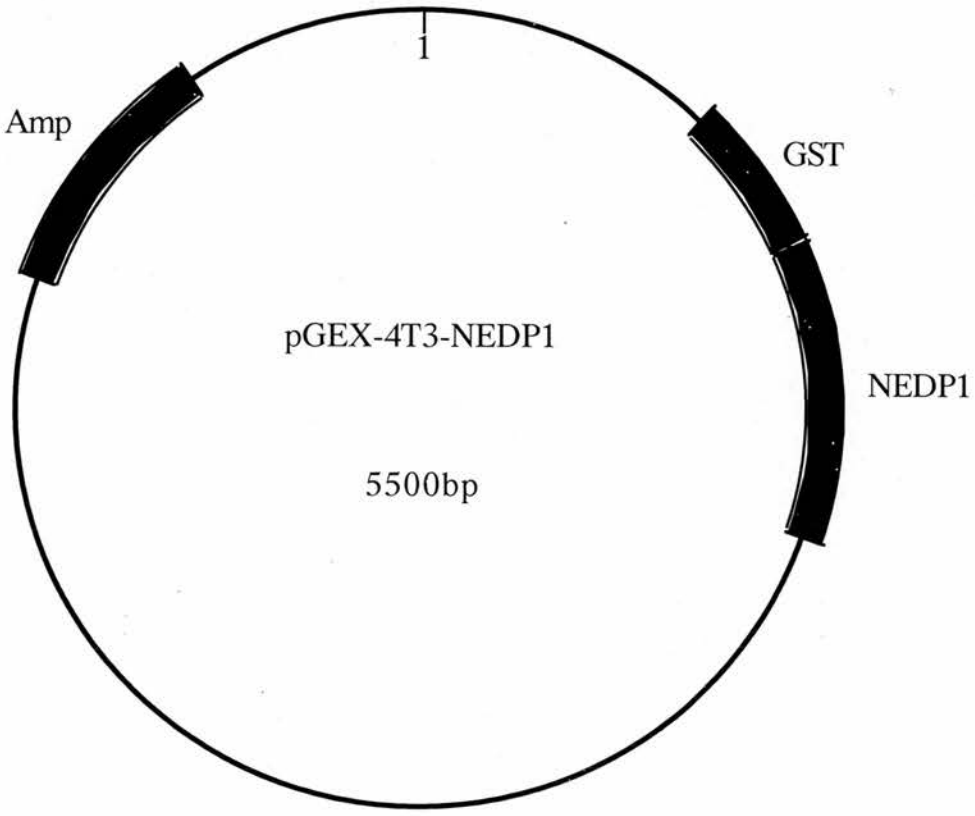

Cloning primers:

5'-GCGGGATCCCAGATCTTCGTGAAGACCCTG-3'

5'-GCGGAATTCCACCACCTCTCAGACGCAGGAC-3'

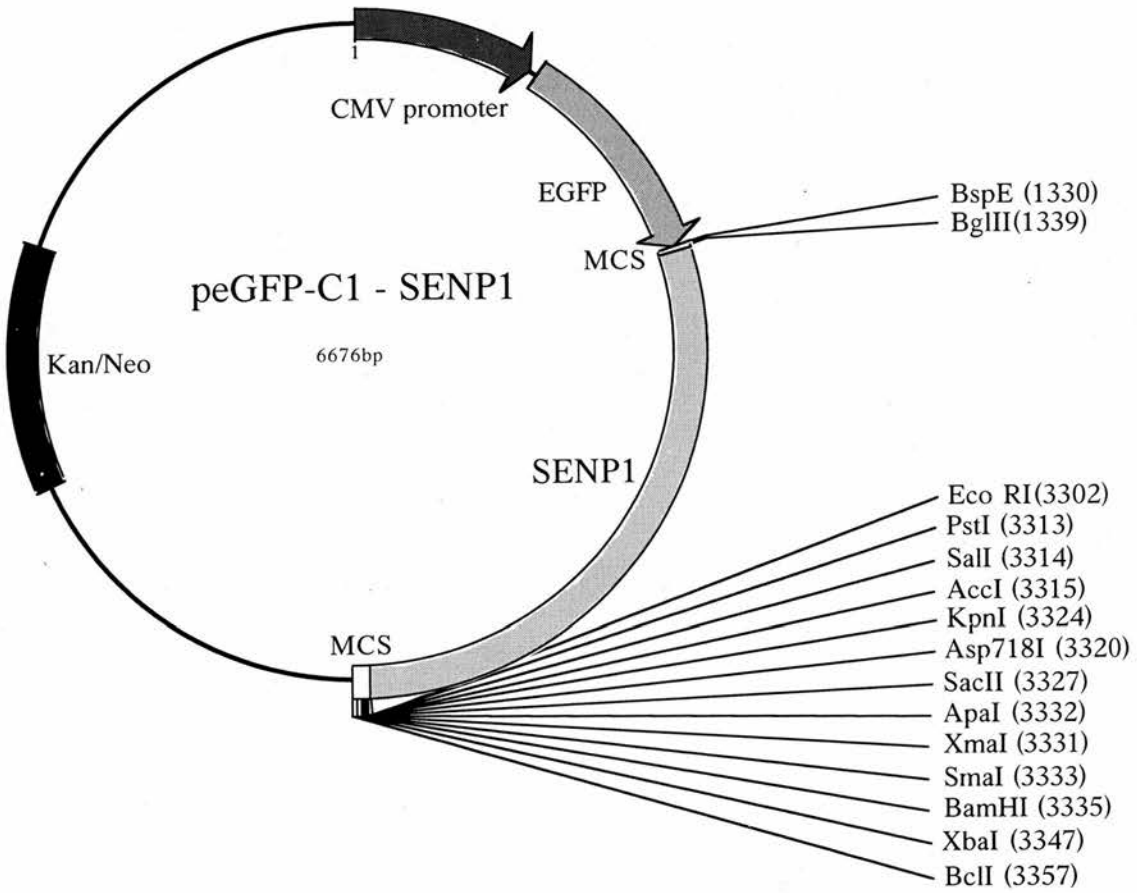

Cloning primers:

5'-TTGAGATCTCTTACAGAGGACATGGAAAAG-3'

5'-ATTGAATTCTCACAGCAACTGCTGATGAAG-3'

9.BIBLIOGRAPHY

1. Larsen, C.N. and H. Wang, *The ubiquitin superfamily: Membranes, features and phylogenies.* Journal of Proteome Research, 2002. **1**: p. 411-419.
2. Tatham, M.H. and R.T. Hay, *Ubiquitin and Ubiquitin-like modifiers: Conserved mechanisms and diverse functions.* Chemtracts-Biochemistry and Molecular Biology, 2003. **16**: p. 759-782.
3. Wilkinson, K.D., *Ubiquitination and deubiquitination: targeting of proteins for degradation by the proteasome.* Semin Cell Dev Biol, 2000. **11**(3): p. 141-8.
4. Hershko, A. and A. Ciechanover, *The ubiquitin system.* Annu Rev Biochem, 1998. **67**: p. 425-79.
5. Aberle, H., A. Bauer, J. Stappert, A. Kispert, and R. Kemler, *beta-catenin is a target for the ubiquitin-proteasome pathway.* Embo J, 1997. **16**(13): p. 3797-804.
6. Hicke, L., *Ubiquitin-dependent internalization and down-regulation of plasma membrane proteins.* Faseb J, 1997. **11**(14): p. 1215-26.
7. Shih, S.C., K.E. Sloper-Mould, and L. Hicke, *Monoubiquitin carries a novel internalization signal that is appended to activated receptors.* Embo J, 2000. **19**(2): p. 187-98.

8. Goldknopf, I.L., C.W. Taylor, R.M. Baum, L.C. Yeoman, M.O. Olson, A.W. Prestayko, and H. Busch, *Isolation and characterization of protein A24, a "histone-like" non-histone chromosomal protein.* J Biol Chem, 1975. **250**(18): p. 7182-7.

9. Momand, J., H.H. Wu, and G. Dasgupta, *MDM2-master regulator of the p53 tumour supressor protein.* GENE, 2002. **242**: p. 15-29.

10. Brummelkamp, T.R., S.M. Nijman, A.M. Dirac, and R. Bernards, *Loss of the cylindromatosis tumour suppressor inhibits apoptosis by activating NF-kappaB.* Nature, 2003. **424**(6950): p. 797-801.

11. Leroy, E., R. Boyer, G. Auburger, B. Leube, G. Ulm, E. Mezey, G. Harta, M.J. Brownstein, S. Jonnalagada, T. Chernova, A. Dehejia, C. Lavedan, T. Gasser, P.J. Steinbach, K.D. Wilkinson, and M.H. Polymeropoulos, *The ubiquitin pathway in Parkinson's disease.* Nature, 1998. **395**(6701): p. 451-2.

12. Jackson, P.K., A.G. Eldridge, E. Freed, L. Furstenthal, J.Y. Hsu, B.K. Kaiser, and J.D. Reimann, *The lore of the RINGs: substrate recognition and catalysis by ubiquitin ligases.* Trends in Cell Biology, 2000. **10**(10): p. 429-39.

13. Peters, J.M., *SCF and APC: the Yin and Yang of cell cycle regulated proteolysis.* Current Opinion in Cell Biology, 1998. **10**(6): p. 759-68.

14. Koepp, D.M., J.W. Harper, and S.J. Elledge, *How the cyclin became a cyclin: regulated proteolysis in the cell cycle.* Cell, 1999. **97**(4): p. 431-4.

15. Nasmyth, K., J.M. Peters, and F. Uhlmann, *Splitting the chromosome: cutting the ties that bind sister chromatids.* Science, 2000. **288**(5470): p. 1379-85.

16. Kim, W. and W.G. Kaelin, *The von Hippel-Lindau tumor supressor protein: new insights into oxygen sensing and cancer.* Curr Opin Genet Dev, 2003. **13**: p. 55-60.

17. Berra, E., E. Benizri, A. Ginouves, V. Volmat, D. Roux, and J. Pouyssegur, *HIF prolyl-hydroxylase 2 is the key oxygen sensor setting low steady-state levels of HIF-1alpha in normoxia.* Embo J, 2003. **22**(16): p. 4082-90.

18. Chung, C.H. and S.H. Baek, *Deubiquitinating enzymes: their diversity and emerging roles.* Biochem Biophys Res Commun, 1999. **266**(3): p. 633-40.

19. Hadari, T., J.V. Warms, I.A. Rose, and A. Hershko, *A ubiquitin C-terminal isopeptidase that acts on polyubiquitin chains. Role in protein degradation.* J Biol Chem, 1992. **267**(2): p. 719-27.

20. Huang, Y., R.T. Baker, and J.A. Fischer-Vize, *Control of cell fate by a deubiquitinating enzyme encoded by the fat facets gene.* Science, 1995. **270**(5243): p. 1828-31.

21. Baek, S.H., Y.J. Yoo, K. Tanaka, and C.H. Chung, *Molecular cloning of chick UCH-6 which shares high similarity with human UCH-L3: its*

unusual substrate specificity and tissue distribution. Biochem Biophys Res Commun, 1999. **264**(1): p. 235-40.

22. Kovalenko, A., C. Chable-Bessia, G. Cantarella, A. Israel, D. Wallach, and G. Courtois, *The tumour suppressor CYLD negatively regulates NF-kappaB signalling by deubiquitination.* Nature, 2003. **424**(6950): p. 801-5.
23. Trompouki, E., E. Hatzivassiliou, T. Tsichritzis, H. Farmer, A. Ashworth, and G. Mosialos, *CYLD is a deubiquitinating enzyme that negatively regulates NF-kappaB activation by TNFR family members.* Nature, 2003. **424**(6950): p. 793-6.
24. Kim, K.I., S.H. Baek, and C.H. Chung, *Versatile protein tag, SUMO: Its enzymology and biological function.* Journal of Cellular Physiology, 2002. **19**: p. 257-268.
25. Seeler, J.S. and A. Dejean, *Nuclear and unclear functions of SUMO.* Nat Rev, 2003. **4**: p. 690-699.
26. Su, H. and S. Li, *Molecular features of human ubiquitin-like SUMO genes and their encoded proteins.* Gene, 2002. **296**: p. 65-73.
27. Saitoh, H. and J. Hinchey, *Functional heterogeneity of small ubiquitin-related protein modifiers SUMO-1 versus SUMO-2/3.* J Biol Chem, 2000. **275**(9): p. 6252-8.
28. Tatham, M.H., E. Jaffray, O.A. Vaughan, J.M. Desterro, C.H. Botting, J.H. Naismith, and R.T. Hay, *Polymeric chains of SUMO-2 and SUMO-3*

are conjugated to protein substrates by SAE1/SAE2 and Ubc9. J Biol Chem, 2001. **276**(38): p. 35368-74.

29. Sachdev, S., L. Bruhn, H. Sieber, A. Pichler, F. Melchior, and R. Grosschedl, *PIASy, a nuclear matrix-associated SUMO E3 ligase, represses LEF1 activity by sequestration into nuclear bodies.* Genes Dev, 2001. **15**(23): p. 3088-103.
30. Azuma, Y., A. Arnaoutov, and M. Dasso, *SUMO-2/3 regulates topoisomerase II in mitosis.* J Cell Biol, 2003. **163**(3): p. 477-87.
31. Desterro, J.M., M.S. Rodriguez, and R.T. Hay, *SUMO-1 modification of IkappaBalpha inhibits NF-kappaB activation.* Mol Cell, 1998. **2**(2): p. 233-9.
32. Mahajan, R., C. Delphin, T. Guan, L. Gerace, and F. Melchior, *A small ubiquitin-related polypeptide involved in targeting RanGAP1 to nuclear pore complex protein RanBP2.* Cell, 1997. **88**(1): p. 97-107.
33. Matunis, M.J., E. Coutavas, and G. Blobel, *A novel ubiquitin-like modification modulates the partitioning of the Ran-GTPase-activating protein RanGAP1 between the cytosol and the nuclear pore complex.* J Cell Biol, 1996. **135**(6 Pt 1): p. 1457-70.
34. Duprez, E., A.J. Saurin, J.M. Desterro, V. Lallemand-Breitenbach, K. Howe, M.N. Boddy, E. Solomon, H. de The, R.T. Hay, and P.S. Freemont, *SUMO-1 modification of the acute promyelocytic leukaemia*

protein PML: implications for nuclear localisation. J Cell Sci, 1999. **112 (Pt 3)**: p. 381-93.

35. Muller, S., M.J. Matunis, and A. Dejean, *Conjugation with the ubiquitin-related modifier SUMO-1 regulates the partitioning of PML within the nucleus.* Embo J, 1998. **17**(1): p. 61-70.
36. Sternsdorf, T., K. Jensen, and H. Will, *Evidence for covalent modification of the nuclear dot-associated proteins PML and Sp100 by PIC1/SUMO-1.* J Cell Biol, 1997. **139**(7): p. 1621-34.
37. Ishov, A.M., A.G. Sotnikov, D. Negorev, O.V. Vladimirova, N. Neff, T. Kamitani, E.T. Yeh, J.F. Strauss, 3rd, and G.G. Maul, *PML is critical for ND10 formation and recruits the PML-interacting protein daxx to this nuclear structure when modified by SUMO-1.* J Cell Biol, 1999. **147**(2): p. 221-34.
38. Zhong, S., S. Muller, S. Ronchetti, P.S. Freemont, A. Dejean, and P.P. Pandolfi, *Role of SUMO-1-modified PML in nuclear body formation.* Blood, 2000. **95**(9): p. 2748-52.
39. Bayer, P., A. Arndt, S. Metzger, R. Mahajan, F. Melchior, R. Jaenicke, and J. Becker, *Structure determination of the small ubiquitin-related modifier SUMO-1.* J Mol Biol, 1998. **280**(2): p. 275-86.
40. Rodriguez, M.S., C. Dargemont, and R.T. Hay, *SUMO-1 conjugation in vivo requires both a consensus modification motif and nuclear targeting.* J Biol Chem, 2001. **276**(16): p. 12654-9.

41. Desterro, J.M., M.S. Rodriguez, G.D. Kemp, and R.T. Hay, *Identification of the enzyme required for activation of the small ubiquitin-like protein SUMO-1.* J Biol Chem, 1999. **274**(15): p. 10618-24.

42. Johnson, E.S., I. Schwienhorst, R.J. Dohmen, and G. Blobel, *The ubiquitin-like protein Smt3p is activated for conjugation to other proteins by an Aos1p/Uba2p heterodimer.* Embo J, 1997. **16**(18): p. 5509-19.

43. Gong, L., B. Li, S. Millas, and E.T. Yeh, *Molecular cloning and characterization of human AOS1 and UBA2, components of the sentrin-activating enzyme complex.* FEBS Lett, 1999. **448**(1): p. 185-9.

44. Okuma, T., R. Honda, G. Ichikawa, N. Tsumagari, and H. Yasuda, *In vitro SUMO-1 modification requires two enzymatic steps, E1 and E2.* Biochem Biophys Res Commun, 1999. **254**(3): p. 693-8.

45. Desterro, J.M., J. Thomson, and R.T. Hay, *Ubch9 conjugates SUMO but not ubiquitin.* FEBS Lett, 1997. **417**(3): p. 297-300.

46. Johnson, E.S. and G. Blobel, *Ubc9p is the conjugating enzyme for the ubiquitin-like protein Smt3p.* J Biol Chem, 1997. **272**(43): p. 26799-802.

47. Seufert, W., B. Futcher, and S. Jentsch, *Role of a ubiquitin-conjugating enzyme in degradation of S- and M-phase cyclins.* Nature, 1995. **373**(6509): p. 78-81.

48. Johnson, E.S. and A.A. Gupta, *An E3-like factor that promotes SUMO conjugation to the yeast septins.* Cell, 2001. **106**(6): p. 735-44.

49. Jackson, P.K., *A new RING for SUMO: wrestling transcriptional responses into nuclear bodies with PIAS family E3 SUMO ligases.* Genes Dev, 2001. **15**(23): p. 3053-8.

50. Gill, G., *Post-translational modification by the small ubiquitin-related modifier SUMO has big effects on transcription factor activity.* Curr Opin Genet Dev, 2003. **13**(2): p. 108-13.

51. Sapetschnig, A., G. Rischitor, H. Braun, A. Doll, M. Schergaut, F. Melchior, and G. Suske, *Transcription factor Sp3 is silenced through SUMO modification by PIAS1.* Embo J, 2002. **21**(19): p. 5206-15.

52. Xhemalce, B., J.S. Seeler, G. Thon, A. Dejean, and B. Arcangioli, *Role of the fission yeast SUMO E3 ligase Pli1p in centromere and telomere maintenance.* Embo J [in press], 2004.

53. Pichler, A., A. Gast, J.S. Seeler, A. Dejean, and F. Melchior, *The nucleoporin RanBP2 has SUMO1 E3 ligase activity.* Cell, 2002. **108**(1): p. 109-20.

54. Zhang, H., H. Saitoh, and M.J. Matunis, *Enzymes of the SUMO modification pathway localize to filaments of the nuclear pore complex.* Mol Cell Biol, 2002. **22**(18): p. 6498-508.

55. Jacobs, J.J. and M. van Lohuizen, *Polycomb repression: from cellular memory to cellular proliferation and cancer.* Biochim Biophys Acta, 2002. **1602**(2): p. 151-61.

56. Kagey, M.H., T.A. Melhuish, and D. Wotton, *The polycomb protein Pc2 is a SUMO E3.* Cell, 2003. **113**(1): p. 127-37.

57. Li, S.J. and M. Hochstrasser, *A new protease required for cell-cycle progression in yeast.* Nature, 1999. **398**(6724): p. 246-51.

58. Li, S.J. and M. Hochstrasser, *The yeast ULP2 (SMT4) gene encodes a novel protease specific for the ubiquitin-like Smt3 protein.* Mol Cell Biol, 2000. **20**(7): p. 2367-77.

59. Meluh, P.B. and D. Koshland, *Evidence that the MIF2 gene of Saccharomyces cerevisiae encodes a centromere protein with homology to the mammalian centromere protein CENP-C.* Mol Biol Cell, 1995. **6**(7): p. 793-807.

60. Bachant, J., A. Alcasabas, Y. Blat, N. Kleckner, and S.J. Elledge, *The SUMO-1 isopeptidase Smt4 is linked to centromeric cohesion through SUMO-1 modification of DNA topoisomerase II.* Mol Cell, 2002. **9**(6): p. 1169-82.

61. Panse, V.G., B. Kuster, T. Gerstberger, and E. Hurt, *Unconventional tethering of Ulp1 to the transport channel of the nuclear pore complex by karyopherins.* Nat Cell Biol, 2003. **5**(1): p. 21-7.

62. Li, S.J. and M. Hochstrasser, *The Ulp1 SUMO isopeptidase: distinct domains required for viability, nuclear envelope localization, and substrate specificity.* J Cell Biol, 2003. **160**(7): p. 1069-81.

63. Johnston, S.C., C.N. Larsen, W.J. Cook, K.D. Wilkinson, and C.P. Hill, *Crystal structure of a deubiquitinating enzyme (human UCH-L3) at 1.8 A resolution.* Embo J, 1997. **16**(13): p. 3787-96.

64. Mossessova, E. and C.D. Lima, *Ulp1-SUMO crystal structure and genetic analysis reveal conserved interactions and a regulatory element essential for cell growth in yeast.* Mol Cell, 2000. **5**(5): p. 865-76.

65. Tanaka, K., J. Nishide, K. Okazaki, H. Kato, O. Niwa, T. Nakagawa, H. Matsuda, M. Kawamukai, and Y. Murakami, *Characterization of a fission yeast SUMO-1 homologue, pmt3p, required for multiple nuclear events, including the control of telomere length and chromosome segregation.* Mol Cell Biol, 1999. **19**(12): p. 8660-72.

66. Taylor, D.L., J.C. Ho, A. Oliver, and F.Z. Watts, *Cell-cycle-dependent localisation of Ulp1, a Schizosaccharomyces pombe Pmt3 (SUMO)-specific protease.* J Cell Sci, 2002. **115**(Pt 6): p. 1113-22.

67. Rawlings, N.D. and A.J. Barrett, *Evolutionary families of peptidases.* Biochem J, 1993. **290 (Pt 1)**: p. 205-18.

68. Nishida, T., H. Tanaka, and H. Yasuda, *A novel mammalian Smt3-specific isopeptidase 1 (SMT3IP1) localized in the nucleolus at interphase.* Eur J Biochem, 2000. **267**(21): p. 6423-7.

69. Gong, L., S. Millas, G.G. Maul, and E.T. Yeh, *Differential regulation of sentrinized proteins by a novel sentrin-specific protease.* J Biol Chem, 2000. **275**(5): p. 3355-9.

70. Rodriguez, M.S., J.M. Desterro, S. Lain, C.A. Midgley, D.P. Lane, and R.T. Hay, *SUMO-1 modification activates the transcriptional response of p53.* Embo J, 1999. **18**(22): p. 6455-61.

71. Mao, Y., M. Sun, S.D. Desai, and L.F. Liu, *SUMO-1 conjugation to topoisomerase I: A possible repair response to topoisomerase-mediated DNA damage.* Proc Natl Acad Sci U S A, 2000. **97**(8): p. 4046-51.

72. Reverter, D. and C.D. Lima, *A Basis for SUMO Protease Specificity Provided by Analysis of Human Senp2 and a Senp2-SUMO Complex.* Structure (Camb), 2004. **12**(8): p. 1519-31.

73. Yukita, A., T. Michiue, A. Fukui, K. Sakurai, H. Yamamoto, M. Ihara, A. Kikuchi, and M. Asashima, *XSENP1, a novel sumo-specific protease in Xenopus, inhibits normal head formation by down-regulation of Wnt/beta-catenin signalling.* Genes Cells, 2004. **9**(8): p. 723-36.

74. Smith, M., V. Bhaskar, J. Fernandez, and A.J. Courey, *Drosophila Ulp1, a nuclear pore-associated SUMO protease, prevents accumulation of cytoplasmic SUMO conjugates.* J Biol Chem, 2004.

75. Mahajan, R., L. Gerace, and F. Melchior, *Molecular characterization of the SUMO-1 modification of RanGAP1 and its role in nuclear envelope association.* J Cell Biol, 1998. **140**(2): p. 259-70.

76. Matunis, M.J., J. Wu, and G. Blobel, *SUMO-1 modification and its role in targeting the Ran GTPase-activating protein, RanGAP1, to the nuclear pore complex.* J Cell Biol, 1998. **140**(3): p. 499-509.

77. Joseph, J., S.H. Tan, T.S. Karpova, J.G. McNally, and M. Dasso, *SUMO-1 targets RanGAP1 to kinetochores and mitotic spindles.* J Cell Biol, 2002. **156**(4): p. 595-602.

78. Roff, M., J. Thompson, M.S. Rodriguez, J.M. Jacque, F. Baleux, F. Arenzana-Seisdedos, and R.T. Hay, *Role of IkappaBalpha ubiquitination in signal-induced activation of NFkappaB in vivo.* J Biol Chem, 1996. **271**(13): p. 7844-50.

79. Rodriguez, M.S., J. Thompson, R.T. Hay, and C. Dargemont, *Nuclear retention of IkappaBalpha protects it from signal-induced degradation and inhibits nuclear factor kappaB transcriptional activation.* J Biol Chem, 1999. **274**(13): p. 9108-15.

80. Steffan, J.S., N. Agrawal, J. Pallos, E. Rockabrand, L.C. Trotman, N. Slepko, K. Illes, T. Lukacsovich, Y.Z. Zhu, E. Cattaneo, P.P. Pandolfi, L.M. Thompson, and J.L. Marsh, *SUMO modification of Huntingtin and Huntington's disease pathology.* Science, 2004. **304**(5667): p. 100-4.

81. Hoege, C., B. Pfander, G.L. Moldovan, G. Pyrowolakis, and S. Jentsch, *RAD6-dependent DNA repair is linked to modification of PCNA by ubiquitin and SUMO.* Nature, 2002. **419**(6903): p. 135-41.

82. Huang, T., S. Wuerzberger-Davis, Z. Wu, and S. Miyamoto, *Sequential modification of NEMO/IKKgamma by SUMO-1 and ubiquitin mediates NF-kappaB activation by genotoxic stress.* Cell, 2003. **115**: p. 565-676.

83. Girdwood, D.W.H., M.H. Tatham, and R.T. Hay, *SUMO and transcriptional regulation.* Seminars in Cell and Developmental Biology, 2004. **15**: p. 201-210.

84. Verger, A., J. Perdomo, and M. Crossley, *Modification with SUMO. A role in transcriptional regulation.* EMBO Rep, 2003. **4**(2): p. 137-42.

85. Gostissa, M., A. Hengstermann, V. Fogal, P. Sandy, S.E. Schwarz, M. Scheffner, and G. Del Sal, *Activation of p53 by conjugation to the ubiquitin-like protein SUMO-1.* Embo J, 1999. **18**(22): p. 6462-71.

86. Ross, S., J.L. Best, L.I. Zon, and G. Gill, *SUMO-1 modification represses Sp3 transcriptional activation and modulates its subnuclear localization.* Mol Cell, 2002. **10**(4): p. 831-42.

87. Yang, S.H., E. Jaffray, R.T. Hay, and A.D. Sharrocks, *Dynamic interplay of the SUMO and ERK pathways in regulating Elk-1 transcriptional activity.* Mol Cell, 2003. **12**(1): p. 63-74.

88. Girdwood, D., D. Bumpass, O.A. Vaughan, A. Thain, L.A. Anderson, A.W. Snowden, E. Garcia-Wilson, N.D. Perkins, and R.T. Hay, *P300 transcriptional repression is mediated by SUMO modification.* Mol Cell, 2003. **11**(4): p. 1043-54.

89. Kumar, S., Y. Yoshida, and M. Noda, *Cloning of a cDNA which encodes a novel ubiquitin-like protein.* Biochem Biophys Res Commun, 1993. **195**(1): p. 393-9.

90. Kamitani, T., K. Kito, H.P. Nguyen, and E.T. Yeh, *Characterization of NEDD8, a developmentally down-regulated ubiquitin-like protein.* J Biol Chem, 1997. **272**(45): p. 28557-62.

91. Yuan, W. and R.M. Krug, *Influenza B virus NS1 protein inhibits conjugation of the interferon (IFN)-induced ubiquitin-like ISG15 protein.* Embo J, 2001. **20**(3): p. 362-71.

92. Zhao, C., S.L. Beaudenon, M.L. Kelley, M.B. Waddell, W. Yuan, B.A. Schulman, J.M. Huibregtse, and R.M. Krug, *The UbcH8 ubiquitin E2 enzyme is also the E2 enzyme for ISG15, an IFN-alpha/beta-induced ubiquitin-like protein.* Proc Natl Acad Sci U S A, 2004. **101**(20): p. 7578-82.

93. Malakhov, M.P., O.A. Malakhova, K.I. Kim, K.J. Ritchie, and D.E. Zhang, *UBP43 (USP18) specifically removes ISG15 from conjugated proteins.* J Biol Chem, 2002. **277**(12): p. 9976-81.

94. Hemelaar, J., P.J. Galardy, A. Borodovsky, B.M. Kessler, H.L. Ploegh, and H. Ovaa, *Chemistry-based functional proteomics: mechanism-based activity-profiling tools for ubiquitin and ubiquitin-like specific proteases.* J Proteome Res, 2004. **3**(2): p. 268-76.

95. Loeb, K.R. and A.L. Haas, *Conjugates of ubiquitin cross-reactive protein distribute in a cytoskeletal pattern.* Mol Cell Biol, 1994. **14**(12): p. 8408-19.

96. Hochstrasser, M., *Evolution and function of ubiquitin-like protein-conjugation systems.* Nat Cell Biol, 2000. **2**(8): p. E153-7.

97. Furukawa, K., N. Mizushima, T. Noda, and Y. Ohsumi, *A protein conjugation system in yeast with homology to biosynthetic enzyme reaction of prokaryotes.* J Biol Chem, 2000. **275**(11): p. 7462-5.

98. Mizushima, N., H. Sugita, T. Yoshimori, and Y. Ohsumi, *A new protein conjugation system in human. The counterpart of the yeast Apg12p conjugation system essential for autophagy.* J Biol Chem, 1998. **273**(51): p. 33889-92.

99. Mizushima, N., T. Yoshimori, and Y. Ohsumi, *Role of the Apg12 conjugation system in mammalian autophagy.* Int J Biochem Cell Biol, 2003. **35**(5): p. 553-61.

100. Mizushima, N., T. Noda, T. Yoshimori, Y. Tanaka, T. Ishii, M.D. George, D.J. Klionsky, M. Ohsumi, and Y. Ohsumi, *A protein conjugation system essential for autophagy.* Nature, 1998. **395**(6700): p. 395-8.

101. Ichimura, Y., T. Kirisako, T. Takao, Y. Satomi, Y. Shimonishi, N. Ishihara, N. Mizushima, I. Tanida, E. Kominami, M. Ohsumi, T. Noda, and Y. Ohsumi, *A ubiquitin-like system mediates protein lipidation.* Nature, 2000. **408**(6811): p. 488-92.

102. Hemelaar, J., V.S. Lelyveld, B.M. Kessler, and H.L. Ploegh, *A single protease, Apg4B, is specific for the autophagy-related ubiquitin-like*

proteins GATE-16, MAP1-LC3, GABARAP, and Apg8L. J Biol Chem, 2003. **278**(51): p. 51841-50.

103. Scherz-Shouval, R., Y. Sagiv, H. Shorer, and Z. Elazar, *The COOH terminus of GATE-16, an intra-Golgi transport modulator, is cleaved by the human cysteine protease HsApg4A.* J Biol Chem, 2003. **278**(16): p. 14053-8.

104. Paz, Y., Z. Elazar, and D. Fass, *Structure of GATE-16, membrane transport modulator and mammalian ortholog of autophagocytosis factor Aut7p.* J Biol Chem, 2000. **275**(33): p. 25445-50.

105. Tanida, I., E. Tanida-Miyake, T. Ueno, and E. Kominami, *The human homolog of Saccharomyces cerevisiae Apg7p is a Protein-activating enzyme for multiple substrates including human Apg12p, GATE-16, GABARAP, and MAP-LC3.* J Biol Chem, 2001. **276**(3): p. 1701-6.

106. Tanida, I., E. Tanida-Miyake, M. Komatsu, T. Ueno, and E. Kominami, *Human Apg3p/Aut1p homologue is an authentic E2 enzyme for multiple substrates, GATE-16, GABARAP, and MAP-LC3, and facilitates the conjugation of hApg12p to hApg5p.* J Biol Chem, 2002. **277**(16): p. 13739-44.

107. Friedman, J.S., B.F. Koop, V. Raymond, and M.A. Walter, *Isolation of a ubiquitin-like (UBL5) gene from a screen identifying highly expressed and conserved iris genes.* Genomics, 2001. **71**(2): p. 252-5.

108. Dittmar, G.A., C.R. Wilkinson, P.T. Jedrzejewski, and D. Finley, *Role of a ubiquitin-like modification in polarized morphogenesis.* Science, 2002. **295**(5564): p. 2442-6.

109. Luders, J., G. Pyrowolakis, and S. Jentsch, *The ubiquitin-like protein HUB1 forms SDS-resistant complexes with cellular proteins in the absence of ATP.* EMBO Rep, 2003. **4**(12): p. 1169-74.

110. Ramelot, T.A., J.R. Cort, A.A. Yee, A. Semesi, A.M. Edwards, C.H. Arrowsmith, and M.A. Kennedy, *Solution structure of the yeast ubiquitin-like modifier protein Hub1.* J Struct Funct Genomics, 2003. **4**(1): p. 25-30.

111. Raasi, S., G. Schmidtke, and M. Groettrup, *The ubiquitin-like protein FAT10 forms covalent conjugates and induces apoptosis.* J Biol Chem, 2001. **276**(38): p. 35334-43.

112. Stuurman, N., A. de Graaf, A. Floore, A. Josso, B. Humbel, L. de Jong, and R. van Driel, *A monoclonal antibody recognizing nuclear matrix-associated nuclear bodies.* J Cell Sci, 1992. **101 (Pt 4)**: p. 773-84.

113. Hanke, T., P. Szawlowski, and R.E. Randall, *Construction of solid matrix-antibody-antigen complexes containing simian immunodeficiency virus p27 using tag-specific monoclonal antibody and tag-linked antigen.* J Gen Virol, 1992. **73 (Pt 3)**: p. 653-60.

114. Nishida, T., F. Kaneko, M. Kitagawa, and H. Yasuda, *Characterization of a novel mammalian SUMO-1/Smt3-specific isopeptidase, a homologue of rat axam, which is an axin-binding protein promoting beta-catenin degradation.* J Biol Chem, 2001. **276**(42): p. 39060-6.

115. Miska, E.A., C. Karlsson, E. Langley, S.J. Nielsen, J. Pines, and T. Kouzarides, *HDAC4 deacetylase associates with and represses the MEF2 transcription factor.* Embo J, 1999. **18**(18): p. 5099-107.

116. Rodriguez, M.S., J. Wright, J. Thompson, D. Thomas, F. Baleux, J.L. Virelizier, R.T. Hay, and F. Arenzana-Seisdedos, *Identification of lysine residues required for signal-induced ubiquitination and degradation of I kappa B-alpha in vivo.* Oncogene, 1996. **12**(11): p. 2425-35.

117. Jaffray, E., K.M. Wood, and R.T. Hay, *Domain organization of I kappa B alpha and sites of interaction with NF-kappa B p65.* Mol Cell Biol, 1995. **15**(4): p. 2166-72.

118. Mendoza, H.M., L.N. Shen, C. Botting, A. Lewis, J. Chen, B. Ink, and R.T. Hay, *NEDP1, a highly conserved cysteine protease that deNEDDylates Cullins.* J Biol Chem, 2003. **278**(28): p. 25637-43.

119. Bradford, M.M., *A rapid and sensitive method for quantitation of microgram quantities of protein utilizing the principle of protein-dye binding.*

Annal biochem, 1976. **72**: p. 248-254.

120. Whitby, F.G., G. Xia, C.M. Pickart, and C.P. Hill, *Crystal structure of the human ubiquitin-like protein NEDD8 and interactions with ubiquitin pathway enzymes.* J Biol Chem, 1998. **273**(52): p. 34983-91.

121. Kim, K.I., S.H. Baek, Y.J. Jeon, S. Nishimori, T. Suzuki, S. Uchida, N. Shimbara, H. Saitoh, K. Tanaka, and C.H. Chung, *A new SUMO-1-specific protease, SUSP1, that is highly expressed in reproductive organs.* J Biol Chem, 2000. **275**(19): p. 14102-6.

122. Liakopoulos, D., G. Doenges, K. Matuschewski, and S. Jentsch, *A novel protein modification pathway related to the ubiquitin system.* Embo J, 1998. **17**(8): p. 2208-14.

123. Osaka, F., H. Kawasaki, N. Aida, M. Saeki, T. Chiba, S. Kawashima, K. Tanaka, and S. Kato, *A new NEDD8-ligating system for cullin-4A.* Genes Dev, 1998. **12**(15): p. 2263-8.

124. Furukawa, M., Y. Zhang, J. McCarville, T. Ohta, and Y. Xiong, *The CUL1 C-terminal sequence and ROC1 are required for efficient nuclear accumulation, NEDD8 modification, and ubiquitin ligase activity of CUL1.* Mol Cell Biol, 2000. **20**(21): p. 8185-97.

125. Hori, T., F. Osaka, T. Chiba, C. Miyamoto, K. Okabayashi, N. Shimbara, S. Kato, and K. Tanaka, *Covalent modification of all members of human cullin family proteins by NEDD8.* Oncogene, 1999. **18**(48): p. 6829-34.

126. Kamura, T., M.N. Conrad, Q. Yan, R.C. Conaway, and J.W. Conaway, *The Rbx1 subunit of SCF and VHL E3 ubiquitin ligase activates Rub1 modification of cullins Cdc53 and Cul2.* Genes Dev, 1999. **13**(22): p. 2928-33.

127. Wada, H., E.T. Yeh, and T. Kamitani, *The von Hippel-Lindau tumor suppressor gene product promotes, but is not essential for, NEDD8 conjugation to cullin-2.* J Biol Chem, 1999. **274**(50): p. 36025-9.

128. Wada, H., E.T. Yeh, and T. Kamitani, *Identification of NEDD8-conjugation site in human cullin-2.* Biochem Biophys Res Commun, 1999. **257**(1): p. 100-5.

129. Xirodimas, D.P., M.K. Saville, J.C. Bourdon, R.T. Hay, and D.P. Lane, *Mdm2-mediated NEDD8 conjugation of p53 inhibits its transcriptional activity.* Embo J [in press], 2004.

130. del Pozo, J.C. and M. Estelle, *The Arabidopsis cullin AtCUL1 is modified by the ubiquitin-related protein RUB1.* Proc Natl Acad Sci U S A, 1999. **96**(26): p. 15342-7.

131. Lammer, D., N. Mathias, J.M. Laplaza, W. Jiang, Y. Liu, J. Callis, M. Goebl, and M. Estelle, *Modification of yeast Cdc53p by the ubiquitin-related protein rub1p affects function of the SCFCdc4 complex.* Genes Dev, 1998. **12**(7): p. 914-26.

132. Osaka, F., M. Saeki, S. Katayama, N. Aida, E.A. Toh, K. Kominami, T. Toda, T. Suzuki, T. Chiba, K. Tanaka, and S. Kato, *Covalent modifier*

NEDD8 is essential for SCF ubiquitin-ligase in fission yeast. Embo J, 2000. **19**(13): p. 3475-84.

133. Kawakami, T., T. Chiba, T. Suzuki, K. Iwai, K. Yamanaka, N. Minato, H. Suzuki, N. Shimbara, Y. Hidaka, F. Osaka, M. Omata, and K. Tanaka, *NEDD8 recruits E2-ubiquitin to SCF E3 ligase.* Embo J, 2001. **20**(15): p. 4003-12.

134. Chen, Y., D.L. McPhie, J. Hirschberg, and R.L. Neve, *The amyloid precursor protein-binding protein APP-BP1 drives the cell cycle through the S-M checkpoint and causes apoptosis in neurons.* J Biol Chem, 2000. **275**(12): p. 8929-35.

135. Handeli, S. and H. Weintraub, *The ts41 mutation in Chinese hamster cells leads to successive S phases in the absence of intervening G2, M, and G1.* Cell, 1992. **71**(4): p. 599-611.

136. Podust, V.N., J.E. Brownell, T.B. Gladysheva, R.S. Luo, C. Wang, M.B. Coggins, J.W. Pierce, E.S. Lightcap, and V. Chau, *A Nedd8 conjugation pathway is essential for proteolytic targeting of p27Kip1 by ubiquitination.* Proc Natl Acad Sci U S A, 2000. **97**(9): p. 4579-84.

137. Cope, G.A., G.S. Suh, L. Aravind, S.E. Schwarz, S.L. Zipursky, E.V. Koonin, and R.J. Deshaies, *Role of predicted metalloprotease motif of Jab1/Csn5 in cleavage of Nedd8 from Cul1.* Science, 2002. **298**(5593): p. 608-11.

138. Lyapina, S., G. Cope, A. Shevchenko, G. Serino, T. Tsuge, C. Zhou, D.A. Wolf, N. Wei, and R.J. Deshaies, *Promotion of NEDD-CUL1 conjugate cleavage by COP9 signalosome.* Science, 2001. **292**(5520): p. 1382-5.

139. Kapelari, B., D. Bech-Otschir, R. Hegerl, R. Schade, R. Dumdey, and W. Dubiel, *Electron microscopy and subunit-subunit interaction studies reveal a first architecture of COP9 signalosome.* Journal of Molecular Biology, 2000. **300**(5): p. 1169-78.

140. Ledl, A., D. Schmidt, and S. Muller, *SUMO: a regulator of gene expression and genome integrity.* Oncogene, 2004. **23**(11): p. 1998-2008.

141. Ding, J., W.J. McGrath, R.M. Sweet, and W.F. Mangel, *Crystal structure of the human adenovirus proteinase with its 11 amino acid cofactor.* Embo J, 1996. **15**(8): p. 1778-83.

142. Gong, L., T. Kamitani, S. Millas, and E.T. Yeh, *Identification of a novel isopeptidase with dual specificity for ubiquitin- and NEDD8-conjugated proteins.* J Biol Chem, 2000. **275**(19): p. 14212-6.

143. Wada, H., K. Kito, L.S. Caskey, E.T. Yeh, and T. Kamitani, *Cleavage of the C-terminus of NEDD8 by UCH-L3.* Biochem Biophys Res Commun, 1998. **251**(3): p. 688-92.

144. Hochstrasser, M., *Molecular biology. New proteases in a ubiquitin stew.* Science, 2002. **298**(5593): p. 549-52.

145. Schwechheimer, C. and X.W. Deng, *COP9 signalosome revisited: a novel mediator of protein degradation.* Trends Cell Biol, 2001. **11**(10): p. 420-6.

146. Chamovitz, D.A. and D. Segal, *JAB1/CSN5 and the COP9 signalosome. A complex situation.* EMBO Rep, 2001. **2**(2): p. 96-101.

147. Kurz, T., L. Pintard, J.H. Willis, D.R. Hamill, P. Gonczy, M. Peter, and B. Bowerman, *Cytoskeletal regulation by the Nedd8 ubiquitin-like protein modification pathway.* Science, 2002. **295**(5558): p. 1294-8.

148. Kirsh, O., J.S. Seeler, A. Pichler, A. Gast, S. Muller, E. Miska, M. Mathieu, A. Harel-Bellan, T. Kouzarides, F. Melchior, and A. Dejean, *The SUMO E3 ligase RanBP2 promotes modification of the HDAC4 deacetylase.* Embo J, 2002. **21**(11): p. 2682-91.

149. Hang, J. and M. Dasso, *Association of the human SUMO-1 protease SENP2 with the nuclear pore.* J Biol Chem, 2002. **277**(22): p. 19961-6.

150. Kadoya, T., H. Yamamoto, T. Suzuki, A. Yukita, A. Fukui, T. Michiue, T. Asahara, K. Tanaka, M. Asashima, and A. Kikuchi, *Desumoylation activity of Axam, a novel Axin-binding protein, is involved in downregulation of beta-catenin.* Mol Cell Biol, 2002. **22**(11): p. 3803-19.

151. Best, J.L., S. Ganiatsas, S. Agarwal, A. Changou, P. Salomoni, O. Shirihai, P.B. Meluh, P.P. Pandolfi, and L.I. Zon, *SUMO-1 protease-1 regulates gene transcription through PML.* Mol Cell, 2002. **10**(4): p. 843-55.

152. Mullins, J.M. and J.R. McIntosh, *Isolation and initial characterization of the mammalian midbody.* J Cell Biol, 1982. **94**(3): p. 654-61.

153. Minoshima, Y., T. Kawashima, K. Hirose, Y. Tonozuka, A. Kawajiri, Y.C. Bao, X. Deng, M. Tatsuka, S. Narumiya, W.S. May, Jr., T. Nosaka, K. Semba, T. Inoue, T. Satoh, M. Inagaki, and T. Kitamura, *Phosphorylation by aurora B converts MgcRacGAP to a RhoGAP during cytokinesis.* Developmental Cell, 2003. **4**(4): p. 549-60.

154. Zhou, T., J.P. Aumais, X. Liu, L.Y. Yu-Lee, and R.L. Erikson, *A role for Plk1 phosphorylation of NudC in cytokinesis.* Developmental Cell, 2003. **5**(1): p. 127-38.

155. Piel, M., J. Nordberg, U. Euteneuer, and M. Bornens, *Centrosome-dependent exit of cytokinesis in animal cells.* Science, 2001. **23**(291): p. 1550-3.

156. Bailey, D. and P. O'Hare, *Characterisation of the localisation and proteolytic activity of the SUMO-specific protease, SENP1.* J Biol Chem, 2003.

157. Nefkens, I., D.G. Negorev, A.M. Ishov, J.S. Michaelson, E.T. Yeh, R.M. Tanguay, W.E. Muller, and G.G. Maul, *Heat shock and Cd2+ exposure regulate PML and Daxx release from ND10 by independent mechanisms that modify the induction of heat-shock proteins 70 and 25 differently.* J Cell Sci, 2003. **116**(Pt 3): p. 513-24.

158. Strunnikov, A.V., L. Aravind, and E.V. Koonin, *Saccharomyces cerevisiae SMT4 encodes an evolutionarily conserved protease with a role in chromosome condensation regulation.* Genetics, 2001. **158**(1): p. 95-107.

159. Nordberg, J., U. Euteneuer, M. Bornens, and T. Hayashi, *Ubc9 is essential for viability of higher eukaryotic cells.* Science, 2001. **291**(5508): p. 1550-3.

160. Bailey, D. and P. O'Hare, *Herpes simplex virus 1 ICP0 co-localizes with a SUMO-specific protease.* J Gen Virol, 2002. **83**(Pt 12): p. 2951-64.

161. Lippincott, J., K.B. Shannon, W. Shou, R.J. Deshaies, and R. Li, *The Tem1 small GTPase controls actomyosin and septin dynamics during cytokinesis.* Journal of Cell Science, 2001. **114**(Pt 7): p. 1379-86.

162. Johnson, E.S. and G. Blobel, *Cell cycle-regulated attachment of the ubiquitin-related protein SUMO to the yeast septins.* J Cell Biol, 1999. **147**(5): p. 981-94.

163. Surka, M.C., C.W. Tsang, and W.S. Trimble, *The mammalian septin MSF localizes with microtubules and is required for completion of cytokinesis.* Molecular Biology of the Cell, 2002. **13**(10): p. 3532-45.

164. Biggins, S., N. Bhalla, A. Chang, D.L. Smith, and A.W. Murray, *Genes involved in sister chromatid separation and segregation in the*

budding yeast Saccharomyces cerevisiae. Genetics, 2001. **159**(2): p. 453-70.

10.PUBLICATION

Mendoza, H.M., et al., *NEDP1, a highly conserved cysteine protease that deNEDDylates Cullins.* J Biol Chem, 2003. **278**(28): p. 25637-43.